

Coupled-Cluster Studies of Double Quantum Dots

by

Yang Min Wang

THESIS
for the degree of
MASTER OF SCIENCE

(Master in Computational Physics)



Faculty of Mathematics and Natural Sciences
Department of Physics
University of Oslo

June 2011

Acknowledgment

I am very thankful to my supervisor, professor Morten Hjort-Jensen, who has taught me ever since 2008. He has been a mentor and helped me far beyond what I would have expected. His enthusiasm and humor have been a motivation. I am very lucky to have met Morten, and I hope I have in return fulfilled his expectations. I am deeply grateful to the many hours Simen Kvaal have spent helping me to implement the transformations and writing replies to my questions.

It has been interesting to work with such a likable person as Marte Hoel Jørgensen, whom I worked with on the optimization of the CCSD code. I admire her professionalism and discipline, and she has helped me to see things from different perspectives.

I would also thank Gustav Jansen and Øyvind Jensen for their insights and suggestions that have helped me understand the nature of my problems. Magnus Pedersen Lohne have been very helpful and responded every time on email. Thanks to my fellow students David Skålid Amundsen, Andreas Nakkerud, Jørgen Trømborg, Christoffer Hirth, Jørgen Høgberget, who have helped me along the way and made my time at the University of Oslo very enjoyable.

I have enjoyed the physics as well as non-physics discussions with my friends Henrik and Michael, they have broadened my perspectives on what a fruit is and is not. The discussions have been very fruitful to say the least. It has been a challenging year, and skiing has been very relaxing, thanks to Patrick, Vladimir, Morten, Christoffer, Thomas, Henrik and Michael for joining me for some memorable trips in Lillomarka. Shout-out to Henrik Holte for proof-reading my thesis. Another shout-out to Christoffer Hirth for introducing me to NetBeans which have been very helpful.

Finally, I want to give credit to my mother, father, and my sister. Without their encouragement and support there would be no thesis.

Yang Min Wang

“The highest forms of understanding we can achieve is laughter and human compassion.”

R. P. Feynman.

Contents

I	FUNDAMENTALS	11
1	Quantum Mechanics for single-particle systems	13
1.1	Introduction	13
1.1.1	Measurement and Observables	14
1.1.2	The Schrödinger equation	14
1.1.3	The time-independent Schrödinger equation	14
1.1.4	Probabilities	15
1.2	Postulates of Quantum Mechanics	15
1.3	Different Representations of Quantum Mechanics	16
1.3.1	Dirac's Notation	16
1.3.2	Heisenberg's matrix formulation	17
1.4	Angular Momentum and Spin	17
1.4.1	The wavefunction	18
1.5	Simple systems	18
1.5.1	Particle in a Infinite Potential Well	18
1.5.2	Particle in a Harmonic Oscillator Potential Well	19
2	The Quantum Mechanics behind Quantum Dots	21
2.1	Description of the Quantum Dot	21
2.2	The One-electron Quantum Dot	22
2.2.1	Parabolic Quantum Dot with Influence of an Electromagnetic Field	23
2.2.2	Scaling the Hamiltonian	28
2.3	Double Quantum Dots	30
2.3.1	The QR-Algorithm	30
2.3.2	Discretizing the Schrödinger Equation	33
3	Quantum Mechanics for Many-Body Systems	37
3.1	Introduction	37
3.2	The Many-Body Problem	37
3.2.1	The Electronic Hamiltonian	38
3.2.2	Identical Particles	39
3.3	Second Quantization	40
3.3.1	Creation and Annihilation Operators	41
3.3.2	Representation of Operators	42
3.3.3	Wick's Theorem	44
3.3.4	Particle-Hole Formalism	46
3.4	The Normal-Ordered Hamiltonian	48

II	MANY-BODY METHODS	51
4	Hartree-Fock Method	53
4.1	Introduction	53
4.2	Derivation of the Hartree-Fock Equations	54
4.3	Outline of the Algorithm	57
5	Coupled Cluster Theory	59
5.1	Introduction	59
5.2	The Coupled Cluster Formalism	59
5.2.1	Reference state and operators	59
5.2.2	The Exponential Ansatz	61
5.3	Energy equation for the CCSD	61
5.3.1	The Algebraic Approach	62
5.4	Introduction to Coupled Cluster Diagrams	67
5.4.1	Energy Equation	71
5.5	The Amplitude Equations	74
5.6	Concluding Remarks	76
5.6.1	Issues with the Coupled Cluster Method	76
III	Implementation and Results	79
6	Implementations	81
6.1	Implementation of the Configuration Class	81
6.2	Implementation of the Restrictd Hartree-Fock Method	82
6.2.1	Input	83
6.2.2	Output	83
6.2.3	Validation of the Code	83
6.2.4	Code Structure	83
6.3	Implementation of the Coupled Cluster Singles and Doubles	87
6.3.1	Input	87
6.3.2	Output	87
6.3.3	Validation of the Code	87
6.3.4	Code Structure	89
6.4	Implementation of the double dot	122
6.4.1	Scaling the Hamiltonian	122
6.4.2	Finding the eigenvectors and eigenvalues	125
6.4.3	Finding the coefficients	127
6.4.4	Transformation from polar to Cartesian representation	129
6.4.5	Tabulating new quantum numbers	132
6.4.6	Validation of the Code	133
7	Results	135
7.1	Standard Interaction	135
7.2	General Analysis and Discussion	156
8	Conclusions	161
8.1	Continuation of this thesis	162
A	Derivation of the Baker-Campbell-Hausdorff formula	165

Abbreviations

EPV	Exclusion-Principle-Violationg
Eq	Equation
Fig	Figure
BCH	Baker-Campbell-Hausdorff expansion
SD	Slater Determinant
PEP	Pauli Exclusion Principle
HF	Hartree-Fock Method
RHF	Restricted Hartree-Fock Method
DFT	Density functional Theory
MBPT	Many-Body Perturbation Theory
CC	Coupled-Cluster
CCM	Coupled-Cluster Method
CCS	Coupled-Cluster Method with Single Excitations
CCD	Coupled-Cluster Method with Double Excitations
CCSD	Coupled-Cluster with Single and Double Excitations
CCSDT	Coupled-Cluster with Single, Double and Triple Excitations
CCSDTQ	Coupled-Cluster with Single, Double, Triple and Quadruple Excitations
DMC	Diffusion Monte Carlo

Introduction

The goal of this thesis is to show how we can study double quantum dots (and more complicated as well) systems using coupled-cluster theory. During this process we have used Magnus Pedersen Lohnes Master's Thesis [47] as a starting point, and a lot of the work has been devoted to optimize his code. I have been working with Marte Hoel Joergensen [34] with the optimization, and we have developed a method of using a Hartree-Fock calculation as an input to improve the convergence of our coupled-cluster calculations. I have developed a method for solving the manybody problem in a two-dimensional double harmonic oscillator well. Using this method I have seen some interesting effects that will be discussed.

This thesis could be regarded as a academic curiosity. However we will show that the versatility of the CCSD method and the general features of our confining potentials, can be used in linking theory with experiment. This is the main reason why we want to study quantum dots. People have applied Density Functional theories (DFT) to describe such systems [61], but we want to describe it from first principle methods. This is why we use the ab initio coupled-cluster method. Quantum dots form a very active and lively research field in condensedmatter theory. They have been used to develop devices such as single electron transistors, quantum dot lasers [6] and “artificial atoms” [3]. They share similar properties such as shell structure and magic numbers as seen in atoms and nuclei. Lately one of the important applications is the use of colloidal quantum dot for detecting cancer cells [68]. To address such system, we need a proper theoretical description of the electronic system, exchange coupling, correlation energies, and ground state energies.

The quantum dot is essentially a device that can trap electrons. The typical size of these devices are between a micrometer to few nanometers. In these quantum dots we can see quantum mechanical effects such as discrete energy levels. Our quantum mechanical model for the quantum dot is a parabolic quantum well which traps the electrons in two dimensions. Such a model is an idealization of quantum dots that serve as a starting point to understand realistic quantum dots. They are in fact crystalline and have periodic potentials. That is the reason why we are interested in the double quantum dots. This could give us insights of the physics in more real life systems.

Another interesting field is construction of qubits which are states of confined electrons in these type of double well potentials [8]. Lot of experiments have been done in this field [55], [57]. Therefore the importance of understanding the underlying principles of the systems involved are essential. The future computers will probability be constructed with these type of systems.

Structure of Thesis

The thesis is divided into three parts. Part one is an introduction to quantum mechanics. I start by covering the one-body Schrödinger equation and then the development of the many-body theory which we need in part two.

In part two we cover the different many-body theories, *Hartree-Fock* and *CCSD*. Finally, part three contains the results and implementation of our code. We finish off with discussions

of the results and conclusion.

Part I

FUNDAMENTALS

Chapter 1

Quantum Mechanics for single-particle systems

“Quantum mechanics is that mysterious, confusing discipline, which really no one of us understands but which we know how to use. It works perfectly, as far as we can tell, in describing physical reality, but it is a counter-intuitive discipline, as the social scientists would say. Quantum mechanics is not a theory, but rather a framework within which we believe any correct theory must fit.”

Murray Gell-Mann, in Mulvey (1981)

1.1 Introduction

In the late 19th century scientists had problems with their classical understanding of the ways things are. Some experiments showed up that did not coincide with the current theories. The beginning of quantum mechanics was when Max Planck published in a theory of black-body radiation (1900). He explained that atoms can absorb and emit discrete quanta of radiation with energy $\epsilon = hf$, where f is the radiation frequency and h is the fundamental constant called Planck’s constant.

$$h \approx 6.626 \times 10^{-34} \text{Js} \tag{1.1}$$

In classical physics we distinguish between the particle and waves, a classical particle cannot be wavelike and particle like at the same time. But as some experiments have shown, this does not reflect the reality (Young’s famous double slit experiment). Quantum mechanics can sometimes be counterintuitive in that regard, but then again, Newton’s theory of gravity must have been difficult to grasp at first. How do we know about these “invisible” forces which we cannot see?

Another problem people had was that the atoms would be unstable if we had electrons that were particle-like and orbited around defined orbits. The orbiting electrons would radiate electromagnetic energy and eventually fall into the nucleus. We need to have a wavelike description of the atomic electrons in order to explain their stability. Wave-like electrons are confined inside the atom, and at the lowest state, the ground state, the electron cannot radiate away its energy and fall into the nucleus. This gave us a whole new way of looking at nuclear physics. It revolutionized the 20th century physics.

1.1.1 Measurement and Observables

Measurements are done by a subject, usually called an *observer*, that has an instrument which takes measurements on an *object*. During this process we have disturbances and never ideal conditions. In classical physics the disturbance is directly associated with measurement itself and can be made arbitrarily small, depending of how good the engineers are. If we wanted to measure length with 5 decimal precision, we could just get a more precise ruler. But this is not the case in quantum mechanics. Each time we do measurements in quantum mechanics we have a probability distribution of different outcomes. This has nothing to do with the instrument itself, it is a part of the intrinsic nature of formulation of the quantum mechanics called the *Heisenberg uncertainty principle*.

$$\Delta x \Delta p \geq \frac{\hbar}{2} \quad (1.2)$$

This means that if we determine the momentum exactly $\Delta x = 0$, then the momentum is totally uncertain. The concept that particles exist with definite position and momentum is an idealistic classical concept.

1.1.2 The Schrödinger equation

The Schrödinger equation is the quantum mechanical equivalent to Newton's Second Law. It describes the motion of a quantum mechanical particle. This is a partial differential equation which describes how the wave function, representing the particle, *flows*. The Schrödinger equation for a particle moving in a three-dimensional potential is:

$$i\hbar \frac{\partial \Psi}{\partial t} = \hat{H} \Psi \quad (1.3)$$

Where \hat{H} is called the Hamilton operator and Ψ is the wavefunction:

$$\hat{H} = -\frac{\hbar^2}{2m} \nabla^2 + V(\mathbf{r}, t). \quad (1.4)$$

It is important to point out that this equation describes a non-relativistic motion of a quantum particle i.e. $E \gg m_0 c^2$, where m_0 is the rest mass of the quantum particle.

1.1.3 The time-independent Schrödinger equation

If we the potential in Eq. (1.4) does not depend on time, we can guess a solution to the Schrödinger equation Eq. (1.3) by

$$\Psi(\mathbf{r}, t) = \psi(\mathbf{r})T(t). \quad (1.5)$$

Inserting this into Eq. (1.3) and divide it by Ψ gives

$$i\hbar \frac{dT(t)/dt}{T(t)} = \frac{\hat{H}\psi(\mathbf{r})}{\psi(\mathbf{r})}, \quad (1.6)$$

since the left side of the equation depends on t while the right side depends on r , the only way this is valid is if they equal a constant we call E which later will become the energy of the system.

$$i\hbar \frac{dT(t)/dt}{T(t)} \quad (1.7)$$

The solution of this equation are

$$T(t) = T(0)e^{-iEt/\hbar}. \quad (1.8)$$

In addition we get the equation

$$\frac{\hat{H}\psi(\mathbf{r})}{\psi(\mathbf{r})} = E, \quad (1.9)$$

rewritten it yields

$$\hat{H}\psi(\mathbf{r}) = E\psi(\mathbf{r}). \quad (1.10)$$

Which we will refer to as the time-independent Schrödinger equation. We only need to solve this equation for time-independent Hamiltonian \hat{H} , since our time dependence will just be a phase factor and does not affect the wavefunction probability nor our energy. If we have such wavefunctions they will be called *stationary* states. Our potentials are not time dependent, therefore Eq. 1.10 would be the main equation to solve in our thesis and the special solution to the Schrödinger equation would be

$$\Psi(\mathbf{r}, t) = \psi(\mathbf{r})e^{-iEt/\hbar} \quad (1.11)$$

If we have more than one stationary solution to Eq. 1.10, the sum of those solution would also be a solution to the Schrödinger equation and the general solution to Schrödinger equation Eq. (1.3) would be

$$\Psi(\mathbf{r}, t) = \sum_n c_n \psi_n(\mathbf{r})e^{-iE_n t/\hbar} \quad (1.12)$$

1.1.4 Probabilities

Max Born introduced an interpretation of the Schrödinger wavefunction $\Psi(\mathbf{r}, t)$. He pointed out that the probability of detecting a particle at a certain location and time is proportional to $|\Psi(\mathbf{r}, t)|^2$. Thus $|\Psi(\mathbf{r}, t)|^2$ is often viewed as a probability density at the position r and time t . And the wavefunction is often referred to as a probability amplitude. We can normalize our probability density by summing up all the possible position of the particle to one:

$$\int |\Psi(\mathbf{r}, t)|^2 d^3\mathbf{r} = 1. \quad (1.13)$$

The wavefunction could also be a function of momentum and thereby describe the probability for finding a momentum in a certain range.

1.2 Postulates of Quantum Mechanics

We could argue that Newton's law of motion is the postulate in classical mechanics. What are Newton's laws derived from? Likewise quantum mechanics is based on some fundamental "laws of nature" that must be underivable.

A postulate is a statement made without any proof, an "underived" statement. In physics a postulate could be translated into a proposal which could either be verified or falsified based on experiment [9].

Postulate 1 *We describe a system by its state vector $|s\rangle$, an observable q and it's a hermitian operator \hat{Q} which operates on any $|s\rangle$*

Postulate 2 *The time evolution of the quantum state Ψ is governed by the time-dependent Schrödinger equation. Ψ is a function of position coordinates q_n and the time t . \hat{H} is the Hamiltonian*

$$i\hbar \frac{\partial \Psi}{\partial t} = \hat{H}\Psi. \quad (1.14)$$

Postulate 3 *The possible results of measurement of an observable Q , are its eigenvalues q_i of its operator \hat{Q} .*

Postulate 4 *If the results of the measurements is found to be q_i , then after the measurement the system will "collapse" into a corresponding eigenstate $|q_i\rangle$.*

Postulate 5 *The expectation value of an observable is given by*

$$\langle F \rangle = \int \psi^* \hat{F} \psi d\tau \quad (\text{coordinate representation}) \quad (1.15)$$

1.3 Different Representations of Quantum Mechanics

As we have seen, originally the state Ψ was a solution to the Schrödinger equation, which was a partial differential equation, second order in space and first order in time. So the "state function" Ψ has to be a function of time and space coordinates. We will refer to this as the Schrödinger representation. Quantum mechanics could be more abstract and more convenient as shown by Dirac [17]. Another way to represent it is by matrix mechanics introduced by Heisenberg. Those are the main ways that we can use to represent quantum mechanics, and they are mathematically equivalent.

1.3.1 Dirac's Notation

An abstract quantum mechanical state Ψ is represented by a "bra" vector $\langle \Psi |$ or a "ket" vector $|\Psi\rangle$. The distinction between the forms lies in the context in which they are used and will become clearer when we show this. The scalar product in Dirac's notation is the "bracket", which is very convenient compared to writing the integral in the Schrödinger representation.

$$\langle \Phi | \Psi \rangle \equiv \int \Phi^*(\mathbf{r}) \Psi(\mathbf{r}) d\mathbf{r}. \quad (1.16)$$

The expectation value of an operator is:

$$\langle \Phi | \hat{Q} | \Psi \rangle \equiv \int \Phi^*(\mathbf{r}) \hat{Q} \Psi(\mathbf{r}) d\mathbf{r}. \quad (1.17)$$

The time-independent Schrödinger equation in the Dirac notation:

$$\hat{H} |E_i\rangle = E_i |E_i\rangle. \quad (1.18)$$

In this example we see that the label E_i inside the ket tells us about its eigenvalue. The spectra of the eigenvalues to an operator could be discrete or continuous like the operator \hat{x} :

$$\hat{x} |x\rangle = x |x\rangle. \quad (1.19)$$

If we wish to get back to the Schrödinger representation $\Psi(x)$, we could do a "projection" of $|\Psi\rangle$ on the eigenfunction $|x\rangle$:

$$\Psi(x) \equiv \langle x | \Psi \rangle. \quad (1.20)$$

Similarly the complex conjugate:

$$\Psi^*(x) \equiv \langle \Psi | x \rangle. \quad (1.21)$$

1.3.2 Heisenberg's matrix formulation

The state vector $|\Psi\rangle$ is represented as a vector by its projection on a complete set of basis states $|E_1\rangle, |E_2\rangle, \dots$:

$$|\Psi\rangle \equiv \begin{pmatrix} \langle E_1 | \Psi \rangle \\ \langle E_2 | \Psi \rangle \\ \dots \\ \dots \end{pmatrix}. \quad (1.22)$$

Similarly we represent the operators by:

$$\hat{H} \equiv \begin{pmatrix} \langle E_1 | \hat{H} | E_1 \rangle & \langle E_1 | \hat{H} | E_2 \rangle & \langle E_1 | \hat{H} | E_3 \rangle & \dots \\ \langle E_2 | \hat{H} | E_1 \rangle & \langle E_2 | \hat{H} | E_2 \rangle & \dots & \dots \\ \dots & \dots & \dots & \dots \end{pmatrix} \quad (1.23)$$

Since the basis states $|E_n\rangle$ are the eigenstates of \hat{H} , its matrix representation is diagonal, and the diagonal elements are eigenvalues of \hat{H} . To diagonalize an operator in matrix representation is therefore the same as solving the time-independent Schrödinger equation.

1.4 Angular Momentum and Spin

In classical physics angular momentum is defined as:

$$\mathbf{L} = \mathbf{r} \times \mathbf{p}. \quad (1.24)$$

\mathbf{r} is the displacement vector from the origin and \mathbf{p} is the linear momentum. We can write out the components of the angular momentum operator in quantum mechanics by using the substitution

$$p_x \rightarrow -i\hbar \frac{\partial}{\partial x}$$

Goldsmith and Uhlenbeck (in 1925) introduced the concept of internal, purely quantum mechanical, angular momentum called *spin*. This was later experimentally confirmed by the Stern-Gerlach experiment (1922).

The spin eigenstates are:

$$\hat{S}_z |l, m\rangle = m\hbar |l, m\rangle. \quad (1.25)$$

$$\hat{S}^2 |l, m\rangle = l(l+1)\hbar^2 |l, m\rangle. \quad (1.26)$$

And their commutation relation reads

$$[\hat{S}_x, \hat{S}_y] = i\hbar \hat{S}_z \quad [\hat{S}_y, \hat{S}_z] = i\hbar \hat{S}_x \quad [\hat{S}_z, \hat{S}_x] = i\hbar \hat{S}_y. \quad (1.27)$$

This basically means that we cannot determine eigenvalues of two different components, for example \hat{S}_z and \hat{S}_x simultaneously. They are *incompatible* observables. But we can determine one of the directions and \hat{S}^2 . The spin quantum numbers are [24]

$$s = 0, \frac{1}{2}, 1, \frac{3}{2}, \dots \quad (1.28)$$

$$m_s = -s, -s + 1, \dots, s - 1, s \quad (1.29)$$

Where s is defined as the *spin* of the particle. Electrons have a spinvalue of $1/2$ spin while the photons have a spinvalue of 1.

1.4.1 The wavefunction

The total wavefunction of a state vector mentioned in Postulate 1 are composed of a spatial part $\phi(x, y, z)$ and a spin part $|\chi\rangle$. They are from different Hilbert spaces and mathematically the state vector is a tensor product of these two.

$$|\psi\rangle \equiv \psi(r) \equiv \phi(x, y, z) \otimes |\chi\rangle. \quad (1.30)$$

1.5 Simple systems

1.5.1 Particle in a Infinite Potential Well

One of the simplest single-particle systems we could solve exactly the infinite one-dimensional potential well, defined by:

$$V(x) = \begin{cases} -x & \text{if } 0 \leq x \leq a \\ \infty, & \text{otherwise} \end{cases} \quad (1.31)$$

and we want to solve the Schrödinger equation with respect to this potential,

$$-\frac{\hbar^2}{2m} \frac{d^2\psi}{dx^2} + V(x) = E\psi. \quad (1.32)$$

We can rewrite this equation as

$$\frac{d^2\psi}{dx^2} = \frac{2m}{\hbar^2} [V(x) - E] \psi. \quad (1.33)$$

For the case $x > a$ and $x < 0$ where $E < V(x)$, we see that the second derivate always has the same sign and therefore cannot be normalized (ref postulate). Such wavefunctions cannot exist in this range. Therefore the wavefunctions only exist in the range $0 \leq x \leq a$ and the continuity of ψ requires the boundary conditions $\psi(0) = 0$ and $\psi(L) = 0$.

Using standard methods of solving second order differential equations (see [7] for details), we get

$$\psi(x) = A \sin kx, \quad (1.34)$$

$$k \equiv \frac{\sqrt{2mE}}{\hbar}, \quad (1.35)$$

normalizing in order to get the constant A :

$$\int_0^a |A|^2 \sin^2 kx \, dx = |A|^2 \frac{a}{2} = 1 \Rightarrow |A|^2 = \frac{2}{a}, \quad (1.36)$$

We then choose to use the positive root

$$\psi(x) = \sqrt{\frac{2}{a}} \sin kx, \quad (1.37)$$

Next we want to determine the constant k . From the boundary condition we know that $\sin ka = 0$. This means that the possible values for k are

$$k = \frac{n\pi}{a}, \quad \text{with } n = 1, 2, 3, \dots \quad (1.38)$$

and hence the possible values of E from Eq. (1.35) are discrete:

$$E_n = \frac{\hbar^2 k^2}{2m} = \frac{n^2 \pi^2 \hbar^2}{2ma^2}. \quad (1.39)$$

1.5.2 Particle in a Harmonic Oscillator Potential Well

The next simplest problem to solve is the *harmonic oscillator* in one-dimensional case. The Hamiltonian we have is

$$\hat{H} = \frac{\hat{p}^2}{2m} + \frac{1}{2}\omega\hat{x}^2, \quad (1.40)$$

where $\hat{x} = x$ is the position operator and the \hat{p} is the momentum operator, given by

$$\hat{p} = -i\hbar \frac{d}{dx}. \quad (1.41)$$

There are two main approaches to solve this. One of them is the analytical approach [24], in which we get the solutions in Schrödinger representation,

$$\psi_n(x) = \sqrt{\frac{1}{2^n n!}} \left(\frac{m\omega}{\pi\hbar} \right)^{1/4} e^{-\beta^2/2} H_n(\beta), \quad \beta = \sqrt{\frac{m\omega}{\hbar}} x \quad (1.42)$$

And the eigenvalues,

$$E_n = \left(n + \frac{1}{2} \right) \hbar\omega, \quad n = 0, 1, 2, 3, \dots \quad (1.43)$$

The other way is algebraically [24], with which we get solutions in Dirac formalism:

$$|\psi_n\rangle = \frac{1}{\sqrt{n!}} (a_+)^n |0\rangle, \quad (1.44)$$

where $|0\rangle$ is our ground state and $a_+ = (a_-)^\dagger$ is the creation operator

$$a_\pm = \frac{1}{\sqrt{2\hbar m\omega}} (\mp i\hat{p} + m\omega\hat{x}). \quad (1.45)$$

Chapter 2

The Quantum Mechanics behind Quantum Dots

In this chapter we will give a quantum mechanical description for the two-dimensional quantum dot. We will start by solving the Schrödinger equation for a single-electron parabolic quantum dot with an applied magnetic field.

Recent developments in techniques of quantum dot growth have made it possible to create better solar cells, as well as other exotic phenomena such as quantum computing. Quantum dot is a semiconductor on the nanoscale. It can trap one or several electrons in a spatially confined potential. The size of quantum dot ranges from a few hundreds to many thousand atoms [66]. And it can confine everything from one electron to hundreds.

2.1 Description of the Quantum Dot

As we have seen in the chapter 1, quantum dots are artificially created. And there are various techniques and methods for creating quantum dots, which give them different properties. In this thesis we will concentrate on the quantum dots created inside the Gallium Arsenide (GaAs) semiconductors. The semiconductor is sandwiched between layers of Aluminum Gallium Arsenide (AlGaAs) semiconductor material which has a bigger bandgap. This acts like an insulator and results in a confinement in the vertical direction. Our choice for the confinement potential is a parabolic harmonic oscillator $\omega_x = \omega_y = \omega$. Both numerical [40, 51] and experimental [36, 26] studies have shown that this is a reasonable approximation. And in our case the electrons inside will only feel the Coulomb interaction. The Hamiltonian then becomes

$$\hat{H} = \sum_{i=1}^N \left(-\frac{\hbar^2}{2m^*} \nabla_i^2 + \frac{1}{2} m^* \omega^2 r_i^2 \right) + \frac{e^2}{4\pi\epsilon_0\epsilon_r} \sum_{i<j}^N \frac{1}{r_{ij}}. \quad (2.1)$$

The e is the electron charge, ϵ_0 is the vacuum permittivity, ϵ_r is the relative permittivity, and $r_{ij} = |r_i - r_j|$, ω is the oscillator frequency, and r_i is the distance from electron i to the potential minimum ($r = 0$). It is important to notice that the m^* here is the effective electron mass and not to be mistaken for the Newtonian reduced mass which is a classical phenomena. This is a simplification we have made to our problem. The effective electron mass differs from the free-electron mass m and is isotropic and independent of both the position and the energy of the electron. The effective mass is the result of the motion of an electron in a periodic potential [69]. For example in GaAs the electrons appear to carry mass that is only 7% of the free-electron mass [3].

2.2 The One-electron Quantum Dot

We start by deriving the wavefunctions for a general spherical symmetric potential $V(r) = V(-r)$ in two dimensions. Our Hamiltonian in Cartesian coordinates reads

$$-\frac{\hbar^2}{2m^*}\nabla^2\psi(x,y) + V(x,y)\psi(x,y) = E\psi(x,y). \quad (2.2)$$

We want to rewrite this using polar coordinates

$$x = r \cos \theta, \quad (2.3)$$

$$y = r \sin \theta, \quad (2.4)$$

$$r = \sqrt{x^2 + y^2}. \quad (2.5)$$

The Laplacian then becomes

$$\nabla^2 = \frac{1}{r} \frac{\partial}{\partial r} \left(r \frac{\partial}{\partial r} \right) + \frac{1}{r^2} \frac{\partial^2}{\partial \theta^2}. \quad (2.6)$$

Inserting this into Eq. (2.2) gives us the Schrödinger equation in polar coordinates

$$-\frac{\hbar^2}{2m^*} \left(\frac{\partial^2}{\partial r^2} + \frac{1}{r} \frac{\partial}{\partial r} + \frac{1}{r^2} \frac{\partial^2}{\partial \theta^2} \right) \psi(r, \theta) + V(r)\psi(r, \theta) = E\psi(r, \theta). \quad (2.7)$$

Introducing a solution on the form $\psi(r, \theta) = R(r)Y(\theta)$ and multiplying by $\frac{2m^*}{\hbar^2 R(r)Y(\theta)}r^2$ in Eq. (2.7), we get

$$\frac{r^2}{R(r)} \left[\frac{d^2 R}{dr^2} + \frac{1}{r} \frac{dR}{dr} + \frac{2m^*}{\hbar^2} (E - V(r))R(r) \right] = -\frac{1}{Y(\theta)} \frac{\partial^2 Y(\theta)}{\partial \theta^2}, \quad (2.8)$$

the left side of this equation depends on r while the right side depends on θ . This can only be satisfied if each term is equal to a constant $k = m^2$

$$\frac{r^2}{R(r)} \left[\frac{d^2 R}{dr^2} + \frac{1}{r} \frac{dR}{dr} + \frac{2m^*}{\hbar^2} (E - V(r))R(r) \right] = -m^2 \quad (2.9)$$

$$\frac{1}{Y(\theta)} \frac{\partial^2 Y(\theta)}{\partial \theta^2} = m^2. \quad (2.10)$$

The solution to the angular part Eq. (2.10) is

$$Y(\theta) = Ce^{im\theta}. \quad (2.11)$$

Normalization gives us the constant C

$$C^2 = \frac{1}{\int_0^{2\pi} Y(\theta)^2 d\theta} = \frac{1}{2\pi}. \quad (2.12)$$

The normalized solution for the angular part is

$$Y(\theta) = \frac{1}{\sqrt{2\pi}} e^{im\theta}. \quad (2.13)$$

The total wavefunction must satisfy the physical condition that $\psi(r, \theta) = \psi(r, \theta + 2\pi)$. This makes a restriction on the quantum number m which can take integral values

$$m = 0, \pm 1, \pm 2, \dots \quad (2.14)$$

For the Eq. (2.9) we can simplify by defining

$$u(r) = \sqrt{r}R(r) \Rightarrow R(r) = \frac{u(r)}{\sqrt{r}}, \quad (2.15)$$

which yields

$$-\frac{\hbar}{2m^*} \frac{d^2 u}{Dr^2} + \left[V(r) + \frac{\hbar^2}{2m^*} \frac{m^2 - \frac{1}{4}}{r^2} \right] u(r) = Eu(r). \quad (2.16)$$

This is the radial equation. It has the same form as the one-dimensional time-independent Schrödinger equation with an effective potential

$$V_{eff} = V(r) + \frac{\hbar^2}{2m^*} \frac{m^2 - \frac{1}{4}}{r^2}. \quad (2.17)$$

The radial function Eq. (2.15) must satisfy the normalization conditions

$$\int_0^\infty |u(r)|^2 Dr = 1. \quad (2.18)$$

For this to be normalizable we require the boundary conditions

$$u(0) = C \text{ and } u(\infty) = 0, \quad \text{where } C \text{ is a constant.} \quad (2.19)$$

Finally the general solutions to the spherical symmetrical potential is

$$\psi(r, \theta) = R(r) \frac{1}{\sqrt{2\pi}} e^{im\theta}. \quad (2.20)$$

2.2.1 Parabolic Quantum Dot with Influence of an Electromagnetic Field

As an academic exercise we shall solve the one-electron Schrödinger equation for a two dimensional quantum dot. Most of the derivation here is taken from [31]. The classical Hamiltonian of a charged electron in an electromagnetic field reads

$$H = \frac{1}{2m} (\mathbf{p} - e \mathbf{A})^2 + e\phi, \quad (2.21)$$

with \mathbf{A} and ϕ as the electromagnetic vector and scalar potentials, m is the electron mass, e is the charge, and \mathbf{p} is the momentum vector. The electromagnetic fields are related to the potentials

$$\mathbf{E} = -\frac{1}{c} \frac{\partial \mathbf{A}}{\partial t} - \nabla \phi, \quad (2.22)$$

$$\mathbf{B} = \nabla \times \mathbf{A}, \quad (2.23)$$

where \mathbf{E} is electric field, and \mathbf{B} is the magnetic field, which satisfies Maxwells equations. The quantum mechanical Hamiltonian consists of and additional term which couples the spin to the electromagnetic field $-\mu \cdot \mathbf{B}$, where μ is the magnetic moment of the electron.

$$\hat{H} = \frac{1}{2m^*} (\hat{p} - e \mathbf{A})^2 + e\phi + \frac{1}{2} m^* \omega_0^2 r^2 - \hat{\mu} \cdot \mathbf{B}. \quad (2.24)$$

Here the \hat{p} is a quantum mechanical momentum operator. The time-independent Schrödinger we want to solve is

$$\frac{1}{2m^*} (\hat{p} - e \mathbf{A})^2 + e\phi + \frac{1}{2} m^* \omega_0^2 r^2 - \hat{\mu} \cdot \mathbf{B} \psi(\mathbf{r}) = E \psi(\mathbf{r}), \quad (2.25)$$

$$H_r = \frac{1}{2m^*}(\hat{p} - e\mathbf{A})^2 + \frac{1}{2}m^*\omega_0^2 r^2, \quad (2.26)$$

$$H_s = -\hat{\mu} \cdot \mathbf{B}. \quad (2.27)$$

where the wavefunction $\psi(\mathbf{r})$ also include the spin part which is decoupled with the spatial part, i.e. their expectation are uncorrelated, and we can therefore write the wavefunction as a product of each.

$$\psi(\mathbf{r}) = R(r) \otimes |m_s\rangle. \quad (2.28)$$

Here the quantum number is $m_s = \pm\frac{1}{2}$, since electrons are fermions. Inserting this into Eqs. (2.26) and (2.27) we obtain two equations, one spatial and one spin dependent

$$\left(\frac{1}{2m^*}(\hat{p} - e\mathbf{A})^2 + e\phi + \frac{1}{2}m^*\omega_0^2 r^2 \right) R(r) = E_r R(r), \quad (2.29)$$

$$-(\mu \cdot \mathbf{B})|m_s\rangle = E_s|m_s\rangle. \quad (2.30)$$

Which gives us the total energy

$$E = E_r + E_s + e\phi. \quad (2.31)$$

We want to do a gauge transformation on the potential \mathbf{A} with the Coulomb gauge condition. This will not change the potentials \mathbf{E} and \mathbf{B} .

$$\nabla \cdot \mathbf{A} = 0. \quad (2.32)$$

A choice that satisfies this condition is

$$\mathbf{A} = \frac{1}{2}\mathbf{B} \times (x\mathbf{i} + y\mathbf{j}). \quad (2.33)$$

We want to expand the first term in the spatial Hamiltonian \hat{H}_r Eq. (2.26) using the condition Eq. (2.33)

$$(\hat{p}^2 - e\mathbf{A})^2 = \hat{p}^2 - e(\hat{p}\mathbf{A} + \mathbf{A}\hat{p}) + e^2\mathbf{A}, \quad (2.34)$$

$$= \hat{p}^2 - 2e\mathbf{A} \cdot \hat{p} + e^2\mathbf{A}^2, \quad (2.35)$$

$$= \hat{p}^2 - e\mathbf{B} \cdot \hat{L} + \frac{e^2}{4}(\mathbf{B} \times (x\mathbf{i} + y\mathbf{j}))^2, \quad (2.36)$$

In Eq. (2.35) we have used that \hat{p} and \mathbf{A} commute because of the Coulomb gauge.

$$\hat{p} \cdot \mathbf{A}\psi = -i\hbar\nabla \cdot (\mathbf{A}\psi) = -i\hbar \left(\underbrace{\nabla \cdot \mathbf{A}}_{=0} + \mathbf{A} \cdot \nabla \psi \right) = \mathbf{A} \cdot (-i\hbar\nabla\psi) = \mathbf{A} \cdot \hat{p}\psi \quad (2.37)$$

And in Eq. (2.36) we have used the relation

$$(\mathbf{B} \times \mathbf{r}) \cdot \mathbf{p} = \mathbf{B} \cdot (\mathbf{r} \times \mathbf{p}) = \mathbf{B} \cdot \mathbf{L}. \quad (2.38)$$

The applied magnetic field is constant and homogeneous along the z-axis. $\mathbf{B} = B_0\mathbf{k}$. Then our spatial Hamiltonian \hat{H}_r simplifies to

$$\hat{H}_r = \frac{1}{2m^*} \left[\hat{p}^2 - eB_0(x\hat{p}_y - y\hat{p}_x) + \frac{e^2 B_0^2}{4}(x^2 + y^2) \right] + \frac{1}{2}m^*\omega_0^2(x^2 + y^2). \quad (2.39)$$

Introducing

$$\omega_B \equiv \frac{eB_0}{2m^*}, \quad (2.40)$$

and

$$\omega \equiv \omega_0 + \omega_B^2, \quad (2.41)$$

the Hamiltonian becomes

$$\hat{H}_r = \frac{1}{2m^*} \left(\hat{p}^2 - eB_0 \hat{L}_z \right) + \frac{1}{2} m^* \omega^2 (x^2 + y^2). \quad (2.42)$$

Where \hat{L}_z is the angular momentum in the z -direction. $L_z = x\hat{p}_y - y\hat{p}_x$ [28]. The next step is to transform the Hamiltonian Eq. (2.42) from a Cartesian coordinate representation to a polar coordinate representation. Then the angular momentum can be expressed as [28]

$$\hat{L}_z = -i\hbar \frac{\partial}{\partial \theta}, \quad (2.43)$$

which yields the time-independent Schrödinger equation for \hat{H}_r Eq. (2.26)

$$\left[-\frac{\hbar^2}{2m^*} \left(\frac{\partial^2}{\partial r^2} + \frac{1}{r} \frac{\partial}{\partial r} + \frac{1}{r^2} \frac{\partial^2}{\partial \theta^2} - \frac{ieB_0}{\hbar} \frac{\partial}{\partial \theta} \right) + \frac{1}{2} m^* \omega^2 r^2 \right] \psi(r, \theta) = E \psi(r, \theta). \quad (2.44)$$

This is almost the same as Eq. (2.7) which we have solved, except we now have an additional term $\frac{ieB_0}{\hbar} \frac{\partial}{\partial \theta}$ caused by the magnetic field. But this can be separated from the radial equation, since it only depends on the angle θ . The wavefunction can still be separated in an angular and a radial part, and we will use the same ansatz as Eq. (2.20)

$$\psi(r, \theta) = R(r) \frac{1}{\sqrt{2\pi}} e^{im\theta}, \quad m = 0, \pm 1, \pm 2, \dots \quad (2.45)$$

Inserting this into Eq. (2.7)

$$\left[-\frac{\hbar^2}{2m^*} \left(\frac{\partial^2}{\partial r^2} + \frac{1}{r} \frac{\partial}{\partial r} + \frac{1}{r^2} \frac{\partial^2}{\partial \theta^2} + \frac{meB_0}{\hbar} \frac{\partial}{\partial \theta} \right) + \frac{1}{2} m^* \omega^2 r^2 \right] R(r) = E_r R(r), \quad (2.46)$$

the solution of this radial equation is

$$R_{nm}(r) = \sqrt{\frac{2n!}{(n+|m|)!}} \beta^{\frac{1}{2}(|m|+1)} r^{|m|} e^{-\frac{1}{2}\beta r^2} L_n^{|m|}(\beta r^2). \quad (2.47)$$

Here the subscript n denotes the principal quantum number, and m is the angular momentum number

$$n = 0, 1, 2, 3, \dots \quad (2.48)$$

$$m = 0, \pm 1, \pm 2, \pm 3, \dots \quad (2.49)$$

$L_n^{|m|}$ is the associated Laguerre polynomials [2], and β is defined as

$$\beta = \frac{m^* \omega}{\hbar}. \quad (2.50)$$

The final eigenfunction to the spatial Hamiltonian H_r is then

$$\psi(r, \theta) = \sqrt{\frac{n!}{\pi(n+|m|)!}} \beta^{\frac{1}{2}(|m|+1)} r^{|m|} e^{-\frac{1}{2}\beta r^2} L_n^{|m|}(\beta r^2) e^{im\theta}, \quad (2.51)$$

with the corresponding eigenvalues

$$E_r = (1 + |m| + 2n)\hbar\omega + m\hbar\omega_B. \quad (2.52)$$

See Appendix in [47] and [19] for details.

Now we will consider the spin Hamiltonian H_s Eq. (2.27). The quantum mechanical magnetic moment \widehat{mu} is given by [24]

$$\widehat{\mu} = \frac{eg}{2m^*} \widehat{S}. \quad (2.53)$$

where g is the g -factor and approximate 2 for the electron. \widehat{S} is the spin operator. Since the magnetic field is $\mathbf{B} = B_0 \mathbf{k}$, the Schrödinger equation reads

$$-\frac{egB_0}{2m^*} S_z |m_s\rangle = E_s |m_s\rangle. \quad (2.54)$$

\widehat{S}_z is the z -component of the total spin \widehat{S} . The eigenvectors and eigenvalues of this operator are given by [28]

$$E_s = -\frac{eg\hbar B_0}{2m^*} m_s = gm_s \hbar \omega_B. \quad (2.55)$$

The total eigenvalue for the system becomes

$$E = (1 + |m| + 2n)\hbar\omega + m\hbar\omega_B + gm_s \hbar \omega_B + e\phi, \quad (2.56)$$

and the corresponding eigenstate

$$\psi_{nmm_s}(\mathbf{r}, \theta) = \sqrt{\frac{n!}{\pi(n + |m|)!}} \beta^{\frac{1}{2}(|m|+1)} r^{|m|} e^{-\frac{1}{2}\beta r^2} L_n^{|m|}(\beta r^2) e^{im\phi} \otimes |m_s\rangle. \quad (2.57)$$

Without any external magnetic field $\mathbf{B} = 0$, the energy becomes spin-independent because $\omega_B = 0$

$$E_{nm}^0 = (1 + |m| + 2n)\hbar\omega_0 \quad (2.58)$$

In the spirit of perturbation theory we denote this with a superscript 0. We will have a degeneracy in spin since the Hamiltonian is spin-independent. For each pair of the quantum numbers $\{n, m\}$ we have two different quantum states, one with $m_s = -\frac{1}{2}$ and the other with $m_s = \frac{1}{2}$.

$$R \equiv (1 + |m| + 2n). \quad (2.59)$$

R is defined as the *shellnumber*, it corresponds to the energy level and the degeneracy for each level R is

$$g(R) = 2R. \quad (2.60)$$

This system has a *shell structure*, Figure 2.1, i.e. the energy levels are equidistant from each other and we have a defined degeneracy. This is similar to the shell model in nuclear physics, for which Goeppert-Mayer, Wiger and Jensen was awarded the Nobel Prize in Physics (1963). The total number of spin-orbitals for a given shellnumber R is

$$N = \sum_{R=0}^{R'} g(R) = 2R' + 2(R' - 1) + 2(R' - 3) + \dots + 2. \quad (2.61)$$

We have tabulated some of the values in Table 2.1

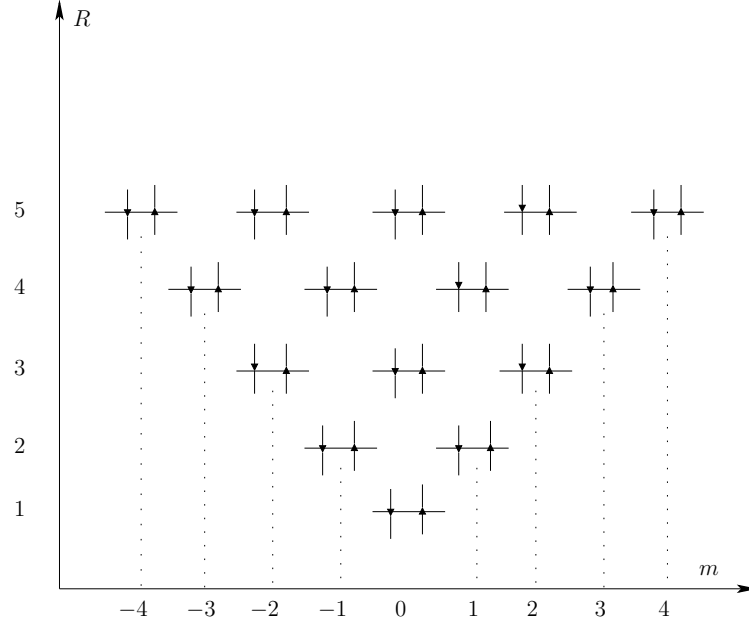


Figure 2.1: Shell structure of a single-electron parabolic quantum dot for $\mathbf{B} = \mathbf{0}$, where R is the shell number defined in Eq. (2.59) and m is the angular quantum number. The arrows $\uparrow\downarrow$ denote the spin quantum number $m_s = \pm\frac{1}{2}$

R	$g(R)$	N
1	2	2
2	4	6
4	8	20
8	16	72
10	20	110
15	30	240
20	40	420

Table 2.1: This table shows some values for different shellnumbers R , where $g(R)$ is the degeneracy. N is the total number of single-electron spin-orbitals occupied in R -number of shells. This is often referred to as *magic numbers* which indicate the number of spin-orbitals needed to complete the shells.

If we take a look at Eq. (2.56), we see that in the presence of a magnetic field, the degenerate energy levels would split because of the sign of m . If we simplify by neglecting the spin quantum number $m_s = 0$, and setting the constant $e\phi = 0$, we can express the energy in Eq. (2.56) by

$$\frac{E_{nm}}{\hbar\omega_0} = (1 + |m| + 2n) \sqrt{1 + \frac{\omega_B^2}{\omega_0^2}} + m \frac{\omega_B}{\omega_0}. \quad (2.62)$$

If we plot $\frac{E_{nm}}{\hbar\omega_0}$ as a function of $\frac{\omega_B}{\omega_0}$ we get the Fock-Darwin energy spectrum, which was first solved by V.Fock [21] and later by C.G. Darwin [14].

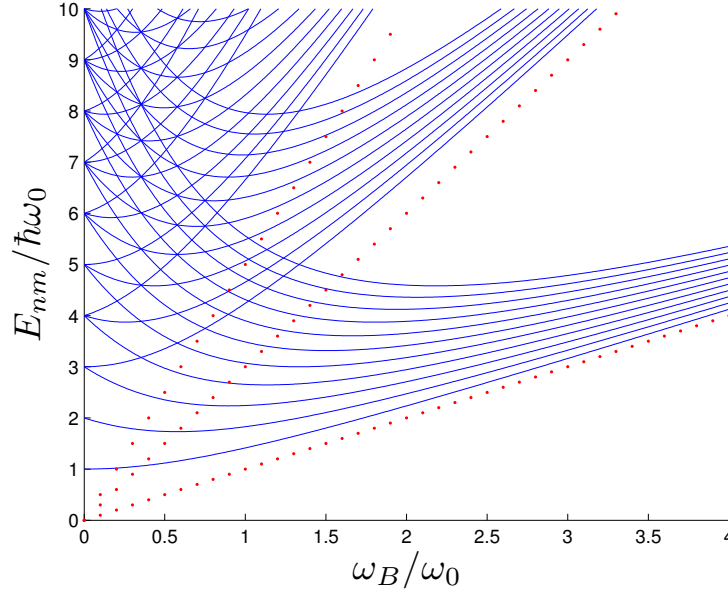


Figure 2.2: This is the Fock-Darwin energy spectrum for a single-electron quantum dot. When $\omega_B = 0$, all the quantum states with equal R are degenerate, after ω_B increases the levels begin to split due to the angular momentum contribution from $m\hbar\omega_B$. The degeneracy can reappear for certain levels and certain ω_B 's. The energy levels will shift back and forth between (n, m) pairs, but they all appear to reach an asymptote in the high field limit, forming the famous Landau levels [60], indicated by the red line. The landau levels are plotted for $N_L = 0, 1, 2$ in Eq. (2.64)

The energy of the different states will then decrease or increase with stronger magnetic field ω_B , depending on m . States that belong to different shells for $\mathbf{B} = 0$ will become degenerate, and when the magnetic field increases even more, we would reach an asymptote for the energies, as we clearly see in Figure 2.62. These energy levels are popularly called Landau levels, which Landau discovered in 1930 at an age of 22 [48].

We are interested in the energy levels when $\omega_B \rightarrow \infty$ for the lowest energy levels $m < 0$

$$\lim_{\omega_B \rightarrow \infty} E_{nm} = (1 + 2n)\hbar\omega_B. \quad (2.63)$$

The Landau levels appear when $N_L \equiv n = 0, 1, 2, 3, \dots$. And the energy only depends on n in the high limit of \mathbf{B}

$$E_L \approx (1 + 2N_L)\hbar\omega_B. \quad (2.64)$$

2.2.2 Scaling the Hamiltonian

When we do computations it is a good thing to have dimensionless parameters. The fewer things that can go wrong in the calculation the better. Therefore we want to rescale our many-body Hamiltonian Eq. (2.1) so that its dimensionless. The following derivation is based on examples [29, 47]

$$\omega = \omega_c \bar{\omega}, \quad (2.65)$$

$$\mathbf{r} = r_c \bar{\mathbf{r}}, \quad (2.66)$$

$$\nabla = \frac{1}{r_c} \bar{\nabla}, \quad (2.67)$$

$$r_i^2 = r_c^2 \bar{r}_i^2, \quad (2.68)$$

$$r_{ij} = r_c \bar{r}_{ij}. \quad (2.69)$$

Here the variables with the subscript c is just a constant with the same dimensions as the variable we want to rescale. The variables with a bar is the dimensionless variables that we want. Inserting these into our Hamiltonian Eq. (2.1) gives

$$\hat{H} = -\frac{\hbar^2}{2m^* r_c^2} \sum_{i=1}^N \bar{\nabla}_i^2 + \frac{1}{2} m^* \omega_c^2 \bar{\omega}^2 r_c^2 \sum_{i=1}^N \bar{r}_i^2 + \frac{\hbar}{\epsilon r_c} \sum_{i<j}^N \frac{1}{\bar{r}_{ij}}, \quad (2.70)$$

where

$$\epsilon = \frac{4\pi\epsilon_0\epsilon_r}{e^2}. \quad (2.71)$$

Furthermore we define the oscillator length to be

$$r_c = \sqrt{\frac{\hbar}{m^* \omega}} \quad (2.72)$$

Inserting this into our Hamiltonian Eq. (2.70)

$$\hat{H} = -\frac{\omega_c \bar{\omega} \hbar}{2} \sum_{i=1}^N \bar{\nabla}_i^2 + \frac{\hbar}{2} \omega_c \bar{\omega} \sum_{i=1}^N \bar{r}_i^2 + \frac{\hbar}{\epsilon} \sqrt{\frac{m^* \omega_c \bar{\omega}}{\hbar}} \sum_{i<j}^N \frac{1}{\bar{r}_{ij}}. \quad (2.73)$$

We want to scale the Hamiltonian as well, so that it has units of the Hartree energy E_h [53]

$$\bar{H} = \hat{H} / E_h. \quad (2.74)$$

where the Hartree energy is defined as

$$E_h = m^* \left(\frac{e^2}{4\pi\epsilon_0\epsilon_r \hbar} \right)^2 = \frac{m^*}{\epsilon^2}. \quad (2.75)$$

The scaled Hamiltonian becomes

$$\bar{H} = -\frac{\omega_c \bar{\omega} \hbar \epsilon^2}{2m^*} \sum_{i=1}^N \bar{\nabla}_i^2 + \frac{\hbar \epsilon^2}{2m^*} \omega_c \bar{\omega} \sum_{i=1}^N \bar{r}_i^2 + \frac{\hbar \epsilon}{m^*} \sqrt{\frac{m^* \omega_c \bar{\omega}}{\hbar}} \sum_{i<j}^N \frac{1}{\bar{r}_{ij}}. \quad (2.76)$$

To make it dimensionless we have to define

$$\omega_c = \frac{m^*}{\hbar \epsilon}, \quad (2.77)$$

which is fine since ω_c has the dimension of $[1/s]$ which is the same as ω . Our final dimensionless N-electron scaled Hamiltonian reads

$$\bar{H} = -\frac{\omega_c}{2} \sum_{i=1}^N \bar{\nabla}_i^2 + \frac{1}{2} \omega_c \sum_{i=1}^N \bar{r}_i^2 + \sqrt{\omega_c} \sum_{i<j}^N \frac{1}{\bar{r}_{ij}}. \quad (2.78)$$

2.3 Double Quantum Dots

The rapid development of nanotechnology has made the quantum computer a more realistic achievement. One of the possible candidates to the quantum bit is a double quantum dot. Experiments of this have been done both with a trapped nucleus [59] and electrons [58]. We will investigate a model based on [64]. Our one-electron Hamiltonian is the same as before but now with a change in the potential

$$\hat{H} = -\frac{\hbar^2}{2m^*} \nabla_i^2 + V_c(x, y), \quad (2.79)$$

where the confinement potential is

$$V_c(x, y) = \frac{1}{2} m^* \omega_0^2 \cdot [x^2 + y^2 - 2L_x|x| + L_x^2]. \quad (2.80)$$

From [64] we use GaAs material parameters $m^* = 0.067m_e$, and the confinement strength $\hbar\omega_0 = 3.0$ meV. Which correspond to a harmonic oscillator length of $\sqrt{\hbar/\omega_0 m^*} \approx 5.3$ nm. And with the minima separated by a distance of $2L_x$ from each other. The values of $V_c(x, 0)$ are plotted in Fig. 2.3.

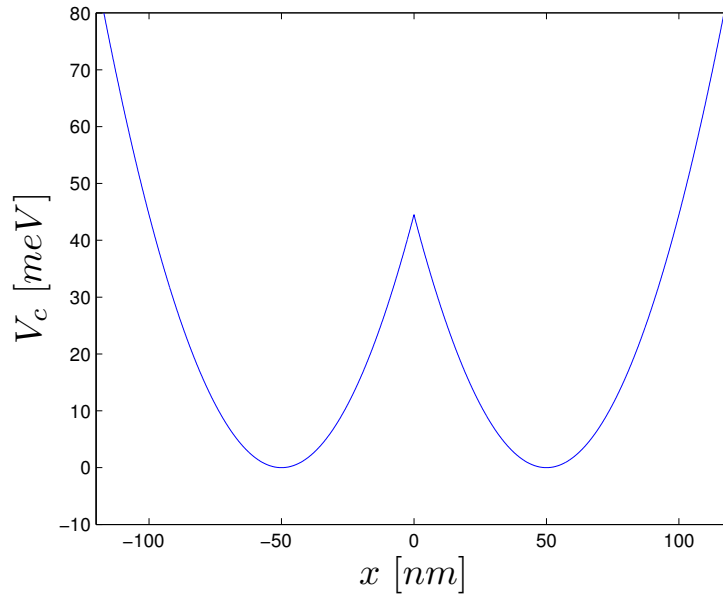


Figure 2.3: Confinement potential for $V_c(x, 0)$ and $L_x = 50$ nm.

We will then solve the two-dimensional Schrödinger equation by using a finite difference method with a three-point Laplacian [32]. This will give us a Hermitian matrix for which the eigenvalues and eigenvectors can be solved using the QR-algorithm [20]. This algorithm was independently introduced in 1960s by Kublanovskaya [38] and Francis [22]. And have been recognized as one the most important algorithms of the 21st century [18].

2.3.1 The QR-Algorithm

The idea is surprisingly simple. First step is to factor the matrix A into a product of an orthogonal matrix Q_1 and positive upper triangular matrix R_1 . This also referred to as an

QR-decomposition and solved by using the Gram-Schmidt algorithm [44].

$$A_1 = Q_1 R_1, \quad (2.81)$$

next step is to multiply Q and R in a reversed order

$$A_2 = R_1 Q_1, \quad (2.82)$$

we repeat this process by finding the Q and R values to A_2

$$A_2 = Q_2 Q_2. \quad (2.83)$$

The complete algorithm can be written as

$$A = Q_1 R_1, \quad R_k Q_k = A_{k+1} = Q_{k+1} R_{k+1}, \quad k = 1, 2, 3, \dots \quad (2.84)$$

Where R_k, Q_k is from the previous steps, and Q_{k+1} is still an orthogonal matrix ($Q^T Q = 1$) and R_{k+1} is a positive upper triangular. The iteration will finally create a matrix \tilde{A} whose diagonal

Algorithm 1 *QR-Algorithm*

```

for  $i = 1 \rightarrow n$  do
     $Q_i R_i = A_i$ 
     $A_{i+1} = R_i Q_i$ 
end for
    
```

entries are eigenvalues of A . The reason why this works is because all the A_k are similar to each other and therefore they have a common set of eigenvalues with different eigenvectors, i.e.

Proof. **If** $Ax = \lambda x$ **and** $\tilde{A} = S^T A S$ ($S S^T = 1$) $\Rightarrow S^T A S x = \lambda x \Rightarrow A(Sx) = \lambda(Sx)$ \square

And

$$A_{k+1} = R_k Q_k = Q_k^T (Q_k R_k) Q_k = Q_k^T A_k Q_k. \quad (2.85)$$

We will not go in to rigorous details for why this works, but readers are recommended to read [10]. Instead we will give an numerical example. Given a Hermitian matrix

$$A = \begin{bmatrix} 5 & 4 & 1 \\ 4 & 3 & 2 \\ 1 & 2 & 1 \end{bmatrix}, \quad (2.86)$$

the *exact* eigenvalues found by `eig(A)` in MATLAB are

$$\begin{aligned} \lambda_1 &= 8.6625 \\ \lambda_2 &= 1.1444 \\ \lambda_3 &= -0.8070 \end{aligned} \quad (2.87)$$

Then the initial QR-factorization $A_1 = Q_1 R_1$ produces

$$Q_1 = \begin{bmatrix} 0.7715 & -0.0392 & -0.6350 \\ 0.6172 & -0.1960 & 0.7620 \\ 0.1543 & 0.9798 & 0.1270 \end{bmatrix} \quad R_1 = \begin{bmatrix} 6.4807 & 5.2463 & 2.1602 \\ 0 & 1.2150 & 0.5487 \\ 0 & 0 & 1.0160 \end{bmatrix}, \quad (2.88)$$

which in turn gives us the new A_2

$$A_2 = R_1 Q_1 = \begin{bmatrix} 8.5714 & 0.8346 & 0.1568 \\ 0.8346 & 0.2995 & 0.9955 \\ 0.1568 & 0.9955 & 0.1290 \end{bmatrix}. \quad (2.89)$$

We continue this procedure

$$A_3 = R_2 Q_2 = \begin{bmatrix} 8.6611 & 0.1033 & 0.0168 \\ 0.1033 & 0.5392 & 0.9035 \\ 0.0168 & 0.9035 & -0.2003 \end{bmatrix}, \quad (2.90)$$

$$A_4 = R_3 Q_3 = \begin{bmatrix} 8.6625 & 0.0131 & 0.0017 \\ 0.0131 & 0.7871 & 0.7548 \\ 0.0017 & 0.7548 & -0.4496 \end{bmatrix}. \quad (2.91)$$

After 17 iterations the off-diagonal elements are practically zero, and the eigenvalues on the diagonal correspond to the eigenvalues found in Eq. (2.87).

$$A_{17} = R_{16} Q_{16} = \begin{bmatrix} 8.6625 & 0.0000 & -0.0000 \\ 0.0000 & 1.1444 & 0.0098 \\ 0.0000 & 0.0098 & -0.8069 \end{bmatrix}. \quad (2.92)$$

But if we want to increase the precision, this method becomes rather slow. As we can see, the convergence of this method is not that impressive, assuming MATLAB is using the Householder's QR factorization method [23], we are going to have $O(n^3)$ flops per iteration, in addition we have a matrix-matrix multiplication.

One of the optimization we could do is to use Householder's method for tridiagonalization [32], i.e. we want to find a tridiagonal matrix T that is a similar transformed of the matrix A .

$$T = S^T A S, \quad S = S_1 S_2 \dots S_{n-2} \quad (2.93)$$

This would speed up the iteration since we have fewer off-diagonal elements to worry about. A second optimization is the QR-algorithm. We could improve the convergence by introducing a *shift* on the diagonal. This is popularly called *The accelerated QR-algorithm* or *The shifted QR-algorithm* [35]

For a general tridiagonal matrix

$$T_m = \begin{bmatrix} \alpha_1^m & \beta_1^m & 0 & 0 & \dots & 0 \\ \beta_1^m & \alpha_2^m & \beta_2^m & 0 & & \\ & \beta_2^m & \alpha_3^m & \beta_3 & & \vdots \\ \vdots & & \ddots & \ddots & \ddots & \\ 0 & & & \beta_{n-2}^m & \alpha_{n-1}^m & \beta_{n-1}^m \\ & & \dots & \beta_{n-1}^m & \alpha_n^m & \end{bmatrix}. \quad (2.94)$$

Algorithm 2 *The accelerated QR-Algorithm*

```

for  $i = 1 \rightarrow n$  do
     $T_m - \alpha_n^m I = Q_m R_m$ 
     $T_{m+1} = R_m Q_m + \alpha_n^m I$ 
end for
    
```

It was interesting to see how well this algorithm works compared to a, and we have therefore mad a plot for comparison in Fig. 2.4

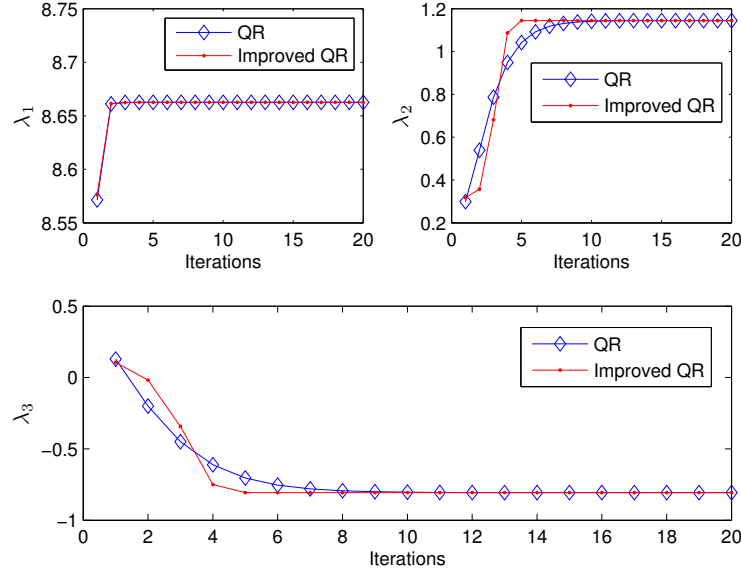


Figure 2.4: This is a plot of different eigenvalues as a function of iteration. The blue line with diamond points represents our normal QR-algorithm on the matrix A Eq. (2.86), and the red line with points represents the accelerated QR-algorithm on a tridiagonalized matrix A . The improved QR-algorithm converges faster for the lower eigenvalues.

The final issue is the numerical precision, or more correctly, the numerical imprecision. It is important to know the error when we do this type of calculations. The details of the mathematics can be read in [49]. We will take use of the Hoffman-Wielandt Theorem which states that

Theorem 2.3.1. *Let A and E be a real symmetric $n \times n$. And let $T = A + E$ with eigenvalues $\{\gamma_i\}$. And $\{\lambda_i\}$ the eigenvalues of A , arranged in increasing order. Then*

$$\left[\sum_{j=1}^n (\lambda_i - \gamma_i) \right]^{\frac{1}{2}} \leq F(E), \quad (2.95)$$

where $F(E) = \left(\sum_{ij} |a_{ij}|^2 \right)^{1/2}$ is the Frobenius norm of E

Let T be a tridiagonal matrix and let \tilde{T} be the new matrix obtained by deleting β_{n-1} from the off-diagonal positions $(n-1, n)$ and $(n, n-1)$ of T . And let $\{\lambda_j\}$ and $\{\tilde{\lambda}_i\}$ denote the eigenvalues respectively. Then from the Wielandt-Hoffman theorem

$$\left[\sum_{j=1}^n (\lambda_i - \tilde{\lambda}_i) \right]^{\frac{1}{2}} \leq F(T - \tilde{T}) = \sqrt{2}|\beta_{n-1}|, \quad (2.96)$$

since β_{n-1} is the only term that was left after the subtraction. The conclusion of this is that we are closest to the exact eigenvalues when the off-diagonals are smallest.

2.3.2 Discretizing the Schrödinger Equation

Our one-electron Hamiltonian from Eq. (2.79) reads

$$\hat{H} = -\frac{\hbar^2}{2m^*}\nabla_i^2 + \frac{1}{2}m^*\omega_0^2 \cdot [x^2 + y^2 - 2L_x|x| + L_x^2]. \quad (2.97)$$

Using the rescaled parameters in section 2.2.2 we get

$$\bar{H} = -\frac{\omega_c}{2}\nabla^2 + \frac{1}{2}\omega_c^2 \cdot V_c(\bar{x}, \bar{y}). \quad (2.98)$$

The time-independent Schrödinger equation of this Hamiltonian is then

$$-\frac{\omega_c}{2} \left[\frac{\partial}{\partial \bar{x}^2} + \frac{\partial}{\partial \bar{y}^2} \right] u(\bar{x}, \bar{y}) + \frac{1}{2}\omega_c^2 \cdot V_c(\bar{x}, \bar{y})u(\bar{x}, \bar{y}) = Eu(\bar{x}, \bar{y}) \quad (2.99)$$

Where $u(\bar{x}, \bar{y})$ is the single-electrons eigenfunctions. From here on the dimensionless coordinates \bar{x} and \bar{y} would be referred to as x and y . And we would set the constant $\omega_c = 1$. The differential equation can be solved as a matrix diagonalization problem. By subtracting two Taylor series we get the numerical second derivate [32]

$$u(x+h) + u(x-h) = 2u(x) + h^2 f''(x) + O(h^4), \quad (2.100)$$

$$u(y+h) + u(y-h) = 2u(y) + h^2 f''(y) + O(h^4), \quad (2.101)$$

$$f''(x) = \frac{u(x+h) - 2u(x) + u(x-h)}{h^2} + O(h^2), f''(y) = \frac{u(y+h) - 2u(y) + u(y-h)}{h^2} + O(h^2). \quad (2.102)$$

For the two-dimensional case the Laplacian becomes

$$\nabla^2 \approx \frac{1}{h_x^2} (u_{i-1,j} - 2u_{i,j} + u_{i+1,j}) + \frac{1}{h_y^2} (u_{i,j-1} - 2u_{i,j} + u_{i,j+1}) + O(h^2). \quad (2.103)$$

Where we have used the more compact way of writing $u(x \pm h, y) = u_{i \pm 1, j}$, $u(x, y \pm h) = u_{i, j \pm 1}$. An example could be a grid with integration points $n_x = 3$, and step $h = h_x = h_y = \frac{x_{\max} - x_{\min}}{n_x} = \frac{1}{3}$, $x = x_{\min} + ih$, $y = y_{\min} + jh$, where $(i, j) \in \{1, 2, 3\}$. See Figure 2.5

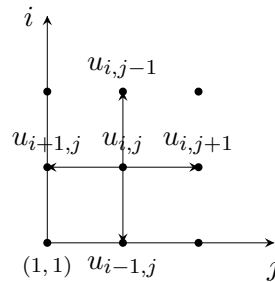


Figure 2.5: The discretized unit grid in our example. The indices are arranged in lexical order

Inserting Eq. (2.103) into the Schrödinger equation Eq. (2.99), gives

$$d_{ij}u_{i,j} - eu_{i,j-1} - eu_{i,j+1} - eu_{i-1,j} - eu_{i+1,j} = \lambda u_{i,j}, \quad (2.104)$$

where we have defined

$$d_{ij} = \frac{4}{h^2} + V_{ij} \quad e = -\frac{1}{h^2}. \quad (2.105)$$

The left side is the discretized Poisson equation in two dimensions. This gives us a set of linear equations that can be written as a matrix eigenvalue problem.

$$\begin{bmatrix} -4 & 1 & 0 & 1 & & & & \\ 1 & -4 & 1 & 0 & 1 & & & \\ 0 & 1 & -4 & 0 & 0 & 1 & & \\ 1 & 0 & 0 & -4 & 1 & 0 & 1 & \\ & 1 & 0 & 1 & -4 & 1 & 0 & 1 \\ & & 1 & 0 & 1 & -4 & 0 & 0 \\ & & & 1 & 0 & 0 & -4 & 1 \\ & & & & 1 & 0 & 1 & -4 \end{bmatrix} \begin{bmatrix} u_{1,1} \\ u_{2,1} \\ u_{3,1} \\ u_{1,2} \\ u_{2,2} \\ u_{3,2} \\ u_{1,3} \\ u_{2,3} \\ u_{3,3} \end{bmatrix} = \lambda \begin{bmatrix} u_{1,1} \\ u_{2,1} \\ u_{3,1} \\ u_{1,2} \\ u_{2,2} \\ u_{3,2} \\ u_{1,3} \\ u_{2,3} \\ u_{3,3} \end{bmatrix}. \quad (2.106)$$

This is a sparse symmetric matrix which is almost tridiagonal. In reality we would choose larger integration points and the number of entries in the matrix grows with n^4 . A lot of those entries are zero.

Since the x -coordinates are separable, i.e.

$$\hat{H}(x, y) = \hat{H}_X(x) + \hat{H}_Y(y) \quad (2.107)$$

$$\Rightarrow E = E_X + E_Y, \quad (2.108)$$

we do not need to discretize in two dimensions, since we already know the eigenvalues for \hat{H}_Y , they are the same as for the one-dimensional case, see section 1.5.2. The Laplacian in one dimension is Eq. (2.102)

$$\frac{d^2}{dx^2} = \frac{u_{i-1} - 2u_i + u_{i+1}}{h^2} + O(h^2), \quad (2.109)$$

where h is our step defined as

$$h = \frac{x_{\max} - x_{\min}}{N}, \quad (2.110)$$

where N is the number of steps or gridpoints. Inserting Eq. (2.109) into the one-dimensional Schrödinger equation

$$-\frac{u_{i+1} - 2u_i + u_{i-1}}{h^2} + V_i u_i = E_X u_i. \quad (2.111)$$

This can be written as a tridiagonal matrix eigenvalue equation.

$$d_i u_i + e_{i-1} u_{i-1} + e_{i+1} u_{i+1} = \lambda u_i, \quad (2.112)$$

where

$$e_i = -\frac{1}{h^2}, \quad d_i = \frac{1}{h^2} + V_i, \quad (2.113)$$

$$\begin{bmatrix} d_1 & e_1 & 0 & 0 & \cdots & 0 & 0 \\ e_1 & d_2 & e_2 & 0 & \cdots & 0 & 0 \\ 0 & e_2 & d_3 & e_3 & \cdots & 0 & 0 \\ \vdots & \vdots & \ddots & \ddots & \ddots & 0 & 0 \\ 0 & 0 & 0 & 0 & \cdots & d_{N-2} & e_{N-1} \\ 0 & 0 & 0 & 0 & \cdots & e_{N-1} & d_N \end{bmatrix} \begin{bmatrix} u_1 \\ u_2 \\ u_3 \\ \vdots \\ u_{N-1} \end{bmatrix} = E_X \begin{bmatrix} u_1 \\ u_2 \\ u_3 \\ \vdots \\ u_{N-1} \end{bmatrix}. \quad (2.114)$$

Chapter 3

Quantum Mechanics for Many-Body Systems

In this chapter, we introduce the notation that is common in many-body physics. We will also introduce the formalism of second-quantization and Wick's theorem.

3.1 Introduction

The underlying fundamentals of quantum mechanics as we know today have not changed much since its birth. We still need to know the Hamiltonian and solve the Schrödinger equation. But how we use this theory is a different story. In the real world we have to deal with systems of more than one quantum particle, we therefore need to expand our Schrödinger equation to include those particles, and this we call the many-body Schrödinger equation. The degrees of freedom increase as our system size gets bigger. We are not able to solve our manybody Schrödinger equation with conventional techniques, not analytically nor numerically. Another limiting factor is our knowledge of the interactions, as the exact Hamiltonian is not known.

Therefore we have to make some assumptions and use approximations, and here is where the *many-body methods* comes in. The first approximation we use is to the Hartree-Fock method on closed shells, assuming that all our electrons interact in the same way. The next method we are going to use is the coupled cluster (CC) method. They are all different in the sense that they have their regions of effectiveness. HF is very fast and gives reasonable result compared to when we have small systems for very closed shells and the ground state is stable. The CC method, on the other hand, has applications for systems up to 40 electrons, but has problems with convergence and non-variational energies.

3.2 The Many-Body Problem

Let us assume that we have a non-relativistic isolated system of N particles. And assume we can describe the system with a time-independent Hamilton operator \hat{H} , then we could reduce the problem to solve the time-independent Schrödinger equation:

$$\hat{H}(r_1, r_2, \dots, r_N)\psi_\lambda(r_1, r_2, \dots, r_N) = E_\lambda\psi_\lambda(r_1, r_2, \dots, r_N). \quad (3.1)$$

where the r_i represents particle i with spin $|m_s\rangle$. λ denotes the set of quantum numbers for particles 1,...N.

The many-body wavefunction Ψ_λ is a N-body *vector* in the composite Hilbert space:

$$\psi_\lambda \in \mathcal{H}_N := \mathcal{H}_1 \oplus \mathcal{H}_1 \oplus \dots \oplus \mathcal{H}_1, \quad (3.2)$$

or

$$|\Psi_\lambda\rangle = |\psi_1\rangle \oplus |\psi_2\rangle \oplus \dots \oplus |\psi_N\rangle \equiv |\psi_1\psi_2\dots\psi_N\rangle, \quad (3.3)$$

where $|\psi_i\rangle$ is a state in a single-particle Hilbert space \mathcal{H}_1 , which is the space of square integrable function over $\mathbb{R}^d \oplus (\sigma)$, or formally:

$$\mathcal{H}_1 := L^2(\mathbb{R}^d \oplus (\sigma)). \quad (3.4)$$

3.2.1 The Electronic Hamiltonian

We want to describe our physical system with an *ab initio* method, which basically means that we want our Hamiltonian to include the basic forces with no parametrization, in atomic units ($\hbar = c = m_e = 1$) the Hamiltonian is:

$$\hat{H} = \hat{T} + \hat{V}. \quad (3.5)$$

Where \hat{T} is the total kinetic energy operator, and \hat{V} is the total potential energy operator.

$$\hat{T} = \sum_k \hat{t}_k. \quad (3.6)$$

\hat{t}_k is the kinetic energy operator for particle k .

In general we have:

$$\hat{V} = \hat{V}_1 + \hat{V}_2 + \dots \quad (3.7)$$

where

$$\hat{V}_n = \frac{1}{n!} \sum_{abc\dots z} \hat{v}_{abc\dots z}^{(n)} \quad (3.8)$$

$n!$ is because we have indistinguishable particles. For systems of electrons like quantum dots, we will truncate our total potential operator to include up to the two-body potential operator \hat{V}_2 . But some papers in nuclear physics (ref(papers of three body force)) have proven that the three-body force is a important contributor to the binding energy. Then the electronic Hamiltonian the reads (in atomic units)

$$\hat{H} = \sum_k \hat{t}_k + \frac{1}{2} \sum_{ij} \hat{v}_{ij}, \quad (3.9)$$

where (in atomic units)

$$\hat{h}_k = -\frac{1}{2} \nabla_k^2 + \sum_A \hat{c}_{kA}, \quad \hat{v}_{ij} = \frac{1}{r_{ij}}. \quad (3.10)$$

Where the last sum is the Coulomb contribution of interaction of the single-particles with the *core* particles A , e.g. electrons around a proton core.

3.2.2 Identical Particles

In quantum mechanics particles are indistinguishable, and thus we can not tell which of the electrons are in which state. This means that the expectation value would have to be the same when we interchange the coordinates of particle i and j .

$$|\Psi_\lambda(r_1, r_2, \dots, r_i, \dots, r_j, \dots, r_N)|^2 = |\Psi_\lambda(r_1, r_2, \dots, r_j, \dots, r_i, \dots, r_N)|^2, \quad (3.11)$$

gives us possible antisymmetric ($-$) and symmetric ($+$) solutions

$$\Psi_\lambda(r_1, r_2, \dots, r_i, \dots, r_j, \dots, r_N) = \pm \Psi_\lambda(r_1, r_2, \dots, r_j, \dots, r_i, \dots, r_N). \quad (3.12)$$

We will later refer to the symmetric solution as bosons, and the other as fermions. Introducing the Permutation operator

$$\hat{P}_{ij}\Psi_\lambda(r_1, r_2, \dots, r_i, \dots, r_j, \dots, r_N) = \Psi_\lambda(r_1, r_2, \dots, r_j, \dots, r_i, \dots, r_N) \quad (3.13)$$

The eigenvalue equation for \hat{P} gives

$$\hat{P}_{ij}\Psi_\lambda(r_1, r_2, \dots, r_i, \dots, r_j, \dots, r_N) = \beta\Psi_\lambda(r_1, r_2, \dots, r_i, \dots, r_j, \dots, r_N), \quad (3.14)$$

$$\beta = \pm 1 \quad \text{Since} \quad \hat{P}_{ij}^2 = 1. \quad (3.15)$$

wavefunctions with ($\beta = +1$) are the bosons, and ($\beta = -1$) are the fermions. The Hamiltonian is invariant under the interchange of particles and therefore commutes with the permutation operator.

Proof.

$$\hat{P}_{jk}\hat{H}\Psi = \hat{P}_{jk}(\hat{H}_{jk}\Psi_{jk}) = \hat{H}_{kj}\Psi_{kj} \quad (3.16)$$

$$\hat{H}\hat{P}_{jk}\Psi = \hat{H}_{jk}\hat{P}_{jk}\Psi_{jk} = \hat{H}_{jk}\Psi_{kj} \quad (3.17)$$

We then subtract equation Eq. (3.16) with Eq. (3.17)

$$\hat{P}_{jk}(\hat{H}\Psi) - \hat{H}(\hat{P}_{jk}\Psi) = \hat{H}_{kj}\Psi_{kj} - \hat{H}_{jk}\Psi_{kj} \quad (3.18)$$

or equivalently

$$[\hat{P}_{jk}, \hat{H}] = (\hat{H}_{kj} - \hat{H}_{jk}) \Psi_{kj} \quad (3.19)$$

□

The permutation operator commutes with the Hamiltonian if and only if $\hat{H}_{kj} = \hat{H}_{jk}$.

According to Eq. (3.6) and Eq. (3.7) Hamiltonian is a sum of onebody and two-body operators. The sums converge and are therefore interchangeable with respect to particles without changing our Hamiltonian.

$$H_{jk} = H_1 \dots + H_j + \dots + H_k + \dots = H_1 \dots + H_k + \dots + H_j + \dots = H_{kj}. \quad (3.20)$$

Then it follows that \hat{H} and \hat{P} are compatible observable ([24]). i.e. there exists eigenfunctions for \hat{H} that are also eigenfunctions of \hat{P} . We know we need to construct symmetric wavefunctions for the bosons and antisymmetric for the fermions. One way of doing this is using a symmetrization operator for bosons

$$\hat{S} = \frac{1}{N!} \sum_p \hat{P} \quad (3.21)$$

where p is the called the permutation number and is the *set* of all possible permutations including the empty set. $p = \{\emptyset, [1, 2], [1, 3], [2, 3]\}$ for three particles. The normalized symmetric state Φ_S is then given by

$$\Phi_S(r_1, r_2, \dots, r_N) = \sqrt{\frac{N!}{n_\alpha! n_\beta! \dots n_\gamma!}} \hat{S} \phi_\alpha(r_1) \phi_\beta(r_2) \dots \phi_\gamma(r_N) \quad (3.22)$$

Similarly we have the anti-symmetrization operator for fermions

$$\hat{A} = \frac{1}{N!} \sum_p (-1)^p \hat{P}, \quad (3.23)$$

and the normalized antisymmetric states

$$\Phi_{AS}(r_1, r_2, \dots, r_N) = \sqrt{N!} \hat{A} \psi_\alpha(r_1) \psi_\beta(r_2) \dots \psi_\gamma(r_N). \quad (3.24)$$

or equivalently

$$\Phi_{\alpha\beta\dots\gamma}(r_1, r_2, \dots, r_N) = \frac{1}{\sqrt{N!}} \begin{vmatrix} \phi_\alpha(r_1) & \phi_\beta(r_1) & \dots & \phi_\gamma(r_1) \\ \phi_\alpha(r_2) & \phi_\beta(r_2) & \dots & \phi_\gamma(r_2) \\ \vdots & \vdots & \ddots & \vdots \\ \phi_\alpha(r_N) & \phi_\beta(r_N) & \dots & \phi_\gamma(r_N) \end{vmatrix}. \quad (3.25)$$

This was first introduced by J.C. Slater [67] in 1929 and is popularly called a Slater determinant. It obeys the Pauli Exclusion Principle (PEP): The determinant would be zero if two of the single-particle wavefunctions have the same quantum numbers $\alpha, \beta, \dots, \gamma$.

The most general way of writing our wavefunction of the N-fermion system is to have a linear combination of the Slater determinants Eq. (3.25).

$$\Psi_\lambda(r_1, r_2, \dots, r_N) = \sum_{\alpha\beta\dots\gamma} C_{\alpha\beta\dots\gamma}^\lambda \Phi_{\alpha\beta\dots\gamma}(r_1, r_2, \dots, r_N). \quad (3.26)$$

3.3 Second Quantization

The second-quantization formalism was first introduced by Dirac (1927) and extended to fermion systems by Jordan and Klein (1927) and by Jordan and Wigner (1928) [65]. The formalism of *second quantization* is just a simplification in the description of a many-body system, a reformulation of the original Schrödinger equation. The quantum mechanical states are represented by annihilation and creation operators working on the physical vacuum state.

We will look at fermionic systems, therefore we will restrict the many-particle functions to be antisymmetric and choose the *Slater determinant* Eq. (3.25) as our candidate. And introduce the occupancy notation for Slater determinants

$$\Phi_{\alpha_1\alpha_2\dots\alpha_N} \equiv |\alpha_1\alpha_2\dots\alpha_N\rangle. \quad (3.27)$$

Note: this is not the same as the product states in Eq. (3.3). This is antisymmetrized

$$|\alpha_1\dots\alpha_i\alpha_j\dots\alpha_N\rangle = -|\alpha_1\dots\alpha_j\alpha_i\dots\alpha_N\rangle. \quad (3.28)$$

And the state "lies" in what we called the Fock space, which is a tensor product space of antisymmetric Hilbert spaces:

$$\mathcal{F}_N = \bigoplus_{n=0}^N \mathcal{H}_n^{AS}. \quad (3.29)$$

In this case we have a state in an N -dimensional Fock space.

3.3.1 Creation and Annihilation Operators

The creation and annihilation operators are mappings between different N and $N \pm 1$ dimensional Hilbert spaces,

$$a_\alpha^\dagger : \mathcal{H}_N^{AS} \rightarrow \mathcal{H}_{N+1}^{AS}, \quad (3.30)$$

$$a_\alpha : \mathcal{H}_N^{AS} \rightarrow \mathcal{H}_{N-1}^{AS}, \quad (3.31)$$

where

$$\alpha \in \mathcal{H}_1. \quad (3.32)$$

A creation operator a_α^\dagger will create a fermion with quantum number(s) α from the antisymmetric state Eq. (3.27)

$$a_\alpha^\dagger |0\rangle = |\alpha\rangle. \quad (3.33)$$

$|0\rangle$ is the vacuum state. If α is already occupied, the result is zero due to PEP.

$$a_\alpha^\dagger |\alpha\rangle = 0. \quad (3.34)$$

An annihilation operator a_α will remove a fermion with quantum number(s) α from the antisymmetric state Eq. (3.27)

$$a_\alpha |\alpha\rangle = |0\rangle, \quad (3.35)$$

$$a_\alpha |0\rangle = 0. \quad (3.36)$$

If α does not exist, the result is zero due to annihilation of a vacuum state.

$$a_\alpha \underbrace{|\alpha_1 \alpha_2 \dots \alpha_N\rangle}_{\alpha \notin} = 0. \quad (3.37)$$

Our Slater determinant (3.27) can now be written as a product of creation operators

$$|\alpha_1 \alpha_2 \dots \alpha_N\rangle = \prod_{i=1}^N a_{\alpha_i}^\dagger |0\rangle. \quad (3.38)$$

Using the antisymmetry of the states Eq. (3.28) we can show that

$$a_{\alpha_i}^\dagger a_{\alpha_k}^\dagger = -a_{\alpha_k}^\dagger a_{\alpha_i}^\dagger, \quad (3.39)$$

leading to the anticommutation rule for creation operators

$$\{a_\alpha^\dagger, a_\beta^\dagger\} = a_\alpha^\dagger a_\beta^\dagger + a_\beta^\dagger a_\alpha^\dagger = 0. \quad (3.40)$$

Note: If $\alpha = \beta$ we would also get zero because of PEP. The hermitian conjugate (adjoint) of a_α^\dagger is the annihilation operator,

$$(a_\alpha^\dagger)^\dagger = a_\alpha \quad (3.41)$$

We have the following anticommutation relation for the annihilation operators (see [65] for details)

$$\{a_\alpha, a_\beta\} = a_\alpha a_\beta + a_\beta a_\alpha = 0 \quad (3.42)$$

and

$$\{a_\alpha^\dagger, a_\beta\} = \{a_\alpha, a_\beta^\dagger\} = \delta_{\alpha\beta} \quad (3.43)$$

where $\delta_{\alpha\beta}$ is 0 if $\alpha \neq \beta$ and 1 if $\alpha = \beta$.

3.3.2 Representation of Operators

Now that we have a formalism for our states, we want to calculate matrix elements and expectation values of our *many-body* operators. Starting with the number-operator. It is a way to test that our many-body formalism conserves the particle number.

$$\hat{N} = \sum_{\alpha} a_\alpha^\dagger a_\alpha, \quad (3.44)$$

and operating this on a state gives us the eigenvalue of n , which is the number of fermions in that state.

$$\hat{N}|\alpha_1\alpha_2...\alpha_N\rangle = \sum_{\alpha} a_\alpha^\dagger a_\alpha|\alpha_1\alpha_2...\alpha_N\rangle = n|\alpha_1\alpha_2...\alpha_N\rangle \quad (3.45)$$

Because from Eq. (3.33), Eq. (3.37) and Eq. (3.37) we get

$$a_\alpha^\dagger a_\alpha|\alpha_1\alpha_2...\alpha_N\rangle = \begin{cases} 0 & \alpha \notin \{\alpha_i\} \\ |\alpha_1\alpha_2...\alpha_N\rangle & \alpha \in \{\alpha_i\} \end{cases}. \quad (3.46)$$

The number operator is a one-body operator since it acts on one single-particle state at a time. Another type is the one-body operator [65].

$$\hat{F} = \sum_{\alpha\beta} \langle\alpha|\hat{f}|\beta\rangle|\alpha\rangle\langle\beta| \quad (3.47)$$

where $|\alpha\rangle, |\beta\rangle$ is the chosen single-particle basis. It can be rewritten and expressed with creation and annihilation operators. The second quantization form of \hat{F}

$$\hat{F} = \sum_{\alpha\beta} \langle\alpha|\hat{f}|\beta\rangle a_\alpha^\dagger a_\beta \quad (3.48)$$

The operator \hat{F} removes a fermion from the state β and creates a new one in state α . This transition is given by the probability amplitude $\langle\alpha|\hat{f}|\beta\rangle$.

Generally we can do this for an N-body operator. But we will only consider a two-body operator:

$$\hat{V} = \sum_{\alpha\beta\gamma\delta} \langle\alpha\beta|v|\gamma\delta\rangle|\gamma\delta\rangle\langle\alpha\beta|. \quad (3.49)$$

For an N -particle system we have

$$V_N = \sum_{i < j=1}^N \hat{v}_{ij} = \frac{1}{2} \sum_{i \neq j}^N \hat{v}_{ij}. \quad (3.50)$$

This can be used to rewrite \hat{V} to

$$\hat{V} = \frac{1}{2} \sum_{\alpha\beta\gamma\delta} \langle \alpha\beta | v | \gamma\delta \rangle a_\alpha^\dagger a_\beta^\dagger a_\delta a_\gamma \quad (3.51)$$

$$= \frac{1}{4} \sum_{\alpha\beta\gamma\delta} \langle \alpha\beta || v || \gamma\delta \rangle a_\alpha^\dagger a_\beta^\dagger a_\delta a_\gamma \quad (3.52)$$

where we have defined the antisymmetric matrix element to be

$$\langle \alpha\beta || v || \gamma\delta \rangle = \langle \alpha\beta | v | \gamma\delta \rangle - \langle \alpha\beta | v | \delta\gamma \rangle. \quad (3.53)$$

see [33] and [16] for details of this derivation. The interpretation of the operator \hat{V} is that it removes two fermions in the states γ and δ , and creates two others in states α, β . This is done with probability amplitude $\frac{1}{4} \langle \alpha\beta | v | \gamma\delta \rangle_{\text{AS}}$. But what is interesting here is to calculate expectation values of the operator Eq. (3.52). Let us find the expectation value of \hat{V} with respect to the two-particle product states $|\alpha_1\alpha_2\rangle$ and $|\beta_1\rangle\beta_2$

$$\langle \alpha_1\alpha_2 | \hat{V} | \beta_1\beta_2 \rangle = \frac{1}{4} \sum_{\alpha\beta\gamma\delta} \langle \alpha\beta || v || \gamma\delta \rangle \langle \alpha_1\alpha_2 | a_\alpha^\dagger a_\beta^\dagger a_\delta a_\gamma | \beta_1\beta_2 \rangle, \quad (3.54)$$

$$= \frac{1}{4} \sum_{\alpha\beta\gamma\delta} \langle \alpha\beta || v || \gamma\delta \rangle \langle 0 | a_{\alpha_1} a_{\alpha_2} a_\alpha^\dagger a_\beta^\dagger a_\delta a_\gamma a_{\beta_1}^\dagger a_{\beta_2}^\dagger | 0 \rangle. \quad (3.55)$$

Using the anticommutation relations Eq. (3.40), Eq. (3.42) and Eq. (3.43), we get

$$\begin{aligned} & \langle 0 | a_{\alpha_1} a_{\alpha_2} a_\alpha^\dagger a_\beta^\dagger a_\delta a_\gamma a_{\beta_1}^\dagger a_{\beta_2}^\dagger | 0 \rangle \\ &= \langle 0 | a_{\alpha_1} a_{\alpha_2} a_\alpha^\dagger a_\beta^\dagger \left(a_\delta \delta_{\gamma\beta_1} a_{\beta_2}^\dagger - a_\delta a_{\beta_1}^\dagger a_\gamma a_{\beta_2}^\dagger \right) | 0 \rangle \end{aligned} \quad (3.56)$$

$$= \langle 0 | a_{\alpha_1} a_{\alpha_2} a_\alpha^\dagger a_\beta^\dagger \left(\delta_{\gamma\beta_1} \delta_{\delta\beta_2} - \delta_{\gamma\beta_1} a_{\beta_2}^\dagger a_\delta - a_\delta a_{\beta_1}^\dagger \delta_{\gamma\beta_2} + a_\delta a_{\beta_1}^\dagger a_{\beta_2}^\dagger a_\gamma \right) | 0 \rangle \quad (3.57)$$

$$= \langle 0 | a_{\alpha_1} a_{\alpha_2} a_\alpha^\dagger a_\beta^\dagger \left(\delta_{\gamma\beta_1} \delta_{\delta\beta_2} - \delta_{\gamma\beta_1} a_{\beta_2}^\dagger a_\delta - \delta_{\delta\beta_1} \delta_{\gamma\beta_2} \delta_{\gamma\beta_2} + \delta_{\gamma\beta_2} a_{\beta_1}^\dagger a_\delta + a_\delta a_{\beta_1}^\dagger a_{\beta_2}^\dagger a_\gamma \right) | 0 \rangle \quad (3.58)$$

The only terms that survive are the terms with only Kronecker deltas, because all the other terms have an annihilation operator to the left, which yields zero with vacuum state, Eq. (3.36).

$$\langle 0 | a_{\alpha_1} a_{\alpha_2} a_\alpha^\dagger a_\beta^\dagger a_\delta a_\gamma a_{\beta_1}^\dagger a_{\beta_2}^\dagger | 0 \rangle = (\delta_{\gamma\beta_1} \delta_{\delta\beta_2} - \delta_{\delta\beta_1} \delta_{\gamma\beta_2}) \langle 0 | a_{\alpha_2} a_{\alpha_1} a_\alpha^\dagger a_\beta^\dagger | 0 \rangle. \quad (3.59)$$

Similarity we can rewrite

$$\langle 0 | a_{\alpha_2} a_{\alpha_1} a_\alpha^\dagger a_\beta^\dagger | 0 \rangle = \delta_{\alpha\alpha_1} \delta_{\beta\alpha_2} - \delta_{\beta\alpha_1} \delta_{\alpha\alpha_2}. \quad (3.60)$$

This gives us the following expectation value

$$\langle \alpha_1 \alpha_2 | \hat{V} | \beta_1 \beta_2 \rangle = \frac{1}{2} [\langle \alpha_1 \alpha_2 | v | \beta_1 \beta_2 \rangle - \langle \alpha_1 \alpha_2 | v | \beta_2 \beta_1 \rangle - \langle \alpha_2 \alpha_1 | v | \beta_1 \beta_2 \rangle + \langle \alpha_2 \alpha_1 | v | \beta_2 \beta_1 \rangle], \quad (3.61)$$

$$= \langle \alpha_1 \alpha_2 | v | \beta_1 \beta_2 \rangle - \langle \alpha_1 \alpha_2 | v | \beta_2 \beta_1 \rangle, \quad (3.62)$$

$$= \langle \alpha_1 \alpha_2 | v | \beta_1 \beta_2 \rangle_{\text{AS}}. \quad (3.63)$$

As we see, this can be very tedious and inefficient as we have to write out contributions that gives us zero. But we can use Wick's theorem to more easily find those terms that give us contribution. This will be our next topic. The second-quantized form of electronic Hamiltonian from Eq. (3.9, Eq. 3.10) is then

$$\hat{H} = \sum_{ij} \langle i | \hat{h} | j \rangle a_i^\dagger a_j + \frac{1}{4} \sum_{ijkl} \langle ij | \hat{v} | kl \rangle a_i^\dagger a_j^\dagger a_l a_k. \quad (3.64)$$

And its vacuum expectation value:

$$\langle 0 | \hat{H} | 0 \rangle = \sum_i \langle i | h | i \rangle + \frac{1}{4} \sum_{ij} \langle ij | v | ij \rangle. \quad (3.65)$$

3.3.3 Wick's Theorem

Originally Gian-Carlo Wick established this method (1950) in order to evaluate the S -matrix in quantum field theory (see for [72] and [11] for details). He introduced two concepts: *normal ordering* and *contractions*. Normal ordering is just a way to write products of annihilation and creation operators in a systematic manner.

The operators $\hat{A}, \hat{B}, \hat{C}, \dots$ represents both creation and annihilation operators. Then the *normal ordering* of the operators $\{\hat{A}\hat{B}\hat{C}\dots\}$ are defined as the rearrangement such that all of the annihilation operators are to the left of the creation operators, multiplied with a phase factor which is -1 for each permutation of the nearest neighbor operators.

$$\{\hat{A}\hat{B}\dots\hat{U}\hat{V}\} \equiv (-1)^p u^\dagger v^\dagger w^\dagger \dots cba \quad (3.66)$$

The superscript p denotes the number of permutations needed to bring the original operator product into the normal ordered form.

Example:

$$\begin{aligned} \{a^\dagger b\} &= a^\dagger b, & \{ab^\dagger\} &= -b^\dagger a, \\ \{ab\} &= ab = -ba, \\ \{a^\dagger bc^\dagger d\} &= a^\dagger c^\dagger db = c^\dagger a^\dagger bd = -a^\dagger c^\dagger bd = -c^\dagger a^\dagger db. \end{aligned} \quad (3.67)$$

Note that the normal ordered form of operators is not unique since creation and annihilation operators can permute among themselves. Also note that one of the important properties of normal ordered operators is that its vacuum expectation value is zero.

$$\langle 0 | \{\hat{A}\hat{B}\dots\} | 0 \rangle = 0. \quad (3.68)$$

Because of

$$a_\alpha | 0 \rangle = 0. \quad (3.69)$$

$$\langle 0 | a_\alpha^\dagger = 0. \quad (3.70)$$

A contraction between two operators is defined as

$$\overline{\hat{A}\hat{B}} \equiv \hat{A}\hat{B} - \{\hat{A}\hat{B}\}. \quad (3.71)$$

And we have only four possible contractions

$$\overline{a_\alpha^\dagger a_\beta^\dagger} = a_\alpha^\dagger a_\beta^\dagger - a_\alpha^\dagger a_\beta^\dagger = 0 \quad (3.72)$$

$$\overline{a_\alpha a_\beta} = a_\alpha a_\beta = 0 \quad (3.73)$$

$$\overline{a_\alpha^\dagger a_\beta} = a_\alpha^\dagger a_\beta - a_\alpha^\dagger a_\beta = 0 \quad (3.74)$$

$$\overline{a_\alpha a_\beta^\dagger} = a_\alpha a_\beta^\dagger - (-a_\beta^\dagger a_\alpha) = \delta_{\alpha\beta} \quad \text{from (3.43)} \quad (3.75)$$

We can have contractions between operators inside a normal ordered product,

$$\{\hat{A}\hat{B}\hat{C}\dots\overline{\hat{P}\hat{Q}}\dots\overline{\hat{X}\hat{Y}}\dots\} = (-1)^p \overline{\hat{P}\hat{Q}}\overline{\hat{X}\hat{Y}}\{\hat{A}\hat{B}\hat{C}\dots\} \quad (3.76)$$

Wick's theorem states that we can express any product of creation and annihilation operators as sum of normal ordered products with all possible ways of contractions, i.e.

$$\begin{aligned} \hat{A}\hat{B}\hat{C}\hat{D}\dots\hat{V}\hat{X}\hat{Y}\hat{Z} &= \{\hat{A}\hat{B}\hat{C}\hat{D}\dots\hat{V}\hat{X}\hat{Y}\hat{Z}\} \\ &+ \sum_{(1)} \{\overline{\hat{A}\hat{B}}\hat{C}\hat{D}\dots\hat{V}\hat{X}\hat{Y}\hat{Z}\} \\ &+ \sum_{(2)} \{\overline{\hat{A}\hat{B}}\overline{\hat{C}\hat{D}}\dots\hat{V}\hat{X}\hat{Y}\hat{Z}\} \\ &+ \dots \\ &+ \sum_{(N/2)} \{\overline{\hat{A}\hat{B}}\overline{\hat{C}\hat{D}}\dots\overline{\hat{V}\hat{X}}\overline{\hat{Y}\hat{Z}}\} \end{aligned} \quad (3.77)$$

$\sum_{(m)}$ means sum over all terms with m representing the number of contractions. N is the total number of creation and annihilation operators. If there are different numbers of creation and annihilation operators, the vacuum expectation value would be zero, because of Eq. (3.69) and Eq. (3.70). If N is odd, one of the operators would not be contracted and we would get zero as well. In order to get contribution one must contract all of the operators. For details of the proof see [56] or [65].

The generalized Wick's theorem follows directly from Wick's theorem and states that the normal ordered product of operators strings $\{\dots\}$ are the same as the sum of the normal ordered product of the total group with all possible ways of contractions, i.e.

$$\begin{aligned}
 \{\widehat{A}\widehat{B}\widehat{C}\widehat{D}..\}\{\widehat{V}\widehat{X}\widehat{Y}\widehat{Z}..\} &= \{\widehat{A}\widehat{B}\widehat{C}\widehat{D}..\widehat{V}\widehat{X}\widehat{Y}\widehat{Z}\} \\
 &+ \sum_{(1)} \{\overbrace{\widehat{A}\widehat{B}\widehat{C}\widehat{D}..\widehat{V}\widehat{X}\widehat{Y}\widehat{Z}}^{(1)}\} \\
 &+ \sum_{(2)} \{\overbrace{\widehat{A}\widehat{B}\widehat{C}\widehat{D}..\widehat{V}\widehat{X}\widehat{Y}\widehat{Z}}^{(2)}\} \\
 &+ \dots \\
 &+ \sum_{(N/2)} \{\overbrace{\widehat{A}\widehat{B}\widehat{C}\widehat{D}..\widehat{V}\widehat{X}\widehat{Y}\widehat{Z}}^{(N/2)}\}
 \end{aligned} \tag{3.78}$$

Note that the only contribution to the vacuum expectation value comes from the full contractions, only the last sum will give contribution. There are no *internal* contractions, i.e. contraction between pairs of operators inside each operator string $\{..\}$.

As an example, we can now use Wick's theorem to find the vacuum expectation value of the following products:

$$\langle 0|a_i a_j^\dagger|0\rangle = \{\overbrace{a_i a_j^\dagger}^{(1)}\} = \delta_{ij} \tag{3.79}$$

$$\begin{aligned}
 \langle 0|a_{\alpha_2} a_{\alpha_1} a_\alpha^\dagger a_\beta^\dagger|0\rangle &= \{\overbrace{a_{\alpha_2} a_{\alpha_1} a_\alpha^\dagger a_\beta^\dagger}^{(1)}\} + \{\overbrace{a_{\alpha_2} a_{\alpha_1} a_\alpha^\dagger a_\beta^\dagger}^{(2)}\} + \underbrace{\{\overbrace{a_{\alpha_2} a_{\alpha_1} a_\alpha^\dagger a_\beta^\dagger}^{(3)}\}}_{=0} \\
 &= \delta_{\alpha\alpha_1} \delta_{\beta\alpha_2} - \delta_{\beta\alpha_1} \delta_{\alpha\alpha_2}.
 \end{aligned} \tag{3.80}$$

3.3.4 Particle-Hole Formalism

One of the advantages with second quantization is that we can easily introduce a reference SD: $|c\rangle$ instead of using the physical vacuum state $|0\rangle$. This reduces the dimensionality of the problem and the new reference state would be defined by a boldfaced zero

$$|\mathbf{0}\rangle \equiv |\Phi_0\rangle = |ijk\dots n\rangle. \tag{3.81}$$

The new reference state $|\mathbf{0}\rangle$ is also referred to as the *Fermi vacuum*, this is now our Fermi level which is the level of our last occupied quantum state, usually the highest occupied orbital.

In this representation we have hole states in addition to particle states. We will define what the hole-states are after the following example. Assume that we have three states that are successively filled with $n-1, n$ and $n+1$ single-particle states α_i

$$|\Phi_0\rangle \equiv |\alpha_1 \alpha_2 \dots \alpha_n\rangle \quad (\text{reference state}), \tag{3.82}$$

$$|\Phi_{\alpha_1}\rangle \equiv |\alpha_2 \alpha_3 \dots \alpha_n\rangle = a_{\alpha_1} |\Phi_0\rangle \quad (\text{creation of a hole}), \tag{3.83}$$

$$|\Phi^\alpha\rangle \equiv |\alpha \alpha_1 \alpha_2 \dots \alpha_n\rangle = a_\alpha^\dagger |\Phi_0\rangle \quad (\text{creation of a particle}). \tag{3.84}$$

And assume that the energies of the single-particle orbitals is such that (see Fig. 3.1)

$$\epsilon_{\alpha_{n+1}} > \epsilon_{\alpha_n} > \epsilon_{\alpha_{n-1}} > \dots \epsilon_{\alpha_2} > \epsilon_{\alpha_1}. \tag{3.85}$$

Let us then define our Fermi level to be α_n , a *hole* is then a state that is below or equal to the Fermi level $\alpha_i \leq \alpha_n$. And a *particle* is a state above $\alpha_i > \alpha_n$.

When we change our reference state from the physical vacuum state $|0\rangle$ to a particle-hole vacuum $|\mathbf{0}\rangle$, we have to introduce new operators as well.

$$a_\alpha|\mathbf{0}\rangle \neq 0. \quad (3.86)$$

since $\alpha \in |\mathbf{0}\rangle$, while for the physical vacuum we have $a_\alpha|0\rangle = 0$ for all α . The new operators need to have the relation $b_\alpha|\mathbf{0}\rangle = 0$.

The new operators are called *quasi*- annihilation and creation operators, viz

$$b_\alpha^\dagger = \begin{cases} a_\alpha^\dagger, & \alpha > \alpha_F \\ a_\alpha, & \alpha \leq \alpha_F \end{cases} \quad (3.87)$$

$$b_\alpha = \begin{cases} a_\alpha, & \alpha > \alpha_F \\ a_\alpha^\dagger, & \alpha \leq \alpha_F \end{cases} \quad (3.88)$$

Where α_F is the Fermi level representing the last occupied single-particle orbit of the reference state $|c\rangle$. And we have the following anticommutation relations

$$\{b_\alpha, b_\beta\} = 0, \quad (3.89)$$

$$\{b_\alpha^\dagger, b_\beta^\dagger\} = 0, \quad (3.90)$$

$$\{b_\alpha^\dagger, b_\beta\} = \delta_{\alpha\beta}. \quad (3.91)$$

The reference state is normalized

$$\langle c|c\rangle = 1 \quad (3.92)$$

A quasi particle state is defined by a state which has one or more particles/holes added to the reference state $|c\rangle$.

$$|abcd\dots i j k l \dots p q r s \dots\rangle \equiv b_a^\dagger b_b^\dagger b_c^\dagger b_d^\dagger \dots b_i^\dagger b_j^\dagger b_k^\dagger b_l^\dagger \dots b_p^\dagger b_q^\dagger b_r^\dagger b_s^\dagger |c\rangle. \quad (3.93)$$

The convention is that indices $i, j, k, l \dots$ indicate states which are occupied by holes. Indices $a, b, c, d \dots$ indicate the states which are occupied by particles. And $p, q, r, s \dots$ indicate any state. We are going to simplify the notation further

$$\begin{aligned} b_i^\dagger &= a_i = i && (\text{creation of a hole} = \text{removing a state below } \alpha_F), \\ b_i &= a_i^\dagger = i^\dagger && (\text{annihilation of a hole} = \text{creating a state below } \alpha_F), \\ b_a^\dagger &= a_a^\dagger = a^\dagger && (\text{creation of a particle} = \text{adding a state above } \alpha_F), \\ b_a &= a_a = a && (\text{annihilation of a particle} = \text{removing a state above } \alpha_F). \end{aligned} \quad (3.94)$$

with the following contractions

$$\overline{p^\dagger q^\dagger}^\dagger = \overline{pq} = 0 \quad (3.95)$$

$$\overline{i^\dagger j} = \delta_{ij} \quad (3.96)$$

$$\overline{ij}^\dagger = 0 \quad (3.97)$$

$$\overline{ab}^\dagger = \delta_{ab} \quad (3.98)$$

$$\overline{a^\dagger b} = 0. \quad (3.99)$$

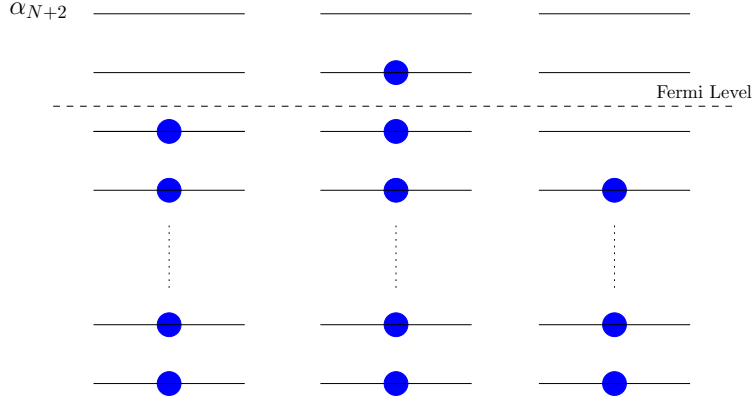


Figure 3.1: The dashed line represents our Fermi level, and the blue dots are our quantum states

3.4 The Normal-Ordered Hamiltonian

We want to rewrite the second-quantized form of the electronic Hamiltonian Eq. (3.64)

$$\hat{H} = \sum_{pq} \langle p|h|q \rangle p^\dagger q + \frac{1}{4} \sum_{pqrs} \langle pq||v||rs \rangle p^\dagger q^\dagger sr. \quad (3.100)$$

using Wick's theorem,

$$\begin{aligned} p^\dagger q &= \{p^\dagger q\} + \underbrace{\{\overline{p^\dagger q}\}}_{p=i, q=j} = \{p^\dagger q\} + \delta_{ij} \\ p^\dagger q^\dagger sr &= \{p^\dagger q^\dagger sr\} + \{\overline{p^\dagger q^\dagger sr}\} + \{\overline{p^\dagger q^\dagger sr}\} + \{\overline{p^\dagger q^\dagger sr}\} + \{\overline{p^\dagger q^\dagger sr}\} \\ &\quad + \{\overline{p^\dagger q^\dagger sr}\} + \{\overline{p^\dagger q^\dagger sr}\} \\ &= \{p^\dagger q^\dagger sr\} - \underbrace{\overline{p^\dagger s}}_{p=i, s=j} \{q^\dagger r\} + \underbrace{\overline{p^\dagger r}}_{p=i, r=j} \{q^\dagger s\} + \underbrace{\overline{q^\dagger s}}_{q=i, s=j} \{p^\dagger r\} - \underbrace{\overline{q^\dagger r}}_{q=i, r=j} \{p^\dagger s\} \\ &\quad - \overline{p^\dagger s q^\dagger r} + \overline{p^\dagger r q^\dagger s} \quad \text{only contribution when } p=i, s=j, q=k, r=l \\ &= \{p^\dagger q^\dagger sr\} - \delta_{ij} \{q^\dagger r\} + \delta_{ij} \{q^\dagger s\} + \delta_{ij} \{p^\dagger r\} - \delta_{ij} \{p^\dagger s\} \\ &= \delta_{ij} \delta_{kl} + \delta_{ij} \delta_{kl}. \end{aligned} \quad (3.102)$$

Here we have done contractions relative to a reference state $|\mathbf{0}\rangle$ and followed the relations Eqs. (3.95)-(3.99). Then the normal-ordered one-body Hamiltonian is

$$\hat{H}_1 = \sum_{pq} \langle p|h|q \rangle \{p^\dagger q\} + \sum_i \langle i|h|i \rangle. \quad (3.103)$$

And the two-body

$$\begin{aligned} \hat{H}_2 &= \frac{1}{4} \sum_{pqrs} \langle pq||v||rs \rangle \{p^\dagger q^\dagger sr\} - \frac{1}{4} \sum_{qri} \langle iq||v||ri \rangle \{p^\dagger r\} + \frac{1}{4} \sum_{qsi} \langle iq||v||is \rangle \{q^\dagger s\}, \\ &\quad + \frac{1}{4} \sum_{pri} \langle pi||v||ri \rangle \{p^\dagger r\} - \frac{1}{4} \sum_{psi} \langle pi||v||is \rangle \{p^\dagger s\} + \frac{1}{4} \sum_{ij} [\langle ij||v||ij \rangle - \langle ij||v||ji \rangle]. \end{aligned} \quad (3.104)$$

The second term is equal to the fourth term. And the third terms is equal to the fifth term.

$$\begin{aligned}\hat{H} = & \sum_{pq} \langle p|h|q \rangle \left\{ p^\dagger q \right\} + \sum_i \langle i|h|i \rangle + \frac{1}{4} \sum_{pqrs} \langle pq||v||rs \rangle \left\{ p^\dagger q^\dagger sr \right\}, \\ & + \frac{1}{2} \sum_{pri} \langle ip||v||ri \rangle \left\{ p^\dagger r \right\} - \frac{1}{2} \sum_{psi} \langle pi||v||is \rangle \left\{ p^\dagger s \right\} + \frac{1}{2} \sum_{ij} \langle ij||v||ij \rangle.\end{aligned}\quad (3.105)$$

We have changed summation variables $s, r \rightarrow q$

$$\begin{aligned}\hat{H} = & \sum_{pq} \langle p|h|q \rangle \left\{ p^\dagger q \right\} + \sum_i \langle i|h|i \rangle + \frac{1}{4} \sum_{pqrs} \langle pq||v||rs \rangle \left\{ p^\dagger q^\dagger sr \right\}, \\ & + \sum_{pq} \left(\langle p|h|q \rangle + \sum_i \langle ip||v||qi \rangle \right) \left\{ p^\dagger q \right\} + \frac{1}{2} \sum_{ij} \langle ij||v||ij \rangle.\end{aligned}\quad (3.106)$$

And define the following

$$f_q^p \equiv \langle p|h|q \rangle + \sum_i \langle ip||v||qi \rangle, \quad (3.107)$$

$$\hat{F}_N \equiv \sum_{pq} f_q^p \left\{ p^\dagger q \right\}, \quad (3.108)$$

$$\hat{V}_N \equiv \frac{1}{4} \sum_{pqrs} \langle pq||v||rs \rangle \left\{ p^\dagger q^\dagger sr \right\}, \quad (3.109)$$

$$\hat{H}_N \equiv \hat{F}_N + \hat{V}_N. \quad (3.110)$$

From Eq. (3.106) we see that only the last term survives and expectation value would be

$$\langle \mathbf{0} | \hat{H} | \mathbf{0} \rangle = \sum_i \langle i|h|i \rangle + \frac{1}{2} \sum_{ij} \langle ij||v||ij \rangle. \quad (3.111)$$

Finally the Hamiltonian reads

$$\hat{H} = \hat{H}_N + \langle \mathbf{0} | \hat{H} | \mathbf{0} \rangle. \quad (3.112)$$

And the normal-ordered electronic Hamiltonian

$$\hat{H}_N = \hat{H} - \langle \mathbf{0} | \hat{H} | \mathbf{0} \rangle. \quad (3.113)$$

This is nothing but a shift by a constant for the expectation value. The usefulness of this will be clearer when we introduce the Coupled Cluster Theory.

Part II

MANY-BODY METHODS

Chapter 4

Hartree-Fock Method

The exact solution to the Schrödinger equation cannot be obtained in most of the systems of chemical interest (see [27]). The number of particles involved in those problems are just too big for computers to solve. Therefore approximations are needed. The approximations would of course depend on the physical system. We could just try some potential and interactions that work. But the many-body theories have hierarchical structure when it comes to approximations. The advantages of this is the fact that we build up experience about the given models. And we can do benchmarks and comparison tests. This allows us to differentiate between different type of *effects* in the theories. In this chapter we are going to look into one of the first approximations, the Hartree-Fock method.

4.1 Introduction

The independent particle picture is an assumption that the electron-electron interaction is rather weak. And each electron could be viewed as independent particles which sees an effective field set up by the other electrons. This is the philosophies of the Hartree-Fock theories and Density functional theories.

The Hartree-Fock method is an optimization problem using Lagrange multipliers as the mathematical tool. The integral we want to minimize are in general

$$E[\Phi] = \int_a^b f(\Phi(r), \frac{\partial \Phi}{\partial r}, r) d^3r. \quad (4.1)$$

We want to find a function Φ that minimizes the *functional* $E[\Phi]$. The set of functions V have the following conditions: $V = \{\Phi : [-\infty, \infty] \rightarrow \mathbb{R} : \Phi \text{ is continuous and differentiable} : \langle \Phi | \Phi \rangle = 1\}$. The unknowns are the functions in V , $\frac{\partial \Phi}{\partial r}$ and r . Although the integral limits a, b are defined, the integration path is not. We want to find a path with a given set of unknowns such that $\delta E = 0$. This will give us minima, maxima or saddle points. So we have to check if we have a minima after finding the solution.

The quantum mechanical functional we want to minimize is

$$E[\Phi] = \frac{\langle \Phi | \hat{H} | \Phi \rangle}{\langle \Phi | \Phi \rangle} = \frac{\int \Phi^* \hat{H} \Phi d\tau}{\int \Phi^* \Phi d\tau}. \quad (4.2)$$

If Φ is an eigenstate of the \hat{H} , then the functional will be stationary

$$\hat{H}|\Phi\rangle = E_0|\Phi\rangle \Rightarrow E[\Phi] = E_0 \Rightarrow \delta E[\Phi] = 0. \quad (4.3)$$

Conversely we can show that a stationary point is an eigenstates of the Hamiltonian (4.3), and therefore a solution of the Schrödinger equation.

Proof. From (4.2) and the fact that setting $\delta E[\Phi] = 0$ gives us

$$\begin{aligned}
 0 &= \delta[\langle \Phi | \hat{H} | \Phi \rangle - E[\Phi] (\langle \Phi | \Phi \rangle - 1)], \\
 0 &= \delta[\langle \Phi | (\hat{H} - E[\Phi]) | \Phi \rangle + E[\Phi]], \\
 0 &= \langle \delta\Phi | (\hat{H} - E[\Phi]) | \Phi \rangle + \langle \Phi | (\hat{H} - E[\Phi]) | \delta\Phi \rangle + \delta E[\Phi], \\
 0 &= \langle \delta\Phi | (\hat{H} - E[\Phi]) | \Phi \rangle + \langle \Phi | (\hat{H} - E[\Phi]) | \delta\Phi \rangle.
 \end{aligned} \tag{4.4}$$

We can add a phase $\delta\Phi \rightarrow i\delta\Phi$. Adding a phase to a wavefunction will not change the expectation value. Then we get two sets of equations

$$I. \quad \langle \delta\Phi | (\hat{H} - E) | \Phi \rangle + \langle \Phi | (\hat{H} - E) | \delta\Phi \rangle = 0, \tag{4.5}$$

$$II. \quad \langle \delta\Phi | (\hat{H} - E) | \Phi \rangle - \langle \Phi | (\hat{H} - E) | \delta\Phi \rangle = 0. \tag{4.6}$$

We have multiplied with i in (II) and remember that $i|\delta\Phi\rangle = -i\langle\delta\Phi|$. And adding them together

$$\langle \delta\Phi | (\hat{H} - E) | \Phi \rangle = 0. \tag{4.7}$$

The choice of $\langle\delta\Phi|$ is arbitrary, so the equation must hold for all possible $\langle\delta\Phi|$'s. Therefore this can only be satisfied if Φ is an eigenfunction to \hat{H} . \square

This is equivalent to Rayleigh-Ritz principle [2] that tells us that the functional $\Omega_{RR} = \langle \Psi | \hat{H} - E | \Psi \rangle$ is stationary at any eigenfunctions $H|\Phi_m\rangle = E_m|\Phi_m\rangle$. One important feature of the functional (4.2) is that errors are in the second order in $\delta\Phi$.

Proof. Our trial wavefunction is $|\phi\rangle = |\psi_0\rangle + \lambda|\psi\rangle$. $|\psi_0\rangle$ is a stationary state, $|\psi\rangle$ is our guess, and λ is a complex number. Using the relations

$$\begin{aligned}
 (\hat{H} - E_0)|\psi_0\rangle &= 0, \\
 (\hat{H} - E_0)[|\phi\rangle - \lambda|\psi\rangle] &= 0, \\
 (\hat{H} - E_0)|\phi\rangle &= \lambda(\hat{H} - E_0)|\psi\rangle.
 \end{aligned} \tag{4.8}$$

we get

$$\begin{aligned}
 E[\Phi] - E_0 &= \frac{\langle \phi | (\hat{H} - E_0) | \phi \rangle}{\langle \phi | \phi \rangle}, \\
 &= \frac{\langle \lambda\psi | (\hat{H} - E_0) | \lambda\psi \rangle}{\langle \phi | \phi \rangle}, \\
 &= |\lambda|^2 \frac{\langle \psi | (\hat{H} - E_0) | \psi \rangle}{\langle \phi | \phi \rangle}.
 \end{aligned} \tag{4.9}$$

\square

4.2 Derivation of the Hartree-Fock Equations

The HF ansatz reads

$$\Phi_{\text{HF}} = |pqrs\dots\rangle. \tag{4.10}$$

Where $pqr\dots$ are the HF spin-orbitals. Φ_{HF} is a SD with N states written in second quantization formalism. We could vary these directly, giving us the Hartree-Fock-Roothaan method [63]. Another possibility is to expand our spin-orbitals $|a\rangle$ as a linear combination of a finite number of basis states $|\alpha\rangle$. The sum goes to infinite in general but we do a truncation.

$$|a\rangle = \sum_{\alpha}^n C_{a\alpha} |\alpha\rangle. \quad (4.11)$$

$C_{a\alpha}$ is the expansion coefficient of an unitary matrix $C^\dagger C = 1$. Writing the Hamiltonian in this basis up to two-body interactions gives

$$\hat{H} = \sum_{ab} \langle a|h|b\rangle a_a^\dagger a_b + \frac{1}{2} \sum_{abcd} \langle ab|v|cd\rangle a_a^\dagger a_b^\dagger a_d a_c. \quad (4.12)$$

Note that the Hamiltonian is in second quantization form (see section 3.3 and [65] for details). h is just the one-body operator, and v is the two-body operator. We will restrict our system to a closed shell system (RHF-equations, see cite...), i.e. all possible spin-orbital levels are filled. Our trial wavefunction $|\Phi_{\text{HF}}\rangle$ will be the *Fermi vacuum* $|\mathbf{0}\rangle$ (see section 3.3.4). We will use Wick's theorem to evaluate $\langle \mathbf{0}|\hat{H}|\mathbf{0}\rangle$. First the Hamiltonian (4.12) have to be rewritten in the quasi-operator representation

$$\hat{H} = \sum_{ij} \langle i|h|j\rangle b_i b_j^\dagger + \frac{1}{2} \sum_{ijkl} \langle ij|v|kl\rangle b_i b_j b_l^\dagger b_k^\dagger. \quad (4.13)$$

Wick's theorem on quasi-operators

$$\langle \mathbf{0}|b_i b_j^\dagger|\mathbf{0}\rangle = \delta_{ij} \quad \text{from (3.79),} \quad (4.14)$$

$$\langle \mathbf{0}|b_i b_j b_l^\dagger b_k^\dagger|\mathbf{0}\rangle = \delta_{kj} \delta_{li} - \delta_{lj} \delta_{ki} \quad \text{from (3.80).} \quad (4.15)$$

lead us to the following energy functional

$$\begin{aligned} E[\Phi_{\text{HF}}] &= \langle \mathbf{0}|\hat{H}|\mathbf{0}\rangle = \sum_i \langle i|h|i\rangle + \frac{1}{2} \sum_{ijkl} [\langle ij|v|ij\rangle - \langle ij|v|ji\rangle], \\ &= \sum_i \langle i|h|i\rangle + \frac{1}{2} \sum_{ij} \langle ij|v|ij\rangle_{\text{AS}}. \end{aligned} \quad (4.16)$$

Inserting the new basis states (4.11) in this expression yields

$$E[\Phi_{\text{HF}}] = \sum_a^N \sum_{\alpha\beta}^n C_{a\alpha}^* C_{b\beta} \langle \alpha|h|\beta\rangle + \frac{1}{2} \sum_{ab}^N \sum_{\alpha\beta\gamma\delta}^n C_{a\alpha}^* C_{b\beta}^* C_{a\gamma} C_{b\delta} \langle \alpha\beta|v|\gamma\delta\rangle_{\text{AS}}, \quad (4.17)$$

The second-quantized form of an operator is unchanged under a unitary transformation of the basis (see [65]).

As mentioned, the method of choice for minimizing $E[\Phi_{\text{HF}}]$ is the Lagrange multipliers method (see [7]).

In general we want to find a stationary point $p = (x_1, x_2, \dots, x_n)$ of a function $f(p)$ with multiple constraints

$$\begin{aligned} g_1(p) &= 0, \\ g_2(p) &= 0, \\ &\vdots \\ g_N(p) &= 0. \end{aligned} \quad (4.18)$$

Then a point p is a stationary if and only if

$$\nabla_\nu f(p) - \sum_{i=1}^N \lambda_i \nabla_\nu g_i(p) = 0, \quad \forall \nu \in p. \quad (4.19)$$

λ_i is the Lagrangian multipliers. We get a system of $N \cdot n$ equations to be solved for the $(N+n)$ -set of variables $\lambda_1, \lambda_2, \dots, \lambda_N, x_1, x_2, \dots, x_n$. In our case the constraint is the HF spin-orbitals are orthonormal

$$\langle a|b \rangle = \sum_{\alpha}^n C_{a\alpha}^* C_{b\alpha} = \delta_{ab}. \quad (4.20)$$

We want to find the stationary point of the energy functional (4.17) with respect to a specific coefficient $C_{k\mu}^*$ in (4.11). We do not have to do the same for $C_{k\mu}$ since they only differ by a phase. This means that for our HF spin-orbitals $|a\rangle \rightarrow i|a\rangle$ will not change the expectation value.

We define

$$\begin{aligned} F &\equiv E[\Phi_{\text{HF}}] - \sum_a^N \lambda_a g_a, \\ &= E[\Phi_{\text{HF}}] - \sum_a^N \lambda_a \sum_{\alpha}^n C_{a\alpha}^* C_{a\alpha}. \end{aligned} \quad (4.21)$$

Then we take the partial derivate of F with respect to $C_{k\mu}^*$ using Eq. (4.19), yielding

$$\begin{aligned} \frac{\partial}{\partial C_{k\mu}^*} &\left(\sum_a^N \sum_{\alpha\beta}^n C_{a\alpha}^* C_{b\beta} \langle \alpha|h|\beta \rangle + \frac{1}{2} \sum_{ab}^N \sum_{\alpha\beta\gamma\delta}^n C_{a\alpha}^* C_{b\beta}^* C_{a\gamma} C_{b\delta} \langle \alpha\beta|v|\gamma\delta \rangle_{\text{AS}} - \sum_a^N \lambda_a \sum_{\alpha}^n C_{a\alpha}^* C_{a\alpha} \right) \\ &= \sum_{\alpha\beta}^n C_{k\beta} \langle \alpha|h|\beta \rangle + \frac{1}{2} \sum_a^N \sum_{\alpha\beta\gamma\delta}^n C_{a\beta}^* C_{k\gamma} C_{a\delta} \langle \alpha\beta|v|\gamma\delta \rangle_{\text{AS}} - \lambda_k \sum_{\alpha}^n C_{k\alpha} \end{aligned} \quad (4.22)$$

$$= \sum_{\alpha}^n \left(\sum_{\beta}^n C_{k\beta} \langle \alpha|h|\beta \rangle + \frac{1}{2} \sum_a^N \sum_{\beta\gamma\delta}^n C_{a\beta}^* C_{k\gamma} C_{a\delta} \langle \alpha\beta|v|\gamma\delta \rangle_{\text{AS}} - \lambda_k C_{k\alpha} \right) = 0. \quad (4.23)$$

The factor 1/2 disappears because of the product rule when we derivate $C_{a\alpha}^* C_{b\beta}^* C_{a\gamma} C_{b\delta}$, we get two cases, when $\{a = k, \alpha = \mu\}$ and $\{b = k, \beta = \mu\}$. We rewrite Eq. (4.23)

$$\sum_{\gamma}^n C_{k\gamma} \langle \alpha|h|\gamma \rangle + \frac{1}{2} \sum_a^N \sum_{\beta\gamma\delta}^n C_{a\beta}^* C_{k\gamma} C_{a\delta} \langle \alpha\beta|v|\gamma\delta \rangle_{\text{AS}} = \lambda_k C_{k\alpha}. \quad (4.24)$$

where we have changed the summation index $\beta \rightarrow \gamma$ in the first sum. And this can then be simplified further

$$\sum_{\gamma}^n \left(\langle \alpha|h|\gamma \rangle + \frac{1}{2} \sum_a^N \sum_{\beta\delta}^n C_{a\beta}^* C_{a\delta} \langle \alpha\beta|v|\gamma\delta \rangle_{\text{AS}} \right) C_{k\gamma} = \lambda_k C_{k\alpha}. \quad (4.25)$$

By defining the Hartree-Fock Hamiltonian as

$$h_{\alpha\gamma}^{\text{HF}} \equiv \langle \alpha|h|\gamma \rangle + \frac{1}{2} \sum_a^N \sum_{\beta\delta}^n C_{a\beta}^* C_{a\delta} \langle \alpha\beta|v|\gamma\delta \rangle_{\text{AS}}, \quad (4.26)$$

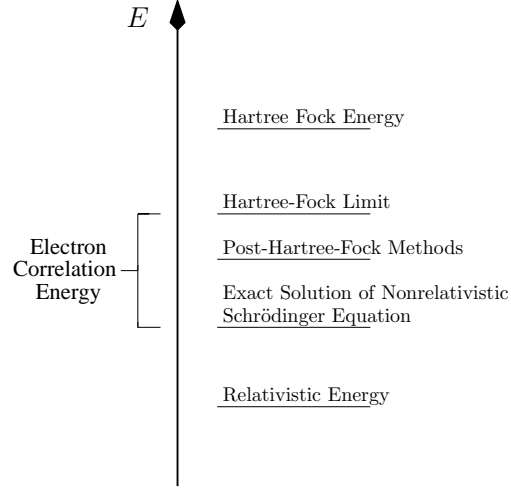


Figure 4.1: A schematic overview over different energies for different approximations

We finally obtain the Hartree-Fock equation

$$\sum_{\gamma}^n h_{\alpha\gamma}^{\text{HF}} C_{k\gamma} = \lambda_k C_{k\alpha}. \quad (4.27)$$

$$E_{\text{corr}} = E_{\text{exact}} - E_{\text{HF}}. \quad (4.28)$$

It is the difference between the exact nonrelativistic energy (i.e. the FCI energy) and the Hartree-Fock energy. This gives us some indication of how much the electron-electron interaction contributes to our system.

4.3 Outline of the Algorithm

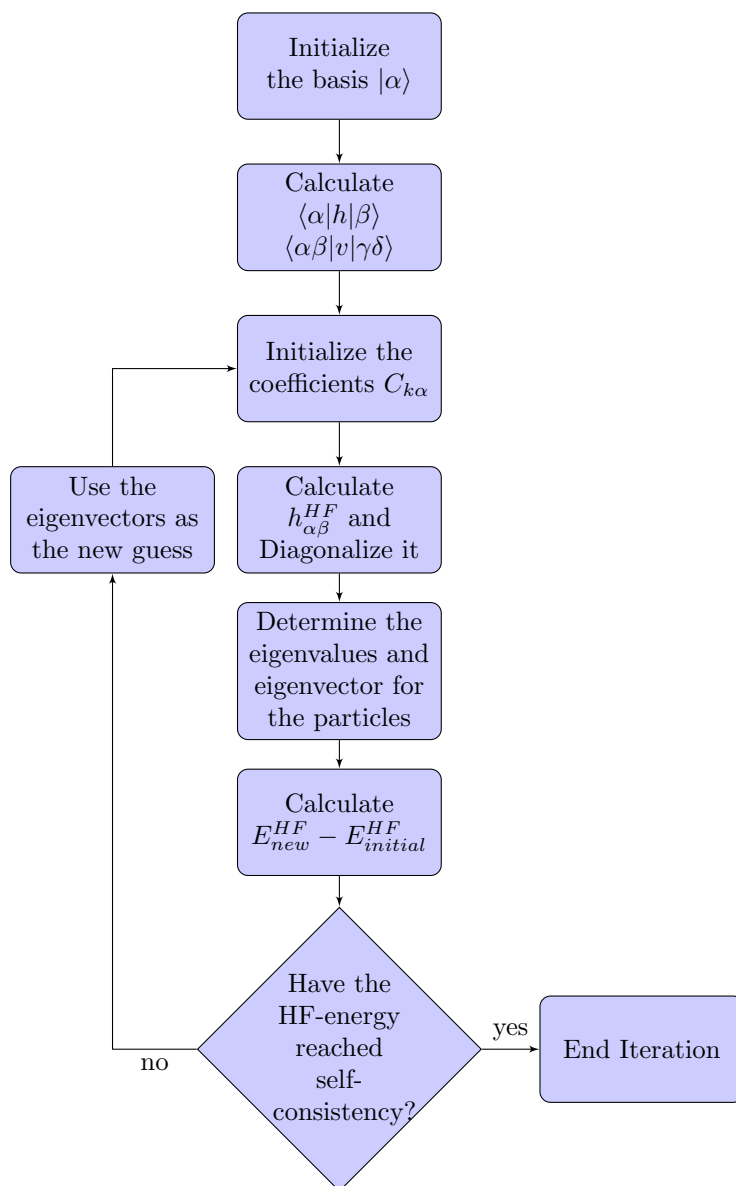


Figure 4.2: Flowchart of Hartree-Fock Algorithm. Self-consistency is the condition that $E[\Phi_{new}] - E[\Phi_{old}] = 0$

Chapter 5

Coupled Cluster Theory

*”In theoretical physics, the analog of the word is the mathematical formula” (From
“Surely you’re joking mr. Feynman“)*

R. P. Feynman

In this chapter we will introduce the Coupled Cluster Theory [13] and derive the Coupled Cluster Equations for Single and Double Excitations (CCSD).

5.1 Introduction

The theoretical framework of Coupled Cluster Theory was developed in the late 1960s by Coester and Kümmel. They applied it to problems in nuclear and subnuclear physics. Later it was introduced into quantum chemistry in the 1960s by Čížek [70, 71]. Kümmel said that he found it remarkable that a quantum chemist would open an issue of a nuclear physics journal [12]. Then Monkhorst [54] developed the CC response theory for calculating the molecular properties. And with the revolution of microprocessors the computational power increased rapidly. People like Pople et al. [30] and Bartlett et al. [5] began to look into more realistic systems by developing the spin-orbital CCD programs. Since then people have tried to develop efficient CCSD energy codes, and inclusion of higher excitations in the wavefunction. And there is still ongoing work with developing methods for open shell calculations (Equation of Motion CCSD) [37]. The CCM is a numerical method for solving the many-body problem (see section 3.2). It is a popular choice with respect to computability (~ 50 nucleons) [25]. Other *ab initio* many-body methods such as Green’s Function Monte Carlo have great precision compared to experiment but have exponential growth in computational need [15].

5.2 The Coupled Cluster Formalism

In this section we will discuss the notation that is going to be used and derive the theory behind the CC equations.

5.2.1 Reference state and operators

We will use the particle-hole formalism (see section 3.3.4). The reference state is defined as

$$|0\rangle \equiv |\Phi_0\rangle, \tag{5.1}$$

where $|\Phi_0\rangle$ is a SD with single-particle orbitals up to the Fermi-level

$$|\Phi_0\rangle = a_{\alpha_1}^\dagger a_{\alpha_2}^\dagger \dots a_{\alpha_F}^\dagger |0\rangle, \quad (5.2)$$

where α_F denotes the quantum number that is on the Fermi-level. Annihilation and creation operators with subscripts $ijk\dots$ will denote hole states, and the subscripts $abc\dots$ will denote the particle states. Subscripts that are $pqr\dots$ are in either of these groups. For the creation and annihilation operators we will use the standard ones a_α and a_α^\dagger with respect to the physical vacuum $|0\rangle$. But we will keep the *quasi*-annihilation b_α and creation operator b_α^\dagger . Eq. (3.87), Eq. (3.88) in mind when we use Wick's theorem.

Products of annihilation and creation operators can be used to construct different states $|\Phi^a\rangle$ with respect to our reference state $|\Phi_0\rangle$ as shown in Eq. (3.83, Eq. 3.84). The subscripts will denote the hole states, and the superscripts will denote the particle states.

A general state can be represented by

$$|\Phi_{ijk\dots}^{abc\dots}\rangle. \quad (5.3)$$

where total number of particles in a system are given by

$$N = N' + n_p - n_h. \quad (5.4)$$

N' is the number of particles in the reference state. And n_p is the number of particles, n_h is the number of holes. We define the single-orbital excitation operator (cluster operator) as

$$t_i \equiv \sum_a t_i^a a_a^\dagger a_i, \quad (5.5)$$

and the two-orbital excitation operator

$$t_{ij} \equiv \frac{1}{2} \sum_a t_{ij}^{ab} a_a^\dagger a_b^\dagger a_j a_i. \quad (5.6)$$

In general the n -orbital excitation operator is defined as

$$t_{ijk\dots}^{abc\dots} \equiv \frac{1}{n!} \sum_{\underbrace{abc\dots}_n} t_{ijk\dots}^{abc\dots} a_a^\dagger a_b^\dagger a_c^\dagger \dots a_j a_i a_k \dots \quad (5.7)$$

$t_{ij\dots}^{ab\dots}$ is the n -orbital excitation amplitude. The factor $\frac{1}{n!}$ is due to the fact that we have an unrestricted summation over the particle states, and there are $n!$ ways of permuting n -particles which give rise to the same final state. The total excitation amplitudes is the sum of all possible excitations

$$\hat{T}_1 \equiv \sum_i \hat{t}_i \quad (5.8)$$

$$\hat{T}_2 \equiv \frac{1}{2} \sum_{ij} t_{ij}^{ab} \quad (5.9)$$

$$\vdots \quad \vdots$$

$$\hat{T}_n \equiv \sum_{\underbrace{ijk\dots}_n} \underbrace{t_{ijk\dots}^{abc\dots}}_n \quad (5.10)$$

5.2.2 The Exponential Ansatz

Our ansatz is that the exact wavefunction $|\Psi\rangle$ can be written as

$$|\Psi\rangle = e^{\hat{T}}|\Phi_0\rangle, \quad (5.11)$$

where \hat{T} is the total excitation operator

$$\hat{T} \equiv \sum_n^{\infty} \hat{T}_n. \quad (5.12)$$

and $|\Phi_0\rangle$ is the reference state.

This would be the exact solution to our many-body Schrödinger equation. But we have to truncate this sum and these truncations give rise to errors in the CC calculation. The fewer term we truncate the closer we are to the exact solution. Different CC schemes are determined by the level of truncation,

$$\hat{T} = \hat{T}_1 \quad (\text{CCS}) \quad (5.13)$$

$$\hat{T} = \hat{T}_1 + \hat{T}_2 \quad (\text{CCSD}) \quad (5.14)$$

$$\hat{T} = \hat{T}_1 + \hat{T}_2 + \hat{T}_3 \quad (\text{CCSDT}) \quad (5.15)$$

$$\hat{T} = \hat{T}_1 + \hat{T}_2 + \hat{T}_3 + \hat{T}_4 \quad (\text{CCSDTQ}) \quad (5.16)$$

We will focus on the CCSD scheme in this thesis.

5.3 Energy equation for the CCSD

The problem we want to solve is the many-body Schrödinger equation defined in Eq. (3.1)

$$\hat{H}|\Psi\rangle = E|\Psi\rangle \quad (5.17)$$

with our Exponential ansatz

$$\hat{H}e^{\hat{T}}|\Phi_0\rangle = Ee^{\hat{T}}|\Phi_0\rangle, \quad (5.18)$$

we can left-multiply to get the energy eigenvalue

$$\langle\Phi_0|\hat{H}e^{\hat{T}}|\Phi_0\rangle = E, \quad (5.19)$$

where $\langle\Phi_0|\Phi_{CC}\rangle = 1$, because of $\langle\Phi_0|\Phi_0\rangle = 1$ and $\langle\Phi_{ijk\dots}^{abc\dots}|\Phi_0\rangle = 0$. This can be taken further by multiplying with a general excited states

$$\langle\Phi_{ijk\dots}^{abc\dots}|\hat{H}e^{\hat{T}}|\Phi_0\rangle = \langle\Phi_{ijk\dots}^{abc\dots}|Ee^{\hat{T}}|\Phi_0\rangle \quad (5.20)$$

This gives us a set of equations involving the excitation amplitude $t_{ijk\dots}^{abc\dots}$. And they are non-linear because of $e^{\hat{T}}$. But formally they are solved exactly when \hat{T} is not truncated (ref?????). We want to decouple the energy and the excitation amplitudes. This can be done by multiplying with $\langle\Phi_0|e^{\hat{T}}$.

$$\langle \Phi_0 | e^{-\hat{T}} \hat{H} e^{\hat{T}} | \Phi_0 \rangle = E \quad (5.21)$$

$$\langle \Phi_i^a | e^{-\hat{T}} \hat{H} e^{\hat{T}} | \Phi_0 \rangle = 0 \quad (5.22)$$

$$\langle \Phi_{ij}^{ab} | e^{-\hat{T}} \hat{H} e^{\hat{T}} | \Phi_0 \rangle = 0 \quad (5.23)$$

$$\vdots$$

$$\langle \Phi_{ijk...}^{abc...} | e^{-\hat{T}} \hat{H} e^{\hat{T}} | \Phi_0 \rangle = 0 \quad (5.24)$$

Which are the CC equations. The first one Eq. (5.21) is the CC energy equation. The next ones are the *amplitude* equations, which we have to solve to get the excitation amplitudes $t_{ijk...}^{abc...}$.

We can write the similarity transformed Hamiltonian as a nested sum of commutators using the Baker-Campbell-Hausdorff relation (see Appendix A).

$$e^{-\hat{T}} \hat{H} e^{\hat{T}} = \hat{H} + [\hat{H}, \hat{T}] + \frac{1}{2!} [[\hat{H}, \hat{T}], \hat{T}] + \frac{1}{3!} [[[\hat{H}, \hat{T}], \hat{T}], \hat{T}] + \dots \quad (5.25)$$

Instead of the Hamiltonian we are going to use the normal-ordered \hat{H}_N to derive the CCSD equations, and truncate such that $\hat{T} = \hat{T}_1 + \hat{T}_2$. We define the similarity transformed normal-ordered Hamiltonian, $\mathbf{H} \equiv e^{-\hat{T}} \hat{H}_N e^{\hat{T}}$. Inserting this into Eqs. (5.21)-(5.23)

$$\langle \Phi_0 | \mathbf{H} | \Phi_0 \rangle + \langle \Phi_0 | \hat{H} | \Phi_0 \rangle = E \quad (5.26)$$

$$\langle \Phi_i^a | \mathbf{H} | \Phi_0 \rangle = 0 \quad (5.27)$$

$$\langle \Phi_{ij}^{ab} | \mathbf{H} | \Phi_0 \rangle = 0 \quad (5.28)$$

We define the CCSD energy as

$$E_{\text{CCSD}} = \langle \Phi_0 | \mathbf{H} | \Phi_0 \rangle + E_0, \quad (5.29)$$

where $E_0 \equiv \langle \Phi_0 | \hat{H} | \Phi_0 \rangle$ is the vacuum expectation energy. There are two ways to derive the set of energy equations Eqs. (5.26)-(5.27), the diagrammatic and the algebraic. We are going to do the latter first.

5.3.1 The Algebraic Approach

Now we want to do a BCH-expansion on \mathbf{H}

$$\mathbf{H} = \hat{H}_N + [\hat{H}_N, \hat{T}] + \frac{1}{2!} [[\hat{H}_N, \hat{T}], \hat{T}] \quad (5.30)$$

The expansion goes to infinity but terminates since \hat{H}_N (Eq. 3.106) is a two-particle operator and therefore can at most de-excite a state that has been twofold excited. This is important because the orthonormality of the reference state $|\Phi_0\rangle$. Therefore we will never get contributions from \hat{T}^3 and higher, because $\langle \Phi_0 | \hat{H}_N \hat{T}_1^3 | \Phi_0 \rangle = 0$. This is due to the type of Hamilton operator and not electron numbers. Inserting for $\hat{T} = \hat{T}_1 + \hat{T}_2$

$$\begin{aligned} \mathbf{H} = & \hat{H}_N + [\hat{H}_N, \hat{T}_1] + [\hat{H}_N, \hat{T}_2] + \frac{1}{2} [[\hat{H}_N, \hat{T}_1], \hat{T}_1] \\ & + \frac{1}{2} [[\hat{H}_N, \hat{T}_2], \hat{T}_2] + \frac{1}{2} [[\hat{H}_N, \hat{T}_1], \hat{T}_2] + \frac{1}{2} [[\hat{H}_N, \hat{T}_2], \hat{T}_1] \end{aligned} \quad (5.31)$$

We know that the \hat{T}_n operators commute with each other because of commutation relations Eq. (3.89)-(3.91). This gives us the following relation

$$\left[\left[\hat{H}_N, \hat{T}_2\right], \hat{T}_1\right] = \left[\left[\hat{H}_N, \hat{T}_1\right], \hat{T}_2\right], \quad (5.32)$$

and the following Hamiltonian

$$\begin{aligned} \mathbf{H} = & \underbrace{\hat{H}_N}_{\text{1th term}} + \underbrace{\left[\hat{H}_N, \hat{T}_1\right]}_{\text{2nd term}} + \underbrace{\left[\hat{H}_N, \hat{T}_2\right]}_{\text{3rd term}} + \underbrace{\frac{1}{2} \left[\left[\hat{H}_N, \hat{T}_1\right], \hat{T}_1\right]}_{\text{4th term}} \\ & + \underbrace{\frac{1}{2} \left[\left[\hat{H}_N, \hat{T}_2\right], \hat{T}_2\right]}_{\text{5th term}} + \underbrace{\left[\left[\hat{H}_N, \hat{T}_1\right], \hat{T}_2\right]}_{\text{6th term}} \end{aligned} \quad (5.33)$$

We need to express these commutation relations in a second-quantized form which leads us to the algebraic approach.

First term

The first term gives us the contribution

$$\langle \Phi_0 | \hat{H}_N | \Phi_0 \rangle = 0 \rightarrow E_{\text{CCSD}}^{(1)} \quad (5.34)$$

Second term

$$\left[\hat{H}_N, \hat{T}_1\right] = \left[\hat{F}_N, \hat{T}_1\right] + \left[\hat{V}_N, \hat{T}_1\right] \quad (5.35)$$

$$\hat{V}_N \hat{T}_1 = \frac{1}{4} \sum_{pqrs} \sum_{ia} \langle pq || v || rs \rangle t_i^a \{a_p^\dagger a_q^\dagger a_s a_r\} \{a_a^\dagger a_i\} \quad (5.36)$$

There are four operators in the first operator string and two in the second. Using the general Wick's theorem we see that we cannot obtain fully contracted terms and therefore this does not contribute to the CCSD energy. Contractions within the operator strings gives zero since they are already on a normal-ordered form.

$$\langle \Phi_0 | [\hat{V}_N, \hat{T}_1] | \Phi_0 \rangle = 0 \rightarrow E_{\text{CCSD}}^{(2)} \quad (5.37)$$

Let us find a second-quantized form of the first commutator

$$\hat{F}_N \hat{T}_1 = \sum_{pq} \sum_{ia} f_q^p t_i^a \{a_p^\dagger a_q\} \{a_a^\dagger a_i\} \quad (5.38)$$

$$\hat{T}_1 \hat{F}_N = \sum_{pq} \sum_{ia} f_q^p t_i^a \{a_a^\dagger a_i\} \{a_p^\dagger a_q\} \quad (5.39)$$

From section 3.3.4 we have the following contraction relations

$$\overline{a_i^\dagger a_j} = \delta_{ij} \quad (5.40)$$

$$\overline{a_a a_b^\dagger} = \delta_{ab} \quad (5.41)$$

$$\overline{a_a^\dagger a_b} = 0 \quad (5.42)$$

$$\overline{a_i a_j^\dagger} = 0 \quad (5.43)$$

Using the generalized form of Wick's theorem from Eq. (3.78) on the operator strings

$$\begin{aligned} \{a_p^\dagger a_q\} \{a_a^\dagger a_i\} &= \{a_p^\dagger a_q a_a^\dagger a_i\} + \{\overline{a_p^\dagger a_q a_a^\dagger a_i}\} + \{a_p^\dagger \overline{a_q a_a^\dagger a_i}\} + \{\overline{a_p^\dagger a_q a_a^\dagger a_i}\} \\ &= \{a_p^\dagger a_q a_a^\dagger a_i\} + \delta_{pi} \{a_q a_a^\dagger\} + \delta_{qa} \{a_p^\dagger a_i\} + \delta_{pi} \delta_{qa} \end{aligned} \quad (5.44)$$

$$\{a_a^\dagger a_i\} \{a_p^\dagger a_q\} = \{a_a^\dagger a_i a_p^\dagger a_q\} = \{a_p^\dagger a_q a_a^\dagger a_i\} \quad (5.45)$$

The non-contracted terms cancel and the commutation relation reads

$$[\hat{F}_N, \hat{T}_1] = \sum_{qia} f_q^i t_i^a \{a_q a_a^\dagger\} + \sum_{pia} f_a^p t_i^a \{a_p^\dagger a_i\} + \sum_{ia} f_i^a t_i^i \quad (5.46)$$

And the contribution from the second term to the energy

$$\langle \Phi_0 | [\hat{H}_N, \hat{T}_1] | \Phi_0 \rangle = \sum_{ia} f_a^i t_i^a \rightarrow E_{\text{CCSD}}^{(2)} \quad (5.47)$$

Third term

$$[\hat{H}_N, \hat{T}_2] = [\hat{F}_N, \hat{T}_2] + [\hat{V}_N, \hat{T}_2] \quad (5.48)$$

Using the same argumentation we had for $[\hat{V}_N, \hat{T}_1]$, we see that $[\hat{F}_N, \hat{T}_2]$ does not contribute to the energy

$$\hat{F}_N \hat{T}_2 = \frac{1}{4} \sum_{abji} \sum_{pq} f_p^q t_{ij}^{ab} \{a_p^\dagger a_q\} \{a_a^\dagger a_b^\dagger a_j a_i\} \quad (5.49)$$

$$\langle \Phi_0 | [\hat{F}_N, \hat{T}_2] | \Phi_0 \rangle = 0 \rightarrow E_{\text{CCSD}} \quad (5.50)$$

The second part of the commutation relation of the third term gives

$$\hat{V}_N \hat{T}_2 = \frac{1}{16} \sum_{pqrs} \sum_{ijab} t_{ij}^{ab} \langle pq || v || rs \rangle \{a_p^\dagger a_q^\dagger a_s a_r\} \{a_a^\dagger a_b^\dagger a_j a_i\} \quad (5.51)$$

$$\hat{V}_2 \hat{V}_N = \frac{1}{16} \sum_{pqrs} \sum_{ijab} t_{ij}^{ab} \langle pq || v || rs \rangle \{a_a^\dagger a_b^\dagger a_j a_i\} \{a_p^\dagger a_q^\dagger a_s a_r\} \quad (5.52)$$

Using the generalized Wick's theorem

$$\begin{aligned} \{a_p^\dagger a_q^\dagger a_s a_r\} \{a_a^\dagger a_b^\dagger a_j a_i\} &= \{a_p^\dagger a_q^\dagger a_s a_r a_a^\dagger a_b^\dagger a_j a_i\} + \{\overline{a_p^\dagger a_q^\dagger a_s a_r a_a^\dagger a_b^\dagger a_j a_i}\} + \{\overline{a_p^\dagger a_q^\dagger a_s a_r a_a^\dagger a_b^\dagger a_j a_i}\} \\ &\quad + \{\overline{a_p^\dagger a_q^\dagger a_s a_r a_a^\dagger a_b^\dagger a_j a_i}\} + \{\overline{a_p^\dagger a_q^\dagger a_s a_r a_a^\dagger a_b^\dagger a_j a_i}\} + \dots \end{aligned} \quad (5.53)$$

$$\begin{aligned} &= \{a_p^\dagger a_q^\dagger a_s a_r a_a^\dagger a_b^\dagger a_j a_i\} + \delta_{pi} \delta_{qj} \delta_{sb} \delta_{ra} - \delta_{pi} \delta_{qj} \delta_{sa} \delta_{rb} \\ &\quad - \delta_{pj} \delta_{qi} \delta_{sb} \delta_{ra} + \delta_{pj} \delta_{qi} \delta_{sa} \delta_{rb} + \dots \\ \{a_a^\dagger a_b^\dagger a_j a_i\} \{a_p^\dagger a_q^\dagger a_s a_r\} &= \{a_a^\dagger a_b^\dagger a_j a_i a_p^\dagger a_q^\dagger a_s a_r\} = \{a_p^\dagger a_q^\dagger a_s a_r a_a^\dagger a_b^\dagger a_j a_i\} \end{aligned} \quad (5.54)$$

The non-contracted term cancels, but we are only interested in the fully contracted terms

$$\begin{aligned} [\widehat{V}_N, \widehat{T}_2] &= \frac{1}{16} \sum_{ijab} [\langle ij||\hat{v}||ab \rangle - \langle ij||\hat{v}||ba \rangle - \langle ji||\hat{v}||ab \rangle + \langle ji||\hat{v}||ba \rangle] t_{ij}^{ab} \\ &= \frac{1}{4} \sum_{ijab} \langle ij||\hat{v}||ab \rangle t_{ij}^{ab}, \end{aligned} \quad (5.55)$$

and the contribution to the energy

$$\langle \Phi_0 | [\widehat{H}_N, \widehat{T}_2] | \Phi_0 \rangle = \frac{1}{4} \sum_{ijab} \langle ij||\hat{v}||ab \rangle t_{ij}^{ab} \rightarrow E_{\text{CCSD}}^{(3)} \quad (5.56)$$

Fourth term

$$[[\widehat{H}_N, \widehat{T}_1], \widehat{T}_1] = [[\widehat{F}_N, \widehat{T}_1], \widehat{T}_1] + [[\widehat{V}_N, \widehat{T}_1], \widehat{T}_1] \quad (5.57)$$

From Eqs. (5.9) and (5.46) we obtain these expressions

$$[\widehat{F}_N, \widehat{T}_1] \widehat{T}_1 = \sum_{qia} \sum_{jb} f_q^i t_j^a t_j^b \{a_q a_a^\dagger\} \{a_b^\dagger a_j\} + \sum_{pia} \sum_{jb} f_a^p t_i^a t_j^b \{a_p^\dagger a_i\} \{a_b^\dagger a_j\} + \sum_{ia} \sum_{jb} f_i^a t_a^i t_j^b \{a_b^\dagger a_j\} \quad (5.58)$$

$$\widehat{T}_1 [\widehat{F}_N, \widehat{T}_1] = \sum_{qia} \sum_{jb} f_q^i t_j^a t_j^b \{a_b^\dagger a_j\} \{a_q a_a^\dagger\} + \sum_{pia} \sum_{jb} f_a^p t_i^a t_j^b \{a_b^\dagger a_j\} \{a_p^\dagger a_i\} + \sum_{ia} \sum_{jb} f_i^a t_a^i t_j^b \{a_b^\dagger a_j\} \quad (5.59)$$

The last two terms cancel each other in a commutation, and all possible contractions are zero. In Eq. (5.59) the particle creation operator a_b^\dagger gives zero in contraction with a particle or hole operator from the left, because of Eq. (5.42). And in Eq. (5.58) the contractions between a particle and hole operator pairs always give zero. Therefore there is no contribution to the energy from this part of the fourth term.

$$[\widehat{V}_N, \widehat{T}_1] \widehat{T}_1 = \frac{1}{4} \sum_{pqrs} \sum_{ia} \sum_{jb} \langle pq||v||rs \rangle t_i^a t_j^b \{a_p^\dagger a_q^\dagger a_s a_r\} \{a_a^\dagger a_i\} \{a_b^\dagger a_j\} \quad (5.60)$$

$$- \frac{1}{4} \sum_{pqrs} \sum_{ia} \sum_{jb} \langle pq||\hat{v}||rs \rangle t_i^a t_j^b \{a_a^\dagger a_i\} \{a_p^\dagger a_q^\dagger a_s a_r\} \{a_b^\dagger a_j\} \quad (5.61)$$

$$\widehat{T}_1 [\widehat{V}_N, \widehat{T}_1] = \frac{1}{4} \sum_{pqrs} \sum_{ia} \sum_{jb} \langle pq||v||rs \rangle t_i^a t_j^b \{a_b^\dagger a_j\} \{a_p^\dagger a_q^\dagger a_s a_r\} \{a_a^\dagger a_i\} \quad (5.62)$$

$$- \frac{1}{4} \sum_{pqrs} \sum_{ia} \sum_{jb} \langle pq||\hat{v}||rs \rangle t_i^a t_j^b \{a_a^\dagger a_i\} \{a_b^\dagger a_j\} \{a_p^\dagger a_q^\dagger a_s a_r\} \quad (5.63)$$

We see that the only term that contribute to the expectation value is the first term in Eq. (5.61). All the other terms have a particle creation operator in the leftmost operator string, and the contractions with this operator therefore leads to zero from Eq. (5.42). Using the generalized

Wick's theorem on the first term in Eq. (5.61)

$$\{a_p^\dagger a_q^\dagger a_s a_r\} \{a_a^\dagger a_i\} \{a_b^\dagger a_j\} = \{a_p^\dagger a_q^\dagger a_s a_r a_a^\dagger a_i a_b^\dagger a_j\} + \{a_p^\dagger a_q^\dagger a_s a_r a_a^\dagger a_i a_b^\dagger a_j\} \quad (5.64)$$

$$+ \{a_p^\dagger a_q^\dagger a_s a_r a_a^\dagger a_i a_b^\dagger a_j\} + \{a_p^\dagger a_q^\dagger a_s a_r a_a^\dagger a_i a_b^\dagger a_j\} + \dots \quad (5.65)$$

$$= -\delta_{pj}\delta_{qi}\delta_{ra}\delta_{sb} + \delta_{pj}\delta_{qi}\delta_{rb}\delta_{sa} + \delta_{pi}\delta_{qj}\delta_{ra}\delta_{sb} - \delta_{pi}\delta_{qj}\delta_{rb}\delta_{sa} + \dots \quad (5.66)$$

The expectation value of the fourth term is then

$$\langle \Phi_0 | [[\hat{V}_N, \hat{T}_1], \hat{T}_1] | \Phi_0 \rangle = \frac{1}{4} \sum_{ia} \sum_{jb} t_i^a t_j^b [\langle ij || \hat{v} || ba \rangle - \langle ij || \hat{v} || ab \rangle - \langle ji || \hat{v} || ba \rangle + \langle ji || \hat{v} || ab \rangle] \quad (5.67)$$

$$= \sum_{ijab} t_i^a t_j^b \langle ij || \hat{v} || ab \rangle \quad (5.68)$$

The contribution to the energy is then

$$\langle \Phi_0 | \frac{1}{2} [[\hat{H}_N, \hat{T}_1], \hat{T}_1] | \Phi_0 \rangle = \frac{1}{2} \sum_{ijab} t_i^a t_j^b \langle ij || \hat{v} || ab \rangle \rightarrow E_{\text{CCSD}}^{(4)} \quad (5.69)$$

Fifth term

$$[[\hat{H}_N, \hat{T}_2], \hat{T}_2] = [[\hat{F}_N, \hat{T}_2], \hat{T}_2] + [[\hat{V}_N, \hat{T}_2], \hat{T}_2] \quad (5.70)$$

The expectation value of $[\hat{F}_N, \hat{T}_2]$ is zero Eq. (5.49), and we are left with finding $[\hat{V}_N, \hat{T}_2]\hat{T}_2$,

$$[\hat{V}_N, \hat{T}_2]\hat{T}_2 = \frac{1}{16} \sum_{pqrs} \sum_{abij} \sum_{cdkl} \langle pq || \hat{v} || rs \rangle t_{ij}^{ab} t_{kl}^{cd} \{a_p^\dagger a_q^\dagger a_s a_r\} \{a_a^\dagger a_b^\dagger a_j a_i\} \{a_c^\dagger a_d^\dagger a_l a_k\} \quad (5.71)$$

$$- \frac{1}{16} \sum_{pqrs} \sum_{abij} \sum_{cdkl} \langle pq || \hat{v} || rs \rangle t_{ij}^{ab} t_{kl}^{cd} \{a_a^\dagger a_b^\dagger a_j a_i\} \{a_p^\dagger a_q^\dagger a_s a_r\} \{a_c^\dagger a_d^\dagger a_l a_k\} \quad (5.72)$$

There are in total four hole-annihilation operators a_s, a_r, a_k, a_l and only two-hole creation operators a_p^\dagger, a_q^\dagger , this term will therefore not be fully contracted. For the same reason $\hat{T}_2[\hat{V}_N, \hat{T}_2]$ will not contribute to the energy.

$$\langle \Phi_0 | \frac{1}{2} [[\hat{H}_N, \hat{T}_2], \hat{T}_2] | \Phi_0 \rangle = 0 \rightarrow E_{\text{CCSD}}^{(5)} \quad (5.73)$$

Sixth term

The mixed term $\hat{H}_N \hat{T}_1 \hat{T}_2$ have three annihilation-creation pairs (one from \hat{T}_1 and two from \hat{T}_2), while \hat{H}_N only have two. This term can therefore never be fully contracted and gives no contribution to the energy

$$\langle \Phi_0 | \frac{1}{2} [[\hat{H}_N, \hat{T}_1], \hat{T}_2] | \Phi_0 \rangle = 0 \rightarrow E_{\text{CCSD}}^{(6)} \quad (5.74)$$

Final term

The final expression becomes

$$E_{\text{CCSD}} - E_0 = \sum_{ia} f_a^i t_i^a + \frac{1}{4} \sum_{ijab} \langle ij || \hat{v} || ab \rangle t_{ij}^{ab} + \frac{1}{2} \sum_{ijab} \langle ij || \hat{v} || ab \rangle t_i^a t_j^b \quad (5.75)$$

This equation is valid for CCSDT and other schemes. Since the higher terms \hat{T}_3 and \hat{T}_4 etc. cannot produce fully contracted terms with the two-body Hamiltonian, as we have seen. However the higher order excitation operators contribute through the amplitude equations Eqs. (5.22)-(5.24).

5.4 Introduction to Coupled Cluster Diagrams

Even though Wick's theorem have simplified the method of evaluating expectation values. However the algebraic approach to the amplitude equations would involve even longer operator strings and be very time consuming. Another method is the diagrammatic approach popularized by Kucharski and Bartlett [39]. We will use their approach to derive the energy equation Eq. (5.75) and the amplitude equations. The particle-hole formalism is still in use, lines represent a particle or a hole with respect to the reference state $|\Phi_0\rangle$. Lines with downward arrows represent the hole states, and lines with the upward arrows represent the particle states (see Fig. 5.1).

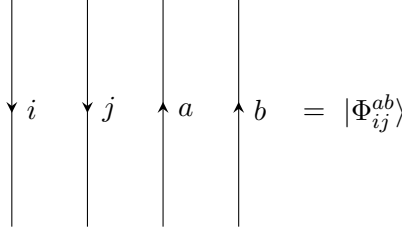


Figure 5.1: Representation of particle and holes

Notice that the convention is to write the rightmost particle/hole first, this has no physical significance since we have a sum of all particles and holes. It is just a phase factor of (-1) difference, $|\Phi_{ij}^{ab}\rangle = -|\Phi_{ji}^{ab}\rangle = |\Phi_{ji}^{ab}\rangle$. Since we already have defined the directions of particles and holes, we want to be consistent with the algebraic ordering of the operators, and have a convention that the rightmost operators start always at the bottom of this page which is the reference state $|\Phi_0\rangle$.

The matrix elements of an interaction with a one-body operator $\langle b|h|a\rangle$ is represented with a vertex (the black dot), $\bullet - - - \times$. Where the dashed line indicate our interaction potential.

Diagram rules part 1

Rule 1: When expressing operators: Any unlabeled particle/hole-line is summed

Rule 2: Incoming lines in a vertex $\bullet - - - \times$ represent an annihilation operator and correspond to the $|\rangle$ ket-part of the matrix element. Outgoing lines represent an creation operator and correspond to the $\langle|$ bra-part of the matrix element.

$$\langle \text{leftmost-out} \dots \text{rightmost-out} | u | \text{leftmost-in} \dots \text{rightmost-in} \rangle \quad (5.76)$$

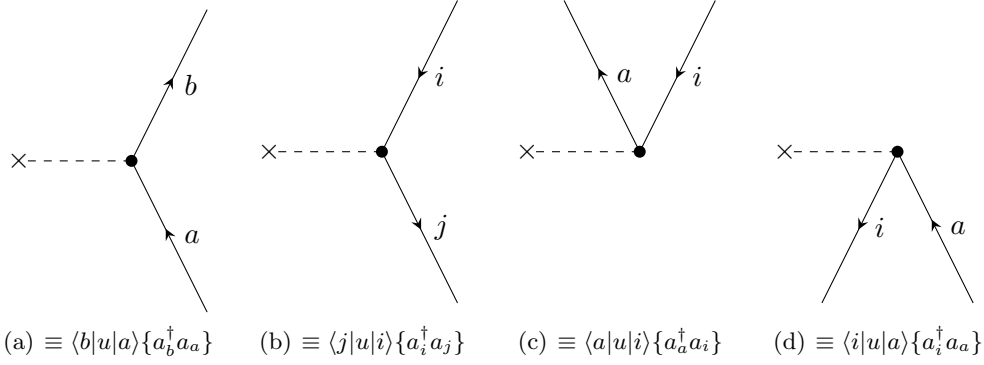


Figure 5.2: Diagrammatic representation of one-body operators. As we can see from Fig. 5.2 the quasi-creation operators lie above the interaction line while the quasi-annihilation operators lie below.

Rule 3: Lines that follow the same direction can be contracted. And a phase factor of -1 is multiplied when contracting two holes

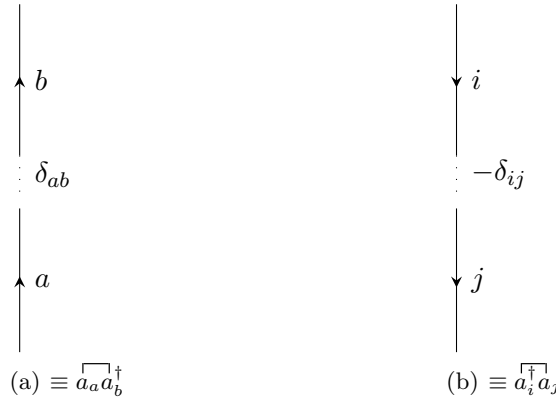


Figure 5.3: Non-zero contractions

Our one-body operator \hat{F}_N Eq. (3.108) is then a sum of all the different diagrams in Fig. 5.2 and of all the indices.

$$\begin{aligned}
 \hat{F}_N &= \sum_{ab} f_b^a \{a_a^\dagger a_b\} + \sum_{ij} f_j^i \{a_i^\dagger a_j\} + \sum_{ia} f_a^i \{a_i^\dagger a_a\} + \sum_{ai} f_i^a \{a_a^\dagger a_i\} \\
 &\equiv \begin{array}{c} \text{Diagram 1} \end{array} + \begin{array}{c} \text{Diagram 2} \end{array} + \begin{array}{c} \text{Diagram 3} \end{array} + \begin{array}{c} \text{Diagram 4} \end{array} \quad (5.77) \\
 &\quad \epsilon_1 = 0 \quad \quad \quad \epsilon_2 = 0 \quad \quad \quad \epsilon_3 = -1 \quad \quad \quad \epsilon_4 = +1 \quad (5.78)
 \end{aligned}$$

ϵ_n is the excitation level of diagram number n and defined by the difference between the number of quasi-creation operators \mathcal{N}_c and the quasi-annihilation operators \mathcal{N}_a divided by 2.

$$\epsilon = \frac{\mathcal{N}_c - \mathcal{N}_a}{2} \quad (5.79)$$

A two-body operator will be represented by two vertices, $\bullet - - - \bullet$ and the matrix elements are defined as before by diagram the rule 2. The diagrammatic representation of \hat{V}_N then becomes

$$\begin{aligned} \hat{V}_N = & \frac{1}{4} \sum_{abcd} \langle ab || \hat{v} || cd \rangle \{a_a^\dagger a_b^\dagger a_d a_c\} + \frac{1}{4} \sum_{ijkl} \langle ij || \hat{v} || kl \rangle \{a_i^\dagger a_j^\dagger a_l a_k\} + \sum_{iabj} \langle ia || \hat{v} || bj \rangle \{a_i^\dagger a_a^\dagger a_j a_b\} \\ & + \frac{1}{2} \sum_{aibc} \langle aj || \hat{v} || bc \rangle \{a_a^\dagger a_i^\dagger a_c a_b\} + \frac{1}{2} \sum_{ijka} \langle ij || \hat{v} || ka \rangle \{a_i^\dagger a_j^\dagger a_a a_k\} + \frac{1}{2} \sum_{abci} \langle ab || \hat{v} || ci \rangle \{a_a^\dagger a_b^\dagger a_i a_c\} \\ & + \frac{1}{2} \sum_{iakl} \langle ia || \hat{v} || kj \rangle \{a_i^\dagger a_a^\dagger a_k a_j\} + \frac{1}{4} \sum_{abij} \langle ab || \hat{v} || ij \rangle \{a_a^\dagger a_b^\dagger a_j a_i\} + \frac{1}{4} \sum_{ijab} \langle ij || \hat{v} || ab \rangle \{a_i^\dagger a_j^\dagger a_b a_a\} \\ \equiv & \begin{array}{ccc} \text{Diagram 1} & + & \text{Diagram 2} & + & \text{Diagram 3} \\ \epsilon_1 = 0 & & \epsilon_2 = 0 & & \epsilon_3 = 0 \end{array} \\ & + \begin{array}{ccc} \text{Diagram 4} & + & \text{Diagram 5} & + & \text{Diagram 6} \\ \epsilon_4 = -1 & & \epsilon_5 = -1 & & \epsilon_6 = +1 \end{array} \\ & + \begin{array}{ccc} \text{Diagram 7} & + & \text{Diagram 8} & + & \text{Diagram 9} \\ \epsilon_7 = +1 & & \epsilon_8 = +2 & & \epsilon_9 = -2 \end{array} . \end{aligned} \quad (5.80)$$

Notice that the \hat{V}_N is a sum of indices p, q, r, s which could either be a particle or hole, we would have $2^4 = 16$ sums, but some of the sums are equivalent. For instance we have used the following

$$\begin{aligned} \frac{1}{4} \sum_{iabj} \langle ia || \hat{v} || bj \rangle \{a_i^\dagger a_a^\dagger a_j a_b\} & + \frac{1}{4} \sum_{iabj} \langle ai || \hat{v} || bj \rangle \{a_a^\dagger a_i^\dagger a_j a_b\} + \frac{1}{4} \sum_{iabj} \langle ia || \hat{v} || jb \rangle \{a_i^\dagger a_a^\dagger a_b a_j\} \\ & + \frac{1}{4} \sum_{iabj} \langle ai || \hat{v} || bj \rangle \{a_a^\dagger a_i^\dagger a_b a_j\} = \sum_{iabj} \langle ai || \hat{v} || jb \rangle \{a_i^\dagger a_a^\dagger a_j a_b\} \end{aligned} \quad (5.81)$$

Which is term 3 in \hat{V}_N . Each vertex is unique $A \bullet - - - \bullet B$, i.e. we can therefore permute the lines leaving or entering the vertex A or B , it will give different diagrams but the same matrix element with a phase factor. For example, the third diagram in \hat{V}_N which is the sum of

$\langle ia || \hat{v} || jb \rangle \{a_i^\dagger a_a^\dagger a_j a_b\}$ can be written in four different ways which is the diagrammatic equivalent of Eq. (5.81).

(5.82)

The diagrams are antisymmetric with respect to permutation of hole and particle pairs. Permutation means placing them in different vertices.

In addition we have the cluster operator $\hat{T} = \hat{T}_1 + \hat{T}_2$

$$\begin{aligned} \hat{T} &= \sum_{ia} t_i^a \{a_a^\dagger a_i\} + \frac{1}{4} \sum_{ijab} t_{ij}^{ab} \{a_a^\dagger a_b^\dagger a_j a_i\} \\ &\equiv \text{Diagram 1} + \text{Diagram 2} \end{aligned} \quad (5.83)$$

$\epsilon_{\hat{T}_1} = +1$
 $\epsilon_{\hat{T}_2} = +2$

where the interaction is represented by a solid bar " — ".

Now that we have established diagrams for the operators, we can now show how the matrix elements of operators between SDs are represented.

$$\langle \Phi_i^a | \hat{T}_1 | \Phi_0 \rangle = \text{Diagram 1} \rightarrow \text{Diagram 2} \quad (5.84)$$

As mentioned earlier the diagrams are read from bottom to top. We have the reference state on bottom, which is *white space* followed by an N-body operator with an interaction in the middle and then finally the *bra*-state on top.

$$\langle \Phi_{ij}^{ab} | \hat{T}_1 | \Phi_0 \rangle = \text{Diagram 1} \rightarrow \text{Diagram 2} \quad (5.85)$$

All the lines in the N-body operator have to be contracted in order to give non-zero matrix elements, additional particle/hole lines which are not involved in the interaction will be written on the right side.

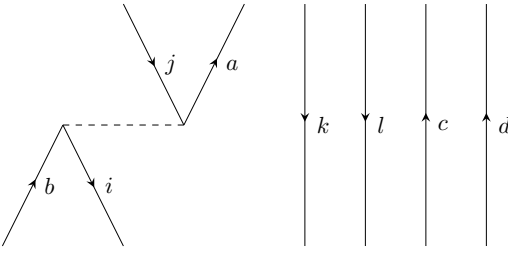
$$\langle \Phi_{ikl}^{acd} | \hat{V}_N | \Phi_{jkl}^{bcd} \rangle =$$

(5.86)

Diagram 3 in \hat{V}_N is therefore the only non-zero contribution for the given the SD. Diagrams that represent the energy equations can be created in the same way. We must remember that our reference state is white space, so we cannot have lines above or below our interaction, i.e. the *excitation level* have to be zero. This will be the condition that gives us the natural truncation to include only \hat{T}^2 diagrams. Since \hat{T}^3 has at least an excitation level of 3, but \hat{H}_N has at an excitation level between -2 and 2 .

5.4.1 Energy Equation

We can write out the commutators in Eq. (5.31) and only include those terms in which the Hamiltonian is to the left of the cluster operators. The reason for this is because of Wick's theorem, we cannot get a full contraction when we have a particle creation operator a_a^\dagger to the left, as we have seen an example of in Eqs. (5.39) and (5.45), i.e. $\langle \Phi_0 | \hat{T}_1 \hat{H}_N | \Phi_0 \rangle = 0$.

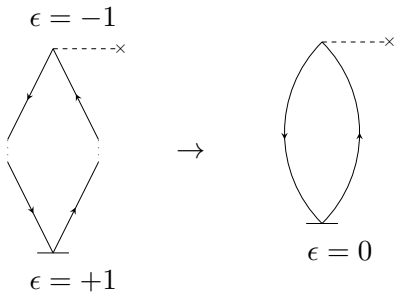
$$\mathbf{H}_c = \hat{H}_N + \hat{H}_N \hat{T}_1 + \hat{H}_N \hat{T}_2 + \frac{1}{2} \hat{H}_N \hat{T}_1^2 + \frac{1}{2} \hat{H}_N \hat{T}_2^2 + \hat{H}_N \hat{T}_1 \hat{T}_2 \quad (5.87)$$

The subscript c indicates that we have a *connected cluster* form of the similarity-transformed Hamiltonian.

Since both \hat{T}_2 and $\hat{T}_1 \hat{T}_2$ have excitation levels bigger than $+2$, we would not get contributions from the last two terms. We are going to consider the first non-zero contribution to the coupled cluster energy

$$E_{CCSD} - E_0 = \langle \Phi_0 | \hat{H}_N \hat{T}_1 | \Phi_0 \rangle + \langle \Phi_0 | \hat{H}_N \hat{T}_2 | \Phi_0 \rangle + \frac{1}{2} \langle \Phi_0 | \hat{H}_N \hat{T}_1^2 | \Phi_0 \rangle \quad (5.88)$$

A \hat{T}_1 -diagram have an excitation level of $+1$, we have to combine this with a diagram in \hat{H}_N that has an excitation level of -1 to get an non-zero contribution. There are several diagrams in \hat{F}_N and \hat{V}_N that fulfill this criterion, but only diagram 3 in \hat{F}_N that has the reference state on top.

$$\langle \Phi_0 | \hat{F}_N \hat{T}_1 | \Phi_0 \rangle =$$

(5.89)

Next we consider $\langle \Phi_0 | \hat{H}_N \hat{T}_2 | \Phi_0 \rangle$, here the \hat{T}_2 has an excitation level of $+2$, which has to be combined with diagram 9 in \hat{V}_N with an excitation level of -2 and reference state on top.

$$\langle \Phi_0 | \hat{V}_N \hat{T}_2 | \Phi_0 \rangle = \begin{array}{c} \epsilon = -2 \\ \text{Diagram 1} \\ \epsilon = +2 \end{array} \rightarrow \begin{array}{c} \text{Diagram 2} \\ \epsilon = 0 \end{array} \quad (5.90)$$

The only contribution left is $\langle \Phi_0 | \hat{H}_N \hat{T}_1^2 | \Phi_0 \rangle$, the excitation level of \hat{T}_1 is the same as the sum of each which is +2. This can only be coupled to diagram 9 in \hat{V}_N .

$$\frac{1}{2} \langle \Phi_0 | \hat{V}_N \hat{T}_1^2 | \Phi_0 \rangle = \begin{array}{c} \epsilon = -2 \\ \text{Diagram 3} \\ \epsilon = +2 \end{array} \rightarrow \begin{array}{c} \text{Diagram 4} \\ \epsilon = 0 \end{array} \quad (5.91)$$

The factor 1/2 seem to be very arbitrary, but the diagrammatic rules are consistent with using Wick's theorem and this factor is taken care of when we imply the diagrammatic rules. The energy equation in the diagrammatic form is then

$$E_{CCSD} - E_0 = \begin{array}{c} \text{Diagram 5} \end{array} + \begin{array}{c} \text{Diagram 6} \end{array} + \begin{array}{c} \text{Diagram 7} \end{array} \quad (5.92)$$

Haven written out the energy equation in a diagrammatic form, we now want to translate this into the algebraic equations we got from Eq. (5.75). First we have to introduce some rules to how diagrams can be interpreted.

Diagram rules part 2

Rule 4: Label the hole lines with indices $ijk..$, and particle lines with indices $abc..$.

Rule 5: Each interaction line contributes with a matrix element f_{in}^{out} or an amplitude $t_{ijk..}^{abc..}$, it is consistent with **Rule 2**

Rule 6: Sum of all indices that is associated with lines that begin and end at interaction lines (internal lines).

Rule 7: The phase of the diagram is $(-1)^{(l+h)}$, where h is number of hole lines. l is the number of **loops** that we have in our diagram. A **loop** is a route along a series of lines that returns to its beginning or begins at one external line and ends at another [13].

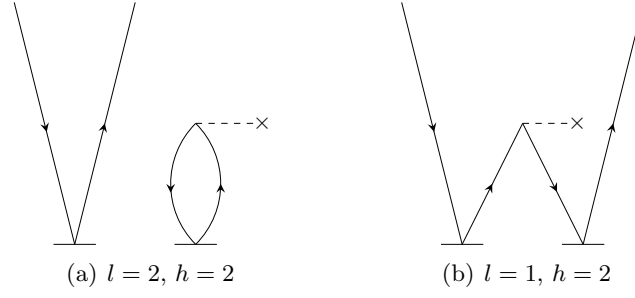


Figure 5.4: Examples of some loops

Rule 8: Each pair of equivalent vertices and equivalent lines give a factor of $\frac{1}{2}$ to be multiplied onto the algebraic expression. Particle/hole-lines that begin and end at the same interactions are equivalent lines. Equivalent vertices are connected by two \hat{T}_N operators to \hat{V}_N in the exact same way, i.e. same incoming and outgoing arrows.

Rule 9: Each pair of **unique** external holes or particle lines give rise to a permutation operator $P(p, q)$. **Unique** means that the external holes and particles enter/leave different interaction lines. This rule makes the total diagram antisymmetric and includes the Pauli Principle which is already included in the interaction.

$$P(p, q)f(p, q) = f(p, q) - f(q, p) \quad (5.93)$$

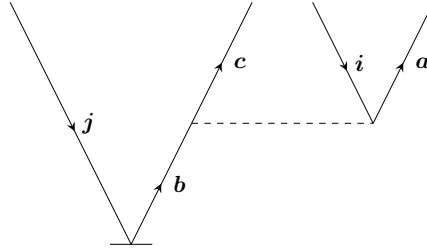


Figure 5.5: Here i and j enters two different interactions and they are therefore a **unique** hole pair. We have to multiply with $P(i, j)$

Now that we have established the diagram rules we can express them in an algebraic form

$$= \sum_{ia} f_a^i t_i^a \quad (5.94)$$

In this diagram we have two loops and two hole lines, one amplitude, one matrix element and two internal indices that have to be summed, which gives us a factor +1 in total.

$$= \frac{1}{4} \sum_{ijab} \langle ij || \hat{v} || ab \rangle t_i^a \quad (5.95)$$

In this diagram we have two loops and two hole lines, two amplitudes, one matrix element and four internal indices that have to be summed. And it also has two pair of equivalent lines that gives us a factor $+\frac{1}{4}$ in total.

$$\begin{array}{c} \text{Diagram: Two loops connected by two horizontal lines. The left loop has vertices labeled } j \text{ and } b. \text{ The right loop has vertices labeled } i \text{ and } a. \end{array} = \frac{1}{2} \sum_{ijab} \langle ij || \hat{v} || ab \rangle t_i^a t_j^b \quad (5.96)$$

In this diagram we have two loops and two hole lines, two amplitudes, two matrix elements and four internal indices that have to be summed. And one pair of equivalent vertices that gives us a factor of $+\frac{1}{2}$. This is the same expressions as Eq. (5.75) when we used Wick's theorem.

5.5 The Amplitude Equations

We will use the same procedure for amplitude equations. The *connected cluster* form of the similarity-transformed Hamiltonian for both the singles and doubles equations

$$\langle \Phi_i^a | \hat{H}_N \left(1 + \hat{T}_1 + \hat{T}_2 + \frac{1}{2} \hat{T}_1^2 + \hat{T}_1 \hat{T}_2 + \frac{1}{3!} \hat{T}_1^3 \right) | \Phi_0 \rangle = 0 \quad (5.97)$$

$$\langle \Phi_{ij}^{ab} | \hat{H}_N \left(1 + \hat{T}_1 + \hat{T}_2 + \frac{1}{2} \hat{T}_1^2 + \hat{T}_1 \hat{T}_2 + \frac{1}{2} \hat{T}_2^2 + \frac{1}{2} \hat{T}_1^2 \hat{T}_2 + \frac{1}{3!} \hat{T}_1^3 + \frac{1}{4!} \hat{T}_1^4 \right) | \Phi_0 \rangle = 0 \quad (5.98)$$

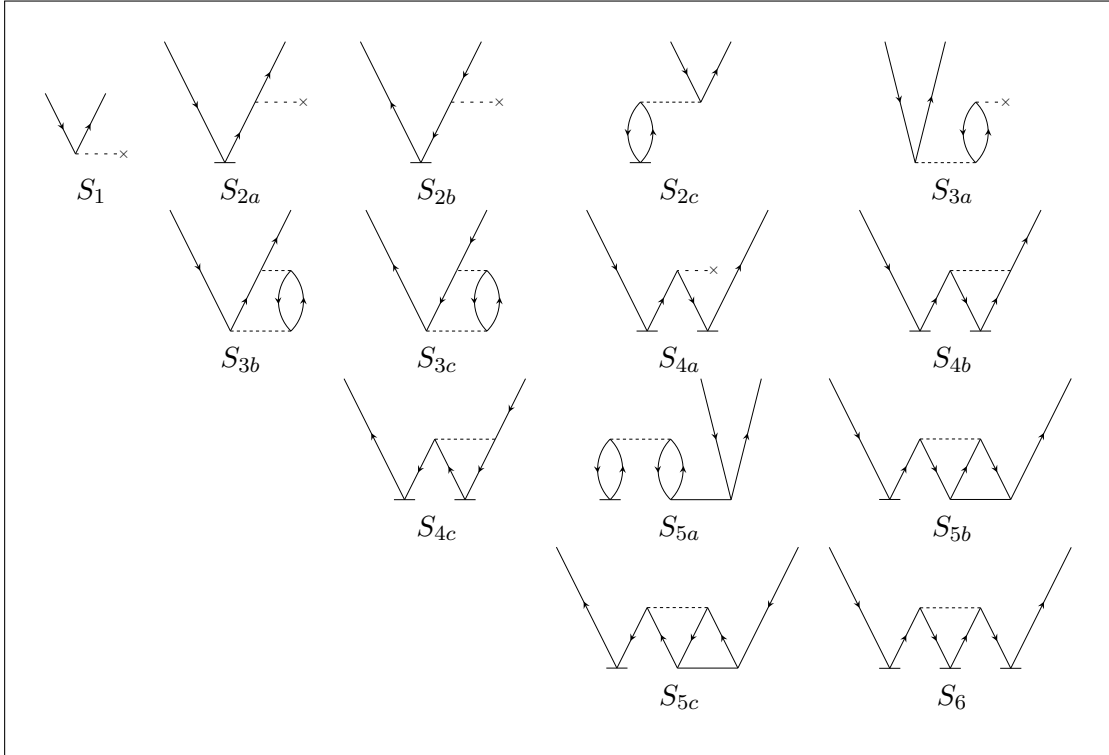


Figure 5.6: Diagrams of the \hat{T}_1 amplitude equation Eq. (5.97)

Table 5.1: Algebraic expression of \hat{T}_1 -amplitude diagrams from Fig. 5.6

Interaction	Contraction	ϵ	Diagram	Expression
$\langle \Phi_i^a \hat{H}_N \Phi_0 \rangle$	$\hat{F}_{N,4}$	+1	S_1	f_i^a
$\langle \Phi_i^a \hat{H}_N \hat{T}_1 \Phi_0 \rangle$	$\hat{F}_{N,1}$	0	S_{2a}	$\sum_c f_c^a t_i^c$
$\langle \Phi_i^a \hat{H}_N \hat{T}_1 \Phi_0 \rangle$	$\hat{F}_{N,2}$	0	S_{2b}	$\sum_c^c f_i^k t_k^a$
$\langle \Phi_i^a \hat{H}_N \hat{T}_1 \Phi_0 \rangle$	$\hat{V}_{N,3}$	0	S_{2c}	$\sum_{kc} \langle ka \hat{v} ci \rangle t_k^c$
$\langle \Phi_i^a \hat{H}_N \hat{T}_2 \Phi_0 \rangle$	$\hat{F}_{N,3}$	-1	S_{3a}	$\sum_{kc} f_c^k t_{ik}^{ac}$
$\langle \Phi_i^a \hat{H}_N \hat{T}_2 \Phi_0 \rangle$	$\hat{V}_{N,4}$	-1	S_{3b}	$\frac{1}{2} \sum_{kcd} \langle ka \hat{v} cd \rangle t_{ki}^{cd}$
$\langle \Phi_i^a \hat{H}_N \hat{T}_2 \Phi_0 \rangle$	$\hat{V}_{N,5}$	-1	S_{3c}	$-\frac{1}{2} \sum_{klc} \langle kl \hat{v} ci \rangle t_{kl}^{ca}$
$\langle \Phi_i^a \frac{1}{2} \hat{H}_N \hat{T}_1^2 \Phi_0 \rangle$	$\hat{F}_{N,3}$	-1	S_{4a}	$-\sum_{kc} f_c^k t_i^c t_k^a$
$\langle \Phi_i^a \frac{1}{2} \hat{H}_N \hat{T}_1^2 \Phi_0 \rangle$	$\hat{V}_{N,4}$	-1	S_{4b}	$-\sum_{klc} \langle kl \hat{v} ci \rangle t_k^c t_l^a$
$\langle \Phi_i^a \frac{1}{2} \hat{H}_N \hat{T}_1^2 \Phi_0 \rangle$	$\hat{V}_{N,5}$	-1	S_{4c}	$\sum_{kcd} \langle ka \hat{v} cd \rangle t_k^c t_i^d$
$\langle \Phi_i^a \hat{H}_N \hat{T}_1 \hat{T}_2 \Phi_0 \rangle$	$\hat{V}_{N,9}$	-2	S_{5a}	$\sum_{klcd} \langle kl \hat{v} cd \rangle t_k^c t_{li}^{da}$
$\langle \Phi_i^a \hat{H}_N \hat{T}_1 \hat{T}_2 \Phi_0 \rangle$	$\hat{V}_{N,9}$	-2	S_{5b}	$-\frac{1}{2} \sum_{klcd} \langle kl \hat{v} cd \rangle t_{kl}^{ca} t_d^i$
$\langle \Phi_i^a \hat{H}_N \hat{T}_1 \hat{T}_2 \Phi_0 \rangle$	$\hat{V}_{N,9}$	-2	S_{5c}	$-\frac{1}{2} \sum_{klcd} \langle kl \hat{v} cd \rangle t_{ki}^{cd} t_l^a$
$\langle \Phi_i^a \frac{1}{3!} \hat{H}_N \hat{T}_1^3 \Phi_0 \rangle$	$\hat{V}_{N,9}$	-2	S_6	$-\sum_{klcd} \langle kl \hat{v} cd \rangle t_k^c t_i^d t_l^a$

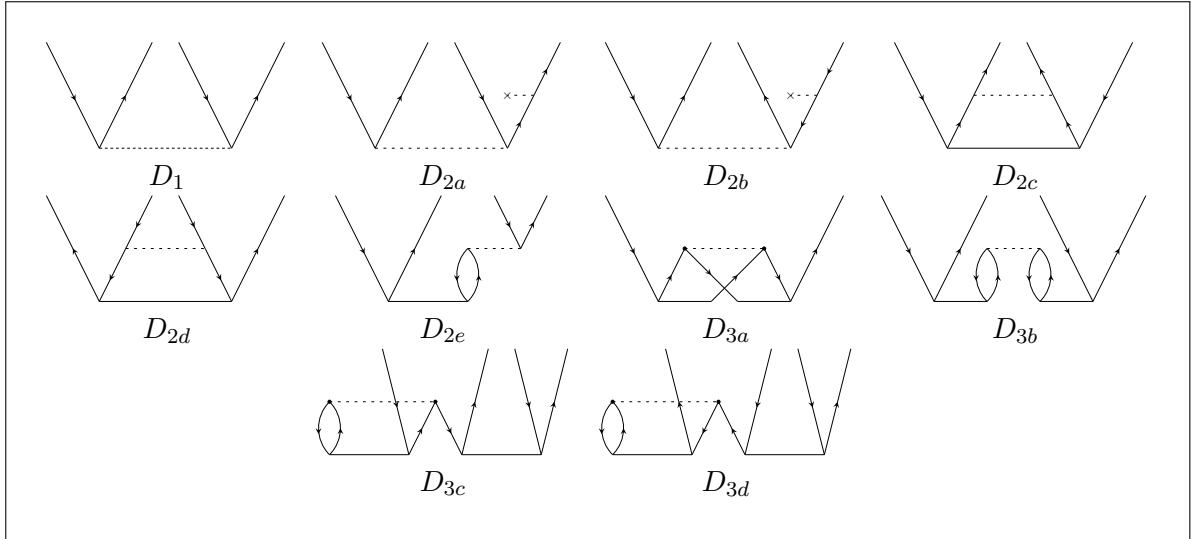
Figure 5.7: Diagrams of the \hat{T}_2 amplitude equation Eq. (5.98), with \hat{T}_2 contractions only (CCD)

Table 5.2: Algebraic expression of \hat{T}_2 -amplitude diagrams from Fig. 5.7

Interaction	Contraction	ϵ	Diagram	Expression
$\langle \Phi_{ij}^{ab} \hat{H}_N \Phi_0 \rangle$	$\hat{V}_{N,8}$	+2	D_1	$\langle ab \hat{v} ij \rangle$
$\langle \Phi_{ij}^{ab} \hat{H}_N \hat{T}_2 \Phi_0 \rangle$	$\hat{F}_{N,1}$	0	D_{2a}	$P(ab) \sum_c f_c^b t_{ij}^{ac}$
$\langle \Phi_{ij}^{ab} \hat{H}_N \hat{T}_2 \Phi_0 \rangle$	$\hat{F}_{N,2}$	0	D_{2b}	$-P(ij) \sum_k f_j^k t_{ik}^{ab}$
$\langle \Phi_{ij}^{ab} \hat{H}_N \hat{T}_2 \Phi_0 \rangle$	$\hat{V}_{N,1}$	0	D_{2c}	$\frac{1}{2} \sum_{cd} \langle ab \hat{v} cd \rangle t_{ij}^{cd}$
$\langle \Phi_{ij}^{ab} \hat{H}_N \hat{T}_2 \Phi_0 \rangle$	$\hat{V}_{N,2}$	0	D_{2d}	$\frac{1}{2} \sum_{kl} \langle kl \hat{v} ij \rangle t_{kl}^{ab}$
$\langle \Phi_{ij}^{ab} \hat{H}_N \hat{T}_2 \Phi_0 \rangle$	$\hat{V}_{N,3}$	0	D_{2e}	$P(ij)P(ab) \sum_{kc} \langle kb \hat{v} cj \rangle t_{ik}^{ac}$
$\langle \Phi_{ij}^{ab} \frac{1}{2} \hat{H}_N \hat{T}_2^2 \Phi_0 \rangle$	$\hat{V}_{N,9}$	-2	D_{3a}	$\frac{1}{4} \sum_{klcd} \langle kl \hat{v} cd \rangle t_{ij}^{ac} t_{kl}^{ab}$
$\langle \Phi_{ij}^{ab} \frac{1}{2} \hat{H}_N \hat{T}_2^2 \Phi_0 \rangle$	$\hat{V}_{N,9}$	-2	D_{3b}	$P(ij) \sum_{klcd} \langle kl \hat{v} cd \rangle t_{ik}^{ac} t_{jl}^{bd}$
$\langle \Phi_{ij}^{ab} \frac{1}{2} \hat{H}_N \hat{T}_2^2 \Phi_0 \rangle$	$\hat{V}_{N,9}$	-2	D_{3c}	$-\frac{1}{2} P(ij) \sum_{klcd} \langle kl \hat{v} cd \rangle t_{ik}^{dc} t_{lj}^{ab}$
$\langle \Phi_{ij}^{ab} \frac{1}{2} \hat{H}_N \hat{T}_2^2 \Phi_0 \rangle$	$\hat{V}_{N,9}$	-2	D_{3d}	$-\frac{1}{2} P(ab) \sum_{klcd} \langle kl \hat{v} cd \rangle t_{lk}^{ac} t_{ij}^{db}$

5.6 Concluding Remarks

5.6.1 Issues with the Coupled Cluster Method

The CC equations for the energy do not have a variational condition. The result of this is that we could in theory get lower energy than the *exact* when we truncate \hat{T} [13].

One of the fundamental postulates in quantum mechanics states that observables are eigenvalues to an Hermitian operator, but the similarity-transformed Hamiltonian $e^{-\hat{T}} \hat{H} e^{\hat{T}}$ is not Hermitian for any \hat{T} .

$$\left(e^{-\hat{T}} \hat{H} e^{\hat{T}} \right)^\dagger = e^{\hat{T}^\dagger} \hat{H} e^{-\hat{T}^\dagger} \neq e^{-\hat{T}} \hat{H} e^{\hat{T}} \quad (5.99)$$

The similarity-transformed Hamiltonian \hat{H}' and \hat{H} have the same eigenvalues:

Proof.

$$|\Psi\rangle = e^{\hat{T}} |\Phi_0\rangle$$

$$\hat{H} |\Psi\rangle = \hat{H} (e^{\hat{T}} |\Phi_0\rangle) = e^{\hat{T}} e^{-\hat{T}} \hat{H} e^{\hat{T}} |\Phi_0\rangle = e^{\hat{T}} \hat{H}' |\Phi_0\rangle = \lambda (e^{\hat{T}} |\Phi_0\rangle) = \lambda |\Psi\rangle$$

□

$|\Phi_0\rangle$ is the eigenfunction of \hat{H}' and $|\Psi\rangle$ is the eigenfunction of \hat{H} . Both gives the same eigenvalues. The $\hat{T} = \hat{T}_1$ gives us the Hartree-Fock approximation,

$$E_{CCSD} - E_0 = \sum_{ia} f_a^i t_i^a + \frac{1}{2} \sum_{ijab} \langle ij || \hat{v} || ab \rangle t_i^a t_j^b \quad (5.100)$$

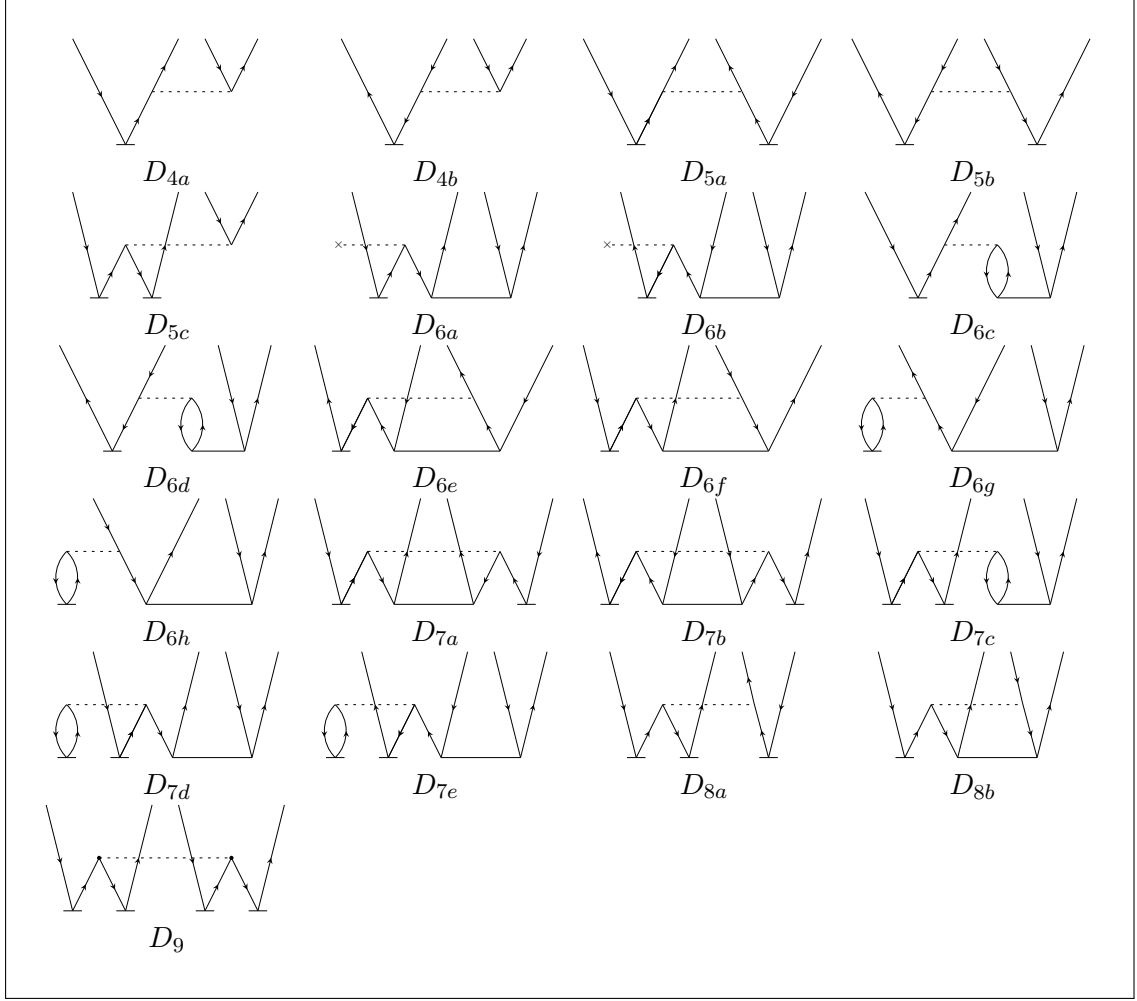


Figure 5.8: Diagrams of the \hat{T}_2 amplitude equation Eq. (5.98), with $\hat{T}_1 + \hat{T}_2$ contractions (CCSD)

and the expression for the \hat{T}_1 -amplitude

$$f_i^a + \sum_c f_c^a t_i^c + \sum_{kc} \langle ka || \hat{v} || ci \rangle t_k^c = 0 \quad (5.101)$$

Table 5.3: Algebraic expression of $\hat{T}_1 + \hat{T}_2$ -amplitude diagrams from Fig. 5.8

Interaction	Contraction	ϵ	Diagram	Expression
$\langle \Phi_{ij}^{ab} \hat{H}_N \hat{T}_1 \Phi_0 \rangle$	$\hat{V}_{N,6}$	+1	D_{4a}	$P(ij) \sum_c \langle ab \hat{v} cj \rangle t_i^c$
$\langle \Phi_{ij}^{ab} \hat{H}_N \hat{T}_1 \Phi_0 \rangle$	$\hat{V}_{N,7}$	+1	D_{4b}	$-P(ab) \sum_k \langle kb \hat{v} ij t_k^a \rangle$
$\langle \Phi_{ij}^{ab} \frac{1}{2} \hat{H}_N \hat{T}_1^2 \Phi_0 \rangle$	$\hat{V}_{N,1}$	0	D_{5a}	$\frac{1}{2} P(ij) \sum_{cd} \langle ab \hat{v} cd \rangle t_i^c t_j^d$
$\langle \Phi_{ij}^{ab} \frac{1}{2} \hat{H}_N \hat{T}_1^2 \Phi_0 \rangle$	$\hat{V}_{N,2}$	0	D_{5b}	$\frac{1}{2} P(ab) \sum_{kl} \langle kl \hat{v} ij \rangle t_k^a t_l^b$
$\langle \Phi_{ij}^{ab} \frac{1}{2} \hat{H}_N \hat{T}_1^2 \Phi_0 \rangle$	$\hat{V}_{N,3}$	0	D_{5c}	$-P(ij ab) \sum_{kc} \langle kb \hat{v} cj \rangle t_i^c t_k^a$
$\langle \Phi_{ij}^{ab} \hat{H}_N \hat{T}_1 \hat{T}_2 \Phi_0 \rangle$	$\hat{F}_{N,1}$	-1	D_{6a}	$-P(ij) \sum_{kc} f_c^k t_i^c t_{kj}^{ab}$
$\langle \Phi_{ij}^{ab} \hat{H}_N \hat{T}_1 \hat{T}_2 \Phi_0 \rangle$	$\hat{F}_{N,1}$	-1	D_{6b}	$-P(ab) \sum_{kc} f_c^k t_a^k t_{ij}^{cb}$
$\langle \Phi_{ij}^{ab} \hat{H}_N \hat{T}_1 \hat{T}_2 \Phi_0 \rangle$	$\hat{V}_{N,4}$	-1	D_{6c}	$P(ij ab) \sum_{kcd} \langle kd \hat{v} cd \rangle t_k^a t_{ij}^{cd}$
$\langle \Phi_{ij}^{ab} \hat{H}_N \hat{T}_1 \hat{T}_2 \Phi_0 \rangle$	$\hat{V}_{N,5}$	-1	D_{6d}	$-\frac{1}{2} P(ab) \sum_{kcd} \langle kb \hat{v} cd \rangle t_k^a t_{ij}^{cd}$
$\langle \Phi_{ij}^{ab} \hat{H}_N \hat{T}_1 \hat{T}_2 \Phi_0 \rangle$	$\hat{V}_{N,4}$	-1	D_{6e}	$P(ab) \sum_{kcd} \langle ka \hat{v} cd \rangle t_k^c t_{ij}^{db}$
$\langle \Phi_{ij}^{ab} \hat{H}_N \hat{T}_1 \hat{T}_2 \Phi_0 \rangle$	$\hat{V}_{N,5}$	-1	D_{6f}	$-P(ij ab) \sum_{klc} \langle kl \hat{v} ic \rangle t_i^c t_{kl}^{ab}$
$\langle \Phi_{ij}^{ab} \hat{H}_N \hat{T}_1 \hat{T}_2 \Phi_0 \rangle$	$\hat{V}_{N,4}$	-1	D_{6g}	$\frac{1}{2} P(ij) \sum_{klc} \langle kl \hat{v} cj \rangle t_i^c t_{kl}^{ab}$
$\langle \Phi_{ij}^{ab} \hat{H}_N \hat{T}_1 \hat{T}_2 \Phi_0 \rangle$	$\hat{V}_{N,5}$	-1	D_{6h}	$-P(ij) \sum_{klc} \langle kl \hat{v} ci \rangle t_k^c t_{lj}^{ab}$
$\langle \Phi_{ij}^{ab} \frac{1}{2} \hat{H}_N \hat{T}_1^2 \hat{T}_2 \Phi_0 \rangle$	$\hat{V}_{N,9}$	-2	D_{7a}	$\frac{1}{4} P(ij) \sum_{klcd} \langle kl \hat{v} cd \rangle t_i^c t_{kl}^{ab} t_j^d t_{lj}^{ab}$
$\langle \Phi_{ij}^{ab} \frac{1}{2} \hat{H}_N \hat{T}_1^2 \hat{T}_2 \Phi_0 \rangle$	$\hat{V}_{N,9}$	-2	D_{7b}	$\frac{1}{4} P(ab) \sum_{klcd} \langle kl \hat{v} cd \rangle t_k^a t_{ij}^{cd} t_l^b t_{lj}^{ab}$
$\langle \Phi_{ij}^{ab} \frac{1}{2} \hat{H}_N \hat{T}_1^2 \hat{T}_2 \Phi_0 \rangle$	$\hat{V}_{N,9}$	-2	D_{7c}	$-P(ij ab) \sum_{klcd} \langle kl \hat{v} cd \rangle t_i^c t_a^k t_{lj}^{db} t_{lj}^{ab}$
$\langle \Phi_{ij}^{ab} \frac{1}{2} \hat{H}_N \hat{T}_1^2 \hat{T}_2 \Phi_0 \rangle$	$\hat{V}_{N,9}$	-2	D_{7d}	$-P(ij) \sum_{klcd} \langle kl \hat{v} cd \rangle t_k^c t_i^d t_{lj}^{ab} t_{lj}^{ab}$
$\langle \Phi_{ij}^{ab} \frac{1}{2} \hat{H}_N \hat{T}_1^2 \hat{T}_2 \Phi_0 \rangle$	$\hat{V}_{N,9}$	-2	D_{7e}	$-P(ab) \sum_{klcd} \langle kl \hat{v} cd \rangle t_k^c t_l^a t_{ij}^{db} t_{lj}^{ab}$
$\langle \Phi_{ij}^{ab} \frac{1}{2} \hat{H}_N \hat{T}_1^2 \hat{T}_2 \Phi_0 \rangle$	$\hat{V}_{N,9}$	-2	D_{8a}	$\frac{1}{2} P(ij ab) \sum_{klc} \langle kl \hat{v} cd \rangle t_i^c t_{kl}^{ab} t_j^d t_{lj}^{ab}$
$\langle \Phi_{ij}^{ab} \frac{1}{2} \hat{H}_N \hat{T}_1^2 \hat{T}_2 \Phi_0 \rangle$	$\hat{V}_{N,9}$	-2	D_{8b}	$\frac{1}{2} P(ij ab) \sum_{klc} \langle kl \hat{v} cd \rangle t_i^c t_{kl}^{ab} t_j^d t_{lj}^{ab}$
$\langle \Phi_{ij}^{ab} \frac{1}{2} \hat{H}_N \hat{T}_1^2 \hat{T}_2 \Phi_0 \rangle$	$\hat{V}_{N,9}$	-2	D_9	$\frac{1}{4} P(ij ab) \sum_{klcd} \langle kl \hat{v} cd \rangle t_i^c t_j^d t_k^a t_l^b t_{lj}^{ab}$

Part III

Implementation and Results

Chapter 6

Implementations

”There’s beauty not just at the dimension of one centimeter; there’s also a beauty at smaller dimensions.” (From “What do you care what other people think?”)

R. P. Feynman

6.1 Implementation of the Configuration Class

The code-development made in this thesis is done in collaboration with Marte Hoel Jørgensen. Before we start getting into the algorithms, we first want to introduce the ”Configuration“-Class or just refer to it as ”Config”. This is the class that is linked both to the Hartree-Fock and The Coupled-Cluster program. It keeps track of our single particle orbital quantum numbers. We choose the harmonic oscillator functions as the basis functions. We have the following mapping of our basis.

$$\begin{aligned} |0\rangle &= \{n = 0, m = 0, m_s = -0.5\}, \\ |1\rangle &= \{n = 0, m = 0, m_s = 0.5\}, \\ |2\rangle &= \{n = 0, m = -1, m_s = -0.5\}, \\ |3\rangle &= \{n = 0, m = -1, m_s = 0.5\}, \\ |4\rangle &= \{n = 0, m = +1, m_s = -0.5\}, \\ |5\rangle &= \{n = 0, m = +1, m_s = 0.5\}. \end{aligned}$$

Our basis is numbered such that the lowest subshells are filled first, and there is a special sequence for doing this. From Eq. (2.59) we know that given shellnumber R and m we can find the radial quantum

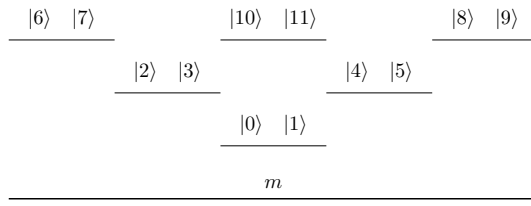


Figure 6.1: We fill the states such that the we start with the negative m valued subshells then the positive m ones, and last we label the $m = 0$ subshells. The spin down state m_s are always the even numbers.

number n by

$$n = \frac{R - 1 - |m|}{2}. \quad (6.1)$$

Next we want to tabulate pairs of states that have equal total $M = m_1 + m_2$ and $M_s = m_{s_1} + m_{s_2}$. This will be used later for the calculation of the interaction elements. For example for two shells we have

Algorithm 3 *Algorithm for the mapping*

1. Loop over *shellnumber*
2. Loop over $m = -(shellnumber - 1); m \leq 0; m = m + 2$
3. If $m \neq 0$ Then fill the $m < 0$ first and then $m > 0$ subshell
4. If $m = 0$ Fill this subshell

M	M_s	α	State
-2	0	1	$ 3, 2\rangle$
-1	-1	3	$ 2, 0\rangle$
-1	0	4	$ 3, 0\rangle$
-1	0	4	$ 2, 1\rangle$
-1	1	5	$ 3, 1\rangle$
0	-1	6	$ 4, 2\rangle$
0	0	7	$ 1, 0\rangle$
0	0	7	$ 5, 2\rangle$
0	0	7	$ 4, 3\rangle$
0	1	8	$ 5, 3\rangle$
1	-1	9	$ 4, 0\rangle$
1	0	10	$ 5, 0\rangle$
1	0	10	$ 4, 1\rangle$
1	1	11	$ 5, 1\rangle$
2	0	13	$ 5, 4\rangle$

Table 6.1: In this table we have paired orbitals with same M and M_s . Where $\alpha \in \{0, \dots, N\}$ and N is the number of pairs $\{M, M_s\}$. Notice that for $\alpha = 1$ we only have one pair, and for $\alpha = 4$, we have two pairs.

The algorithm for this is to loop over a pair of single-particle states and test if they have the same α value, i.e. the same $\{M, M_s\}$ -pair. This information is stored in the array `c_bc` which is a class member of the `config` class.

In this class there are also methods that distinguish between a hole-hole pair `c_hh`, particle-particle pair `c_pp` and particle-hole pair `c_ph` for a given α . This becomes useful later when we store the two-particle interaction elements.

Note that the states always are classified such that the biggest spin-orbital quantum numbers are labeled first, but this is not uniquely defined, so that the permutations must be considered as well. This is done in the calculations, where we make sure to permute where it needs to be permuted.

6.2 Implementation of the Restrictred Hartree-Fock Method

In this chapter we shall present the algorithms involved in the Restrictred Hartree-Fock Method (RHF) for a two-dimensional parabolic quantum dot. The restricted Hartree-Fock means that we only consider the closed shell systems, ie all the orbitals in the last shell are filled. We have implemented the Hartree-Fock Scheme presented in Chapter 4. The Hartree-Fock orbitals are expanded in a Harmonic Oscillator basis. The minima of the Hartree Fock Energy is found iteratively and we use the identity-matrix as our first guess. A Hartree-Fock calculation is needed to accelerate the convergence of the coupled cluster energy.

6.2.1 Input

The input parameters of our system are

- nh is the number of holes in our systems
- np is the number of particles in our systems
- tol is the tolerance needed to stop the iteration
- max_iter is the maximum number of iteration
- $\langle \alpha|h|\beta \rangle$ is the one-particle interaction element
- $\langle \alpha\beta|v|\gamma\delta \rangle$ is the two-particle interaction element

The spin-orbital quantum numbers $|\alpha\rangle$ of our system are enumerated according to the config class. Next we need the single-particle interaction elements $\langle \alpha|h|\beta \rangle$, which we get from the config class. And we also need the two-particle interaction elements $\langle \alpha\beta|v|\gamma\delta \rangle$. Note that the interaction elements $\langle \alpha\beta|v|\gamma\delta \rangle$ are antisymmetrized.

$$\langle \alpha\beta|v|\gamma\delta \rangle_{AS} = \langle \alpha\beta|v|\gamma\delta \rangle - \langle \alpha\beta|v|\delta\gamma \rangle. \quad (6.2)$$

We will from here on use the notation $\langle \alpha\beta|v|\gamma\delta \rangle$ for the antisymmetric interaction $\langle \alpha\beta|v|\gamma\delta \rangle_{AS}$, if nothing else is specified.

6.2.2 Output

The program prints the Hartree-Fock energy for each iteration. When the energy has converged it use the unitary coefficient-matrix $C_{\alpha\beta}$ to create new single-particle interaction elements $\langle \alpha'|h|\beta' \rangle$ and two-particle interaction elements $\langle \alpha'\beta'|v|\gamma'\delta' \rangle$.

6.2.3 Validation of the Code

We validate the the Hartree-Fock code by testing the code for a given situation where we know the answer analytically, i.e. the non-interacting system [ref]. For $N = 2, 6, 12$ and 20 , the non-interacting energy is $2\hbar\omega$, $10\hbar\omega$, $28\hbar\omega$ and $60\hbar\omega$, respectively. However, this is merely an indication that the code is correct. In order to be satisfied we need to get the same results as [47],[52] and [50], for the interacting system.

6.2.4 Code Structure

The Program is structured into a class, with class methods. This makes the structure of the program flexible and we can modify functions without changing the whole program. The code is tailored for a parabolic quantum dot, but can easily be changed to deal with other quantum systems. As mentioned the Hartree-Fock program is linked up to the config class which establishes the mapping:

$$|\alpha\rangle \rightarrow |nmm_s\rangle. \quad (6.3)$$

And also pairs

$$|\alpha\beta\rangle \rightarrow |MM_s\rangle. \quad (6.4)$$

Where M is the total angular momentum

$$M = m_\alpha + m_\beta. \quad (6.5)$$

And the M_s is the total spin

$$M_s = m_{s_1} + m_{s_2}. \quad (6.6)$$

The single-particle interaction $\langle \alpha|h|\beta \rangle$ is diagonal for the harmonic oscillator basis

$$\langle \alpha|h|\beta \rangle = \delta_{\alpha\beta}\epsilon_\alpha \quad (6.7)$$

These interaction elements are stored in an array $\mathbf{sp}[\mathbf{n}]$, where \mathbf{n} is the index for the spin-orbital quantum number. $\mathbf{sp}[\mathbf{n}]$ is an array from the config class. The two-particle interaction elements have to be feed

in externally from a binary file generated by a program `tabulate.cc`, created by Simen Kvaal, see [43]. The binary file is stored with the first four quantum numbers $\alpha, \beta, \gamma, \delta$ as `short int` (This is because we operate mostly with at most 3 digit numbers), the fifth number is stored as a double and represent our interaction value. The number of elements are therefore given by

```
int number_of_elements = filestat.st_size / (sizeof (double) + 4 * sizeof (
short int));
```

We store all the four quantum numbers in a c++ vector struct `<string,double>` called `mymap`. The quantum numbers are stored as a string type in `mymap`, while the interaction value are stored as double, this can be regarded as a dictionary in Python language terms, where the quantum numbers are the *key*, and the interaction is the *value* from the key.

```
for (int i = 0; i < number_of_elements; i++) {
    Ifile.read((char*) &q, sizeof (short int));
    Ifile.read((char*) &r, sizeof (short int));
    Ifile.read((char*) &s, sizeof (short int));
    Ifile.read((char*) &t, sizeof (short int));
    Ifile.read((char*) &vvalue, sizeof (double));
    sprintf(key, "%d %d %d %d", q, r, s, t);
    mymap.insert(MapType::value_type(key, value));
}
```

The reason we want to store the two-particle interaction in such a way is to be able to search for the elements faster. We know that the Hamiltonian does not change spin nor the angular momentum. Therefore the only contribution from the two-particle elements are when M and M_s are conserved.

$$\langle MM_s | v | M' M'_s \rangle = \delta_{MM', M_s M'_s}. \quad (6.8)$$

```
for (int alpha = 0; alpha < Conf->dim_alpha; alpha++) {
    n1_map = 0;
    for (int n1 = 0; n1 < 2 * Conf->n_bc[alpha]; n1 += 2) {
        n2_map = 0;
        for (int n2 = 0; n2 < 2 * Conf->n_bc[alpha]; n2 += 2) {
            p = Conf->c_bc[alpha][n1];
            q = Conf->c_bc[alpha][n1 + 1];
            r = Conf->c_bc[alpha][n2];
            s = Conf->c_bc[alpha][n2 + 1];
            sprintf(configuration, "%d %d %d %d", p, q, r, s);
            search_value = mymap.find(configuration);
            v_matrix[alpha][n1_map][n2_map] = search_value->second;
            n2_map++;
        }
        n1_map++;
    }
}
```

For each `alpha`, i.e. $\{M, M_s\}$ - pair, we loop over pairs p, q and r, s and store the value in the three-dimensional array `v_matrix`, where `n1_map` and `n2_map` indicate which of the pairs that give contribution to our interaction elements. The number of pairs in each `alpha` would vary as we see in Table 6.1. So it is necessary to know the number of pairs for each `alpha` in advance. This information is stored in the array `n_bc` which is a class member of the `config` class.

The main Hartree-Fock program is initiated from the constructor of the `HF-iter` class.

```

HFinter::HFinter(int nh, int np, double tol, char *filename, Config *Conf) {
    this->Conf = Conf;
    this->iter = iter;
    this->filename = filename;
    this->tol = tol;
    shellnumber = int(-1 / 2 + sqrt(1 + 4 * (m_nh + m_np))) / 2);
    sp_states = shellnumber * (shellnumber + 1);
    max_mvalue = 2 * (shellnumber - 1);
    dim_alpha = 2 * (max_mvalue) * 3 + 3;

    //Set up the two-particle interaction
    setup_coulombmatrix();

    //Start Hartree Fock Iteration
    setup_hf();

    //Create new single-particle and two-particle interaction elements
    setup_coulombmatrix_hf();
} //end Constructor
    
```

The philosophy of the Hartree-Fock Method is to diagonalize the Hartree-Fock Hamiltonian

$$H_{\alpha,\beta}^{HF} = \begin{bmatrix} H_{11} & H_{12} & \dots & H_{1n} \\ H_{21} & H_{22} & \dots & H_{2n} \\ \vdots & \vdots & \ddots & \vdots \\ H_{n1} & H_{n2} & \dots & H_{nn} \end{bmatrix}, \quad (6.9)$$

where

$$H_{\alpha,\beta}^{HF} = \langle \alpha | h | \beta \rangle + \sum_a^N \sum_{\gamma\delta} C_{a\gamma}^* C_{a\delta}^* \langle \alpha\gamma | v | \beta\delta \rangle_{AS}. \quad (6.10)$$

The eigenvalue equation gives

$$H^{HF} \mathbf{C}_k = \lambda_k \mathbf{C}_k. \quad (6.11)$$

Where \mathbf{C}_k are our eigenvectors corresponding to the given eigenvalue λ_k . The eigenvector contains the expansion coefficients of the k -th HF-orbital Eq. 4.11. Since the HF-matrix are dependent on the coefficient vectors \mathbf{C}_k , the equation is non-linear and can be solved iteratively.

$$\mathbf{C}_k = \begin{pmatrix} C_{k1} \\ C_{k2} \\ C_{k3} \\ \vdots \\ C_{kn} \end{pmatrix}. \quad (6.12)$$

There are several LAPACK routines for diagonalization. And we could do this by brute force, but the HF-matrix is very sparse. The two-body operator v and the onebody operator h does not change the spin nor the angular momentum of the harmonic oscillator basis, therefore we can divide the HF-matrix into blocks of $\{m, m_s\}$. That is we can only couple spin-orbitals with the same m and m_s -values. For three shells we have the following block matrices

m	m_s	Block
-2	-0.5	$[H_{6,6}]$
-2	0.5	$[H_{7,7}]$
-1	-0.5	$[H_{2,2}]$
-1	0.5	$[H_{3,3}]$
0	-0.5	$\begin{bmatrix} H_{0,0} & H_{0,10} \\ H_{10,0} & H_{10,10} \end{bmatrix}$
0	0.5	$\begin{bmatrix} H_{1,1} & H_{1,11} \\ H_{11,1} & H_{11,11} \end{bmatrix}$
1	-0.5	$[H_{4,4}]$
1	0.5	$[H_{5,5}]$
2	-0.5	$[H_{8,8}]$
2	0.5	$[H_{9,9}]$

Table 6.2: Table of the block we have to diagonalize for three shells, note that the quantum numbers for our HF-basis are indicated as subscript. The corresponding eigenvectors are found and placed in

m	m_s	Block
-2	-0.5	$[C_{6,6}]$
-2	0.5	$[C_{7,7}]$
-1	-0.5	$[C_{2,2}]$
-1	0.5	$[C_{3,3}]$
0	-0.5	$\begin{bmatrix} C_{0,0} & C_{0,10} \\ C_{10,0} & C_{10,10} \end{bmatrix}$
0	0.5	$\begin{bmatrix} C_{1,1} & C_{1,11} \\ C_{11,1} & C_{11,11} \end{bmatrix}$
1	-0.5	$[C_{4,4}]$
1	0.5	$[C_{5,5}]$
2	-0.5	$[C_{8,8}]$
2	0.5	$[C_{9,9}]$

Table 6.3: Table of diagonalized blocks for 3 shells, note that eigenvectors C_{ka} are sorted, so that the lowest eigenvalue is in the leftmost place

The coefficient matrix is set to equal the identity matrix as our first guess $\mathbf{C}_{m,n} = \delta_{m,n}$.

Algorithm 4 *Hartree - Fock Algorithm*

1. Calculate $\langle \alpha|h|\beta \rangle$ and $\langle \alpha\beta|v|\gamma\delta \rangle$
2. Initialize $C_{n,m} = \delta_{n,m}$
3. Check if $E_{new} - E_{old} < tolerance$
 1. Calculate the HF matrix.
 2. Block-diagonalize the HF matrix and find the eigenvalues and eigenvectors
 3. Sort the eigenvalues and eigenvectors such that the lowest is $k = 0$ for \mathbf{C}_k
 4. Calculate the HF energy

Output: HF energy and new interaction elements $\langle a|h|b \rangle$ and $\langle ab|v|cd \rangle$

The new one-body interaction elements are defined in the new basis as

$$\langle a|h|b \rangle = \sum_{\alpha}^N \sum_{\beta}^N C_{a\alpha}^* C_{b\beta} \langle \alpha|h|\beta \rangle \quad (6.13)$$

And the two-body interaction elements

$$\langle ab|v|cd \rangle = \sum_{\alpha}^N \sum_{\beta}^N \sum_{\gamma}^N \sum_{\delta}^N C_{a\alpha}^* C_{b\beta}^* C_{c\gamma} C_{d\delta} \langle \alpha|\langle \beta|v|\gamma\delta \rangle. \quad (6.14)$$

The Hartree Fock energy is defined by

$$E_{HF} = \sum_{k=1}^{nh} \lambda_k + \frac{1}{2} \sum_{ab}^{nh} \sum_{\alpha\beta\gamma\delta}^N C_{a\alpha}^* C_{b\beta}^* C_{c\gamma} C_{d\delta} \langle \alpha|\langle \beta|v|\gamma\delta \rangle. \quad (6.15)$$

Where nh is the number of hole states in our system.

6.3 Implementation of the Coupled Cluster Singles and Doubles

In the following section we will give a general outline of our CCSD code. It is based on Magnus Pedersen Lohnes original code [47]. We (Yang Min Wang and Marte Hoel Joergensen) have jointly optimized the code so that it in some cases has run 200 times faster. The optimization include rewriting the expressions into matrix multiplication so that we could use OpenMP to make it run in parallel CPUs, and storing the interaction elements in a better way, so that we loop over the configurations that give contribution. It is here the config class becomes useful. In comparison the code in [47] used 36 hours to run 10 H.O. shells and 20 particles. While our optimized code are using 4 minutes and 20 seconds! Much of that is the overhead caused by Bliz++, and it's ineffective way of accessing elements in the memory.

The code still only calculates the energy and the amplitudes t_i^a and t_{ij}^{ab} for a closed shell system. The coupled code have a option to run a Hartree-Fock calculation. If we run the Hartree-Fock calculation it will get new single-particle and two-particle elements for the CCSD input.

6.3.1 Input

The input parameters of our system are

- nh is the number of holes in our systems
- np is the number of particles in our systems
- tol is the tolerance needed to stop the iteration
- max_iter is the maximum number of iteration
- $\langle \alpha|h|\beta \rangle$ is the one-particle interaction element
- $\langle \alpha\beta|v|\gamma\delta \rangle$ is the two-particle interaction element

The matrix elements $\langle \alpha|h|\beta \rangle$ and $\langle \alpha\beta|v|\gamma\delta \rangle$ are tabulated in a binary file with the ordering

- $\alpha \quad \beta \quad \langle \alpha|h|\beta \rangle$
- $\alpha \quad \beta \quad \gamma \quad \delta \quad \langle \alpha\beta|v|\gamma\delta \rangle$

$\alpha, \beta, \gamma, \delta$ are the single-particle quantum numbers mapped according to section 6.1

6.3.2 Output

The program prints the CCSD Energy for each iteration. When the energy has converged it has the option to write the T-amplitudes t_i^a and t_{ij}^{ab} to a textfile.

6.3.3 Validation of the Code

One of the first checks we can do is to run the code for the non-interacting case, where analytical expressions can be obtained. The program reproduce these results. Next we need to validate the with interacting part of the program.

The CCSD code should be compared to an exact diagonalization of the Hamiltonian for the two-particle. The ground state energies should be equal since we only have single and double excitation. The exact diagonalization is popularly called Full Configuration Interaction method (FCI) [42]. We will give a brief outline.

In general the Schrödinger equation can be solved as a matrix eigenvalue problem, section 1.3.2.

$$H|\Psi\rangle = E|\Psi\rangle, \quad (6.16)$$

where $|\Psi\rangle$ is a linear combination of Slater determinants

$$|\Psi\rangle = \sum_{i=1}^d C_i |\Phi_i\rangle. \quad (6.17)$$

Since our system is the parabolic dot, we will choose the Harmonic oscillator as our basis for the Slater determinant $|\Phi\rangle$

$$|\Phi\rangle = \frac{1}{\sqrt{N!}} \sum_p (-1)^p \hat{P} \prod_{i=1}^d |\alpha_i\rangle. \quad (6.18)$$

The basis

$$\mathcal{B} \equiv \{|\alpha_i\rangle\}_{i=1}^d. \quad (6.19)$$

The Hamiltonian in secondquantized form is given by

$$\hat{H} = \sum_{ij} \langle i|\hat{h}|j\rangle a_i^\dagger a_j + \frac{1}{4} \sum_{ijkl} \langle ij|\hat{v}|kl\rangle a_i^\dagger a_j^\dagger a_l a_k. \quad (6.20)$$

In principle $d \rightarrow \infty$ gives the exact energy eigenvalues and eigenvectors for Eq. (6.16), but we must truncate our model space, yielding an approximation to the eigenfunctions and eigenvalues. The diagonalization and the CCSD should give us the same energy given the same model space.

Using Wick's theorem Eq. (3.77), the matrix elements $H_{ij} = \langle \Phi_i|\hat{H}|\Phi_j\rangle$ can be evaluated in terms of $\langle \alpha|h|\beta\rangle$ and $\langle \alpha\beta|v|\gamma\delta\rangle$. The onebody part is defined by

$$\langle \alpha|h|\beta\rangle = \delta_{\alpha\beta} \epsilon_\alpha, \quad (6.21)$$

where

$$\epsilon_\alpha = 2n_\alpha + |m_\alpha| + 1. \quad (6.22)$$

The two-particle interaction elements $\langle \alpha\beta|v|\gamma\delta\rangle$ are found analytically from [62]. We are going to validate the CCSD code for the 2-electron case with 6 of the lowest basis functions $d = 6$, i.e. 2 H.O. shells. As in section 6.1 we have the following mapping

$$\begin{aligned} |0\rangle &= \{n = 0, m = 0, m_s = -0.5\} \\ |1\rangle &= \{n = 0, m = 0, m_s = 0.5\} \\ |2\rangle &= \{n = 0, m = -1, m_s = -0.5\} \\ |3\rangle &= \{n = 0, m = -1, m_s = 0.5\} \\ |4\rangle &= \{n = 0, m = +1, m_s = -0.5\} \\ |5\rangle &= \{n = 0, m = +1, m_s = 0.5\} \end{aligned}$$

Since the Coulomb interaction does not depend on spin nor the angular momentum, the only nonzero

$$\begin{array}{c} \begin{array}{cc} |2\rangle & |3\rangle \end{array} \qquad \begin{array}{cc} |4\rangle & |5\rangle \end{array} \\ \hline \begin{array}{cc} |0\rangle & |1\rangle \end{array} \\ \hline m \end{array} \longrightarrow$$

elements are

$$\langle M, M_s|v|M, M_s\rangle, \quad (6.23)$$

where

$$M = m_\alpha + m_\beta = m_\gamma + m_\delta = 0 \quad (6.24)$$

$$M_s = m_{s_\alpha} + m_{s_\beta} = m_{s_\gamma} + m_{s_\delta} = 0 \quad (6.25)$$

Then we can diagonalize for the cases

M	M_s	H	E
-2	0	$\begin{bmatrix} \langle 23 H 23 \rangle \end{bmatrix}$	$\begin{bmatrix} 4.86165 \end{bmatrix}$
-1	-1	$\begin{bmatrix} \langle 02 H 02 \rangle \end{bmatrix}$	$\begin{bmatrix} 3.62666 \end{bmatrix}$
-1	0	$\begin{bmatrix} \langle 03 H 03 \rangle & \langle 03 H 12 \rangle \\ \langle 12 H 03 \rangle & \langle 12 H 12 \rangle \end{bmatrix}$	$\begin{bmatrix} 3.62666 & 4.2533 \end{bmatrix}$
-1	1	$\begin{bmatrix} \langle 13 H 13 \rangle \end{bmatrix}$	$\begin{bmatrix} 3.6267 \end{bmatrix}$
0	-1	$\begin{bmatrix} \langle 24 H 24 \rangle \end{bmatrix}$	$\begin{bmatrix} 4.6267 \end{bmatrix}$
0	0	$\begin{bmatrix} \langle 01 H 01 \rangle & \langle 01 H 25 \rangle & \langle 01 H 34 \rangle \\ \langle 25 H 01 \rangle & \langle 25 H 25 \rangle & \langle 25 H 34 \rangle \\ \langle 34 H 01 \rangle & \langle 34 H 25 \rangle & \langle 34 H 34 \rangle \end{bmatrix}$	$\begin{bmatrix} 3.1523 & 4.6267 & 5.1976 \end{bmatrix}$

Table 6.4: Table of the blocks we have to diagonalize for two shells, where E are the eigenvalues. The diagonalization for $M > 0$ would be exactly the same as $M < 0$

In this case the lowest (groundstates) energy was

$$E = 3.1523, \quad (6.26)$$

which our coupled cluster program reproduces, see [47]. FCI could also be used to validate other CC schemes like CCSDT. For this we would need 3 particles in order to test the 3-particle-3-hole excitation. Since triples have at max 3-particle-3-hole excitations.

6.3.4 Code Structure

The code is structured such that `main.cpp` is linked to three *abstract* classes:

- **CCalgo**: Class containing the CCSD algorithm
 - `ccsd1`: A subclass of **CCalgo**
- **Fmatrix**: Class for handling the F-matrix
 - `fl`: A subclass of **Fmatrix**
- **Interaction**: Class for handling the interaction elements $\langle \alpha\beta|v|\gamma\delta \rangle$
 - `int1`: A subclass of **Interaction**

In addition linked to 3 regular classes:

- **Amplitudes**: Class for calculating the CCSD amplitudes t_i^a and t_{ij}^{ab} .
- **Config**: Class containing the one and two-particle basis map
- **Hfiter**: Class for calculating the Hartree-Fock and new interaction elements
- **DDot**: Class for calculating the interaction elements for our Double Dot

The reason we do this is to be able to expand the program to handle different physical problems in the future. The advantages of an abstract is that the subclasses can share the main class methods. The **CCalgo** class runs the CCSD algorithm and it goes like this. The first thing we do in our CCSD code is setting up the interaction elements $\langle pq|v|rs \rangle$, they are read from file and we want to structure those elements into six arrays:

$$\begin{aligned}
 \text{hhhh} &= \langle ij|v|kl \rangle \\
 \text{phhh} &= \langle aj|v|kl \rangle \\
 \text{pphh} &= \langle ab|v|kl \rangle \\
 \text{phph} &= \langle aj|v|bl \rangle \\
 \text{ppph} &= \langle ab|v|cl \rangle \\
 \text{pppp} &= \langle ab|v|cd \rangle
 \end{aligned}$$

Algorithm 5 *CCSD Algorithm*

1. Setup the model space: nh, np
2. Setup the F-matrix f_p^q and the two-particle interaction elements $\langle \alpha\beta|v|\gamma\delta \rangle$
3. Setup the reference energy $E_0 = \langle \Phi_0|\hat{H}|\Phi_0 \rangle$
4. Initialize the amplitudes t_i^a and t_{ij}^{ab}
5. Check if $E_{new} - E_{old} \leq tolerance$
 1. Calculate the Intermediates
 2. Calculate t_i^a -matrix elements
 3. Calculate t_{ij}^{ab} -matrix elements
 4. Calculate the energy E_{new}
 5. Calculate Set $E_{old} = E_{new}$

Output: HF energy and new interaction elements $\langle a|h|b \rangle$ and $\langle ab|v|cd \rangle$

Where $ijkl\dots$ denote the hole states, and $abcd\dots$ denote the particle states. If we stored the matrix $\langle pq|v|rs \rangle$ in a four dimensional array we would need $8np^4$ bytes of memory. In the case of 20 shells (420 one-particle states) we would need 232 GB! But many of the matrix-elements are zero and we do not need to store those. Since interaction-elements preserve total M and M_s , we can use the Config class to help us find the two-particle pairs that give a nonzero element, viz.

$$hhh[\alpha][1.pair][2.pair] = \langle \underbrace{\alpha\beta}_{1.pair} | v | \underbrace{\gamma\delta}_{2.pair} \rangle \quad (6.27)$$

where α points to the set $\{M, M_s\}$. This makes it possible to calculate for 20 H.O. shells, and we need about 8GB of memory space for this calculation, which is acceptable. Note that our interaction elements are antisymmetrized

$$\langle pq|v|rs \rangle = -\langle pq|v|sr \rangle.$$

This needs to be taken into account, when we use those matrix elements Eq. (6.27) The next step is to setup the single particle interaction elements and the F-matrix:

Fmatrix: CLASS implementation

Fmatrix is an abstract base class with one subclass f1. This class tabulates the single-particle matrix elements $\langle \alpha|h|\beta \rangle$ and they are used for calculating the F-matrix.

The sp-elements are provided in a text file, which is read and tabulated in the f1-class function *read_sp_energy*. See listing 6.1. The class stores the sp-elements in different two-dimensional arrays according to the placement of holes and particles in the element. This gives four different arrays

$$\begin{aligned} \mathbf{s_hh} &= \langle i|\hat{h}|j \rangle, \\ \mathbf{s_hp} &= \langle i|\hat{h}|a \rangle, \\ \mathbf{s_ph} &= \langle a|\hat{h}|i \rangle, \\ \mathbf{s_pp} &= \langle a|\hat{h}|b \rangle. \end{aligned} \quad (6.28)$$

where the subscript h denotes hole states, and the subscript p denotes particle states. Since we have

```

void f1::read_sp_energy(char* filename){
    // open and reading from file
    ifstream file(filename, ios_base::in);
    while(!file.eof()){
        // read <bra| = <q|
        file >> q;
        // read |ket> = |r>
        file >> r;
        // read single-particle energy <q|h_0|r>
        file >> value;

        if(q<(nh+np) && r<(nh+np)){
            if(q<nh && r<nh){
                s_hh[q][r] = value;
            }
            else if(q<nh && r>=nh){
                s_hp[q][r-nh] = value;
            }
            else if(q>=nh && r<nh){
                s_ph[q-nh][r] = value;
            }
            else if(q>=nh && r>=nh){
                s_pp[q-nh][r-nh] = value;
            }
        }
    }
    file.close();
} // end read_sp_energy

```

Listing 6.1: Illustration of the implemented Fmatrix class function read_sp_energy. See the text for description.

a orthogonal basis of harmonic oscillator functions, we only obtain contribution on the form

$$\begin{aligned} \mathbf{s_hh} &= \langle i | \hat{h} | i \rangle, \\ \mathbf{s_pp} &= \langle a | \hat{h} | a \rangle. \end{aligned}$$

However all possibilities are implemented making the code more general. Note that the rescaling of particles numbers encountered in the implementation of the *Interaction* class, is a necessary implementation also for this class, when creating the arrays.

The f1-class function *set_up_fmatrix* calculates the F-matrix defined as

$$f_q^p = \langle p | h | q \rangle + \sum_i^d \langle pi | v | qi \rangle. \quad (6.29)$$

where $pq \dots$ denotes both particle and hole states, i denotes hole states, d is the number of hole states, and the interaction elements are antisymmetrized. Listing 6.2 illustrates the implementation of *set_up_fmatrix*.

```

void f1::set_up_fmatrix(Interaction *interaction) {
    int i, j, k, l; // hole states
    int a, b; // particle states

    int n1_map, n2_map;

    // set up f_hh = <i|h_0|j> + SUM_k <i k||j k>
    for (i = 0; i < nh; i++) {
        for (j = 0; j < nh; j++) {
            f_hh[i][j] = s_hh[i][j];
        }
    }
}

```

```

}
for (int alpha = C->alpha_hh; alpha < C->dim_alpha_hh; alpha++) {
    n1_map = 0;
    for (int n1 = 0; n1 < 2 * C->n_hh[alpha]; n1 += 2) {
        i = C->c_hh[alpha][n1];
        j = C->c_hh[alpha][n1 + 1];
        n2_map = 0;
        for (int n2 = 0; n2 < 2 * C->n_hh[alpha]; n2 += 2) {
            k = C->c_hh[alpha][n2];
            l = C->c_hh[alpha][n2 + 1];
            if (j == l)
                f_hh[i][k] += interaction->hhhh[alpha][n1_map][n2_map];
            if (i == l)
                f_hh[j][k] -= interaction->hhhh[alpha][n1_map][n2_map];
            if (j == k)
                f_hh[i][l] -= interaction->hhhh[alpha][n1_map][n2_map];
            if (i == k)
                f_hh[j][l] += interaction->hhhh[alpha][n1_map][n2_map];
            n2_map++;
        }
        n1_map++;
    }
}

for (int alpha = 0; alpha < C->dim_alpha; alpha++) {
    n1_map = 0;
    for (int n1 = 0; n1 < 2 * C->n_ph[alpha]; n1 += 2) {
        a = C->c_ph[alpha][n1];
        l = C->c_ph[alpha][n1 + 1];
        n2_map = 0;
        for (int n2 = 0; n2 < 2 * C->n_hh[alpha]; n2 += 2) {
            i = C->c_hh[alpha][n2];
            j = C->c_hh[alpha][n2 + 1];
            if (l == j) {
                f_hp[i][a] += interaction->phhh[alpha][n1_map][n2_map];
                f_ph[a][i] += interaction->phhh[alpha][n1_map][n2_map];
            } else if (l == i) {
                f_hp[j][a] = f_hp[j][a] - interaction->phhh[alpha][n1_map][n2_map];
                f_ph[a][j] = f_ph[a][j] - interaction->phhh[alpha][n1_map][n2_map];
            }
            n2_map++;
        }
        n1_map++;
    }
}

// set up f_pp = <a|h_0|b> + SUM_k <a k|| b k>
for (a = 0; a < np; a++) {
    f_pp[a][a] = s_pp[a][a];
}

for (int alpha = C->alpha_ph; alpha < C->dim_alpha_ph; alpha++) {
    n1_map = 0;
    for (int n1 = 0; n1 < 2 * C->n_ph[alpha]; n1 += 2) {
        a = C->c_ph[alpha][n1];
        i = C->c_ph[alpha][n1 + 1];
        n2_map = 0;
        for (int n2 = 0; n2 < 2 * C->n_ph[alpha]; n2 += 2) {
            b = C->c_ph[alpha][n2];
            j = C->c_ph[alpha][n2 + 1];

```

```

        if (i == j)
            f_pp[a][b] += interaction->phph[alpha][n1_map][n2_map];
            n2_map++;
        }
        n1_map++;
    }
} // end set-up-fmatrix

```

Listing 6.2: code-snippet illustrating the implementation of the Fmatrix calculation. See the text for description.

The F-matrix is also tabulated according to the placement of holes and particles, thus we obtain four arrays

$$\begin{aligned}
 \mathbf{f_hh} &= f_i^j, \\
 \mathbf{f_hp} &= f_i^a, \\
 \mathbf{f_ph} &= f_a^i, \\
 \mathbf{f_pp} &= f_a^b.
 \end{aligned} \tag{6.30}$$

In listing 6.2 the implementation of $\mathbf{f_hh}$ and $\mathbf{f_pp}$ is shown explicit. The $\mathbf{C}\rightarrow$ is a pointer to the Config class, and $\mathbf{interaction}\rightarrow$ points to our Interaction class. Next step is to initialize the amplitudes t_i^a and t_{ij}^{ab} .

Amplitudes: CLASS implementation

Amplitudes is an abstract base class with the derived class `amp1`. This class implements the amplitude equations for both \hat{T}_1 and \hat{T}_2 . It calculates the amplitudes iteratively. In this section we present the implementation of the \hat{T}_1 and \hat{T}_2 amplitude equations..

\hat{T}_1 -amplitude equation

Consider the \hat{T}_1 -amplitude equation, note that the summation-notation is omitted. We rearrange this equation as follows:

$$\begin{aligned}
 0 &= f_i^a + \langle ja|v|bi\rangle t_j^b + \frac{1}{2} \langle aj|v|bc\rangle t_{ij}^{bc} + (f_b^a t_i^b + \langle aj|v|bc\rangle t_i^b t_j^c) \\
 &+ \left(-f_i^j t_j^a - f_b^j t_j^a t_i^b - \langle jk|v|ib\rangle t_j^a t_k^b - \langle jk|v|bc\rangle t_i^b t_j^a t_k^c - \frac{1}{2} \langle jk|v|bc\rangle t_j^a t_{ik}^{bc} \right) \\
 &+ \left(-\frac{1}{2} \langle jk|v|ib\rangle t_{jk}^{ab} - \frac{1}{2} \langle jk|v|bc\rangle t_i^b t_{jk}^{ac} \right) + (f_b^j t_{ij}^{ab} + \langle jk|v|bc\rangle t_j^b t_{ik}^{ac})
 \end{aligned} \tag{6.31}$$

which is equivalent to

$$\begin{aligned}
 0 &= f_i^a + \langle ja|v|bi\rangle t_j^b + \frac{1}{2} \langle aj|v|bc\rangle t_{ij}^{bc} + (f_b^a + \langle aj|v|bc\rangle t_j^c) t_i^b \\
 &- \left(f_i^j + f_b^j t_i^b + \langle jk|v|ib\rangle t_k^b + \langle jk|v|bc\rangle t_i^b t_k^c + \frac{1}{2} \langle jk|v|bc\rangle t_{ik}^{bc} \right) t_j^a \\
 &+ \frac{1}{2} (\langle jk|v|ic\rangle + \langle jk|v|bc\rangle t_i^b) t_{jk}^{ca} + (f_c^k + \langle jk|v|bc\rangle t_j^b) t_{ik}^{ac}
 \end{aligned} \tag{6.32}$$

In the above equation we have relabeled some of the indices in the last line, in order to extract a common amplitude from the parenthesis. We simplify this expression further by defining the parenthesis in Eq. (6.32) as intermediates. These intermediates are manipulated such that the matrix elements fit

the ordering of the six matrices implemented in the *Interaction* class.

$$\begin{aligned} [I1]_b^a &= f_b^a + \langle aj|v|bc\rangle t_j^c \\ &= f_b^a + \langle bc|v|aj\rangle t_j^c \end{aligned} \quad (6.33)$$

$$\begin{aligned} [I2]_c^k &= f_c^k + \langle jk|v|bc\rangle t_j^b \\ &= f_c^k + \langle bc|v|jk\rangle t_j^b \end{aligned} \quad (6.34)$$

$$\begin{aligned} [I3]_i^j &= f_i^j + f_b^j t_i^b + \langle jk|v|ib\rangle t_k^b + \langle jk|v|bc\rangle t_i^b t_k^c + \frac{1}{2} \langle jk|v|bc\rangle t_{ik}^{bc} \\ &= f_i^j + \langle jk|v|ib\rangle t_k^b + \frac{1}{2} \langle jk|v|bc\rangle t_{ik}^{bc} + \left(f_b^j + \langle cb|v|kj\rangle t_k^c \right) t_i^b \\ &= f_i^j - \langle bi|v|jk\rangle t_k^b + \frac{1}{2} \langle bc|v|jk\rangle t_{ik}^{bc} + [I2]_b^j t_i^b \end{aligned} \quad (6.35)$$

$$\begin{aligned} [I4]_{ic}^{jk} &= \langle jk|v|ic\rangle + \langle jk|v|bc\rangle t_i^b \\ &= -\langle ci|v|jk\rangle + \frac{1}{2} \langle bc|v|jk\rangle t_i^b + \frac{1}{2} \langle bc|v|jk\rangle t_i^b \\ &= [I5]_{ic}^{jk} + \frac{1}{2} \langle bc|v|jk\rangle t_i^b \end{aligned} \quad (6.36)$$

$$[I5]_{ic}^{jk} = -\langle ci|v|jk\rangle + \frac{1}{2} \langle bc|v|jk\rangle t_i^b \quad (6.37)$$

We insert these definitions into Eq. (6.32), and obtain the \hat{T}_1 amplitude equation:

$$\begin{aligned} 0 &= f_i^a - \langle aj|v|bi\rangle t_j^b + \frac{1}{2} \langle bc|v|aj\rangle t_{ij}^{bc} + [I1]_b^a t_i^b \\ &\quad - [I3]_i^j t_j^a + \frac{1}{2} [I4]_{ic}^{jk} t_{jk}^{ca} + [I2]_c^k t_{ik}^{ac} \end{aligned} \quad (6.38)$$

Next we wish to obtain an equation for the \hat{T}_1 amplitude t_i^a . We accomplish this by performing the trick of adding and subtracting the t_i^a amplitude inside Eq. (6.38). Each term containing a t_x^y amplitude is expressed in terms of the t_i^a amplitude, and added to the equation. This added term is then subtracted by including the original expression multiplied by one or more delta-functions. Thus we obtain

$$\begin{aligned} 0 &= f_i^a - \langle ai|v|ai\rangle t_i^a - (1 - \delta_{ab}\delta_{ij}) \langle aj|v|bi\rangle t_j^b + \frac{1}{2} \langle bc|v|aj\rangle t_{ij}^{bc} \\ &\quad + [I1]_a^a t_i^a + (1 - \delta_{ab}) [I1]_b^a t_i^b - [I3]_i^i t_i^a - (1 - \delta_{ij}) [I3]_i^j t_j^a \\ &\quad + \frac{1}{2} [I4]_{ic}^{jk} t_{jk}^{ca} + [I2]_c^k t_{ik}^{ac} \end{aligned} \quad (6.39)$$

We are now able to extract an equation for the amplitude t_i^a , which reads

$$\begin{aligned} t_i^a &= \frac{1}{D_i^a} \left(f_i^a + \frac{1}{2} \langle bc|v|aj\rangle t_{ij}^{bc} - (1 - \delta_{ab}\delta_{ij}) \langle aj|v|bi\rangle t_j^b \right. \\ &\quad \left. + (1 - \delta_{ab}) [I1]_b^a t_i^b - (1 - \delta_{ij}) [I3]_i^j t_j^a + \frac{1}{2} [I4]_{ic}^{jk} t_{jk}^{ca} + [I2]_c^k t_{ik}^{ac} \right) \end{aligned} \quad (6.40)$$

where D_i^a is given as

$$D_i^a = \langle ai|v|ai\rangle - [I1]_a^a + [I3]_i^i \quad (6.41)$$

The Eq. (6.40) is implemented in the class function `t1_uncoupled_calc`, which is illustrated in Listing 6.3. The implementation of the intermediates will be presented after the derivation of the \hat{T}_2 amplitude equation.

```

void Amplitudes::t1_uncoupled_calc(){
    // calculate t1 intermediates
    t1_uncoupled_intermediates();

    // f_i^a
    for (i=0; i<np; i++){
        for (j=0; j<nh; j++){
            t1[i][j] = F->f_ph[i][j];
        }
    }

    // -(1-delta_{ab})delta_{ij}<aj|v|bi>t_{j}^{b}
    t1_uncoupled_term2(t1);

    // (1-delta_{ab})[I1]_{b}^{a} t_{i}^{b}
    t1_uncoupled_term3(t1);

    // -(1-delta_{ij})[I3]_{i}^{j} t_{j}^{a}
    t1_uncoupled_term4(t1);

    // 0.5<bc|v|aj>t_{ij}^{bc}
    t1_uncoupled_term5(t1);

    // 0.5[I4]_{ic}^{jk} t_{jk}^{ca}
    t1_uncoupled_term6(t1);

    // [I2]_{c}^{k} t_{ik}^{ac}
    t1_uncoupled_term7(t1);

    // calculate t1 denominator
    t1_uncoupled_denom(t1);
} //end t1_uncoupled_calc

```

Listing 6.3: Implementation of the amp1 class function t1_uncoupled_calc()

In Listing 6.3 `t1`, represents a two-dimensional array with dimension `t1[np][nh]`, containing all possible t_i^a amplitudes. We proceed by illustrating the implementation of the term-functions in *t1_uncoupled_calc*, which represent the terms in Eq. (6.40). First the algebraic expression is given, followed by its implementation. Note how we in these implementations loop effectively over contributing interaction elements only. This technique saves much cpu-time compared with the brute force technique of looping over all interaction elements. Also note that the intermediates are calculated prior to the `t1` calculations. These intermediates are tabulated in matrices carrying names including `barh`. These names are not correspondent with the algebraic notation utilized above, however the connection is seen from the algebraic expressions above the implementation. Here we have `B->` which points to the `Config` class.

$$t_i^a D_i^a \leftarrow -(1 - \delta_{ab} \delta_{ij}) \langle aj | v | bi \rangle t_j^b$$

```

void Amplitudes::t1_uncoupled_term2(double **t1) {
    for (alpha = 0; alpha < dim_alpha; alpha++) {
        map1 = 0;
        for (ph = 0; ph < phbcount[alpha]; ph += 2) {
            a = B->c_ph[alpha][ph];
            j = B->c_ph[alpha][ph + 1];
            map2 = 0;
            for (ph2 = 0; ph2 < phbcount[alpha]; ph2 += 2) {
                b = B->c_ph[alpha][ph2];
                i = B->c_ph[alpha][ph2 + 1];
                if (j != i || b != a) {
                    t1[a][i] = t1[a][i] - V->phph[alpha][map1][map2] * t1_old[b][j];
                }
            }
        }
    }
}

```

```

        }
        map2 += 1;
    }
    map1 += 1;
}
} // end t1_uncoupled_term2

```

Listing 6.4: implementation of the amp1 class function t1_uncoupled_term2()

$$t_i^a D_i^a \leftarrow (1 - \delta_{ab}) [I1]_b^a t_i^b$$

```

void Amplitudes::t1_uncoupled_term3(double **t1){

    for (a=0; a<np; a++){
        for (i=0; i<nh; i++){
            temp = 0.0;
            for (b=0; b<np; b++){
                if (b!=a){
                    temp = temp + barh_i02a[a][b]*t1_old[b][i];
                }
            }
            t1[a][i] = t1[a][i] + temp;
        }
    }

} // end t1_uncoupled_term3

```

Listing 6.5: implementation of the amp1 class function t1_uncoupled_term3()

$$t_i^a D_i^a \leftarrow -(1 - \delta_{ij}) [I3]_i^j t_j^a$$

```

void Amplitudes::t1_uncoupled_term4(double **t1){

    for (a=0; a<np; a++){
        for (i=0; i<nh; i++){
            temp = 0.0;
            for (j=0; j<nh; j++){
                if (j!=i){
                    temp = temp + barh_03[j][i]*t1_old[a][j];
                }
            }
            t1[a][i] = t1[a][i] - temp;
        }
    }

} // end t1_uncoupled_term4

```

Listing 6.6: implementation of the amp1 class function t1_uncoupled_term4()

$$t_i^a D_i^a \leftarrow \frac{1}{2} \langle bc|v|aj \rangle t_{ij}^{bc}$$

```

void Amplitudes::t1_uncoupled_term5(double **t1){

    for (alpha=0; alpha<dim_alpha; alpha++){
        for (i=0; i<nh; i++){
            map1=0;
            for (p=0; p<ppbcount[alpha]; p+=2){
                b = B->c_pp[alpha][p];
                c = B->c_pp[alpha][p+1];
                map2=0;
            }
        }
    }
}

```



```

for (ph=0; ph<phbcount[alpha]; ph+=2){
    a = B->c_ph[alpha][ph];
    j = B->c_ph[alpha][ph+1];
    t1[a][i] += 0.5*V->ppph[alpha][map1][map2]*t2_old[b][c][i][j];
    t1[a][i] -= 0.5*V->ppph[alpha][map1][map2]*t2_old[c][b][i][j];
    map2+=1;
}
map1+=1;
}
}
} // end t1_uncoupled_term5
    
```

Listing 6.7: implementation of the amp1 class function t1_uncoupled_term5()

$$t_i^a D_i^a \leftarrow \frac{1}{2} [I4]_{ic}^{jk} t_{jk}^{ca}$$

```

void Amplitudes::t1_uncoupled_term6(double **t1){
    for (a=0; a<np; a++){
        for (i=0; i<nh; i++){
            temp = 0.0;
            for (j=0; j<nh; j++){
                for (k=0; k<nh; k++){
                    for (c=0; c<np; c++){
                        temp = temp + barh_07[j][k][i][c]*t2_old[c][a][j][k];
                    }
                }
            }
            t1[a][i] = t1[a][i] + 0.5*temp;
        }
    }
} // end t1_uncoupled_term6
    
```

Listing 6.8: implementation of the amp1 class function t1_uncoupled_term6()

$$t_i^a D_i^a \leftarrow [I2]_c^k t_{ik}^{ac}$$

```

void Amplitudes::t1_uncoupled_term7(double **t1){
    for (a=0; a<np; a++){
        for (i=0; i<nh; i++){
            temp = 0.0;
            for (k=0; k<nh; k++){
                for (c=0; c<np; c++){
                    temp = temp + barh_01[k][c]*t2_old[a][c][i][k];
                }
            }
            t1[a][i] = t1[a][i] + temp;
        }
    }
} // end t1_uncoupled_term7
    
```

Listing 6.9: implementation of the amp1 class function t1_uncoupled_term7()

$$t_i^a \leftarrow \frac{t_i^a}{D_i^a} = t_i^a / (\langle ai|v|ai \rangle - [I1]_a^a + [I3]_i^i)$$

```

void Amplitudes::t1_uncoupled_denom(double **t1){

    double **C;
    C = new double*[np];
    for (a=0; a<np; a++){
        C[a] = new double[nh];
        for (i=0; i<nh; i++){
            C[a][i] = 0.0;
        }
    }

    //C = [I3]-[I1]
    for (i=0; i<nh; i++){
        for (a=0; a<np; a++){
            C[a][i] = barh_03[i][i] - barh_i02a[a][a];
        }
    }

    //C += <ai|v|ai>
    for (int alpha=0; alpha<dim_alpha; alpha++){
        map1=0;
        for (ph=0; ph<phbcount[alpha]; ph+=2){
            a = B->c_ph[alpha][ph];
            i = B->c_ph[alpha][ph+1];
            C[a][i] += V->phph[alpha][map1][map1];
            map1+=1;
        }
    }

    //t_i^a/D_i^a
    for (i=0; i<nh; i++){
        for (a=0; a<np; a++){
            t1[a][i] = t1[a][i]/C[a][i];
        }
    }

    //deallocating
    for (a=0; a<np; a++)
        delete [] C[a];
    delete [] C;

} // end t1_uncoupled_denom

```

Listing 6.10: implementation of the amp1 class function t1_uncoupled_denom()

\hat{T}_2 -amplitude equation

Consider the \hat{T}_2 -amplitude equation. Again note that the summation-notation is omitted. We rearrange this equation as follows:

$$0 = \langle ij|v|ab \rangle + \frac{1}{2} \langle ab|v|cd \rangle t_{ij}^{cd} \quad (6.42)$$

$$- \left(\hat{P}_{(ij)} f_j^k t_{ik}^{ab} + \hat{P}_{(ij)} f_c^k t_{kj}^{ab} + \hat{P}_{(ij)} \langle kl|v|ci \rangle t_k^c t_{jl}^{ba} + \hat{P}_{(ij)} \langle kl|v|cd \rangle t_k^c t_l^d t_{ij}^{ba} \right. \quad (6.43)$$

$$\left. + \frac{1}{2} \hat{P}_{(ij)} \langle kl|v|cd \rangle t_{ki}^{cd} t_{lj}^{ab} \right) \quad (6.44)$$

$$+ \frac{1}{2} \left(\langle kl|v|ij \rangle t_{kl}^{ab} + \hat{P}_{(ij)} \langle kl|v|cj \rangle t_i^c t_{kl}^{ab} + \frac{1}{2} \langle kl|v|cd \rangle t_{kl}^{ab} t_{ij}^{cd} + \frac{1}{2} \hat{P}_{(ij)} \langle kl|v|cd \rangle t_i^c t_{kl}^{ab} t_j^d \right) \quad (6.45)$$

$$+ \left(\hat{P}_{(ab)} f_c^b t_{ij}^{ac} - \hat{P}_{(ab)} f_c^k t_{kj}^{ac} + \hat{P}_{(ab)} \langle ka|v|cd \rangle t_k^c t_{ij}^{db} - \hat{P}_{(ab)} \langle kl|v|cd \rangle t_k^c t_l^a t_{ij}^{db} \right. \quad (6.46)$$

$$\left. - \frac{1}{2} \hat{P}_{(ab)} \langle kl|v|cd \rangle t_{kl}^{ca} t_{ij}^{db} \right) \quad (6.47)$$

$$+ \left(\hat{P}_{(ab)} \hat{P}_{(ij)} \langle kb|v|cj \rangle t_{ik}^{ac} + \hat{P}_{(ab)} \hat{P}_{(ij)} \langle ak|v|dc \rangle t_i^d t_{jk}^{bc} - \hat{P}_{(ab)} \hat{P}_{(ij)} \langle lk|v|ic \rangle t_l^a t_{kj}^{cb} \right. \quad (6.48)$$

$$\left. + \hat{P}_{(ab)} \hat{P}_{(ij)} \langle kl|v|cd \rangle t_i^c t_k^a t_{jl}^{bd} + \frac{1}{2} \hat{P}_{(ab)} \hat{P}_{(ij)} \langle kl|v|cd \rangle t_{ik}^{ac} t_{jl}^{bd} \right) \quad (6.49)$$

$$+ \left(-\hat{P}_{(ab)} \langle kb|v|ij \rangle t_k^a - \frac{1}{2} \hat{P}_{(ab)} \langle kb|v|cd \rangle t_k^a t_{ij}^{cd} - \hat{P}_{(ab)} \hat{P}_{(ij)} \langle kb|v|cj \rangle t_k^a t_i^c \right. \quad (6.50)$$

$$\left. - \frac{1}{2} \hat{P}_{(ab)} \hat{P}_{(ij)} \langle kb|v|cd \rangle t_k^a t_i^c t_j^d + \frac{1}{2} \hat{P}_{(ab)} \langle kl|v|ij \rangle t_k^a t_l^b + \frac{1}{4} \hat{P}_{(ab)} \langle kl|v|cd \rangle t_k^a t_{ij}^{cd} t_l^b \right. \quad (6.51)$$

$$\left. + \frac{1}{2} \hat{P}_{(ab)} \hat{P}_{(ij)} \langle kl|v|cj \rangle t_k^a t_i^c t_l^b + \frac{1}{4} \hat{P}_{(ab)} \hat{P}_{(ij)} \langle kl|v|cd \rangle t_k^a t_i^c t_l^b t_j^d \right) \quad (6.52)$$

$$+ \left(\hat{P}_{(ij)} \langle ab|v|cj \rangle t_i^c + \frac{1}{2} \hat{P}_{(ij)} \langle ab|v|cd \rangle t_i^c t_j^d \right) \quad (6.53)$$

This is equivalent to:

$$\begin{aligned} 0 = & \langle ij|v|ab \rangle + \frac{1}{2} \langle ab|v|cd \rangle t_{ij}^{cd} \\ & - \hat{P}_{(ij)} \left(f_i^l + f_c^l t_i^c + \langle kl|v|ci \rangle t_k^c + \langle kl|v|cd \rangle t_k^c t_l^d + \frac{1}{2} \langle kl|v|cd \rangle t_{ki}^{cd} \right) t_{lj}^{ab} \\ & + \frac{1}{2} \left(\langle kl|v|ij \rangle + \hat{P}_{(ij)} \langle lk|v|jc \rangle t_i^c + \frac{1}{2} \langle kl|v|cd \rangle t_{ij}^{cd} + \frac{1}{2} \hat{P}_{(ij)} \langle kl|v|cd \rangle t_i^c t_j^d \right) t_{kl}^{ab} \\ & + \hat{P}_{(ab)} \left(f_d^a - f_d^k t_k^a + \langle ka|v|cd \rangle t_k^c - \langle lk|v|cd \rangle t_l^c t_k^a - \frac{1}{2} \langle kl|v|cd \rangle t_{kl}^{ca} \right) t_{ij}^{db} \\ & + \hat{P}_{(ab)} \hat{P}_{(ij)} \left(\langle kb|v|cj \rangle + \langle bk|v|dc \rangle t_j^d - \langle lk|v|jc \rangle t_l^b - \langle kl|v|cd \rangle t_j^d t_l^b + \frac{1}{2} \langle kl|v|cd \rangle t_{jl}^{bd} \right) t_{ik}^{ac} \\ & - \hat{P}_{(ab)} \left(\langle kb|v|ij \rangle + \frac{1}{2} \langle kb|v|cd \rangle t_{ij}^{cd} + \hat{P}_{(ij)} \langle kb|v|cj \rangle t_i^c + \frac{1}{2} \hat{P}_{(ij)} \langle kb|v|cd \rangle t_i^c t_j^d \right. \\ & \quad \left. - \frac{1}{2} \langle kl|v|ij \rangle t_l^b - \frac{1}{4} \langle kl|v|cd \rangle t_{ij}^{cd} t_l^b - \frac{1}{2} \hat{P}_{(ij)} \langle kl|v|cj \rangle t_i^c t_l^b - \frac{1}{4} \hat{P}_{(ij)} \langle kl|v|cd \rangle t_i^c t_l^b t_j^d \right) t_k^a \\ & + \hat{P}_{(ij)} \left(\langle ab|v|cj \rangle + \frac{1}{2} \langle ab|v|cd \rangle t_j^d \right) t_i^c \end{aligned} \quad (6.54)$$

where we have relabeled some indices in the first, third and fourth parenthesis in order to extract common factors. We simplify this equation in a similar manner as for \hat{T}_1 , by defining intermediates. The intermediates corresponding to \hat{T}_2 are given explicitly below. Note that we manipulate these expressions so that they correspond to the six matrices defined in the *Interaction* class.

We recognize the first parenthesis of Eq. (6.54) as the intermediate $[I3]$, already defined for the \hat{T}_1

amplitude Eq. (6.35), viz...

$$\begin{aligned}
 [I3]_i^l &= f_i^l + f_c^l t_i^c + \langle kl|v|ci\rangle t_k^c + \langle kl|v|cd\rangle t_k^c t_i^d + \frac{1}{2} \langle kl|v|cd\rangle t_{ki}^{cd} \\
 &= f_i^l + \langle ci|v|kl\rangle t_k^c + \frac{1}{2} \langle cd|v|kl\rangle t_{ki}^{cd} + (f_c^l + \langle dc|v|kl\rangle t_k^d) t_i^c \\
 &= f_i^l - \langle ci|v|lk\rangle t_k^c + \frac{1}{2} \langle cd|v|lk\rangle t_{ik}^{cd} + (f_c^l + \langle cd|v|lk\rangle t_k^d) t_i^c \\
 &= f_i^l - \langle ci|v|lk\rangle t_k^c + \frac{1}{2} \langle cd|v|lk\rangle t_{ik}^{cd} + [I2]_c^l t_i^c
 \end{aligned} \tag{6.55}$$

The second parenthesis reads

$$\begin{aligned}
 [I6]_{ij}^{kl} &= \langle kl|v|ij\rangle + \hat{P}_{(ij)} \langle lk|v|jc\rangle t_i^c + \frac{1}{2} \langle kl|v|cd\rangle t_{ij}^{cd} + \frac{1}{2} \hat{P}_{(ij)} \langle kl|v|cd\rangle t_i^c t_j^d \\
 &= \langle kl|v|ij\rangle + \frac{1}{2} \langle cd|v|kl\rangle t_{ij}^{cd} + \hat{P}_{(ij)} \left(-\langle cj|v|lk\rangle + \frac{1}{2} \langle cd|v|kl\rangle t_j^d \right) t_i^c \\
 &= \langle lk|v|ji\rangle + \frac{1}{2} \langle dc|v|lk\rangle t_{ij}^{cd} + \hat{P}_{(ij)} \left(-\langle cj|v|lk\rangle + \frac{1}{2} \langle dc|v|lk\rangle t_j^d \right) t_i^c \\
 &= \langle lk|v|ji\rangle + \frac{1}{2} \langle dc|v|lk\rangle t_{ij}^{cd} + \hat{P}_{(ij)} [I5]_{jc}^{lk} t_i^c \\
 &= \langle kl|v|ij\rangle + \frac{1}{2} \langle cd|v|kl\rangle t_{ij}^{cd} + \hat{P}_{(ij)} [I5]_{ic}^{kl} t_j^c
 \end{aligned} \tag{6.56}$$

where the intermediate $[I5]$ is defined in Eq. (6.37). The third parenthesis reads

$$\begin{aligned}
 [I7]_d^a &= f_d^a - f_d^k t_k^a + \langle ka|v|cd\rangle t_k^c - \langle lk|v|cd\rangle t_l^c t_k^a - \frac{1}{2} \langle kl|v|cd\rangle t_{kl}^{ca} \\
 &= (f_d^a + \langle dc|v|ak\rangle t_k^c) - (f_d^k + \langle cd|v|lk\rangle t_l^c) t_k^a - \frac{1}{2} \langle cd|v|kl\rangle t_{kl}^{ca} \\
 &= [I1]_d^a - [I2]_d^k t_k^a - \frac{1}{2} \langle dc|v|kl\rangle t_{kl}^{ac}
 \end{aligned} \tag{6.57}$$

where the intermediates $[I1]$ and $[I2]$ are defined in Eqs. (6.33) and (6.34) respectively. The fourth parenthesis reads

$$\begin{aligned}
 [I8]_{cj}^{kb} &= \langle kb|v|cj\rangle + \langle bk|v|dc\rangle t_j^d - \langle lk|v|jc\rangle t_l^b - \langle kl|v|cd\rangle t_j^d t_l^b + \frac{1}{2} \langle kl|v|cd\rangle t_{jl}^{bd} \\
 &= \left(-\langle bk|v|cj\rangle + \frac{1}{2} \langle dc|v|bk\rangle t_j^d \right) + \frac{1}{2} \langle dc|v|bk\rangle t_j^d \\
 &\quad - \left(-\langle cj|v|lk\rangle + \frac{1}{2} \langle cd|v|kl\rangle t_j^d + \frac{1}{2} \langle cd|v|kl\rangle t_j^d \right) t_l^b \\
 &\quad + \frac{1}{2} \langle cd|v|kl\rangle t_{jl}^{bd} \\
 &= [I9]_{cj}^{kb} + \frac{1}{2} \langle dc|v|bk\rangle t_j^d - [I4]_{jc}^{lk} t_l^b + \frac{1}{2} \langle cd|v|kl\rangle t_{jl}^{bd}
 \end{aligned} \tag{6.58}$$

where $[I4]$ corresponds to Eq. (6.36) and $[I9]$ reads

$$[I9]_{cj}^{kb} = -\langle bk|v|cj\rangle + \frac{1}{2} \langle dc|v|bk\rangle t_j^d \tag{6.59}$$

The fifth parenthesis yields

$$\begin{aligned}
 [I10]_{ij}^{kb} &= \langle kb|v|ij\rangle + \frac{1}{2}\langle kb|v|cd\rangle t_{ij}^{cd} + \hat{P}_{(ij)}\langle kb|v|cj\rangle t_i^c + \frac{1}{2}\hat{P}_{(ij)}\langle kb|v|cd\rangle t_i^c t_j^d \\
 &\quad - \frac{1}{2}\langle kl|v|ij\rangle t_l^b - \frac{1}{4}\langle kl|v|cd\rangle t_{ij}^{cd} t_l^b - \frac{1}{2}\hat{P}_{(ij)}\langle kl|v|cj\rangle t_i^c t_l^b - \frac{1}{4}\hat{P}_{(ij)}\langle kl|v|cd\rangle t_i^c t_l^b t_j^d \\
 &= -\langle bk|v|ij\rangle - \frac{1}{2}\langle cd|v|bk\rangle t_{ij}^{cd} + \hat{P}_{(ij)}\left(-\langle bk|v|cj\rangle + \frac{1}{2}\langle dc|v|bk\rangle t_j^d\right) t_i^c \\
 &\quad - \frac{1}{2}\left(\langle kl|v|ij\rangle + \frac{1}{2}\langle cd|v|kl\rangle t_{ij}^{cd} + \hat{P}_{(ij)}\left(\langle cj|v|kl\rangle + \frac{1}{2}\langle cd|v|kl\rangle t_j^d\right) t_i^c\right) t_l^b \\
 &= -\langle bk|v|ij\rangle - \frac{1}{2}\langle cd|v|bk\rangle t_{ij}^{cd} + \hat{P}_{(ij)}[I9]_{cj}^{kb} t_i^c \\
 &\quad - \frac{1}{2}\left(\langle lk|v|ji\rangle + \frac{1}{2}\langle dc|v|lk\rangle t_{ij}^{cd} + \hat{P}_{(ij)}\left(-\langle cj|v|lk\rangle + \frac{1}{2}\langle dc|v|lk\rangle t_j^d\right) t_i^c\right) t_l^b \\
 &= -\langle bk|v|ij\rangle - \frac{1}{2}\langle cd|v|bk\rangle t_{ij}^{cd} + \hat{P}_{(ij)}[I9]_{cj}^{kb} t_i^c - \frac{1}{2}[I6]_{ij}^{kl} t_l^b
 \end{aligned} \tag{6.60}$$

Finally the sixth parenthesis yields

$$[I11]_{cj}^{ab} = \langle ab|v|cj\rangle + \frac{1}{2}\langle ab|v|cd\rangle t_j^d \tag{6.61}$$

We now reinsert these definitions into Eq. (6.54), and obtain the \hat{T}_2 amplitude equation

$$\begin{aligned}
 0 &= \langle ab|v|ij\rangle + \frac{1}{2}\langle ab|v|cd\rangle t_{ij}^{cd} - \hat{P}_{(ij)}[I3]_i^l t_{lj}^{ab} + \frac{1}{2}[I6]_{ij}^{kl} t_{kl}^{ab} \\
 &\quad + \hat{P}_{(ab)}[I7]_d^a t_{ij}^{db} + \hat{P}_{(ab)}\hat{P}_{(ij)}[I8]_{cj}^{kb} t_{ik}^{ac} - \hat{P}_{(ab)}[I10]_{ij}^{kb} t_k^a + \hat{P}_{(ij)}[I11]_{cj}^{ab} t_i^c
 \end{aligned} \tag{6.62}$$

Similarly, as for the \hat{T}_1 amplitude, we wish to obtain an equation for the \hat{T}_2 amplitude t_{ij}^{ab} . This is obtained by using the same technique as in the case of \hat{T}_1 , thus

$$\begin{aligned}
 0 &= \langle ab|v|ij\rangle + \frac{1}{2}\langle ab|v|ab\rangle t_{ij}^{ab} + \frac{1}{2}(1 - \delta_{ca}\delta_{db})\langle ab|v|cd\rangle t_{ij}^{cd} \\
 &\quad - \hat{P}_{(ij)}[I3]_i^l t_{lj}^{ab} - (1 - \delta_{il})\hat{P}_{(ij)}[I3]_i^l t_{lj}^{ab} + \frac{1}{2}[I6]_{ij}^{ij} t_{ij}^{ab} \\
 &\quad + \frac{1}{2}(1 - \delta_{ki}\delta_{lj})[I6]_{ij}^{kl} t_{kl}^{ab} + \hat{P}_{(ab)}[I7]_d^a t_{ij}^{db} + \hat{P}_{(ab)}(1 - \delta_{da})[I7]_d^a t_{ij}^{db} \\
 &\quad + \hat{P}_{(ab)}\hat{P}_{(ij)}[I8]_{cj}^{kb} t_{ik}^{ac} - \hat{P}_{(ab)}[I10]_{ij}^{kb} t_k^a + \hat{P}_{(ij)}[I11]_{cj}^{ab} t_i^c
 \end{aligned} \tag{6.63}$$

We extract the t_{ij}^{ab} amplitudes and obtain the t_{ij}^{ab} -amplitude equation

$$\begin{aligned}
 t_{ij}^{ab} &= \frac{1}{D_{ij}^{ab}} \left(\langle ab|v|ij\rangle + \frac{1}{2}(1 - \delta_{ca}\delta_{db})\langle ab|v|cd\rangle t_{ij}^{cd} - \hat{P}_{(ij)}(1 - \delta_{il})[I3]_i^l t_{lj}^{ab} \right. \\
 &\quad + \frac{1}{2}(1 - \delta_{ki}\delta_{lj})[I6]_{ij}^{kl} t_{kl}^{ab} + \hat{P}_{(ab)}(1 - \delta_{da})[I7]_d^a t_{ij}^{db} + \hat{P}_{(ab)}\hat{P}_{(ij)}[I8]_{cj}^{kb} t_{ik}^{ac} \\
 &\quad \left. - \hat{P}_{(ab)}[I10]_{ij}^{kb} t_k^a + \hat{P}_{(ij)}[I11]_{cj}^{ab} t_i^c \right)
 \end{aligned} \tag{6.64}$$

where

$$D_{ij}^{ab} = \hat{P}_{(ij)}[I3]_i^l - \frac{1}{2}\langle ab|v|ab\rangle - \frac{1}{2}[I6]_{ij}^{ij} - \hat{P}_{(ab)}[I7]_d^a \tag{6.65}$$

Eq. 6.64 is implemented in the `amp1` class function `t2_uncoupled_calc`, which is illustrated in Listing 6.11

```

void Amplitudes::t2_uncoupled_calc() {
    //calculating t2 intermediates
    t2_uncoupled_intermediates();
}
    
```

```

// <ab|v|ij>
for (a = 0; a < np; a++)
  for (b = 0; b < np; b++)
    for (i = 0; i < nh; i++)
      for (j = 0; j < nh; j++)
        t2[a][b][i][j] = 0.0;
for (int alpha = 0; alpha < dim_alpha; alpha++) {
  map1 = 0;
  for (i = 0; i < ppbcount[alpha]; i += 2) {
    a = B->c_pp[alpha][i];
    b = B->c_pp[alpha][i + 1];
    map2 = 0;
    for (j = 0; j < hhhcount[alpha]; j += 2) {
      m = B->c_hh[alpha][j];
      n = B->c_hh[alpha][j + 1];
      t2[a][b][m][n] = V->pphh[alpha][map1][map2];
      t2[b][a][m][n] = -V->pphh[alpha][map1][map2];
      t2[a][b][n][m] = -V->pphh[alpha][map1][map2];
      t2[b][a][n][m] = V->pphh[alpha][map1][map2];
      map2 += 1;
    }
    map1 += 1;
  }
}

// 0.5(1-delta_{ca}delta_{db}) <ab|v|cd> t_{ij}^{cd}
t2_uncoupled_term2(t2);

// -P_{ij}(1-delta_{il})[I3]_{i}^{l} t_{lj}^{ab}
t2_uncoupled_term3(t2);

// 0.5(1-delta_{ki}delta_{lj})[I6]_{ij}^{kl} t_{kl}^{ab}
t2_uncoupled_term4(t2);

// P_{ab}(1-delta_{da})[I7]_{d}^{a} t_{ij}^{db}
t2_uncoupled_term5(t2);

// P_{ab}P_{ij}[I8]_{cj}^{kb} t_{ik}^{ac}
t2_uncoupled_term6(t2);

// -P_{ab}[I10]_{ij}^{kb} t_{k}^{a}
t2_uncoupled_term7(t2);

// P_{ij}[I11]_{cj}^{ab} t_{i}^{c}
t2_uncoupled_term8(t2);

// calculating t2 denominator
t2_uncoupled_denom(t2);
} // end t2_uncoupled_calc

```

Listing 6.11: Implementation of the amp1 class function t2_uncoupled_calc()

In Listing 6.11, $t2$ represents the four-dimensional array with dimensions `[np] [np] [nh] [nh]`, containing all possible t_{ij}^{ab} amplitudes. Note how we are utilizing the *Config* class (B) and *Interaction* class (V) to get hold of the interaction elements in question. We proceed by illustrating the implementation of each term-function in *t2_uncoupled_calc*, corresponding to the terms of Eq. (6.64). In order to limit the implementation scope, standard procedures, like allocating arrays, are replaced by explanatory comments. The implementations are first presented in listings [6.12-6.19], followed by a more detailed description of

t2_uncoupled_term2 and t2_uncoupled_term4.

$$t_{ij}^{ab} D_{ij}^{ab} \leftarrow \frac{1}{2} (1 - \delta_{ca} \delta_{db}) \langle ab | v | cd \rangle t_{ij}^{cd}$$

```

void Amplitudes::t2_uncoupled_term2(double ****t2){

    /* allocate matrix C[dim_alpha][ppbcount[alpha]][nh*(nh-1)] */

    //filling of t2_pppp matrix = 2dimensional t2-old
    t2pppp_fill();

    //matrix multiplication
    for(alpha=0; alpha<dim_alpha; alpha++){
#pragma omp parallel default(shared) private(v,u,w)
    {
        nthreads = omp_get_num_threads();
#pragma omp for schedule(static)
        for(ab=0; ab<ppbcount[alpha]; ab++){
            for(ij=0; ij<temp; ij++){
                for(cd=0; cd<ppbcount[alpha]; cd++){
                    C[alpha][ab][ij] += 0.5*v_pppp[alpha][ab][cd]
                                     *t2_pppp[alpha][cd][ij];
                }
            }
        }
    }
    //translation from 2dim to 4dim
    translste(t2,C);

    /* deallocate matrix C */
} // end t2_uncoupled_term2

void Amplitudes::t2pppp_fill()
{
    for(int a=0; a<dim_alpha ; a++){
        for(int cd=0; cd<ppbcount[a]; cd+=2){
            map2=0;
            for(int ij=0; ij < 2*nh*(nh-1); ij+=2){
                t2_pppp[a][cd][map2] = t2_old[B->c_pp[a][cd]][B->c_pp[a][cd+1]]
                                     [ij_map[ij]][ij_map[ij+1]];
                t2_pppp[a][cd+1][map2] = t2_old[B->c_pp[a][cd+1]][B->c_pp[a][cd]]
                                     [ij_map[ij]][ij_map[ij+1]];
            }
            map2+=1;
        }
    }
} //end fill

void Amplitudes::translste(double ****t2, double*** C)
{
    for(int alpha=0; alpha<dim_alpha; alpha++){
        for(int ab=0; ab<ppbcount[alpha]; ab+=2){
            map1=0;
            for(int ij=0; ij < 2*nh*(nh-1); ij+=2){
                t2[B->c_pp[alpha][ab]][B->c_pp[alpha][ab+1]]
                [ij_map[ij]][ij_map[ij+1]] += C[alpha][ab][map1];
                t2[B->c_pp[alpha][ab+1]][B->c_pp[alpha][ab]]
                [ij_map[ij]][ij_map[ij+1]] += C[alpha][ab+1][map1];
            }
        }
    }
}

```

```

    map1+=1;
    }
  }
} //end translate

```

Listing 6.12: implementation of the amp1 class function t2_uncoupled_term2()

$$t_{ij}^{ab} D_{ij}^{ab} \leftarrow -\hat{P}_{(ij)}(1 - \delta_{il})[I3]_i^l t_{ij}^{ab}$$

```

void Amplitudes::t2_uncoupled_term3(double ****t2){

  /* allocating new matrix barh03[nh][nh], where if (i!=l)
  is implemented in form of zero elements along the diagonal*/
  for (i=0; i<nh-1; i++){
    for (l=i+1; l<nh; l++){
      barh03[i][l] = barh_03[i][l];
      barh03[l][i] = barh_03[l][i];
    }
  }
  for (i=0; i<nh; i++)
    barh03[i][i]=0.0;

  for (a=0; a<np-1; a++){
    for (b=a+1; b<np; b++){
      for (i=0; i<nh-1; i++){
        for (j=i+1; j<nh; j++){
          temp=0.0;
          for (l=0; l<nh; l++){
            temp -= barh03[l][i]*t2_old[a][b][l][j]
                  -barh03[l][j]*t2_old[a][b][l][i];
          }
          t2[a][b][i][j] += temp;
          t2[b][a][i][j] -= temp;
          t2[a][b][j][i] -= temp;
          t2[b][a][j][i] += temp;
        }
      }
    }
  }

  //deallocating matrix barh03
} // end t2_uncoupled_term3

```

Listing 6.13: implementation of the amp1 class function t2_uncoupled_term3()

$$t_{ij}^{ab} D_{ij}^{ab} \leftarrow \frac{1}{2}(1 - \delta_{ki}\delta_{lj})[I6]_{ij}^{kl} t_{kl}^{ab}$$

```

void Amplitudes::t2_uncoupled_term4(double ****t2){

  /* allocating matrix: A[np^2][nh^2], barh[nh^2][nh^2], C[np^2][nh^2] */
  //filling matrices A, barh:
  for (a=0; a<np; a++)
    for (b=0; b<np; b++)
      for (k=0; k<nh; k++)
        for (l=0; l<nh; l++)
          A[a*np+b][k*nh+l] = t2_old[a][b][k][l];
  for (k=0; k<nh; k++)
    for (l=0; l<nh; l++)
      for (i=0; i<nh; i++)

```



```

    for (j=0; j<nh; j++)
        if (i!=k || j!=1)
            barh[k*nh+1][i*nh+j] = barh_09[k][1][i][j];

    //matrix multiplication
#pragma omp parallel default(shared) private(v,u,w)
    {
        nthreads = omp_get_num_threads();
#pragma omp for schedule(static)
        for (ab=0; ab<np*np; ab++){
            for (ij=0; ij<nh*nh; ij++){
                for (kl=0; kl<nh*nh; kl++){
                    C[ab][ij] += 0.5*A[ab][kl]*barh[kl][ij];
                }
            }
        }
    }
    //translate
    for (a=0; a<np; a++){
        for (b=0; b<np; b++){
            for (i=0; i<nh; i++){
                for (j=0; j<nh; j++){
                    t2[a][b][i][j] = t2[a][b][i][j]+C[a*np+b][i*nh+j];
                }
            }
        }
    }
    //deallocating matrix A, barh, C
} // end t2_uncoupled_term4

```

Listing 6.14: implementation of the amp1 class function t2_uncoupled_term4()

$$t_{ij}^{ab} D_{ij}^{ab} \leftarrow \hat{P}_{(ab)} (1 - \delta_{da}) [I7]_d^a t_{ij}^{db}$$

```

void Amplitudes::t2_uncoupled_term5(double ****t2){
    /*allocating new matrix barh02[np][np], which implement
    if(a!=d) by introducing zero elements along the diagonal*/
    for (a=0; a<np-1; a++){
        for (d=a+1; d<np; d++){
            barh02[a][d] = barh_02[a][d];
            barh02[d][a] = barh_02[d][a];
        }
    }
    for (a=0; a<np; a++){
        barh02[a][a]=0.0;

        for (a=0; a<np-1; a++){
            for (b=a+1; b<np; b++){
                for (i=0; i<nh-1; i++){
                    for (j=i+1; j<nh; j++){
                        temp = 0.0;
                        for (d=0; d<np; d++){
                            temp += barh02[a][d]*t2_old[b][d][i][j]
                                -barh02[b][d]*t2_old[a][d][i][j];
                        }
                        t2[a][b][i][j] += temp;
                        t2[b][a][i][j] -= temp;
                        t2[a][b][j][i] -= temp;
                        t2[b][a][j][i] += temp;
                    }
                }
            }
        }
    }
}

```

```

    }
  }
}

//deallocating barh02
} // end t2_uncoupled_term5

```

Listing 6.15: implementation of the amp1 class function t2_uncoupled_term5()

$$t_{ij}^{ab} D_{ij}^{ab} \leftarrow \hat{P}_{(ab)} \hat{P}_{(ij)} [I8]_{cj}^{kb} t_{ik}^{ac}$$

```

void Amplitudes::t2_uncoupled_term6(double ****t2){

  /*allocating matrix: A[np*nh][np*nh], I[np*nh][np*nh], C[np*nh][np*nh] */

  //filling the matrices
  for(j=0; j<nh; j++){
    for(b=0; b<np; b++){
      for(c=0; c<np; c++){
        for(k=0; k<nh; k++){
          I[k*np+c][j*np+b]= barh.i10c[k][b][c][j];

        for(i=0; i<nh; i++){
          for(a=0; a<np; a++){
            for(c=0; c<np; c++){
              for(k=0; k<nh; k++){
                A[i*np+a][k*np+c] = t2_old[a][c][i][k];

              //multiplication
#pragma omp parallel default(shared) private(v,u,w)
              {
                nthreads = omp_get_num_threads();
#pragma omp for schedule (static)
                for(u=0; u<np*nh; u++){
                  for(v=0; v<np*nh; v++){
                    for(w=0; w<np*nh; w++){
                      C[u][v]+=A[u][w]*I[w][v];
                    }
                  }
                }
              }

              //translate
              for(a=0; a<np; a++){
                for(b=0; b<np; b++){
                  for(i=0; i<nh; i++){
                    for(j=0; j<nh; j++){
                      t2[a][b][i][j] += C[i*np+a][j*np+b];
                      t2[a][b][i][j] -= C[i*np+b][j*np+a];
                      t2[a][b][i][j] -= C[j*np+a][i*np+b];
                      t2[a][b][i][j] += C[j*np+b][i*np+a];
                    }
                  }
                }
              }
            }
          }
        }
      }
    }
  }
  //deallocate matrix: A, I, C
} // end t2_uncoupled_term6

```

Listing 6.16: implementation of the amp1 class function t2_uncoupled_term6()

$$t_{ij}^{ab} D_{ij}^{ab} \leftarrow -\hat{P}_{(ab)}[I10]_{ij}^{kb} t_k^a$$

```

void Amplitudes::t2_uncoupled_term7(double ****t2){

    /* t1 used instead if t1_old for a quicker convergence */
    for (a=0; a<np-1; a++){
        for (b=a+1; b<np; b++){
            for (i=0; i<nh-1; i++){
                for (j=i+1; j<nh; j++){
                    temp = 0.0;
                    for (k=0; k<nh; k++){
                        temp = temp + (barh_i12a[k][b][i][j]*t1[a][k]
                                      - barh_i12a[k][a][i][j]*t1[b][k]);
                    }
                    t2[a][b][i][j] -= temp;
                    t2[b][a][i][j] += temp;
                    t2[a][b][j][i] += temp;
                    t2[b][a][j][i] -= temp;
                }
            }
        }
    }
} // end t2_uncoupled_term7

```

Listing 6.17: implementation of the amp1 class function t2_uncoupled_term7()

$$t_{ij}^{ab} D_{ij}^{ab} \leftarrow \hat{P}_{(ij)}[I11]_{cj}^{ab} t_i^c$$

```

void Amplitudes::t2_uncoupled_term8(double ****t2){

    /* t1 used instead if t1_old for a quicker convergence*/
    for (alpha=0; alpha<dim_alpha; alpha++){
        for (p=0; p<ppbcount[alpha]; p+=2){
            a=B->c_pp[alpha][p];
            b=B->c_pp[alpha][p+1];
            for (j=0; j<nh; j++){
                for (i=0; i<nh; i++){
                    temp1=0.0;
                    temp2=0.0;
                    for (c=0; c<np; c++){
                        temp1 += (barh_i11a[a][b][c][j]*t1[c][i]
                                - barh_i11a[a][b][c][i]*t1[c][j]);
                    }
                    t2[a][b][i][j] +=temp1;
                    t2[b][a][i][j] -=temp1;
                }
            }
        }
    }
} // end t2_uncoupled_term8

```

Listing 6.18: implementation of the amp1 class function t2_uncoupled_term8()

$$t_{ij}^{ab} \leftarrow \frac{t_{ij}^{ab}}{D_{ij}^{ab}} = t_{ij}^{ab} / \left(\hat{P}_{(ij)}[I3]_i^i - \frac{1}{2} \langle ab|v|ab \rangle - \frac{1}{2} [I6]_{ij}^{ij} - \hat{P}_{(ab)}[I7]_a^a \right)$$

```

void Amplitudes::t2_uncoupled_denom(double ****t2){

```

```

/* allocating matrix C[np][np][nh][nh] */

for(a=0; a<np; a++){
  for(b=0; b<np; b++){
    h2ab = barh_02[a][a] + barh_02[b][b];
    for(j=0; j<nh; j++){
      for(i=0; i<nh; i++){
        h3ij = barh_03[i][i] + barh_03[j][j];
        h9ijij = 0.5*barh_09[i][j][i][j];
        C[a][b][i][j] = h3ij - h2ab - h9ijij;
      }
    }
  }
}

double temp;
for(alpha=0; alpha<dim_alpha; alpha++){
  map1=0;
  for(p=0; p<ppbcount[alpha]; p+=2){
    a= B->c_pp[alpha][p];
    b= B->c_pp[alpha][p+1];
    temp=0.5*V->pppp[alpha][map1][map1];
    for(i=0; i<nh; i++){
      for(j=0; j<nh; j++){
        C[a][b][i][j]-= temp;
        C[b][a][i][j]-= temp;
      }
    }
    map1+=1;
  }
}

for(b=0; b<np-1; b++){
  for(a=b+1; a<np; a++){
    for(j=0; j<nh-1; j++){
      for(i=j+1; i<nh; i++){
        t2[b][a][j][i] = t2[b][a][j][i]/C[b][a][j][i];
        t2[a][b][j][i] = -t2[b][a][j][i];
        t2[b][a][i][j] = -t2[b][a][j][i];
        t2[a][b][i][j] = t2[b][a][j][i];
      }
    }
  }
}

//deallocate matrix C
} // end t2_uncoupled_denom

```

Listing 6.19: implementation of the amp1 class function t2_uncoupled_denom()

Let us review the class function `t2_uncoupled_term2` and `t2_uncoupled_term4` in detail. We start with the former. The expression calculated in this function reads

$$\frac{1}{2}(1 - \delta_{ca}\delta_{db})\langle ab|v|cd\rangle t_{ij}^{cd}$$

Originally this calculation was implemented with brute force by M. P. Lohne, see illustration in listing 6.20.

```

void Amplitudes::t2_uncoupled_term2(Array<double,4> ans){

```

```

for (j=0; j<nh; j++){
  for (i=0; i<nh; i++){
    for (b=0; b<np; b++){
for (a=0; a<np; a++){
    temp = 0.0;
    for (d=0; d<np; d++){
      for (c=0; c<np; c++){
        if (a!=c || b!=d){
          temp = temp + V->pppp(a,b,c,d)*t2_old(c,d,i,j);
        }
      }
    }
    ans(a,b,i,j) = 0.5*temp;
  }
}
}
}
} // end t2_uncoupled_term2

```

Listing 6.20: M.P.Lohne's brute force implementation of amp1 class function t2_uncoupled_term2

The first simplification we make, is to utilize the two-particle basis embedded in the class *Config* (B->), and the corresponding interaction matrices in the class *Interaction* (V->). By coupling the a-loop and the b-loop into one loop over the c_pp in *Config*, and repeating this for the c-loop and the d-loop, we obtain the simplification illustrated in listing 6.21

```

void Amplitudes::t2_uncoupled_term2(double ****t2){

  for (alpha=0; alpha<dim_alpha; alpha++){
    for (j=0; j<nh; j++){
      for (i=0; i<nh; i++){
        map1=0;
for (p=0; p<ppbcount[alpha]; p+=2){
          a = B->c_pp[alpha][p];
          b = B->c_pp[alpha][p+1];
          map2=0;
for (p2=0; p2<ppbcount[alpha]; p2+=2){
            c = B->c_pp[alpha][p2];
            d = B->c_pp[alpha][p2+1];
            if (a!=e || b!=f){
              t2[a][b][i][j] = ans[a][b][i][j]
                + 0.5*V->pppp[alpha][map1][map2]*t2_old[c][d][i][j];
              t2[b][a][i][j] = ans[b][a][i][j]
                + 0.5*V->pppp[alpha][map1][map2]*t2_old[d][c][i][j];
            }
            if (b!=e || a!=f){
              t2[b][a][i][j] = ans[b][a][i][j]
                - 0.5*V->pppp[alpha][map1][map2]*t2_old[c][d][i][j];
              t2[a][b][i][j] = ans[a][b][i][j]
                - 0.5*V->pppp[alpha][map1][map2]*t2_old[d][c][i][j];
            }
            map2+=1;
          }
          map1+=1;
        }
      }
    }
  }
} // end t2_uncoupled_term2

```

Listing 6.21: illustrates the first simplification of M.P.Lohne's implementation of amp1 class function t2_uncoupled_term2

Next we notice in listing 6.20 that the interaction matrix **pppp** have two common indices with the four-dimensional matrix **t2_old**. Thus, this multiplication is in reality a matrix multiplication. Therefore, by mapping the four-dimensional **t2_old** into a two-dimensional matrix **t2_pppp**, we can replace these loops by a matrix multiplication. This matrix multiplication results in a significant speed up of our code. The new matrix **t2_pppp** is created in correspondence with the three-dimensional interaction matrix **pppp**. For each possible $\{M, M_s\}$ -value, we create a two-dimensional **t2_pppp**[*cd*][*ij*]-matrix. The common dimension [*cd*] is determined by the **c_pp** in *Config* class, while the dimension of [*ij*] reads

$$ij = nh \cdot (nh - 1)$$

This dimension equals the number of all pairs of *i* and *j*, where *i* and *j* are different. If *i* and *j* are equal it violates the Pauli exclusion principle. The mapping of *i* and *j* into one variable is obtained as illustrated in listing 6.22. We then create an array **ij_map** with twice the size of the [*ij*] dimension Eq. (6.3.4), and tabulate the pairs of *i* and *j* values constituting the new *ij* values. This mapping is performed once in the *Amplitudes* constructor.

```
//mapping i, j -> ij
int ij_map = new int [2*nh*(nh-1)];
temp=0;
for (int i=0; i<nh; i++){
    for (int j=0; j<nh; j++){
        if (i!=j){
            ij_map[temp]=i;
            ij_map[temp+1]=j;
            tmp+=2;
        }
    }
}
```

Listing 6.22: Illustrates the map of the two quantum numbers *i,j* into one number *ij*

We utilize this mapping when filling **t2_pppp**, and when we translate the new two-dimensional system back into the four-dimensional system of *t2*, see the functions **t2pppp_fill** and *translate* respectively, in listing 6.12. The matrix multiplication however, is not straightforward because of the if-statements in both listing 6.20 and 6.21. We therefore create a new interaction matrix **v_pppp**, where these if-statements are incorporated. We incorporate the if-statements by implementing the unwanted matrix elements as zero. The matrix multiplication between **t2_pppp** and **v_pppp** is then carried out, and $t2_{ij}^{ab}$ is obtained by translating back into a four-dimensional system, see listing 6.12.

Next we consider the class function **t2_uncoupled_term4**. This function performs the calculation of the following expression

$$\frac{1}{2}(1 - \delta_{ki}\delta_{lj})[I6]_{ij}^{kl} t_{kl}^{ab}$$

Originally this expression was implemented with brute force by M. P. Lohne, see illustration in listing 6.23

```
void Amplitudes::t2_uncoupled_term4(Array<double,4> ans){

    for (j=0; j<nh; j++){
        for (i=0; i<nh; i++){
            for (b=0; b<np; b++){
                for (a=0; a<np; a++){
                    temp = 0.0;
                    for (l=0; l<nh; l++){
                        for (k=0; k<nh; k++){
                            if (i!=k || j!=l){
                                temp = temp + barh_09(k,l,i,j)*t2_old(a,b,k,l);
                            }
                        }
                    }
                }
            }
        }
    }
    ans(a,b,i,j) = 0.5*temp;
```

```

    }
    }
    }
} // end t2_uncoupled_term4

```

Listing 6.23: M.P.Lohne’s brute force implementation of amp1 class function `t2_uncoupled_term4` [47]

In this implementation there is no direct connections to an interaction element, thus simplification utilizing the two-particle basis embedded in the class *Config* is not obtainable. However, we observe that the four-dimensional matrices `barh_09` and `t2_old` have two common indices `k` and `l`. This means that by mapping the matrices into a two-dimensional form, the performed calculation is equivalent to a matrix multiplication between `barh_09[kl][ij]` and `t2_old[ab][kl]`, which results in a matrix with dimension `[ab][ij]`. We create three new two-dimensional matrices, `barh` representing `barh_09[kl][ij]`, `A` representing `t2_old[ab][kl]`, and `C` for performing the multiplication. The mapping from four to two dimensions is performed with brute force when filling the matrices `A` and `barh` in listing 6.14. The dimensions thus read

$$\begin{aligned}
 ab &= a \cdot b = np^2 \\
 ij &= i \cdot j = nh^2 \\
 kl &= k \cdot l = nh^2
 \end{aligned}$$

Note how the if-statement is incorporated in the new matrix `barh`. From here the matrix multiplication is straightforward, and the final result for `t2` is obtained by mapping back into the four-dimensional system, in the same manner which we mapped into the two-dimensional system.

In both listing 6.12 and 6.14 we are utilizing Open Multi-Processing (OMP), which is an application for parallelizing programs in a shared memory environment. OMP provides tools which create and manage threads automatically, and this makes parallelizing a much easier job. Parallel computing refers to computations where many calculations are carried out simultaneously, such that large and time consuming problems can be divided between threads into smaller ones, and then solved concurrently. Pragmas are special compiler commands, providing the compiler with additional information. OMP contains a set of Pragmas that instructs the compiler to parallelized the code, but only if the compiler support OMP. The most basic pragma is the “`#pragma omp parallel`”, which denotes the region one wishes to parallelize. OMP is thereby a source to speed up our code. However, it is worth noticing that OMP can not run on different remote machines, like in a cluster of machines. This means that the speed up is limited by the number of processors on the single machine performing the calculation.

Intermediates

In the following we present the implementation of the intermediates for both amplitudes \hat{T}_1 and \hat{T}_2 . We calculate the intermediates since those terms appear more than one time in the CCSD equation. Then it would save us some computational time if we just calculate them once. We are not utilizing matrix multiplication when calculating the intermediates, even though this is possible in some of the calculations. We did not prioritize this implementation because the time consumption of calculating the intermediates did not imply that this would constitute a great speed up of our code.

$$[I1]_b^a = f_b^a + \langle bc|v|aj \rangle t_j^c$$

```

void Amplitudes::ccsd_uncoupled_barh_i02a_store() {
    //initializing barh_i02a ([I1]) by including f_{b}^{a}
    for(int a=0; a<np; a++){
        for(int b=a; b<np; b++){
            barh_i02a[a][b] = F->f_pp[a][b];
        }
    }
}

```

```

        barh_i02a[b][a] = F->f_pp[b][a];
    }
}
// calculating second term of [I1]
for(alpha=0; alpha<dim_alpha; alpha++){
    map1=0;
    for(p=0; p<ppbcount[alpha]; p+=2){
        b = B->c_pp[alpha][p];
        c = B->c_pp[alpha][p+1];
        map2=0;
        for(ph=0; ph<phbcount[alpha]; ph+=2){
            a = B->phbasis[alpha][ph];
            j = B->phbasis[alpha][ph+1];
            barh_i02a[a][b] += V->ppph[alpha][map1][map2]*t1[c][j];
            barh_i02a[a][c] -= V->ppph[alpha][map1][map2]*t1[b][j];
            map2+=1;
        }
        map1+=1;
    }
}
} //end [I1]

```

Listing 6.24: implementation of I1 in the amp1 class function ccscd_uncoupled_barh_i02a_store

$$[I2]_c^k = f_c^k + \langle bc|v|jk\rangle t_j^b$$

```

void Amplitudes::ccscd_uncoupled_barh_01_store() {
    //initializing barh_01 ([I2]) by including f_{c}^{\{k\}}
    for(int c=0; c<nh; c++){
        for(int k=0; k<np; k++){
            barh_01[c][k] = F->f_hp[c][k];
        }
    }
    //calculating second term of [I2]
    for(alpha=0; alpha<dim_alpha; alpha++){
        map1=0;
        for(p=0; p<ppbcount[alpha]; p+=2){
            c = B->c_pp[alpha][p];
            b = B->c_pp[alpha][p+1];
            map2=0;
            for(h=0; h<hhbcount[alpha]; h+=2){
                k = B->c_hh[alpha][h];
                j = B->c_hh[alpha][h+1];
                barh_01[k][c] += V->pphh[alpha][map1][map2]*t1[b][j];
                barh_01[k][b] -= V->pphh[alpha][map1][map2]*t1[c][j];
                barh_01[j][c] -= V->pphh[alpha][map1][map2]*t1[b][k];
                barh_01[j][b] += V->pphh[alpha][map1][map2]*t1[c][k];
                map2+=1;
            }
            map1+=1;
        }
    }
}
% } //end [I2]
%

```

Listing 6.25: implementation of I2 in the amp1 class function ccscd_uncoupled_barh_01_store

$$[I3]_i^j = f_i^j - \langle bi|v|jk\rangle t_k^b + \frac{1}{2} \langle bc|v|jk\rangle t_{ik}^{bc} + [I2]_b^j t_i^b$$


```

void Amplitudes::ccsd_uncoupled_barh_03_store(){

    //initializing barh_03 ([I3]) by including f- $\{i\}^{\{j\}}$ 
    for(int i=0; i<nh; i++){
        for(int j=i; j<nh; j++){
            barh_03[i][j] = F->f_hh[i][j];
            barh_03[j][i] = F->f_hh[j][i];
        }
    }
    //calculating [I2]
    for(j=0; j<nh; j++){
        for(i=0; i<nh; i++){
            for(b=0; b<np; b++){
                barh_03[j][i] = barh_03[j][i] + barh_01[j][b]*t1[b][i];
            }
        }
    }
    //calculating second term of [I3]
    for(alpha=0; alpha<dim_alpha; alpha++){
        map1=0;
        for(ph=0; ph<phbcount[alpha]; ph+=2){
            b = B->phbasis[alpha][ph];
            i = B->phbasis[alpha][ph+1];
            map2=0;
            for(h=0; h<hhbcount[alpha]; h+=2){
                j = B->c_hh[alpha][h];
                k = B->c_hh[alpha][h+1];
                barh_03[j][i] -= V->phhh[alpha][map1][map2]*t1[b][k];
                barh_03[k][i] += V->phhh[alpha][map1][map2]*t1[b][j];
                map2+=1;
            }
            map1+=1;
        }
    }
    //calculating third term of [I3]
    for(alpha=0; alpha<dim_alpha; alpha++){
        map1=0;
        for(p=0; p<ppbcount[alpha]; p+=2){
            b = B->c_pp[alpha][p];
            c = B->c_pp[alpha][p+1];
            map2=0;
            for(h=0; h<hhbcount[alpha]; h+=2){
                j = B->c_hh[alpha][h];
                k = B->c_hh[alpha][h+1];
                for(i=0; i<nh; i++){
                    barh_03[j][i] += V->pphh[alpha][map1][map2]*t2[b][c][i][k];
                    barh_03[k][i] -= V->pphh[alpha][map1][map2]*t2[b][c][i][j];
                }
                map2+=1;
            }
            map1+=1;
        }
    }
} //end [I3]

```

Listing 6.26: implementation of I3 in the amp1 class function ccsd_uncoupled_barh_03_store

$$[I4]_{ic}^{jk} = [I5]_{ic}^{jk} + \frac{1}{2} \langle bc|v|jk \rangle t_i^b$$

```

void Amplitudes::ccsd_uncoupled_barh_07_store(){

    //initializing barh_07 ([I4]) by including [I5]-{ic}^{jk}
    for(int j=0; j<nh; j++){
        for(int k=j; k<nh; k++){
            for(int i=0; i<nh; i++){
                for(int c=0; c<np; c++){
                    barh_07[j][k][i][c] = barh_i07a[j][k][i][c];
                    barh_07[k][j][i][c] = barh_i07a[k][j][i][c];
                }
            }
        }
    }

    //calculating second term of [I4]
    for(alpha=0; alpha<dim_alpha; alpha++){
        map1=0;
        for(p=0; p<ppbcount[alpha]; p+=2){
            b = B->c_pp[alpha][p];
            c = B->c_pp[alpha][p+1];
            map2=0;
            for(h=0; h<hhbcount[alpha]; h+=2){
                j = B->c_hh[alpha][h];
                k = B->c_hh[alpha][h+1];
                temp3 = 0.5 * V->pphh[alpha][map1][map2];
                for(i=0; i<nh; i++){
                    temp1 = temp3*t1[f][i];
                    temp2 = temp3*t1[e][i];
                    barh_07[j][k][i][c] += temp1;
                    barh_07[j][k][i][b] -= temp2;
                    barh_07[k][j][i][c] -= temp1;
                    barh_07[k][j][i][b] += temp2;
                }
                map2+=1;
            }
            map1+=1;
        }
    }
} //end [I4]

```

Listing 6.27: implementation of I4 in the amp1 class function ccsd_uncoupled_barh_07_store

$$[I5]_{ic}^{jk} = -\langle ci|v|jk\rangle + \frac{1}{2}\langle bc|v|jk\rangle t_i^b$$

```

void Amplitudes::ccsd_uncoupled_barh_i07a_store(){

    //calculating first term of [I5] (barh_i07a)
    for(alpha=0; alpha<dim_alpha; alpha++){
        map1=0;
        for(ph=0; ph<phbcount[alpha]; ph+=2){
            c = B->phbasis[alpha][ph];
            i = B->phbasis[alpha][ph+1];
            map2=0;
            for(h=0; h<hhbcount[alpha]; h+=2){
                j = B->c_hh[alpha][h];
                k = B->c_hh[alpha][h+1];
                barh_i07a[j][k][i][c] = -V->pphh[alpha][map1][map2];
                barh_i07a[k][j][i][c] = +V->pphh[alpha][map1][map2];
            }
            map2+=1;
        }
        map1+=1;
    }
}

```

```

    }
  }
  //calculating second term of [I5]
  for(alpha=0; alpha<dim-alpha; alpha++){
    map1=0;
    for(p=0; p<ppbcount[alpha]; p+=2){
      b = B->c_pp[alpha][p];
      c = B->c_pp[alpha][p+1];
      map2=0;
      for(h=0; h<hhbcount[alpha]; h+=2){
        j = B->c_hh[alpha][h];
        k = B->c_hh[alpha][h+1];
        temp3 = 0.5*V->pphh[alpha][map1][map2];
        for(i=0; i<nh; i++){
          temp1 = temp3*t1[b][i];
          temp2 = temp3*t1[c][i];
          barh_i07a[j][k][i][c] += temp1;
          barh_i07a[k][j][i][c] -= temp1;
          barh_i07a[k][j][i][b] += temp2;
          barh_i07a[j][k][i][b] -= temp2;
        }
        map2+=1;
      }
      map1+=1;
    }
  }
} //end [I5]

```

Listing 6.28: implementation of I5 in the amp1 class function ccsd_uncoupled_barh_i07a_store

$$[I6]_{ij}^{kl} = \langle kl|v|ij \rangle + \frac{1}{2} \langle cd|v|kl \rangle t_{ij}^{cd} + \hat{P}_{(ij)} [I5]_{ic}^{kl} t_j^c$$

```

void Amplitudes::ccsd_uncoupled_barh_09_store() {
  //calculating first term of [I6] (barh_09)
  for(alpha=0; alpha<dim-alpha; alpha++){
    map1=0;
    for(i=0; i<hhbcount[alpha]; i+=2){
      k = B->c_hh[alpha][i];
      l = B->c_hh[alpha][i+1];
      map2=0;
      for(j=0; j<hhbcount[alpha]; j+=2){
        i=B->c_hh[alpha][j];
        j=B->c_hh[alpha][j+1];
        barh_09[k][l][i][j] = V->hhhh[alpha][map1][map2];
        barh_09[k][l][j][i] = -V->hhhh[alpha][map1][map2];
        barh_09[l][k][i][j] = -V->hhhh[alpha][map1][map2];
        barh_09[l][k][j][i] = V->hhhh[alpha][map1][map2];
        map2+=1;
      }
      map1+=1;
    }
  }
  //calculating the [I5] term of [I6]
  for(k=0; k<nh; k++){
    for(l=0; l<nh; l++){
      for(i=0; i<nh; i++){
        for(j=0; j<nh; j++){
          temp = 0.0;
          for(c=0; c<np; c++){

```

```

        temp = temp + (barh_i07a[k][l][i][c]*t1[c][j]
                      - barh_i07a[k][l][j][c]*t1[c][i]);
    }
    barh_09[k][l][i][j] += temp;
}
}
}
}
//calculating second term of [I6]
for(alpha=0; alpha<dim_alpha; alpha++){
    map1=0;
    for(p=0; p<ppbcount[alpha]; p+=2){
        c = B->c_pp[alpha][p];
        d = B->c_pp[alpha][p+1];
        map2=0;
        for(h=0; h<hhbcount[alpha]; h+=2){
            k = B->c_hh[alpha][h];
            l = B->c_hh[alpha][h+1];
            for(j=0; j<nh; j++){
                for(i=0; i<nh; i++){
                    temp1 = V->pphh[alpha][map1][map2]*t2[c][d][i][j];
                    barh_09[k][l][i][j] += temp1;
                    barh_09[l][k][i][j] -= temp1;
                }
            }
            map2+=1;
        }
        map1+=1;
    }
}
} //end [I6]

```

Listing 6.29: implementation of I6 in the amp1 class function ccscd_uncoupled_barh_09_store

$$[I7]_d^a = [I1]_d^a - [I2]_d^k t_k^a - \frac{1}{2} \langle dc|v|kl \rangle t_{kl}^{ac}$$

```

void Amplitudes::ccscd_uncoupled_barh_02_store() {

    //initializing barh_02 ([I7]) by including [I1]
    for(int a=0; a<np; a++){
        for(int d=a; d<np; d++){
            barh_02[a][d] = barh_i02a[a][d];
            barh_02[d][a] = barh_i02a[d][a];
        }
    }
    //including the [I2] term
    for(a=0; a<np; a++){
        for(d=0; d<np; d++){
            for(k=0; k<nh; k++){
                barh_02[a][d] = barh_02[a][d] - barh_01[k][d] * t1[a][k];
            }
        }
    }
    //calculating the third term of [I7]
    for(alpha=0; alpha<dim_alpha; alpha++){
        for(a=0; a<np; a++){
            map1=0;
            for(p=0; p<ppbcount[alpha]; p+=2){
                d = B->c_pp[alpha][p];
                c = B->c_pp[alpha][p+1];
            }
        }
    }
}

```

```

map2=0;
for (h=0; h<hhbcount[alpha]; h+=2){
  k = B->c_hh[alpha][h];
  l = B->c_hh[alpha][h+1];
  temp1= V->pphh[alpha][map1][map2]*t2[a][c][k][l];
  temp2= V->pphh[alpha][map1][map2]*t2[a][d][k][l];
  barh_02[a][d] -=temp1;
  barh_02[a][c] +=temp2;
  map2+=1;
}
map1+=1;
}
}
} //end[I7]

```

Listing 6.30: implementation of I7 in the amp1 class function ccscd_uncoupled_barh_02_store

$$[I8]_{cj}^{kb} = [I9]_{cj}^{kb} + \frac{1}{2} \langle dc|v|bk \rangle t_j^d - [I4]_{jc}^{lk} t_l^b + \frac{1}{2} \langle cd|v|kl \rangle t_{jl}^{bd}$$

```

void Amplitudes::ccscd_uncoupled_barh_i10b_store() {

  //initializing barh_i10b, equivalent to calculating [I9]
  for (int k=0; k<nh; k++){
    for (int b=0; b<np; b++){
      for (int c=b; c<np; c++){
        for (int j=k; j<nh; j++){
          barh_i10b[k][b][c][j] = barh_i10a[k][b][c][j];
          barh_i10b[j][b][c][k] = barh_i10a[j][b][c][k];
          barh_i10b[k][c][b][j] = barh_i10a[k][c][b][j];
          barh_i10b[j][c][b][k] = barh_i10a[j][c][b][k];
        }
      }
    }
  }

  //calculating second term of [I8]
  for (alpha=0; alpha<dim_alpha; alpha++){
    map1=0;
    for (p=0; p<ppbcount[alpha]; p+=2){
      d = B->c_pp[alpha][p];
      c = B->c_pp[alpha][p+1];
      map2=0;
      for (ph=0; ph<phbcount[alpha]; ph+=2){
        b = B->phbasis[alpha][ph];
        k = B->phbasis[alpha][ph+1];
        temp = 0.5 * V->ppph[alpha][map1][map2];
        for (j=0; j<nh; j++){
          barh_i10b[k][b][c][j] += temp*t1[d][j];
          barh_i10b[k][b][d][j] -= temp*t1[c][j];
        }
        map2+=1;
      }
      map1+=1;
    }
  }

  //calculating 0.5*[I4]
  for (k=0; k<nh; k++){
    for (b=0; b<np; b++){
      for (c=0; c<np; c++){
        for (j=0; j<nh; j++){

```

```

    temp1=0.0;
    for(l=0; l<nh; l++){
        temp1 += 0.5 * barh_07[l][k][j][c]*t1[b][l];
    }
    barh_i10b[k][b][c][j]-=temp1;
}
}
}
}
} //end part of [I8]

void Amplitudes::ccsd_uncoupled_barh_i10c_store(){

//initializing barh_i10c ([I8]) by including barh_i10b
for(int k=0; k<nh; k++){
    for(int b=0; b<np; b++){
        for(int c=b; c<np; c++){
            for(int j=k; j<nh; j++){
                barh_i10c[k][b][c][j] = barh_i10b[k][b][c][j];
                barh_i10c[j][b][c][k] = barh_i10b[j][b][c][k];
                barh_i10c[k][c][b][j] = barh_i10b[k][c][b][j];
                barh_i10c[j][c][b][k] = barh_i10b[j][c][b][k];
            }
        }
    }
}
//calculating 0.5*[I4]
for(k=0; k<nh; k++){
    for(b=0; b<np; b++){
        for(c=0; c<np; c++){
            for(j=0; j<nh; j++){
                temp1=0.0;
                for(l=0; l<nh; l++){
                    temp1 += 0.5 * barh_07[l][k][j][c]*t1[b][l];
                }
                barh_i10b[k][b][c][j]-=temp1;
            }
        }
    }
}
//calculating last term of [I8]
for(b=0; b<np; b++){
    for(alpha=0; alpha<dim_alpha; alpha++){
        map1=0;
        for(p=0; p<ppbcount[alpha]; p+=2){
            d = B->c_pp[alpha][p];
            c = B->c_pp[alpha][p+1];
            map2=0;
            for(h=0; h<hhbcount[alpha]; h+=2){
                l = B->c_hh[alpha][h];
                k = B->c_hh[alpha][h+1];
                temp1 = 0.5*V->pphh[alpha][map1][map2];
                for(j=0; j<nh; j++){
                    barh_i10c[k][b][c][j] += temp1*t2[b][d][j][l];
                    barh_i10c[k][b][d][j] -= temp1*t2[b][c][j][l];
                    barh_i10c[l][b][c][j] -= temp1*t2[b][d][j][k];
                    barh_i10c[l][b][d][j] += temp1*t2[b][c][j][k];
                }
                map2+=1;
            }
            map1+=1;
        }
    }
}

```

```

    }
  }
}
} //end [I8]

```

Listing 6.31: implementation of I8 in the amp1 class function ccscd_uncoupled_barh_i10b_store and ccscd_uncoupled_barh_i10c_store

$$[I9]_{cj}^{kb} = -\langle bk|v|cj\rangle + \frac{1}{2}\langle dc|v|bk\rangle t_j^d$$

```

void Amplitudes::ccscd_uncoupled_barh_i10a_store() {
    //calculating first term of [I9] (barh_i10a)
    for (alpha=0; alpha<dim_alpha; alpha++){
        map1=0;
        for (ph=0; ph<phbcount[alpha]; ph+=2){
            b = B->phbasis[alpha][ph];
            k = B->phbasis[alpha][ph+1];
            map2=0;
            for (ph2=0; ph2<phbcount[alpha]; ph2+=2){
                c = B->phbasis[alpha][ph2];
                j = B->phbasis[alpha][ph2+1];
                barh_i10a[k][b][c][j] = -V->phph[alpha][map1][map2];
                map2+=1;
            }
            map1+=1;
        }
    }
    //calculating second term of [I9]
    for (alpha=0; alpha<dim_alpha; alpha++){
        map1=0;
        for (p=0; p<ppbcount[alpha]; p+=2){
            d = B->c_pp[alpha][p];
            c = B->c_pp[alpha][p+1];
            map2=0;
            for (ph=0; ph<phbcount[alpha]; ph+=2){
                b = B->phbasis[alpha][ph];
                k = B->phbasis[alpha][ph+1];
                temp = 0.5 * V->ppph[alpha][map1][map2];
                for (j=0; j<nh; j++){
                    barh_i10a[k][b][c][j] += temp*t1[d][j];
                    barh_i10a[k][b][d][j] -= temp*t1[c][j];
                }
                map2+=1;
            }
            map1+=1;
        }
    }
} //end [I9]

```

Listing 6.32: implementation of I9 in the amp1 class function ccscd_uncoupled_barh_i10a_store

$$[I10]_{ij}^{kb} = -\langle bk|v|ij\rangle - \frac{1}{2}\langle cd|v|bk\rangle t_{ij}^{cd} + \hat{P}_{(ij)}[I9]_{cj}^{kb} t_i^c - \frac{1}{2}[I6]_{ij}^{kl} t_l^b$$

```

void Amplitudes::ccscd_uncoupled_barh_i12a_store() {
    //calculating first term of [I10] (barh_i12a)
    for (alpha=0; alpha<dim_alpha; alpha++){
        map1=0;

```

```

    for(ph=0; ph<phbcount[alpha]; ph+=2){
        b = B->phbasis[alpha][ph];
        k = B->phbasis[alpha][ph+1];
        map2=0;
        for(h=0; h<hhbcount[alpha]; h+=2){
i = B->c_hh[alpha][h];
j = B->c_hh[alpha][h+1];
barh_i12a[k][b][i][j] = -V->phhh[alpha][map1][map2];
barh_i12a[k][b][j][i] = +V->phhh[alpha][map1][map2];
map2+=1;
        }
        map1+=1;
    }
}
// calculating the [I9] term of [I10]
for(k=0; k<nh; k++){
    for(b=0; b<np; b++){
        for(j=0; j<nh; j++){
for(i=0; i<nh; i++){
            temp = 0.0;
            for(c=0; c<np; c++){
                temp = temp + (barh_i10a[k][b][c][j]*t1[c][i]
                    - barh_i10a[k][b][c][i]*t1[c][j]);
            }
            barh_i12a[k][b][i][j] = barh_i12a[k][b][i][j] + temp;
        }
    }
}
}
// calculating the [I6] term of [I10]
for(k=0; k<nh; k++){
    for(b=0; b<np; b++){
        for(j=0; j<nh; j++){
for(i=0; i<nh; i++){
            temp = 0.0;
            for(l=0; l<nh; l++){
                temp = temp + barh_09[k][l][i][j]*t1[b][l];
            }
            barh_i12a[k][b][i][j] = barh_i12a[k][b][i][j] - 0.5*temp;
        }
    }
}
}
//calculating second term of [I10]
for(alpha=0; alpha<dim_alpha; alpha++){
    map1=0;
    for(p=0; p<ppbcount[alpha]; p+=2){
        c = B->c_pp[alpha][p];
        d = B->c_pp[alpha][p+1];
        map2=0;
        for(ph=0; ph<phbcount[alpha]; ph+=2){
b = B->phbasis[alpha][ph];
k = B->phbasis[alpha][ph+1];
for(i=0; i<nh; i++){
            for(j=0; j<nh; j++){
                barh_i12a[k][b][i][j] -= V->ppph[alpha][map1][map2]*t2[c][d][i][j];
            }
        }
    }
    map2+=1;
}
    map1+=1;
}

```



```

    }
  }
} //end [I10]

```

Listing 6.33: implementation of I10 in the amp1 class function ccscd_uncoupled_barh_i12a_store

$$[I11]_{cj}^{ab} = \langle ab|v|cj\rangle + \frac{1}{2}\langle ab|v|cd\rangle t_j^d$$

```

void Amplitudes::ccscd_uncoupled_barh_i11a_store() {
    //calculating first term of [11] (barh_i11a)
    for (alpha=0; alpha<dim_alpha; alpha++){
        map1=0;
        for (p=0; p<ppbcount[alpha]; p+=2){
            a = B->c_pp[alpha][p];
            b = B->c_pp[alpha][p+1];
            map2=0;
            for (ph=0; ph<phbcount[alpha]; ph+=2){
                c = B->phbasis[alpha][ph];
                j = B->phbasis[alpha][ph+1];
                barh_i11a[a][b][c][j] = V->ppph[alpha][map1][map2];
                barh_i11a[b][a][c][j] = -V->ppph[alpha][map1][map2];
                map2+=1;
            }
            map1+=1;
        }
    }
    //calculating second term of [11]
    for (alpha=0; alpha<dim_alpha; alpha++){
        for (j=0; j<nh; j++){
            map1=0;
            for (p=0; p<ppbcount[alpha]; p+=2){
                a = B->c_pp[alpha][p];
                b = B->c_pp[alpha][p+1];
                map2=0;
                for (p2=0; p2<ppbcount[alpha]; p2+=2){
                    c = B->c_pp[alpha][p2];
                    d = B->c_pp[alpha][p2+1];
                    temp3 = 0.5*V->pppp[alpha][pmap][p2map];
                    temp1 = temp3*t1[f][i];
                    temp2 = temp3*t1[e][i];
                    barh_i11a[a][b][c][j] += temp1;
                    barh_i11a[b][a][c][j] -= temp1;
                    barh_i11a[a][b][d][j] -= temp2;
                    barh_i11a[b][a][d][j] += temp2;
                    map2+=1;
                }
                map1+=1;
            }
        }
    }
} //end [I11]

```

Listing 6.34: implementation of I11 in the amp1 class function ccscd_uncoupled_barh_i11a_store

6.4 Implementation of the double dot

We will in this section outline the numerical methods and algorithms related to finding the one-electron eigenvalues of double dot potential, see section 2.3. The code can take a general potential in two dimensions, and find the eigenvalues and eigenvectors. But for our particular problem, we only diagonalize in x -direction, find the eigenvalues and eigenvectors. Then find the overlap coefficients with an harmonic oscillator basis

$$C_{n'_x, n_X m_X} = \sum_{n_x}^N \langle n'_x | n_X m_X \rangle | n_X m_X \rangle. \quad (6.66)$$

Where n_X and m_X are the radial and angular quantum numbers from a polar basis solution, see Eq. (2.57). Since there is no barrier in the y -direction, the Hamiltonian 2.97 is separable and we get

$$C_{n'_Y m'_Y, n_Y m_Y} = \delta_{n'_Y m'_Y, n_Y m_Y} | n_X m_X \rangle. \quad (6.67)$$

The relations between Cartesian quantum numbers (n_x, n_y) and n, m are as follows

$$E = n_x + n_y + 1 = 2n + |m| + 1 \quad (6.68)$$

Then our new basis states can be expressed as linear combination of harmonic oscillator states

$$|a\rangle = \sum_{\alpha} C_{\alpha} |\alpha\rangle, \quad C_{\alpha} = C_{n'_x, n_X m_X} C_{n_Y m_Y}. \quad (6.69)$$

Our goal is to find the two-particle interaction elements in the new basis

$$\langle ab | v | cd \rangle = \sum_{\alpha\beta\gamma\delta} C_{\alpha}^* C_{\beta}^* C_{\gamma} C_{\delta} \langle \alpha\beta | v | \gamma\delta \rangle \quad (6.70)$$

The interaction elements for the parabolic quantum dot Eq. 2.1 $\langle \alpha\beta | v | \gamma\delta \rangle$ can be obtained from Simen Kvaal's Open FCI code for quantum dots [42]. This is a transformation of the interaction elements from a polar basis to a Cartesian basis. And these basis transformations are costly to calculate, we have tried to optimize as much as we could.

These new interaction elements Eq. 6.70, together with the new spinorbital quantum numbers Eq. 6.69 $|a\rangle$ and single-particle energies $\langle a | b \rangle$ are used as an input in our CCSD and Hartree-Fock.

6.4.1 Scaling the Hamiltonian

One of the potentials we wish to study [64]

$$V(x, y) = \frac{1}{2} m^* \omega_0^2 [x^2 + y^2 - 2L_x |x| + L_x^2]. \quad (6.71)$$

We want our potential to dimensionless in our calculation. Introducing the scaled variables

$$L_x = L_c \bar{L}_x \quad (6.72)$$

$$x = x_c \bar{x} \quad (6.73)$$

$$y = y_c \bar{y} \quad (6.74)$$

$$\omega_0 = \omega_c \bar{\omega} \quad (6.75)$$

Setting

$$L_c = x_c = y_c = l_0 \quad (6.76)$$

$$(6.77)$$

We get

$$\bar{V} = \frac{1}{2} m^* \omega_0 l_0^2 [\bar{x}^2 + \bar{y}^2 - 2|\bar{x}| + \bar{L}_x]. \quad (6.78)$$

And setting

$$l_0 = \sqrt{\frac{\hbar}{m^* \omega_c \bar{\omega}}}. \quad (6.79)$$

Which gives

$$\bar{V}_C = \frac{\hbar}{2} \omega_c \bar{\omega} [\bar{x}^2 + \bar{y}^2 - 2|\bar{x}| + \bar{L}_x]. \quad (6.80)$$

Defining E_h

$$E_h = \frac{m^*}{\epsilon^2} \quad \kappa = \frac{e^2}{4\pi\epsilon_0\epsilon_r\hbar} \quad (6.81)$$

Scaling the Hamiltonian $\hat{H} = E_h \bar{H}$, where E_h is effective Hartrees.

$$\bar{H} = -\frac{\omega_c \bar{\omega} \hbar \kappa^2}{2m^*} \nabla^2 + \frac{\hbar \kappa^2}{2m^*} \omega_c \bar{\omega} [\bar{x}^2 + \bar{y}^2 - 2|\bar{x}| + \bar{L}_x] \quad (6.82)$$

Setting

$$\frac{\hbar \kappa^2 \omega_c}{m^*} = 1 \quad (6.83)$$

We then get the one-body Hamiltonian

$$\bar{H} = -\frac{\bar{\omega}}{2} \nabla^2 + \frac{1}{2} \bar{\omega} [\bar{x}^2 + \bar{y}^2 - 2|\bar{x}| + \bar{L}_x]. \quad (6.84)$$

The two-body interaction is the same as in Eq. 2.78. And the total Hamiltonian for our model becomes

$$\bar{H} = -\frac{\bar{\omega}}{2} \nabla^2 + \frac{1}{2} \bar{\omega} [\bar{x}^2 + \bar{y}^2 - 2|\bar{x}| + \bar{L}_x] + \sqrt{\bar{\omega}} \sum_{i < j}^N \frac{1}{\bar{r}_{ij}} \quad (6.85)$$

In the article [64], they set $L_x = 50$ nm, then we can choose $L_c = 50$ nm and setting $\bar{L}_x = 1$, $\bar{\omega} = 1$.

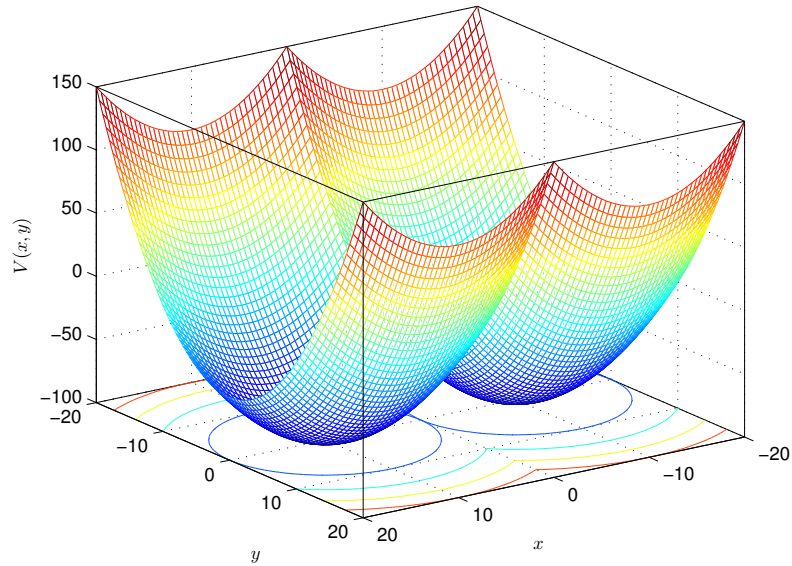


Figure 6.2: Confinement potential for Eq. 6.80 $V(\bar{x}, \bar{y})$, $\bar{L}_x = 10$ and $\bar{\omega} = 1$

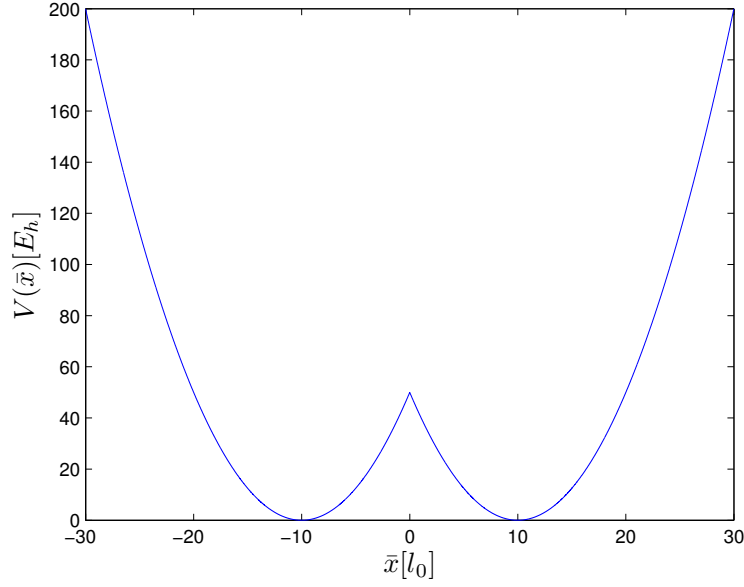


Figure 6.3: Confinement potential for Eq. 6.80 $V(\bar{x}, 0)$, $\bar{L}_x = 10$ and $\bar{\omega} = 1$

The code is so general that we can change the potential, instead of the absolute value barrier $|\bar{x}|$, we can choose a Gaussian curve barrier which is smoother. An example could be

$$\bar{V}_G = \frac{1}{2}\bar{\omega} \left[\bar{x}^2 + \bar{y}^2 + V_0 \exp\left(-\frac{\bar{x}^2}{2\sigma}\right) \right] \quad (6.86)$$

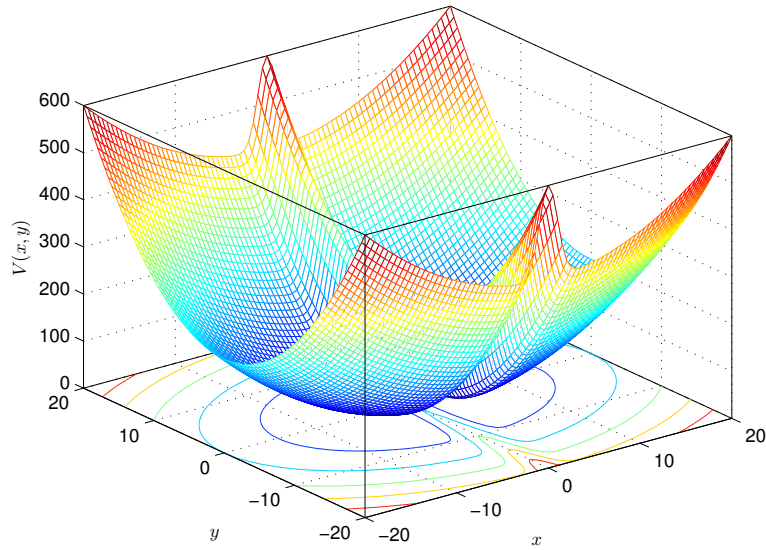


Figure 6.4: Confinement potential for Eq. 6.86 $V(\bar{x}, \bar{y})$, $V_0 = 100$ and $\sigma = 1, \omega = 1$

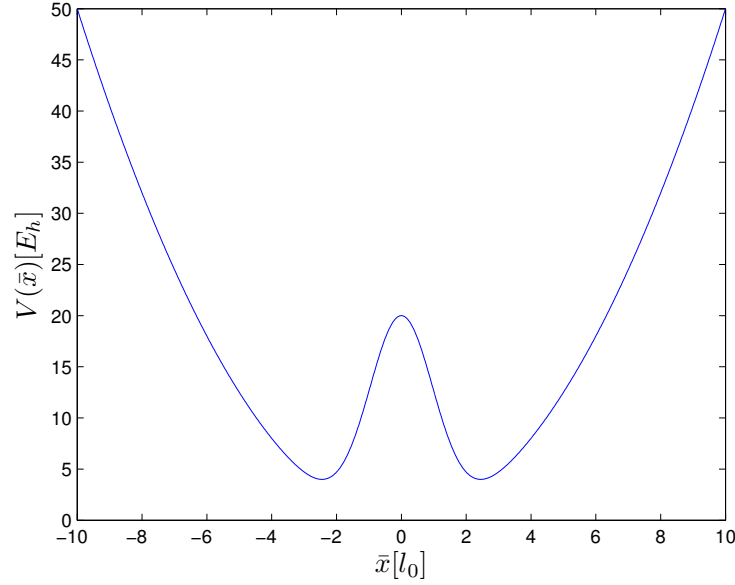


Figure 6.5: Confinement potential for Eq. 6.86 $V(x, 0)$, $V_0 = 20$, $\sigma = 1$ and $\bar{\omega} = 1$

6.4.2 Finding the eigenvectors and eigenvalues

We diagonalize the one-body Hamiltonian in x -direction

$$\hat{H}_X = -\frac{\bar{\omega}}{2} \frac{d}{d\bar{x}^2} + V(\bar{x}). \quad (6.87)$$

In order to find the eigenvalues and the eigenvectors we can use the technique of Discretizing described in section 2.3. We use the algorithm (Listing 6.35) to create the tridiagonal matrix Eq. 2.114

```
double e = 0.5 * (-1.0) / (xstep * xstep);
double f = 1.0 / (xstep * xstep);
double V = 0;
for (int i = 0; i < N - 1; i++) {
    x = xmin + i*xstep;
    V = potential(x);

    //Filling the diagonal
    T[i][i] = f + V;

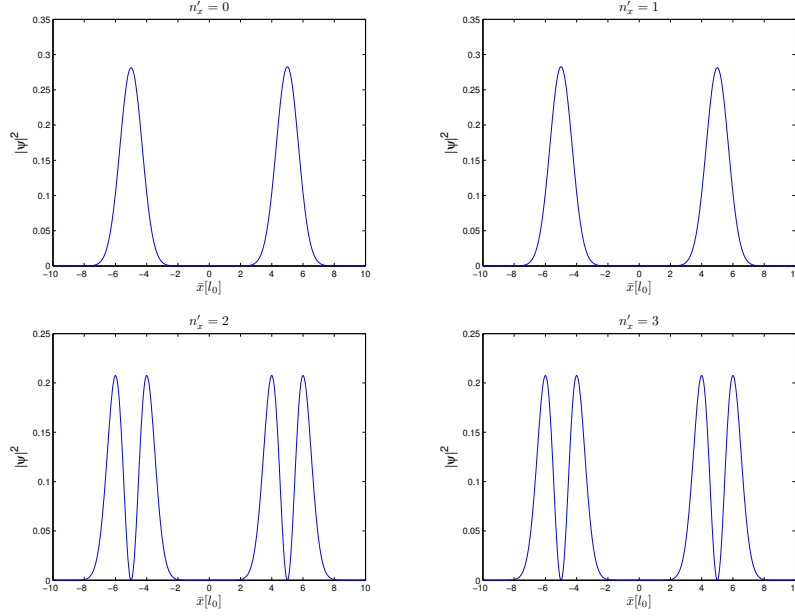
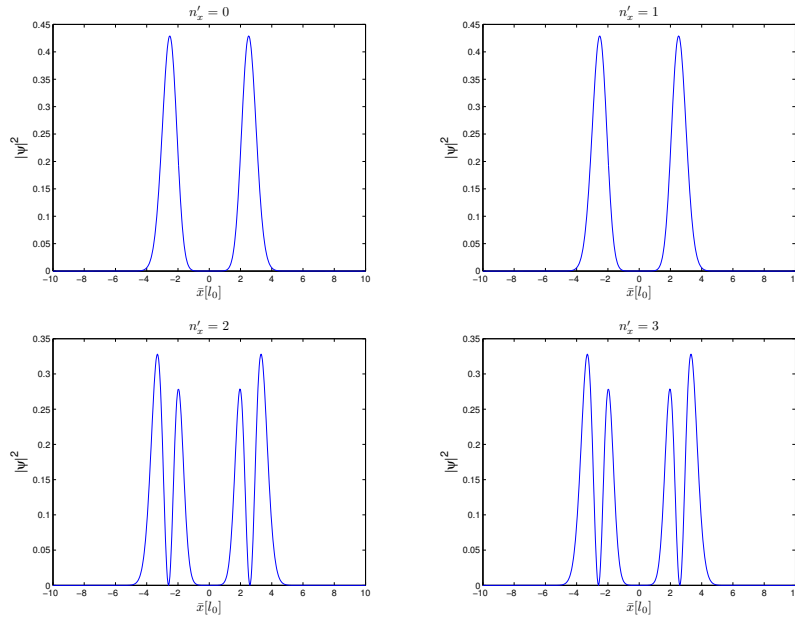
    //Filling the off diagonal;
    T[i][i + 1] = e;
    T[i + 1][i] = e;
}
//Filling the last diagonal element
x = xmin + (N - 1) * xstep;
V = potential(x);
T[N - 1][N - 1] = f + V;
```

Listing 6.35: Filling the tridiagonal matrix

We use the LAPACK routine for solving a symmetric dense matrix, `dsyev()`, which basically use the accelerated QR-Algorithm, section 2.3.1. The eigenvalues $E_{n'_x}$ are then sorted in ascending order,

$$n'_x = 0, 1, 2, \dots, N \quad E_0 \geq E_1 \geq E_2 \geq \dots \geq E_{n'_x=N}. \quad (6.88)$$

$$\psi_{n'_x} = \begin{bmatrix} \psi_{n'_x}(x_{\min}) \\ \psi_{n'_x}(x_1) \\ \vdots \\ \psi_{n'_x}(x_N) \end{bmatrix}, \quad x_j = x_{\min} + j \cdot h, \quad j \in \{0, 1, \dots, N\} \quad (6.89)$$


 Figure 6.6: The probability density of the four lowest eigenstates for $L_x = 5$, $\omega = 1$.

 Figure 6.7: The probability density of the four lowest eigenstates for $V_0 = 20$, $\omega = 1$.

6.4.3 Finding the coefficients

We want to find the overlap coefficients

$$C_{n'_x, n} = \langle \psi_{n'_x} | n \rangle = \sum_n^N \psi_{n'_x}(x_i) \psi_n(x_i) \quad n = 0, 1, 2, \dots, N \quad (6.90)$$

$$x_i = x_{\min} + i \cdot h \quad h = \frac{x_{\max} - x_{\min}}{N} \quad (6.91)$$

Where $\psi_n(x)$ are the harmonic oscillator eigenfunctions in one dimension:

$$\psi_n(x) = \left(\frac{\beta}{\pi}\right)^{1/4} \frac{1}{\sqrt{2^n n!}} H_n(x) e^{-\frac{\beta x^2}{2}} \quad (6.92)$$

$$\beta = \frac{m\omega}{\hbar} \quad (6.93)$$

$H_n(x)$ are the Hermite polynomials [7]. Using the recursive relation for the Hermite polynomials

$$H_{n+1}(x) = 2xH_n(x) - 2nH_{n-1}(x) \quad (6.94)$$

We get

$$\psi_{n+1} = \left(\frac{1}{\pi}\right)^{1/4} \frac{1}{\sqrt{2^{n+1}(n+1)!}} H_{n+1} e^{\frac{1x^2}{2}} \quad (6.95)$$

$$= \left(\frac{1}{\pi}\right)^{1/4} \frac{1}{\sqrt{2^{n+1}(n+1)!}} (2xH_n - 2nH_{n-1}) \quad (6.96)$$

$$= x \sqrt{\frac{2}{n+1}} \psi_n - \sqrt{\frac{n}{n+1}} \psi_{n-1} \quad (6.97)$$

Or

$$\psi_n = x \sqrt{\frac{2}{n}} \psi_{n-1} - \sqrt{\frac{n-1}{n}} \psi_{n-2} \quad (6.98)$$

Where

$$\psi_0 = \left(\frac{1}{\pi}\right)^{1/4} e^{-\frac{x^2}{2}} \quad (6.99)$$

$$\psi_1 = \left(\frac{1}{\pi}\right)^{1/4} \frac{1}{\sqrt{2}} 2xe^{-\frac{x^2}{2}} \quad (6.100)$$

The algorithm for generating the harmonic oscillator wavefunctions and evaluate at x , $\beta = 1$

```
double wf(int n, double x) {
    double *W = new double[n + 2];
    double a = (1.0 / pow(pi, 0.25));
    double b = (1.0 / sqrt(2));

    W[0] = 1.0 * a; //psi_0(x)

    if (n == 0) {
        return W[0] * exp(-0.5 * x * x);
    } else {
        W[1] = sqrt(2) * x * a; //psi_1(x)
        for (int i = 1; i <= n - 1; i++) {
            W[i + 1] = (sqrt(2.0 / (i + 1)) * x * W[i] - sqrt(double(i) / (i + 1))
                * W[i - 1]);
        }
    }
}
```

```

    }
    return W[n] * exp(-0.5 * x * x);
}

delete [] W;

```

The coefficients are then calculated by the following algorithm

```

for (int nxprime = 0; nxprime < nxprime_max; nxprime++) {
    for (int n = 0; n < nmax; n++) {
        innerprod = 0;
        for (int i = 0; i < N; i++) {
            innerprod += xstep * Evecs[i][nxprime] * H[i][n];
        }
        Coeff[n][nxprime] = innerprod;
    }
}

```

Validation

One way to validate the coefficients is to check if it preserve the probability.

$$P(n'_x) = \sum_i^N C_{i,n'_x}^* C_{i,n'_x} \approx 1 \quad (6.101)$$

Another check is to plot the diagonalized curve against the linear expansion and see if the L_2 -norm of the function is a small number

$$\|\psi_{n'_x} - \psi_{n_x}\|_2 = \sqrt{\sum_i^N |\psi_{n'_x}(x_i) - \psi_{n_x}(x_i)|^2} < \epsilon \quad (6.102)$$

For the $L_x = 5, \omega = 1$ we need $n_x > 30$ in order to get reasonable amount of non-zero coefficients $C_{n'_x, n_x}$. But our calculation is with a max $n_x = 20$ due to the heavy time consumption of generating the transformed interaction elements. Besides we are studying small model spaces and only need $n'_x < 10$, in that regard $C_{n'_x, n_x}$ falls off quickly and it is sufficient to have maximal $n_x = 20$

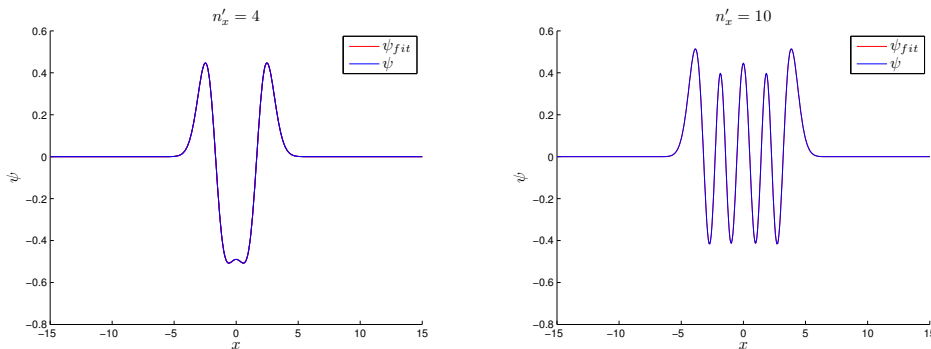


Figure 6.8: Plot of the fitted curve for $L_x = 5, \omega = 1$, and the max value of $n_x = 20$. The L_2 -norm for $n'_x = 10$ was 5.8E-4, while the L_2 -norm for $n'_x = 10$ was 0.0118. Which is a reasonable fit

6.4.4 Transformation from polar to Cartesian representation

Harmonic oscillator wavefunctions in two dimensions for some selected values

$$\psi_{n_x, n_y}^{\text{HO}}(x, y) = \psi_{n_x}^{\text{HO}}(x) \psi_{n_y}^{\text{HO}}(y) \quad (6.103)$$

$$\psi_{n_x, n_y}^{\text{HO}}(x, y) = H_{n_x}(x) H_{n_y}(y) e^{-x^2} e^{-y^2} \quad (6.104)$$

In Cartesian representation (not normalized):

$$\psi_{0,0}^{\text{HO}}(x, y) = e^{-x^2} e^{-y^2} \quad (\epsilon = 1)$$

$$\psi_{1,0}^{\text{HO}}(x, y) = x e^{-x^2} e^{-y^2} \quad (\epsilon = 2)$$

$$\psi_{0,1}^{\text{HO}}(x, y) = y e^{-x^2} e^{-y^2} \quad (\epsilon = 2)$$

$$\psi_{1,1}^{\text{HO}}(x, y) = y x e^{-x^2/2} e^{-y^2} \quad (\epsilon = 3)$$

Where $\epsilon = n_x + n_y + 1$. In polar coordinate representation (not normalize):

$$\psi_{n,m}^{\text{HO}}(r, \theta) = R(r) \phi(\theta) \quad (6.105)$$

$$\psi_{n,m}^{\text{HO}}(r, \theta) = r^{|m|} e^{-r^2} L_n^{|m|} e^{im\theta} \quad (6.106)$$

$$\psi_{0,0}^{\text{HO}}(r, \theta) = e^{-r^2} \quad (\epsilon = 1)$$

$$\psi_{0,1}^{\text{HO}}(r, \theta) = r e^{-r^2} e^{i\theta} \quad (\epsilon = 2)$$

$$\psi_{0,-1}^{\text{HO}}(r, \theta) = r e^{-r^2} e^{-i\theta} \quad (\epsilon = 2)$$

$$\psi_{1,0}^{\text{HO}}(r, \theta) = (-r^2 + 1) e^{-r^2} \quad (\epsilon = 3)$$

Where $\epsilon = 2n + |m| + 1$. We transformation between the representation by the following

$$x = r \cos(\theta)$$

$$y = r \sin(\theta)$$

$$r^2 = x^2 + y^2$$

We have that

$$\cos(\theta) = \frac{e^{i\theta} + e^{-i\theta}}{2} \quad \sin(\theta) = \frac{e^{i\theta} - e^{-i\theta}}{2i} \quad (6.107)$$

We see that (normalized):

$$\psi_{0,0}^{\text{HO}}(x, y) = \psi_{0,0}^{\text{HO}}(r, \theta) \quad (6.108)$$

$$\psi_{1,0}^{\text{HO}}(x, y) = \frac{1}{\sqrt{2}} \psi_{1,1}^{\text{HO}}(r, \theta) + \frac{1}{\sqrt{2}} \psi_{1,-1}^{\text{HO}}(r, \theta) \quad (6.109)$$

$$\psi_{0,1}^{\text{HO}}(x, y) = \frac{i}{\sqrt{2}} \psi_{1,-1}^{\text{HO}}(r, \theta) - \frac{i}{\sqrt{2}} \psi_{1,1}^{\text{HO}}(r, \theta) \quad (6.110)$$

$$(6.111)$$

The Transformation matrix T^N , $N = n_x + n_y$:

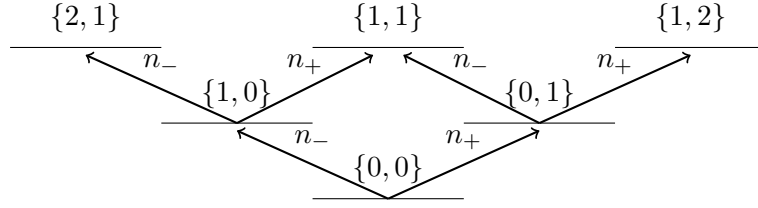


Figure 6.9: Shell structure of the quantum dot, and the relations to the quantum number n_+ , n_- . There is a 1-1 map between the radial quantum number n and angular momentum quantum number m_s to $\{n_+, n_-\}$

$$T^0 = 1 \quad (6.112)$$

$$T^1 = \begin{bmatrix} \frac{1}{\sqrt{2}} & \frac{1}{\sqrt{2}} \\ \frac{1}{\sqrt{2}} & -\frac{1}{\sqrt{2}} \end{bmatrix} \quad (6.113)$$

$$T^2 = \begin{bmatrix} \frac{1}{2} & \frac{1}{\sqrt{2}} & \frac{1}{2} \\ \frac{1}{\sqrt{2}} & 0 & -\frac{1}{\sqrt{2}} \\ \frac{1}{2} & -\frac{1}{\sqrt{2}} & \frac{1}{2} \end{bmatrix} \quad (6.114)$$

$$T^N = \dots \quad (6.115)$$

These transformation matrices are obtained from Simen Kvaal's PhD-thesis [41] Our transformation from a polar basis to a Cartesian one are defined,

$$|a\rangle \equiv |n'_x(a), n'_y(a)\rangle^{CAR} = \sum_{n_x(a)} C_{n_x(a), n'_x(a)} \sum_{n_+(a)}^{N_a} i^{-n'_y(a)} T_{n_+(a), n_x(a)}^{N_a} \quad (6.116)$$

Where $N_a = n_x(a) + n'_y(a)$. Then the interaction elements in the Cartesian space represented by

$$\begin{aligned} \langle ab|v|cd\rangle^{CAR} &= \sum_{n_x(a)} \sum_{n_x(b)} \sum_{n_x(c)} \sum_{n_y(d)} C_{n_x(a), n'_x(a)} C_{n_x(b), n'_x(b)} C_{n_x(c), n'_x(c)} C_{n_x(d), n'_x(d)} \\ &\times \sum_{n_+(a)}^{N_a} \sum_{n_+(b)}^{N_b} \sum_{n_+(c)}^{N_c} \sum_{n_+(d)}^{N_d} T_{n_+(a), n_x(a)}^{N_a} T_{n_+(b), n_x(b)}^{N_b} T_{n_+(c), n_x(c)}^{N_c} T_{n_+(d), n_x(d)}^{N_d} \\ &\times \underbrace{\langle n_+(a) n_-(a) |}_a \underbrace{n_+(b) n_-(b) |}_b v \underbrace{n_+(c) n_-(c) |}_c \underbrace{n_+(d) n_-(d) \rangle}_d^{POL} \\ &\times i^{n'_y(a)} i^{n'_y(b)} i^{-n'_y(c)} i^{-n'_y(d)} \end{aligned}$$

Where

$$m = n_+ - n_- \quad n = \frac{n_+ + n_- - |m|}{2} \quad (6.117)$$

Think of it as a ladder, where number of n_+ , defines how high to the right you move on the ladder, and n_- defines how high to the left. Therefore each of the subshells will be defined by a set of $\{n_+, n_-\}$. Notice that we have a imaginary part. Our interaction elements in the polar basis are real, and the transformation will not change this, therefore the transformations will have the condition.

$$[n_y(a) + n_y(b) - n_y(c) - n_y(d)] = 2n + 1 \iff \langle ab|v|cd\rangle^{CAR} = 0, \quad n \in \mathcal{N} \quad (6.118)$$

We can do a simple example using the parabolic harmonic oscillator potential, i.e. $L_x = 0$ and $V_0 = 0$.

Our system is a harmonic oscillator with 2 shell level, and the basis states are:

$$\begin{aligned}
 |0\rangle &\rightarrow n'_x = 0, n'_y = 0, m'_s = -0.5, & E &= 0.99988 \\
 |1\rangle &\rightarrow n'_x = 0, n'_y = 0, m'_s = 0.5, & E &= 0.99988 \\
 |2\rangle &\rightarrow n'_x = 1, n'_y = 0, m'_s = -0.5, & E &= 1.99943 \\
 |3\rangle &\rightarrow n'_x = 1, n'_y = 0, m'_s = 0.5, & E &= 1.99943 \\
 |4\rangle &\rightarrow n'_x = 0, n'_y = 1, m'_s = -0.5, & E &= 1.99988 \\
 |5\rangle &\rightarrow n'_x = 0, n'_y = 1, m'_s = 0.5, & E &= 1.99988
 \end{aligned}$$

Polar basis:

$$\begin{aligned}
 |0\rangle &= \{n = 0, m = 0, m_s = -0.5\} \\
 |1\rangle &= \{n = 0, m = 0, m_s = 0.5\} \\
 |2\rangle &= \{n = 0, m = -1, m_s = -0.5\} \\
 |3\rangle &= \{n = 0, m = -1, m_s = 0.5\} \\
 |4\rangle &= \{n = 0, m = +1, m_s = -0.5\} \\
 |5\rangle &= \{n = 0, m = +1, m_s = 0.5\}
 \end{aligned}$$

Talmi matrix:

$$T^{(1)} = 1 \quad (6.119)$$

$$T^{(2)} = \begin{bmatrix} \frac{1}{\sqrt{2}} & \frac{1}{\sqrt{2}} \\ \frac{1}{\sqrt{2}} & -\frac{1}{\sqrt{2}} \end{bmatrix} \quad (6.120)$$

Want to find the interaction element $\langle 45|v|45\rangle^{CAR}$:

$$|n'_x n'_y\rangle^{CAR} = \sum_{n_x} C_{n'_x, n_x} \sum_{n_+}^{n_x + n'_y} T_{n_+, n_x}^{n_x + n'_y} |n_+, n_-\rangle^{POL} \quad (6.121)$$

$$|4\rangle^{CAR} = T_{0,0}^{(1)} |n_+ = 0, n_- = 1\rangle^{POL} + T_{1,0}^{(1)} |n_+ = 1, n_- = 0\rangle^{POL} \quad (6.122)$$

$$|5\rangle^{CAR} = T_{0,0}^{(1)} |n_+ = 0, n_- = 1\rangle^{POL} + T_{1,0}^{(1)} |n_+ = 1, n_- = 0\rangle^{POL} \quad (6.123)$$

If we translate these states into the Polar basis quantum numbers we get, and remember that $|4\rangle$ is a spin down states, so $\{n_+, n_-\}$ must map to a state which is spin down:

$$|4\rangle^{CAR} = T_{0,0}^{(1)} |4\rangle^{POL} + T_{1,0}^{(1)} |2\rangle^{POL} \quad (6.124)$$

$$|5\rangle^{CAR} = T_{0,0}^{(1)} |5\rangle^{POL} + T_{1,0}^{(1)} |3\rangle^{POL} \quad (6.125)$$

Then

$$|45\rangle^{CAR} = (T_{0,0}^{(1)})^2 |45\rangle^{POL} + T_{0,0}^{(1)} T_{1,0}^{(1)} |43\rangle^{POL} + T_{1,0}^{(1)} T_{0,0}^{(1)} |25\rangle^{POL} + (T_{1,0}^{(1)})^2 |23\rangle^{POL} \quad (6.126)$$

Then

$$\langle 45|v|45\rangle^{CAR} = \frac{1}{2} \frac{1}{2} \langle 45|v|45\rangle^{POL} + \frac{1}{2} \frac{1}{2} \langle 43|v|25\rangle^{POL} + \frac{1}{2} \frac{1}{2} \langle 43|v|43\rangle^{POL} \quad (6.127)$$

$$+ \frac{1}{2} \frac{1}{2} \langle 25|v|25\rangle^{POL} + \frac{1}{2} \frac{1}{2} \langle 25|v|43\rangle^{POL} + \frac{1}{2} \frac{1}{2} \langle 23|v|23\rangle^{POL} \quad (6.128)$$

List of interaction elements from `tabulate.x` with $\omega = 1.0$ and standard v.v.:

$$\langle 45|v|45\rangle^{POL} = 0.86165 \quad (6.129)$$

$$\langle 43|v|25\rangle^{POL} = 0.23499 \quad (6.130)$$

$$\langle 43|v|43\rangle^{POL} = 0.86165 \quad (6.131)$$

$$\langle 25|v|25\rangle^{POL} = 0.86165 \quad (6.132)$$

$$\langle 25|v|43\rangle^{POL} = 0.23499 \quad (6.133)$$

$$\langle 23|v|23\rangle^{POL} = 0.86165 \quad (6.134)$$

The our interaction element becomes

$$\langle 45|v|45\rangle^{CAR} = 0.86165 + \frac{1}{2}0.23499 = 0.97915 \quad (6.135)$$

$$\langle 45|v|45\rangle^{POL} = 0.86165 \quad (6.136)$$

6.4.5 Tabulating new quantum numbers

In our Cartesian basis, the two-particle interaction still does not change spin. Therefore the total spin is conserved.

$$\langle M_s|v|M'_s\rangle = \delta_{M_s,M'_s} \quad M_s = m_{1s} + m_{2s} \quad (6.137)$$

M_s	α	State
-1	0	$ 0, 2\rangle$
-1	0	$ 0, 4\rangle$
-1	0	$ 2, 4\rangle$

M_s	α	State
0	1	$ 0, 1\rangle$
0	1	$ 0, 3\rangle$
0	1	$ 0, 5\rangle$
0	1	$ 1, 2\rangle$
0	1	$ 1, 4\rangle$
0	1	$ 2, 3\rangle$
0	1	$ 2, 5\rangle$
0	1	$ 3, 4\rangle$
0	1	$ 4, 5\rangle$
0	1	$ 1, 3\rangle$

M_s	α	State
1	2	$ 3, 4\rangle$
1	2	$ 1, 5\rangle$
1	2	$ 3, 5\rangle$

Table 6.5: Tabulated two-particle basis for $M_s = -1$

Table 6.6: Tabulated two-particle basis for $M_s = 0$

Table 6.7: Tabulated two-particle basis for $M_s = 1$

Every odd number is now a spin up state, and even number are spin down. The energy is thereby degenerate in spin.

$$|a\rangle = \begin{cases} a = 2n & \text{if } m_s = -0.5 \\ a = 2n + 1 & \text{if } m_s = 0.5 \end{cases} \quad (6.138)$$

In section 2.2.1 we discussed the shell structure of the parabolic quantum dot. We have the same situation now but with a different kind of subshells. We define a subshell with the set of quantum numbers $\{n'_x, n'_y\}$, where each subshell have the energy

$$E_{sub} = E_{n'_x} + E_{n'_y} \quad (6.139)$$

And $E_{n'_x}$ are the eigenvalues found by diagonalization Eq. 6.88 and Fig. 6.5, Fig. 6.4. While $E_{n'_y} = (0.5 + n'_y)$ are the one-dimensional solution to the harmonic oscillator potential. Example for the potential 6.86, $V = 20, \sigma = 1$, with $N = 500$.

n'_x	$E_{n'_x}$
0	0 5.68161
1	0 5.68162
2	0 7.42767

Table 6.8: Energyeigenvalues for n'_x

n'_y	$E_{n'_y}$
0	0.5
1	1
2	2

Table 6.9: Energyeigenvalues for n'_y

The first 6 spinorbitals are tabulated as

$$\begin{aligned}
 |0\rangle &= \{n'_x = 0, n'_y = 0, m_s = \downarrow\} & E &= 5.68161 \\
 |1\rangle &= \{n'_x = 0, n'_y = 0, m_s = \uparrow\} & E &= 5.68161 \\
 |2\rangle &= \{n'_x = 1, n'_y = 0, m_s = \downarrow\} & E &= 5.68161 \\
 |3\rangle &= \{n'_x = 1, n'_y = 0, m_s = \uparrow\} & E &= 5.68161 \\
 |4\rangle &= \{n'_x = 1, n'_y = 1, m_s = \downarrow\} & E &= 6.68162 \\
 |5\rangle &= \{n'_x = 1, n'_y = 1, m_s = \uparrow\} & E &= 6.68162
 \end{aligned}$$

6.4.6 Validation of the Code

One of the test we can do is to drop the barrier in the x -direction, i.e. $L_x = 0$ in Eq. (6.84). Then we get a harmonic oscillator potential. And we want to do a diagonalization for the 2-shell case. We get 6 single-particle states with eigenvalues in the Cartesian basis:

$$\begin{aligned}
 |0\rangle &\rightarrow \{n'_x = 0, n'_y = 0, m'_s = \downarrow\} & E &= 0.99988 \\
 |1\rangle &\rightarrow \{n'_x = 0, n'_y = 0, m'_s = \uparrow\} & E &= 0.99988 \\
 |2\rangle &\rightarrow \{n'_x = 1, n'_y = 0, m'_s = \downarrow\} & E &= 1.99943 \\
 |3\rangle &\rightarrow \{n'_x = 1, n'_y = 0, m'_s = \uparrow\} & E &= 1.99943 \\
 |4\rangle &\rightarrow \{n'_x = 0, n'_y = 1, m'_s = \downarrow\} & E &= 1.99988 \\
 |5\rangle &\rightarrow \{n'_x = 0, n'_y = 1, m'_s = \uparrow\} & E &= 1.99988
 \end{aligned}$$

If we start with the case $M_s = -1$

$$\mathbf{H} = \begin{bmatrix} \langle \Phi_{02} | H_0 | \Phi_{02} \rangle + \langle \Phi_{02} | V | \Phi_{02} \rangle & \langle \Phi_{02} | H_0 | \Phi_{04} \rangle + \langle \Phi_{02} | V | \Phi_{04} \rangle & \langle \Phi_{02} | H_0 | \Phi_{24} \rangle + \langle \Phi_{02} | V | \Phi_{24} \rangle \\ \langle \Phi_{04} | H_0 | \Phi_{02} \rangle + \langle \Phi_{04} | V | \Phi_{02} \rangle & \langle \Phi_{04} | H_0 | \Phi_{04} \rangle + \langle \Phi_{04} | V | \Phi_{04} \rangle & \langle \Phi_{04} | H_0 | \Phi_{24} \rangle + \langle \Phi_{04} | V | \Phi_{24} \rangle \\ \langle \Phi_{24} | H_0 | \Phi_{02} \rangle + \langle \Phi_{24} | V | \Phi_{02} \rangle & \langle \Phi_{24} | H_0 | \Phi_{04} \rangle + \langle \Phi_{24} | V | \Phi_{04} \rangle & \langle \Phi_{24} | H_0 | \Phi_{24} \rangle + \langle \Phi_{34} | V | \Phi_{24} \rangle \end{bmatrix}$$

Where the Slater determinant is defined as

$$|\Phi_{ab}\rangle \equiv \frac{1}{\sqrt{2}} (|ab\rangle - |ba\rangle) \quad (6.140)$$

Then we get

$$\begin{aligned}
 \mathbf{H} &\approx \begin{bmatrix} 2 + \langle 02 | v | 02 \rangle_{AS} & \langle 02 | v | 04 \rangle_{AS} & \langle 02 | v | 24 \rangle_{AS} \\ \langle 04 | v | 02 \rangle_{AS} & 4 + \langle 04 | v | 04 \rangle_{AS} & \langle 04 | v | 24 \rangle_{AS} \\ \langle 24 | v | 02 \rangle_{AS} & \langle 24 | v | 04 \rangle_{AS} & 4 + \langle 24 | v | 24 \rangle_{AS} \end{bmatrix} \\
 &= \begin{bmatrix} 3.6260 & 0 & 0 \\ 0 & 3.6264 & 0 \\ 0 & 0 & 4.6260 \end{bmatrix}
 \end{aligned}$$

Which is what we get when we diagonalize for $M_s = 0$ in polar basis. The case $M_s = 1$ is exactly the same, and for the $M_s = 0$ we get the eigvalues

$$\begin{aligned}
 E_0 &= 3.1523 & E_1 &= 3.6260 & E_2 &= 3.6264 \\
 E_3 &= 4.2533 & E_4 &= 4.2533 & E_5 &= 4.6267 \\
 E_6 &= 4.8617 & E_7 &= 4.8617 & E_8 &= 5.1976
 \end{aligned}$$

Which is the same as for the polar basis.

Chapter 7

Results

"I've very often made mistakes in my physics by thinking the theory isn't as good as it really is, thinking that there are lots of complications that are going to spoil it - an attitude that anything can happen, in spite of what you're pretty sure should happen." (From "Surely you're joking Mr. Feynman")

R. P. Feynman

7.1 Standard Interaction

In this section we present results from the Hartree-Fock and CCSD calculation for different two-dimensional potentials. Our Hamiltonian reads

$$\hat{H} = -\frac{\hbar^2}{2m^*} \sum_{i=1}^N \nabla_i^2 + \sum_i^N V(r_i) + \frac{e^2}{4\pi\epsilon_0\epsilon_r} \sum_{i=1<j}^N \frac{1}{r_{ij}}, \quad (7.1)$$

in section 2.2.2 we have shown that it can be rescaled to this dimensionless form

$$\bar{H} = -\frac{\omega_c}{2} \sum_{i=1}^N \bar{\nabla}^2 + \omega_c \sum_i^N V(\bar{r}_i) + \sqrt{\omega_c} \sum_{i<j}^N \frac{1}{\bar{r}_{ij}}, \quad (7.2)$$

where

$$\omega_c = \frac{\hbar\kappa^2}{m^*} \omega \quad (7.3)$$

$$\kappa = \frac{4\pi\epsilon_0\epsilon_r\hbar}{e^2} \quad (7.4)$$

$$\bar{r}_i = l_0 r_i, \quad \bar{x} = l_0 x_i, \quad \bar{y} = l_0 y_i \quad (7.5)$$

$$\bar{r}_{ij} = l_0 r_{ij} \quad (7.6)$$

$$\bar{\nabla}_i^2 = \frac{1}{l_0^2} \nabla_i^2 \quad (7.7)$$

$$l_0 = \frac{\hbar\kappa}{m^*} \quad (7.8)$$

Energy are now measured in units of effective Hartrees E_H , defined as

$$E_H \equiv \frac{m^*}{\kappa^2} \quad (7.9)$$

We will be using the potentials V_G Eq. (6.86) and V_C Eq. (6.80). They have the same common dimensionless ω_c that we can draw out of the Hamiltonian. In our CCSD program we are calculating the following Hamiltonian

$$\bar{H} = -\frac{1}{2} \sum_{i=1}^N \bar{\nabla}^2 + \sum_i^N V(\bar{r}_i) + \frac{1}{\sqrt{\omega_c}} \sum_{i < j}^N \frac{1}{\bar{r}_{ij}}, \quad (7.10)$$

the single particle energies and the potentials does not change with ω_c , but the interaction elements does. By multiplying our final energy with ω_c we would have solved for the same Hamiltonian as Eq. (7.2). This is because we have rescaled the interaction elements with $1/\sqrt{\omega_c}$.

It is important to note that we are using the potential with a Gaussian curve Eq. (6.86), the height are denoted by V_0 . And when we are using the potential with an absolute value cusp, we are using the parameter L_x Eq. (6.80).

Optimization results

We have done the following runs for the optimized code and compared to the code from [47].

Run case	Regular code time [s]	Optimized code time [s]	Improvement [%]
$nh = 2, R = 10$	1897	4	4,75E+4
$nh = 6, R = 7$	1595	3	5,32E+4
$nh = 6, R = 8$	4331	6	7,22E+4
$nh = 6, R = 9$	9697	11	8,82E+4
$nh = 6, R = 10$	21356	20	10,68E+4
$nh = 12, R = 7$	11775	23	5,12E+4
$nh = 12, R = 8$	30834	52	5,93E+4

Table 7.1: Here the R is defined as the major oscillator shells, see section 2.2.1. We have turned on the OpenMP in the optimized code and compared with the regular code from [47]. But most of the improvement was due to the fact that we changed from Blitz++ to pointer matrices. We have on average improved the code by a 500 times speed up! And it improves with number of particles.

Benchmark results for $L_x = 0$ and $\omega = 1$

We want to test the code for the parabolic harmonic oscillator potential case and see if we get the same results as in [47]

$nh = 2$				$nh = 6$			
R_m	R	HF	CCSD	R_m	R	HF	CCSD
2	3	3.253314	3.152329	2	3	22.219813	22.219813
4	10	3.162691	3.025231	4	10	20.766919	20.421321
6	21	3.161921	3.013626	6	21	20.720257	20.260893
8	36	3.161909	3.009236	8	36	20.719248	20.221750
10	55	3.161908	3.006938	10	55	20.719217	20.204344

Table 7.2: Ground-state energies for holes states $nh = 2$ and $nh = 6$ in a circular quantum dot using a standard Coulomb interaction for $L_x = 0$. The interaction elements are obtained from a Cartesian basis transformation, section 6.4.4. HF is the Hartree- Fock energy and CCSD is the coupled-cluster energy Eq. (6.80). R_m is the total number of subshells while R_m stands for the number of major oscillator shells Fig. 2.1

$nh = 2$				$nh = 6$			
R_m	R	HF	CCSD	R_m	R	HF	CCSD
2	3	3.253314	3.152329	2	3	22.212981	22.219813
4	10	3.162691	3.025232	4	10	20.766419	20.421325
6	21	3.161921	3.013627	6	21	20.720157	20.260893
8	36	3.161909	3.009237	8	36	20.719248	20.221750
10	55	3.161909	3.006938	10	55	20.719217	20.204345

Table 7.3: Ground-state energies for holes states $nh = 2$ and $nh = 6$ in a double quantum dot. These results are taken from [47] for us to compare with. As we can see they are almost identical with Table 7.2

We shall define a new shell structure, each subshell consist of quantum numbers n'_x and n'_y and they can be occupied with at most 2 electrons. In the special case where we do not have any perturbation in the middle $L_x = 0$ or $V_0 = 0$, some subshells are part of the major oscillator shells which we have discussed in section 2.2.1. The relations are

$$R = \frac{R_m(R_m + 1)}{2}. \quad (7.11)$$

We define the total number of single-particle states in our basis as

$$nh + np = 2R, \quad (7.12)$$

nh are number of hole states and np are number of particle states in our model.

p	n'_x	n'_y	m'_s	E	p	n'_x	n'_y	m'_s	E
0	0	0	-1	1	55	0	6	1	7
1	0	0	1	1	56	7	0	-1	8
2	1	0	-1	2	57	7	0	1	8
3	1	0	1	2	58	6	1	-1	8
4	0	1	-1	2	59	6	1	1	8
5	0	1	1	2	60	5	2	-1	8
6	2	0	-1	3	61	5	2	1	8
7	2	0	1	3	62	4	3	-1	8
8	1	1	-1	3	63	4	3	1	8
9	1	1	1	3	64	3	4	-1	8
10	0	2	-1	3	65	3	4	1	8
11	0	2	1	3	66	2	5	-1	8
12	3	0	-1	4	67	2	5	1	8
13	3	0	1	4	68	1	6	-1	8
14	2	1	-1	4	69	1	6	1	8
15	2	1	1	4	70	0	7	-1	8
16	1	2	-1	4	71	0	7	1	8
17	1	2	1	4	72	8	0	-1	9
18	0	3	-1	4	73	8	0	1	9
19	0	3	1	4	74	7	1	-1	9
20	4	0	-1	5	75	7	1	1	9
21	4	0	1	5	76	6	2	-1	9
22	3	1	-1	5	77	6	2	1	9
23	3	1	1	5	78	5	3	-1	9
24	2	2	-1	5	79	5	3	1	9
25	2	2	1	5	80	4	4	-1	9
26	1	3	-1	5	81	4	4	1	9
27	1	3	1	5	82	3	5	-1	9
28	0	4	-1	5	83	3	5	1	9
29	0	4	1	5	84	2	6	-1	9
30	5	0	-1	6	85	2	6	1	9
31	5	0	1	6	86	1	7	-1	9
32	4	1	-1	6	87	1	7	1	9
33	4	1	1	6	88	0	8	-1	9
34	3	2	-1	6	89	0	8	1	9
35	3	2	1	6	90	9	0	-1	10
36	2	3	-1	6	91	9	0	1	10
37	2	3	1	6	92	8	1	-1	10
38	1	4	-1	6	93	8	1	1	10
39	1	4	1	6	94	7	2	-1	10
40	0	5	-1	6	95	7	2	1	10
41	0	5	1	6	96	6	3	-1	10
42	6	0	-1	7	97	6	3	1	10
43	6	0	1	7	98	5	4	-1	10
44	5	1	-1	7	99	5	4	1	10
45	5	1	1	7	100	4	5	-1	10
46	4	2	-1	7	101	4	5	1	10
47	4	2	1	7	102	3	6	-1	10
48	3	3	-1	7	103	3	6	1	10
49	3	3	1	7	104	2	7	-1	10
50	2	4	-1	7	105	2	7	1	10
51	2	4	1	7	106	1	8	-1	10
52	1	5	-1	7	107	1	8	1	10
53	1	5	1	7	108	0	9	-1	10
54	0	6	-1	7	109	0	9	1	10

Table 7.4: $L_x = 0$, $\omega = 1.0$, here we have defined $m'_s = 2m_s$, and $m_s = \pm 1/2$. E are the energy eigenvalues for the singel-particles.

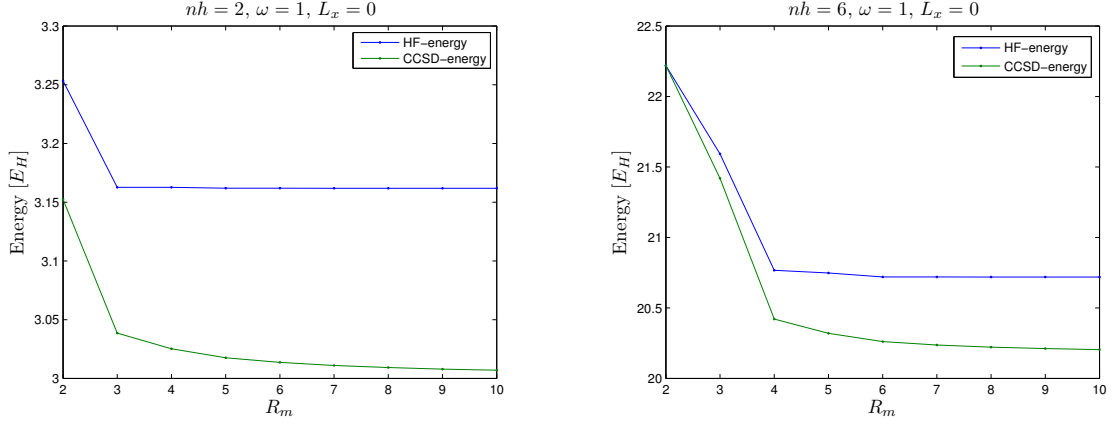


Figure 7.1: CCSD and HF energy as function of major oscillator shells R_m for the 2- and 6-electron system with $L_x = 0$, $\omega = 1$. The energy is measured in effective Hartrees (E_H)

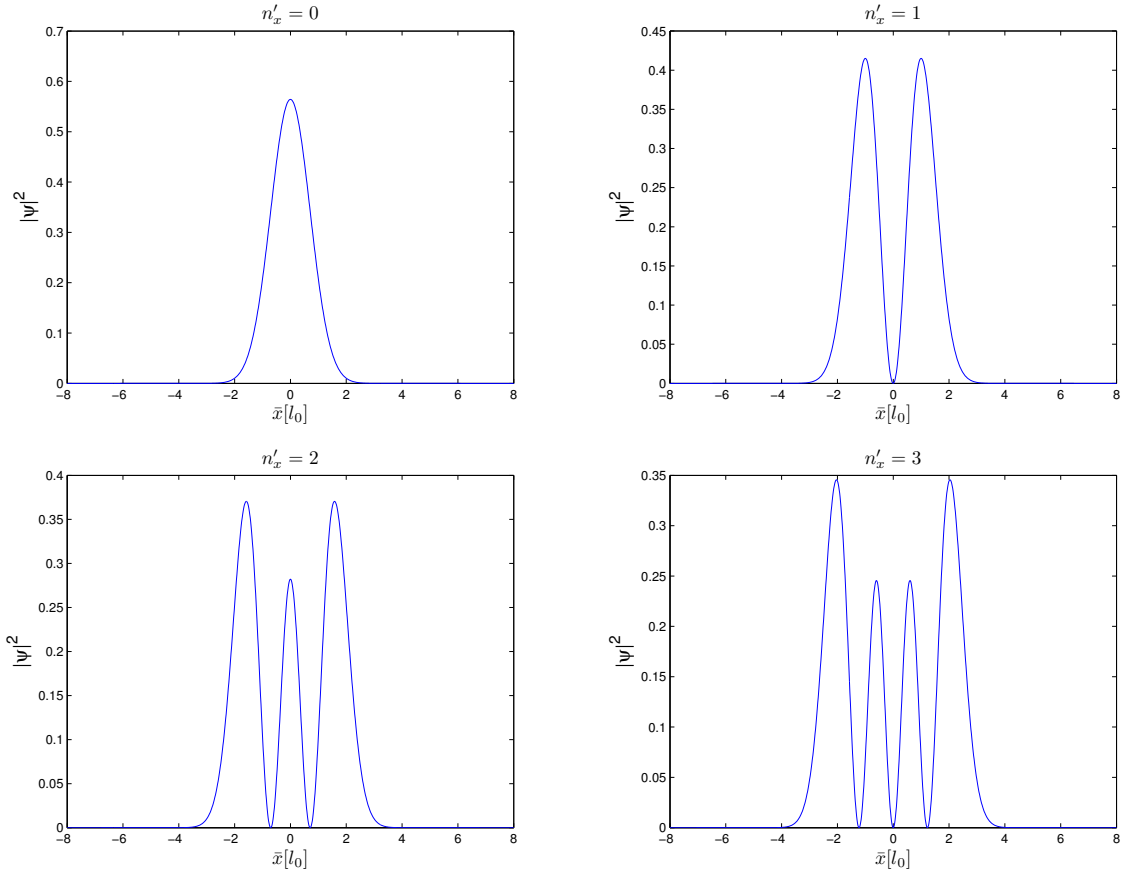


Figure 7.2: The probability density of the four lowest eigenvalues for $L_x = 0$, $\omega = 1$ and $V(x, 0)$.

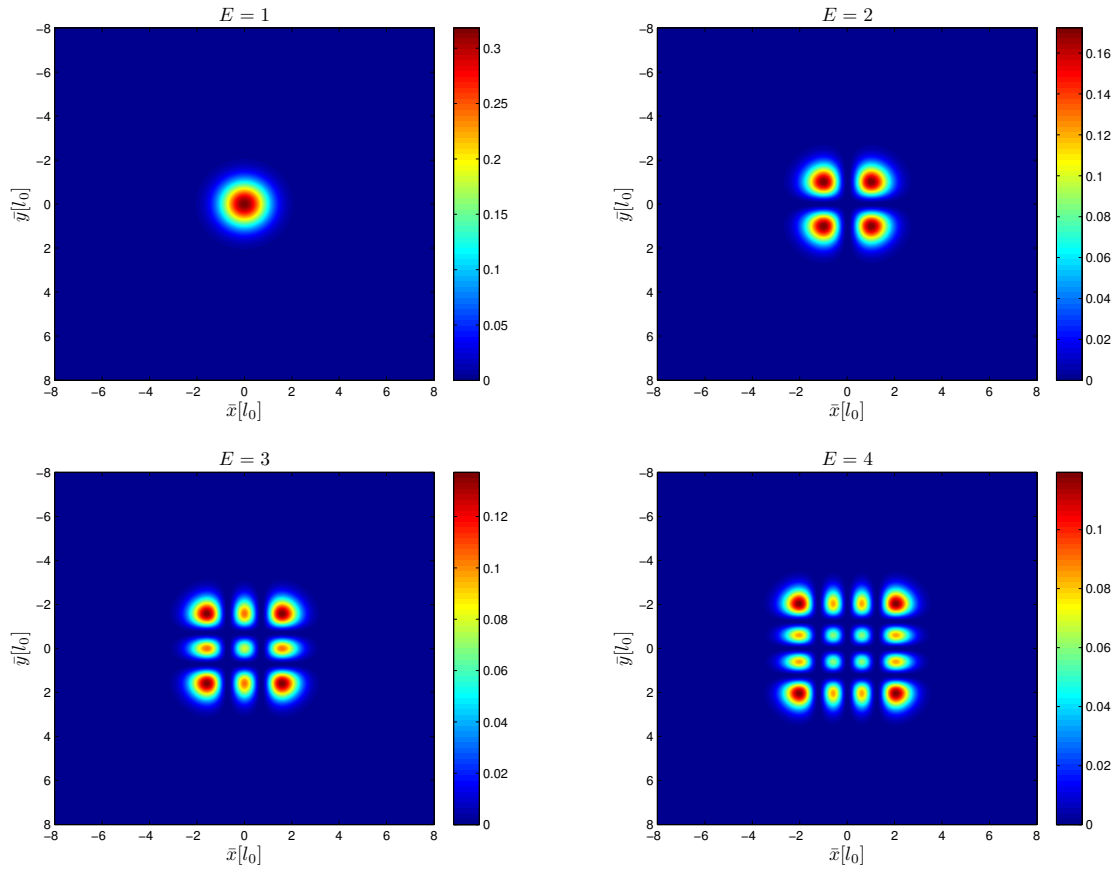


Figure 7.3: The probability density of the four lowest eigenvalues for $L_x = 0$, $\omega = 1$ and $V(x, y)$. The energy E is given in units of $[\hbar\omega]$

Standard Interaction for $L_x = 2.5$, $\omega = 0.8$

p	n'_x	n'_y	m'_s	E
0	0	0	-1	0.9977
1	0	0	1	0.9977
2	1	0	-1	1.0025
3	1	0	1	1.0025
4	2	0	-1	1.9662
5	2	0	1	1.9662
6	0	1	-1	1.9970
7	0	1	1	1.9970
8	1	1	-1	2.0025
9	1	1	1	2.0025
10	3	0	-1	2.0245
11	3	0	1	2.0245
12	4	0	-1	2.8722
13	4	0	1	2.8722
14	2	1	-1	2.9662
15	2	1	1	2.9662
16	0	2	-1	2.9970
17	0	2	1	2.9970
18	1	2	-1	3.0025
19	1	2	1	3.0025
20	3	1	-1	3.0245
21	3	1	1	3.0245
22	5	0	-1	3.8722
23	5	0	1	3.8722

Table 7.5: single-particle states for $L_x = 2.5$, E is the energy eigenvalues and $m'_s = 2m_s$, where $m_s = \pm 1/2$

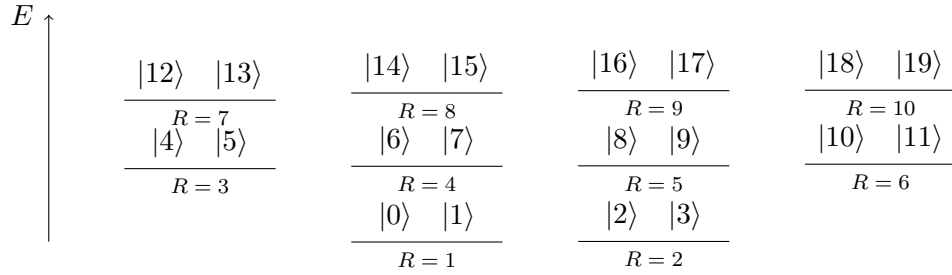


Figure 7.4: Shellstructure for $L_x = 2.5$

$nh = 2$				$nh = 4$			
R	$nh + np$	HF	CCSD	R	$nh + np$	HF	CCSD
1	2	2.8476	2.8466	1	2	-	-
2	4	2.8466	2.7185	2	4	9.5711	9.5719
3	6	2.8337	2.6566	3	6	9.5125	9.6027
4	8	2.8337	2.6608	4	8	9.5125	9.9226
5	10	2.8337	2.6407	5	10	9.5125	not conv.
6	12	2.8337	2.6376	6	12	9.3498	not conv.
7	14	2.8337	2.6373	7	14	9.3498	not conv.
8	16	2.7477	2.5870	8	16	9.0801	not conv.
9	18	2.6978	2.5199	9	18	8.8066	8.3057
10	20	2.6978	not conv.	10	20	8.6306	8.1228
11	22	2.6978	not conv.	11	22	8.6306	8.1119
12	24	2.6978	not conv.	12	24	8.6306	8.1095

Table 7.6: Ground-state energies for hole states $nh = 2$ in a double quantum dot using a standard Coulomb interaction for $L_x = 2.5$, $\omega = 0.8$, where $nh + np$ are the number of holes plus particles in our system.

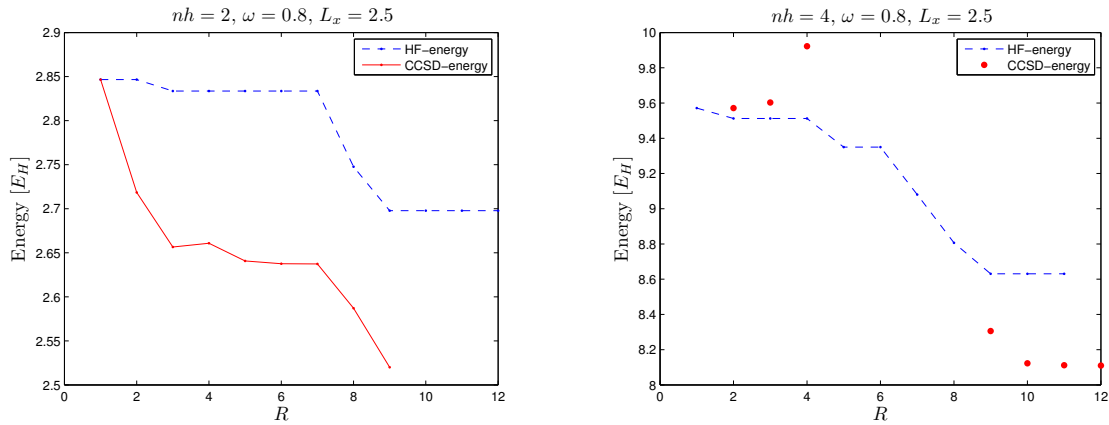


Figure 7.5: CCSD and HF energy as function of subshells R for the 2- and 4-electron system with $L_x = 2.5$, $\omega = 0.8$. The energy is measured in effective Hartrees (E_H)

Standard Interaction for $L_x = 2.5$, $\omega = 1$

$nh = 2$				$nh = 4$			
R	$nh + np$	HF	CCSD	R	$nh + np$	HF	CCSD
1	2	3.3932	3.3931	1	2	-	-
2	4	3.3931	3.2508	2	4	11.1229	11.1229
3	6	3.3808	3.1865*	3	6	11.0769	not conv.
4	8	3.3808	3.1893*	4	8	11.0769	not conv.
5	10	3.3808	3.1634*	5	10	11.0769	not conv.
6	12	3.3808	3.1633*	6	12	10.9337	not conv.
7	14	3.3808	3.1637*	7	14	10.9337	not conv.
8	16	3.2918	3.1119*	8	16	10.6236	not conv.
9	18	3.2400	3.0716*	9	18	10.3394	not conv.
10	20	3.2400	3.0715*	10	20	10.1495	not conv.
11	22	3.2400	not conv.	11	22	10.1495	not conv.
12	24	3.2400	not conv.	12	24	10.1495	not conv.

Table 7.7: Ground-state energies for $nh = 2$ in a double quantum dot using a standard Coulomb interaction for $L_x = 2.5$, $\omega = 1$. I have marked the CCSD energies with (*) where I have extrapolated due to poor convergence.

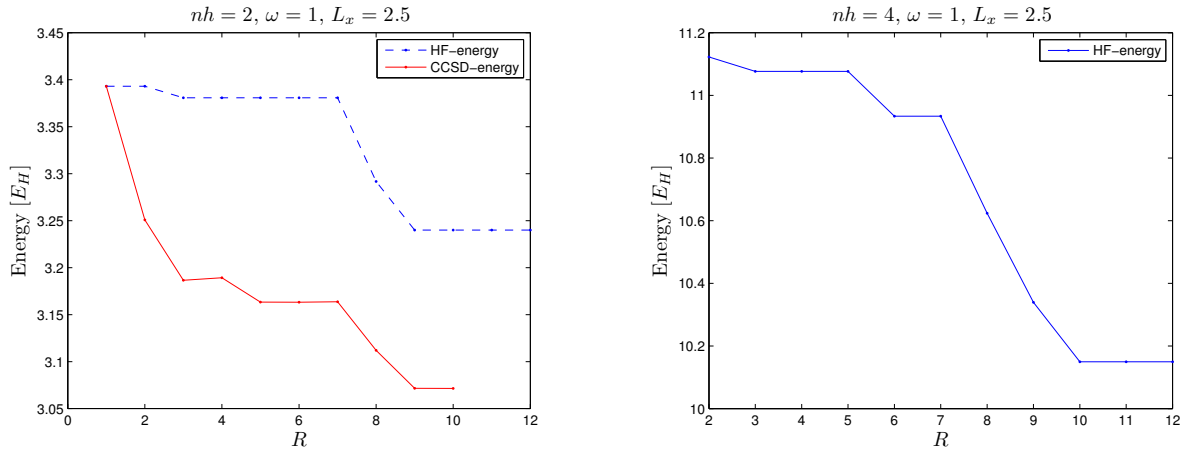


Figure 7.6: CCSD and HF energy as function of subshells R for the 2- and 4-electron system with $L_x = 2.5$, $\omega = 1$. The energy is measured in effective Hartrees (E_H)

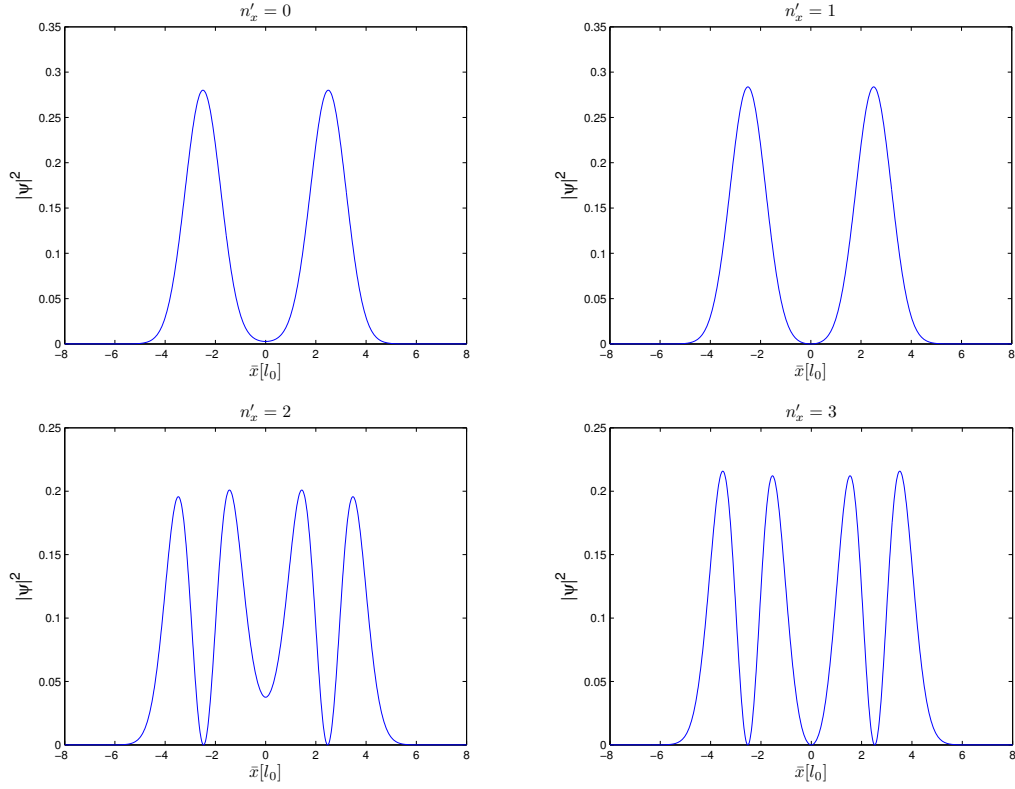


Figure 7.7: The probability density of the six lowest eigenstates for $L_x = 2.5$, $\omega = 1$ and $V(x, 0)$.

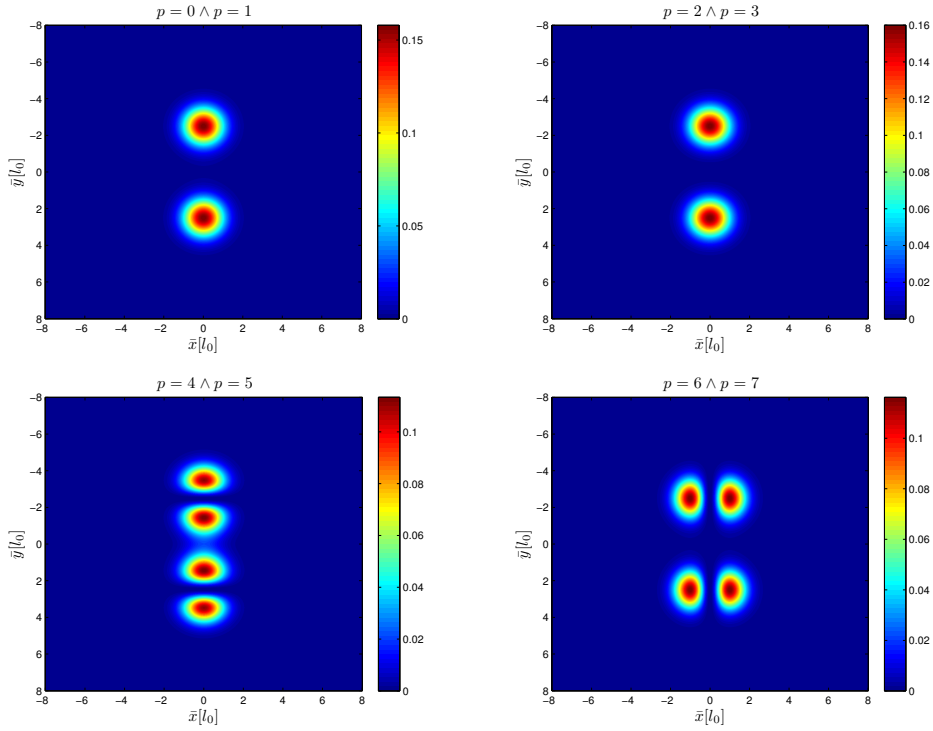


Figure 7.8: The probability density of the six lowest eigenstates for $L_x = 2.5$, $\omega = 1$ and $V(x, 0)$.

Standard Interaction for $V_0 = 8$, $\omega = 1$

p	n'_x	n'_y	m'_s	E	p	n'_x	n'_y	m'_s	E
0	0	0	-1	4.5510	20	0	3	-1	7.5506
1	0	0	1	4.5510	21	0	3	1	7.5506
2	1	0	-1	4.5536	22	1	3	-1	7.5532
3	1	0	1	4.5536	23	1	3	1	7.5532
4	0	1	-1	5.5510	24	4	0	-1	7.8936
5	0	1	1	5.5510	25	4	0	1	7.8936
6	1	1	-1	5.5536	26	5	0	-1	8.1525
7	1	1	1	5.5536	27	5	0	1	8.1525
8	2	0	-1	6.3731	28	2	2	-1	8.3715
9	2	0	1	6.3731	29	2	2	1	8.3715
10	3	0	-1	6.4135	30	3	2	-1	8.3715
11	3	0	1	6.4135	31	3	2	1	8.3715
12	0	2	-1	6.5510	32	0	4	-1	8.4118
13	0	2	1	6.5510	33	0	4	1	8.4118
14	1	2	-1	6.5536	34	1	4	-1	8.5506
15	1	2	1	6.5536	35	1	4	1	8.5506
16	2	1	-1	7.3731	36	4	1	-1	8.8936
17	2	1	1	7.3731	37	4	1	1	8.8936
18	3	1	-1	7.4135	38	5	1	-1	9.1525
19	3	1	1	7.4135	39	5	1	1	9.1525

Table 7.8: single-particle states for $V_0 = 8$, $\omega = 1$. E is the eigenvalues, and m'_s is defined as $m'_s = 2m_s$, where $m_s = \pm 1/2$.

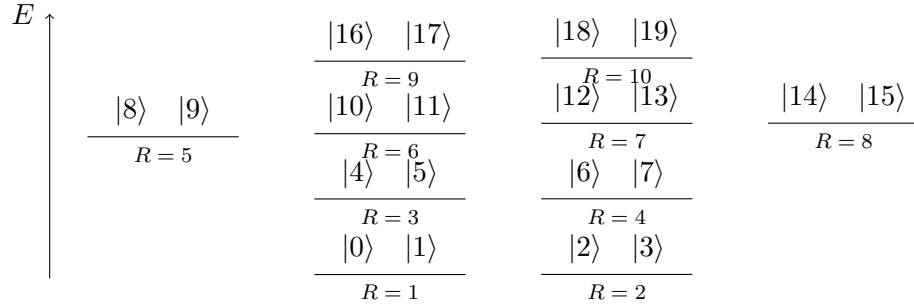


Figure 7.9: Shellstructure for $V_0 = 8$, the levels are drawn with respect to Table 7.8

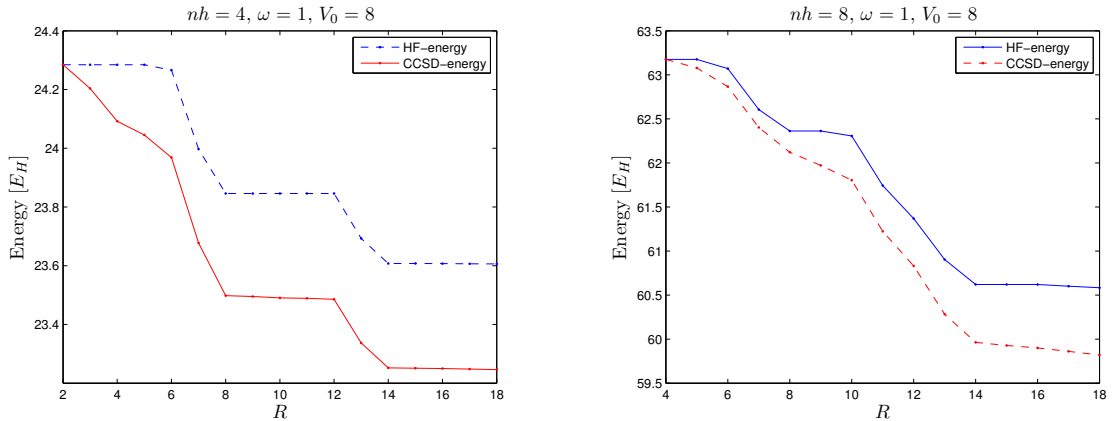


Figure 7.10: CCSD and HF energy as function of subshells R for the 4- and 8-electron system with $V_0 = 8$, $\omega = 1$. The energy is measured in effective Hartrees (E_H)

$nh = 4$				$nh = 8$			
R	$nh + np$	HF	$CCSD$	R	$nh + np$	HF	$CCSD$
2	4	24.2844	24.2844	2	4	-	-
3	6	24.2844	24.2039	3	6	-	-
4	8	24.2844	24.0921	4	8	63.1758	63.1758
5	10	24.2662	24.0452	5	10	63.1757	63.0789
6	12	24.2661	23.9688	6	12	63.0706	62.8668
7	14	23.9971	23.6772	7	14	62.6058	62.4029
8	16	23.8460	23.4980	8	16	62.3627	62.1220
9	18	23.8460	23.4950	9	18	62.3066	61.9723
11	22	23.8460	23.4888	11	22	61.7437	61.8037
12	24	23.8460	23.4857	12	24	61.3687	61.2238
13	26	23.6929	23.3370	13	26	60.9041	60.8306
14	28	23.6074	23.2520	14	28	60.6206	59.9635
15	30	23.6074	23.2510	15	30	60.6206	59.9283
16	32	23.6074	23.2497	16	32	60.6200	59.8997
17	34	23.6074	23.2481	17	34	60.6012	59.8606
18	36	23.6067	23.2463	18	36	60.5834	59.8198

Table 7.9: Ground-state energies for 4 and 8 electrons in a double quantum dot using a standard Coulomb interaction for $V_0 = 8$, $\omega = 1$.

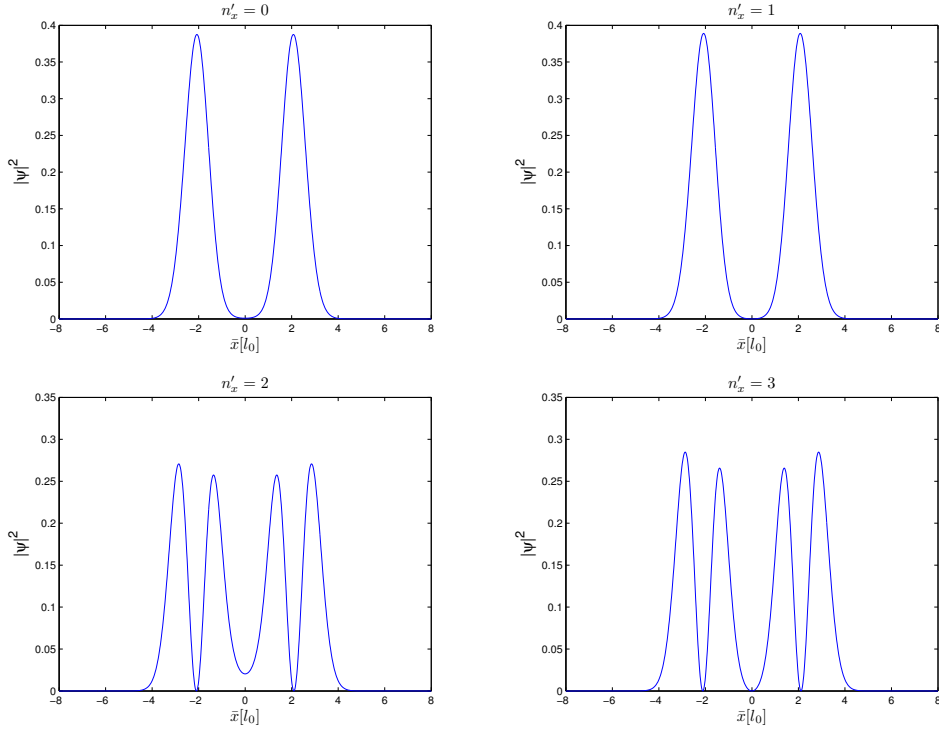


Figure 7.11: The probability density of the six lowest eigenstates for $V_0 = 8$, $\omega = 1$ and $V_G(\bar{x}, 0)$.

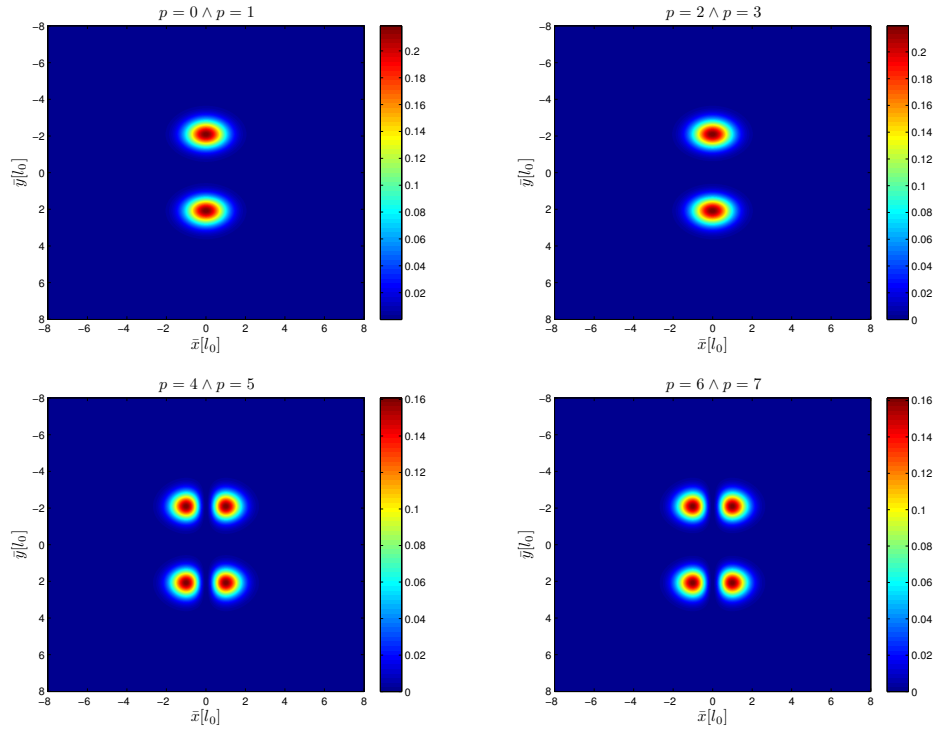


Figure 7.12: The probability density of the six lowest eigenstates for $V_0 = 8$, $\omega = 1$ and $V_G(\bar{x}, \bar{y})$.

Standard Interaction for $V_0 = 10.66$, $\omega = 1$

p	n'_x	n'_y	m'_s	E	p	n'_x	n'_y	m'_s	E
0	0	0	-1	4.9123	20	0	3	1	7.9123
1	0	0	1	4.9123	21	0	3	-1	7.9123
2	1	0	-1	4.9127	22	1	3	1	7.9126
3	1	0	1	4.9127	23	1	3	-1	7.9126
4	0	1	-1	5.9123	24	4	0	1	8.7184
5	0	1	1	5.9123	25	4	0	-1	8.7184
6	1	1	-1	5.9127	26	5	0	1	8.7628
7	1	1	1	5.9127	27	5	0	-1	8.7628
8	2	0	-1	6.9018	28	2	2	1	8.9018
9	2	0	1	6.9018	29	2	2	-1	8.9018
10	3	0	-1	6.9071	30	3	2	1	8.9071
11	3	0	1	6.9071	31	3	2	-1	8.9071
12	0	2	-1	6.9123	32	0	4	1	8.9123
13	0	2	1	6.9123	33	0	4	-1	8.9123
14	1	2	-1	6.9127	34	1	4	1	8.9127
15	1	2	1	6.9127	35	1	4	-1	8.9127
16	2	1	-1	7.9018	36	4	1	1	9.7184
17	2	1	1	7.9018	37	4	1	-1	9.7184
18	3	1	-1	7.9071	38	5	1	1	9.7628
19	3	1	1	7.9071	39	5	1	-1	9.7628

Table 7.10: Tabulated single-particle basis for $V_0 = 10.66$, $\omega = 1.0$, here we have defined $m'_s = 2m_s$, and $m_s = \pm 1/2$.

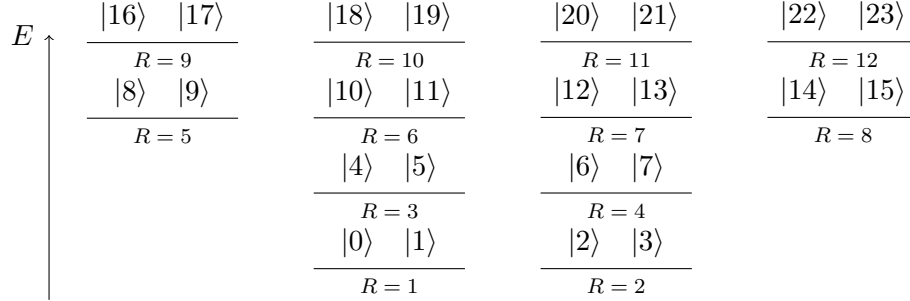


Figure 7.13: Shellstructure for $\omega = 1$, $V_0 = 10.66$ with respect to the single particle energies in Table 7.10

$nh = 8$				$nh = 4$			
R	$nh + np$	HF	$CCSD$	R	$nh + np$	HF	$CCSD$
2	4	65.6857	65.6857	2	4	25.6188	25.6188
4	8	65.5764	65.3979	4	8	25.6188	25.4430
6	12	64.8985	64.6806	6	12	25.5957	25.3295
8	16	63.9310	63.4484	8	16	25.1959	24.8764
12	24	63.9310	62.6858	12	24	25.1959	24.8653
14	28	63.2738	62.6309	14	28	24.9871	24.6589
16	32	63.2729	62.5532	16	32	24.9872	24.6569
18	36	63.2372	62.5532	18	36	24.9858	24.6535
20	40	62.8530	62.1496	20	40	24.9858	24.6511

Table 7.11: Ground-state energies for $nh = 4$ and $nh = 8$ in a double quantum dot using a standard Coulomb interaction for $V_0 = 10.66$, $\omega = 1$.

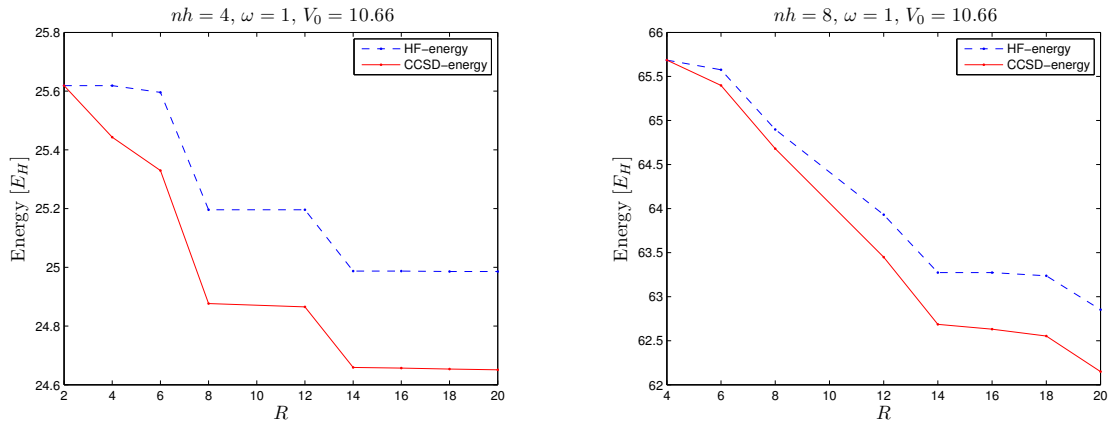


Figure 7.14: CCSD and HF energy as function of subshells R for the 4- and 8-electron system with $V_0 = 10.66$, $\omega = 1$. The energy is measured in effective Hartrees (E_H)

Standard Interaction for $V_0 = 20$, $\omega = 1$

p	n'_x	n'_y	m'_s	E	p	n'_x	n'_y	m'_s	E
0	0	0	-1	5.6822	16	0	3	-1	8.6822
1	0	0	1	5.6822	17	0	3	1	8.6822
2	1	0	-1	5.6822	18	1	3	-1	8.6822
3	1	0	1	5.6822	19	1	3	1	8.6822
4	0	1	-1	6.6822	20	2	1	-1	8.9303
5	0	1	1	6.6822	21	2	1	1	8.9303
6	1	1	-1	6.6822	22	3	1	-1	8.9303
7	1	1	1	6.6822	23	3	1	1	8.9303
8	0	2	-1	7.6822	24	0	4	-1	9.6822
9	0	2	1	7.6822	25	0	4	1	9.6822
10	1	2	-1	7.6822	26	1	4	-1	9.6822
11	1	2	1	7.6816	27	1	4	1	9.6816
12	2	0	-1	7.9303	28	2	2	-1	9.9303
13	2	0	1	7.9303	29	2	2	1	9.9303
14	3	0	-1	7.9303	30	3	2	-1	9.9303
15	3	0	1	7.9303	31	3	2	1	9.9303

Table 7.12: single-particle states for $V_0 = 8$, and E is the eigenvalues, $m'_s = 2m_s$ where m_s is defined as $m_s = \pm 1/2$.

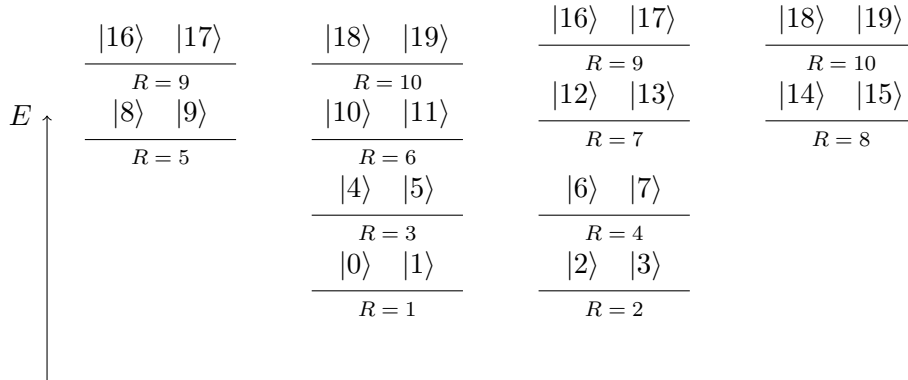


Figure 7.15: Shellstructure for $V_0 = 20$, the levels are drawn with respect to Table 7.12

$nh = 4$				$nh = 8$			
R	$nh + np$	HF	$CCSD$	R	$nh + np$	HF	$CCSD$
2	4	28.5229	28.5229	2	4	-	-
4	8	28.5229	28.3691	4	8	71.2361	71.2361
6	12	28.1446	27.9108	6	12	70.5689	70.4711
8	16	28.1171	27.8315	8	16	70.4506	70.2593
10	20	28.1171	27.8315	10	20	69.5845	69.2638
12	24	28.1171	27.8256	12	24	69.5121	69.0910
14	28	28.1153	27.8217	14	28	69.4645	68.9951
16	32	28.1153	27.8204	16	32	69.4616	68.9481

Table 7.13: Ground-state energies for 4 and 8 electrons in a double quantum dot using a standard Coulomb interaction for $V_0 = 20$, $\omega = 1$.

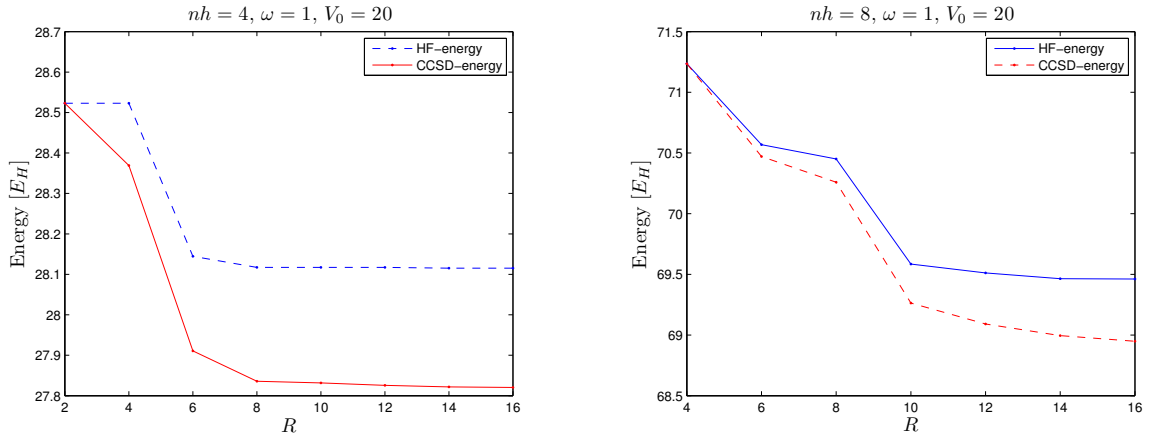


Figure 7.16: CCSD and HF energy as function of subshells R for the 4- and 8-electron system with $V_0 = 20$, $\omega = 1$. The energy is measured in effective Hartrees (E_H)

Potentials

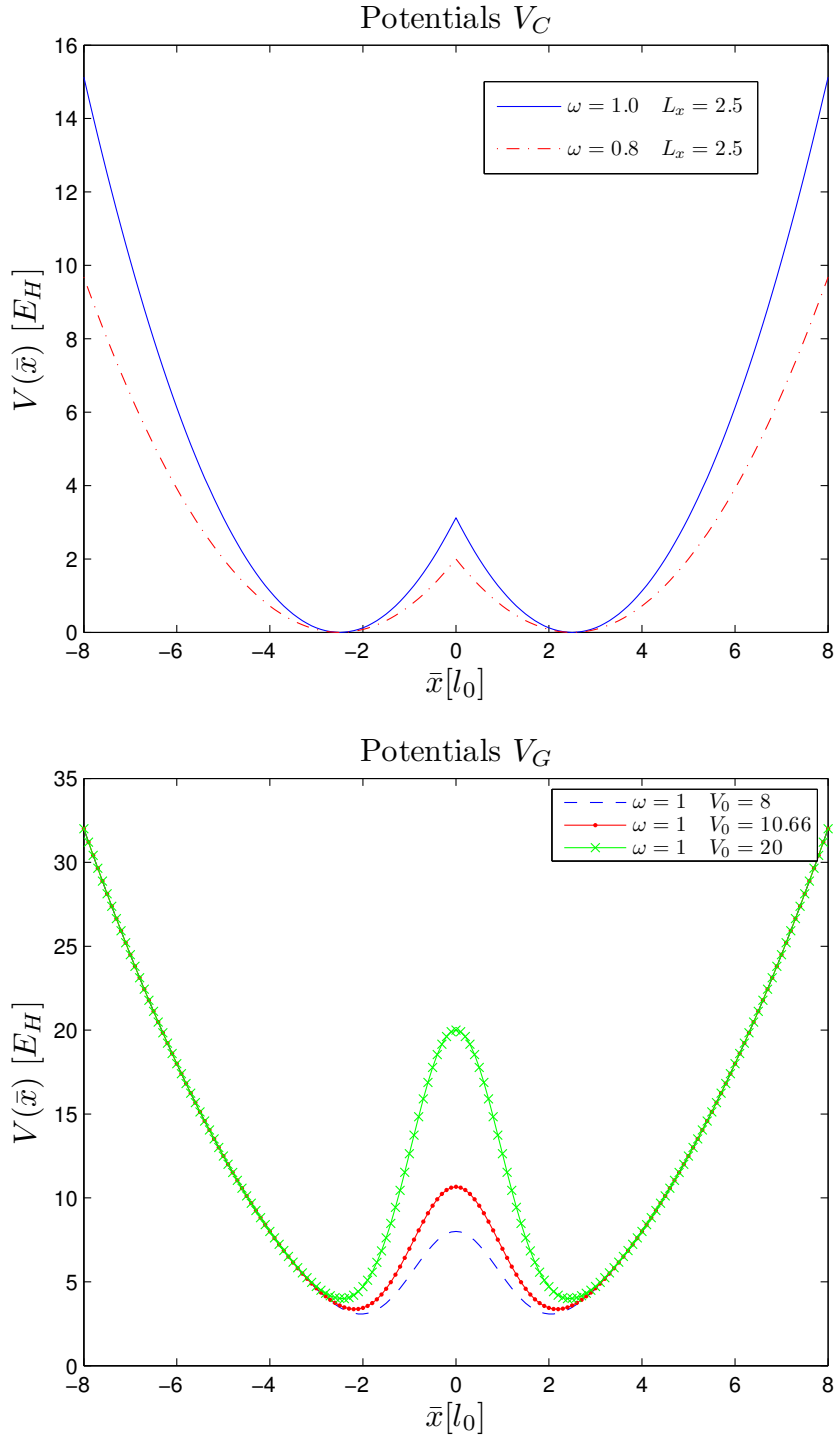


Figure 7.17: The top figure is a plot of the potential Eq. (6.80) for different ω values and $L_x = 2.5$, while the bottom figure show the potential Eq. (6.86) for different V_0 values and $\omega = 1$.

Standard Interaction for $V_0 = 10$, $\omega = 1$, $a = 1.449$, $\sigma = 1$

We want to look at a special potential where they may have 6 electrons in the ground state, a triple quantum dot.

$$V_S = \frac{1}{2}\bar{\omega} \left[\bar{x}^2 + \bar{y}^2 + V_0 \exp\left(-\frac{(\bar{x}-a)^2}{2\sigma}\right) + V_0 \exp\left(-\frac{(\bar{x}+a)^2}{2\sigma}\right) \right] \quad (7.13)$$

Where we have set: $V_0 = 10$, $\omega = 1$, $a = 1.449$, $\sigma = 1$.

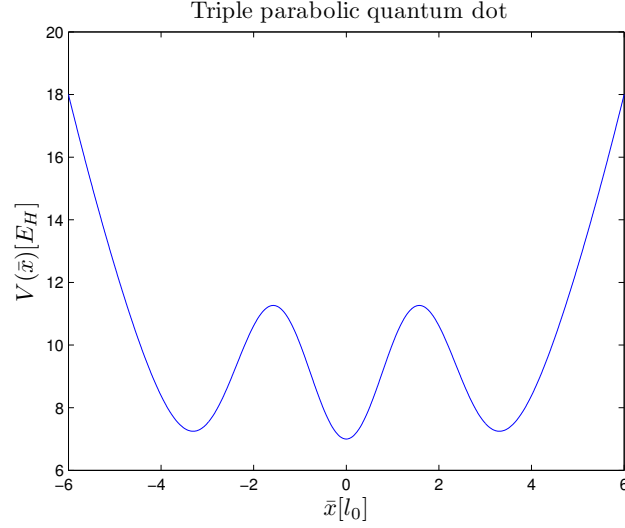


Figure 7.18: Plot of the potential Eq. (7.13) with $V_G(\bar{x}, 0)$ and $V_0 = 10$, $\omega = 1$, $a = 1.449$, $\sigma = 1$.

p	n'_x	n'_y	m'_s	E	p	n'_x	n'_y	m'_s	E
0	0	0	-1	8.8186	20	0	3	1	10.8567
1	0	0	1	8.8186	21	0	3	-1	10.8567
2	1	0	-1	8.8397	22	1	3	1	11.1972
3	1	0	1	8.8397	23	1	3	-1	11.1972
4	0	1	-1	8.8504	24	4	0	1	11.7849
5	0	1	1	8.8504	25	4	0	-1	11.7849
6	1	1	-1	9.8186	26	5	0	1	11.8186
7	1	1	1	9.8186	27	5	0	-1	11.8186
8	2	0	-1	9.8397	28	2	2	1	11.8397
9	2	0	1	9.8397	29	2	2	-1	11.8397
10	3	0	-1	9.8504	30	3	2	1	11.8504
11	3	0	1	9.8504	31	3	2	-1	11.8504
12	0	2	-1	10.7849	32	0	4	1	11.8567
13	0	2	1	10.7849	33	0	4	-1	11.8567
14	1	2	-1	10.8186	34	1	4	1	12.1972
15	1	2	1	10.8186	35	1	4	-1	12.1972
16	2	1	-1	10.8397	36	4	1	1	12.2962
17	2	1	1	10.8397	37	4	1	-1	12.2962
18	3	1	-1	10.8504	38	5	1	1	12.7849
19	3	1	1	10.8504	39	5	1	-1	12.7849

Table 7.14: Tabulated single-particle basis for $V_0 = 10$, $\omega = 1.0$, $a = 1.449$, E is the eigenvalues, and m'_s is defined as $m_s = \pm 1/2$.

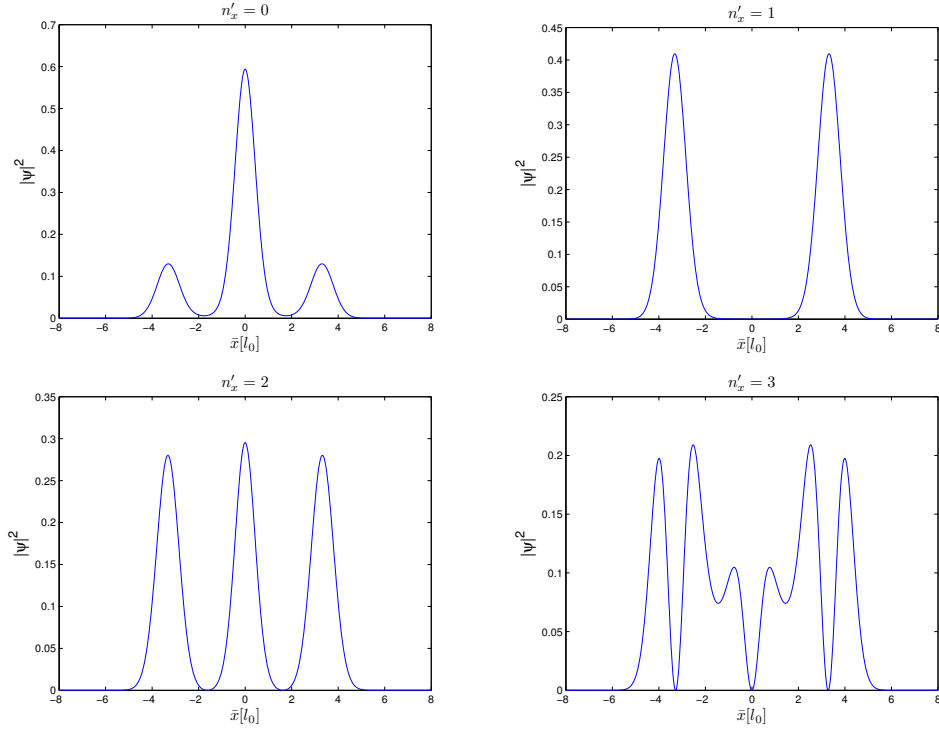


Figure 7.19: The probability density of the six lowest eigenstates for $V_0 = 10$, $\omega = 1$ and $a = 1.449$ for the potential $V_S(\bar{x}, 0)$.

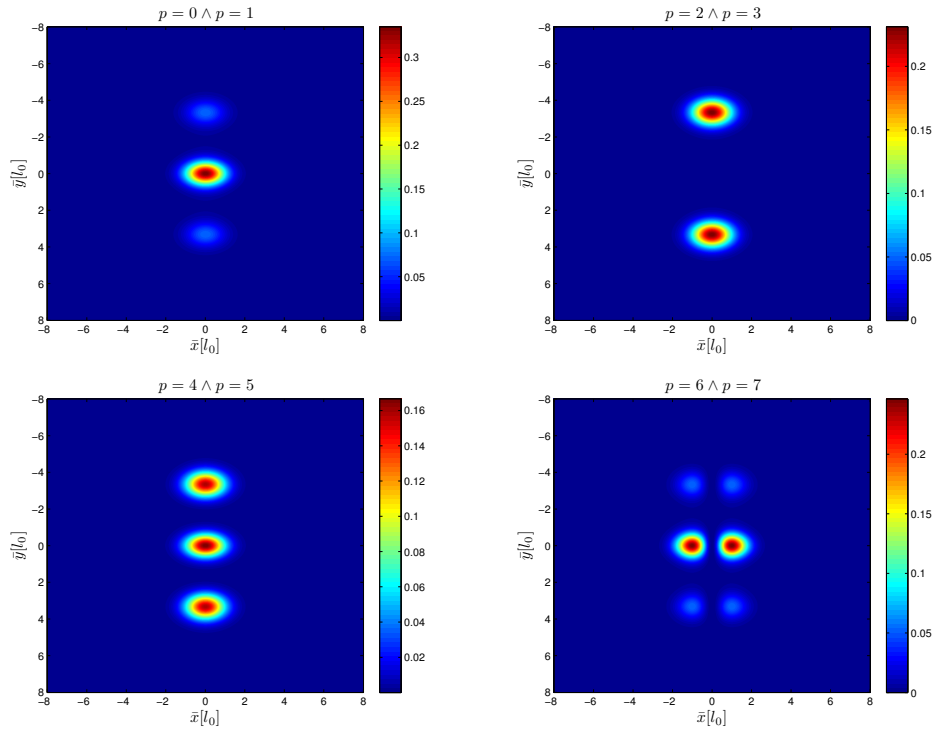


Figure 7.20: The probability density of the six lowest eigenstates for $V_0 = 10$, $\omega = 1$ and $a = 1.449$ for the potential $V_S(\bar{x}, \bar{y})$.

$nh = 2$			$nh = 4$			$nh = 6$		
R	$nh + np$	$CCSD$	R	$nh + np$	$CCSD$	R	$nh + np$	$CCSD$
2	4	18.6711	2	4	41.5660	2	4	-
4	8	18.7212	4	8	no conv.	4	8	67.2539
6	12	18.6911	6	12	no conv.	6	12	no conv.
8	16	18.3337	8	16	no conv.	8	16	no conv.
10	20	22.8665	10	20	no conv.	10	20	no conv.
14	28	24.5351	14	28	no conv.	10	20	no conv.
16	32	18.4136	16	32	no conv.	16	32	no conv.
20	40	26.4021	20	40	no conv.	20	40	no conv.

Table 7.15: Ground-state energies for 2,4,6-electrons in a triple quantum dot using a standard Coulomb interaction for $V_0 = 10$, $\omega = 1$, $a = 1.449$. Here $nh + np$ are the total number of particles for a given R , Eq. (7.12). We have no convergence in most of the cases.

$ 12\rangle$ $ 13\rangle$	$ 14\rangle$ $ 15\rangle$	$ 16\rangle$ $ 17\rangle$	$ 18\rangle$ $ 19\rangle$	$ 20\rangle$ $ 21\rangle$
$R = 7$	$R = 8$	$R = 9$	$R = 10$	$R = 11$
	$ 6\rangle$ $ 7\rangle$	$ 8\rangle$ $ 9\rangle$	$ 10\rangle$ $ 11\rangle$	
	$R = 4$	$R = 5$	$R = 6$	
	$ 0\rangle$ $ 1\rangle$	$ 2\rangle$ $ 3\rangle$	$ 4\rangle$ $ 5\rangle$	
	$R = 1$	$R = 2$	$R = 3$	

Figure 7.21: Shellstructure for the potential V_S with respect to the single particle energies in Table 7.14. We have dotted the level to $R = 1$. We see that $R = 2$ and $R = 3$ is not entirely overlapping with $R = 1$

7.2 General Analysis and Discussion

We start by considering the HF and CCSD results for 2-electron and 6-electron quantum dot for the system $L_x = 0$ and $\omega = 1$, Tables 7.2 and 7.3. We observe that the differences between the energies in our calculation and [47] are of the order 1E-6. This could be caused by the tolerance in the CCSD and HF calculation. I have used a tolerance of 1E-8 in my HF calculation and a tolerance of 1E-7 in the CCSD calculation. While I'm uncertain of what the tolerance of the CCSD and HF calculation are in [47]. Next we consider the double quantum dot potential Eq. (6.80), with $L_x = 2.5$ and $\omega = 1$, see Table 7.7. For the 2-electron system we see that the CCSD calculation have a poor convergence and does not converge at all for $R = 11$ and $R = 12$. If we look at the possibilities for placing two electron in the lowest single-particle states, Table 7.5 and Fig. 7.4: Then we get a total of six Slater determinants

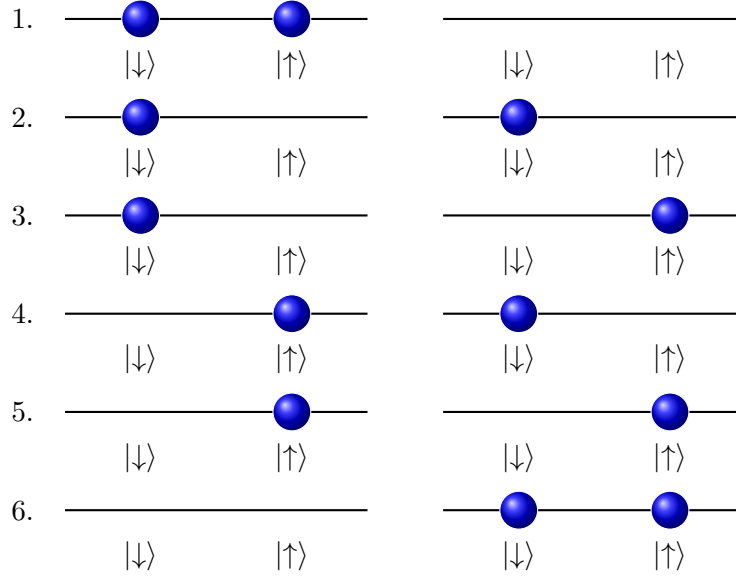


Figure 7.22: Different SD for the single-particle basis in Table 7.5. The blue spheres represent the electrons and the spin configurations of those are denoted beneath. Here we have assumed that the subshells R_1 and R_2 in Fig. 7.4 are degenerate, but in reality they differ in the fourth decimal place.

for this system. A proper way of dealing with this is using a multireference coupled-cluster theory [46]. Which means that the ground state Slater determinant are a linear combination of those six possibilities with a probability amplitude for each. Our calculation in Table 7.7 for the 2-electron system are with the SD no. 3 in Fig. 7.22. The same problem applies to the HF energy as well. In the calculation in Table 7.7 we are assuming that the ground-state Slater determinant is no. 3 in Fig. 7.22. But we have to take into account the other Slater determinants as well which then gives us new coefficients for us to minimize. This is the multi-configurational Hartree-Fock method [1].

For the 4-electron system we have only one possible Slater determinant which have total spin 0, see Table 7.7. We have convergence for the HF energy after $R = 10$. But there is no convergence for the CCSD energy at all. This is because that we do not have a big enough harmonic oscillator basis due to the cusp of the absolute value, remember that our maximal n_x is only 20. Together with the fact that we are using Newton's method when we search for the energy minimum in CCSD makes the calculation unstable. However, when we apply a lower ω -value we see that the ground-state energy goes a down for HF-energy and the 4-electron system. This makes sense since an increased frequency ω , means a steeper potential Fig. 7.17, which means that the electrons are pushed closer together, giving them more kinetic energy. We see this effect in the circular quantum dot ($L_x = 0$), see [47] and [45].

The CCSD energies have good convergence for the potential Eq. (6.86) and we see that the ground-state energy increase with the height of the Gaussian V_0 , see Tables 7.9, 7.9 and 7.13. Comparing the HF energy with CCSD energy, we see that the difference does not change much after the energies have

converged. This is what we expect since the HF-calculations take into account 1p-1h excitation, while the CCSD have the 2p-2h contribution in addition, this will lower the CCSD-energy compared to the HF-energy with a constant value. We have done an analysis of the ground state energies for a model space with $R = 12$. We look at the 4- and 8-electron system with increasing V_0 for the Gaussian potential Eq. (6.86)

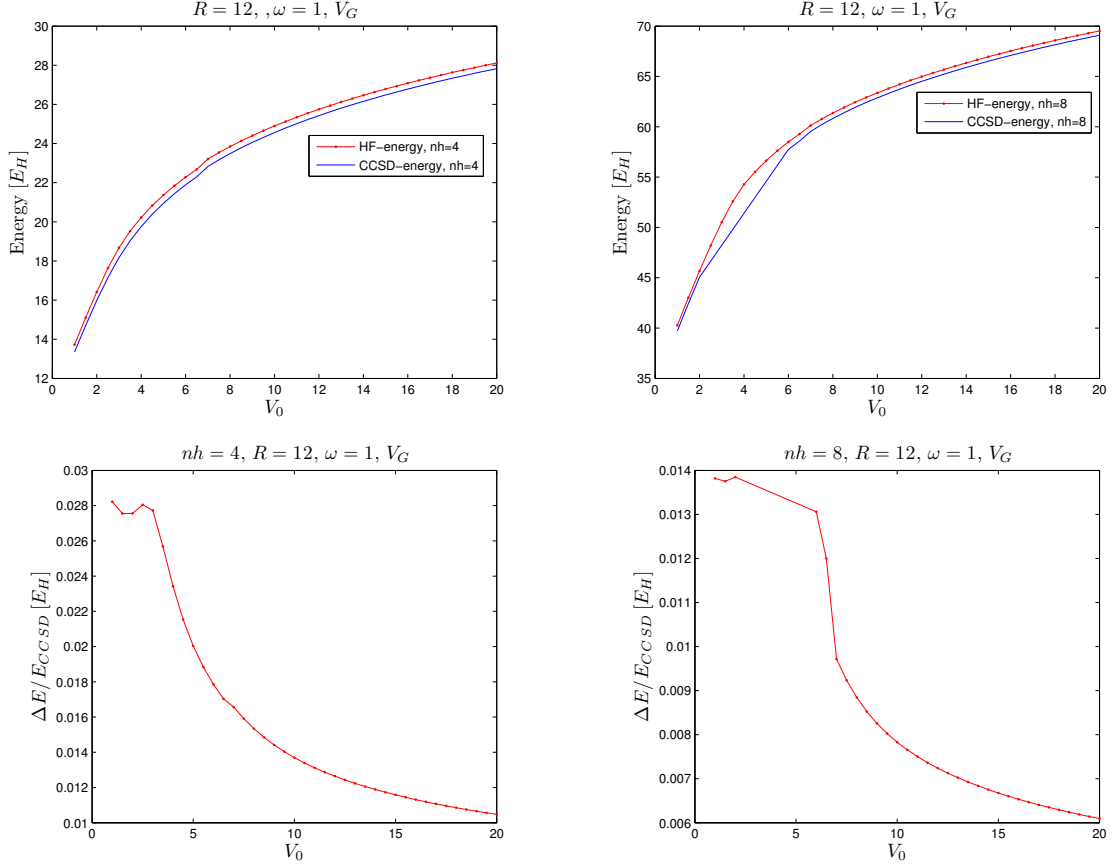


Figure 7.23: On the top left and right, we show the CCSD and HF energies for the 4 and 8-electron system respectively. We have calculated the energy for a $R = 12$ model space, i.e. 24 single-particle orbitals. Next we compare the energy difference of HF and CCSD. ΔE is defined as $\Delta E = E_{HF} - E_{CCSD}$.

For the 8-electron system, the CCSD energy does not converge for $V_0 = 2.5$ to $V_0 = 5.5$. The explanation for this could be that the Slater determinant in that range is wrong. The same problem we saw earlier that we may need a multireference calculation. If we look at the single-particle energies in Fig. 7.24, we see that the single particle states in the range $V_0 = 2.5$ to $V_0 = 5.5$ is overlapping many other excited single-particle states. This is not the case with the 4-electron system.

We define the correlation energy by

$$\%E_{corr} = \frac{E_{CCSD} - \sum_{ij} \langle i | \hat{h} | j \rangle}{E_{CCSD}} \quad (7.14)$$

The contribution to the energy that comes from the correlation energy falls off with increasing V_0 . This is because when V_0 increases the tunneling barrier becomes bigger and the electrons will interact less with each other. Finally we have looked at the triple quantum dots system. Which is essentially two Gaussian functions in the harmonic oscillator well. We tried to adjust the parameters so that we had 6 possible single-orbital states in the ground-state, see Table 7.14. Here we have the states $p = 0$ and $p = 1$ that are exactly degenerate, because of spin. But $p = 1$ and $p = 2$ are not exactly degenerate, they differ in the second decimal place. However $p = 2$ and $p = 3$ are degenerate because of spin. This

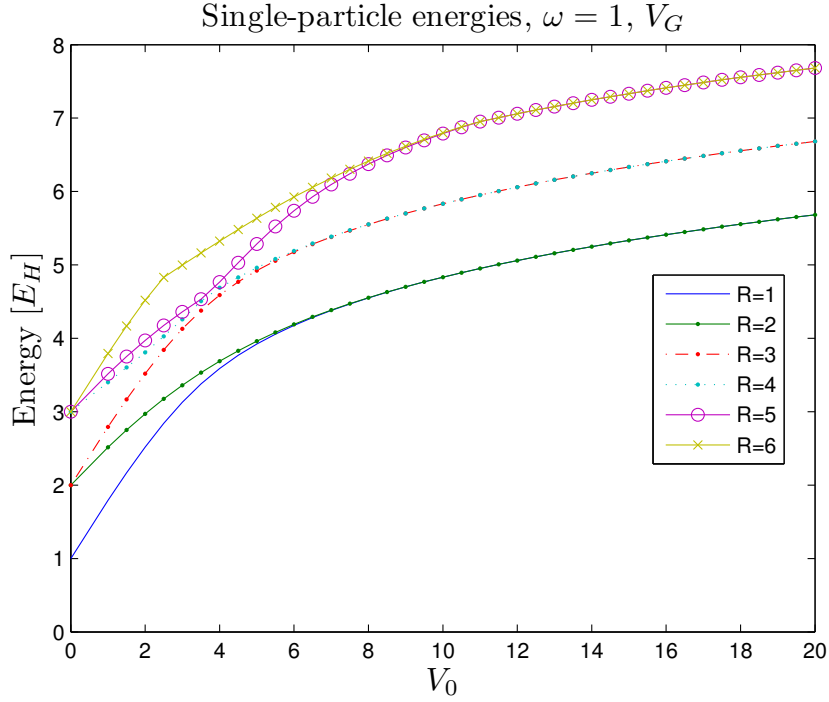


Figure 7.24: We are interested to see how the single-particle energies develops with increasing V_0 in the Gaussian double quantum dots Eq. 6.86. This is a plot over single-particle energies and the R 's denote the subshells, each R can be occupied by two electrons because of spin. We see that in the range $V_0 = 2$ til $V_0 = 6$, the energy levels are tanglet together and it's difficult to make sense of the shellstructure in such a system.

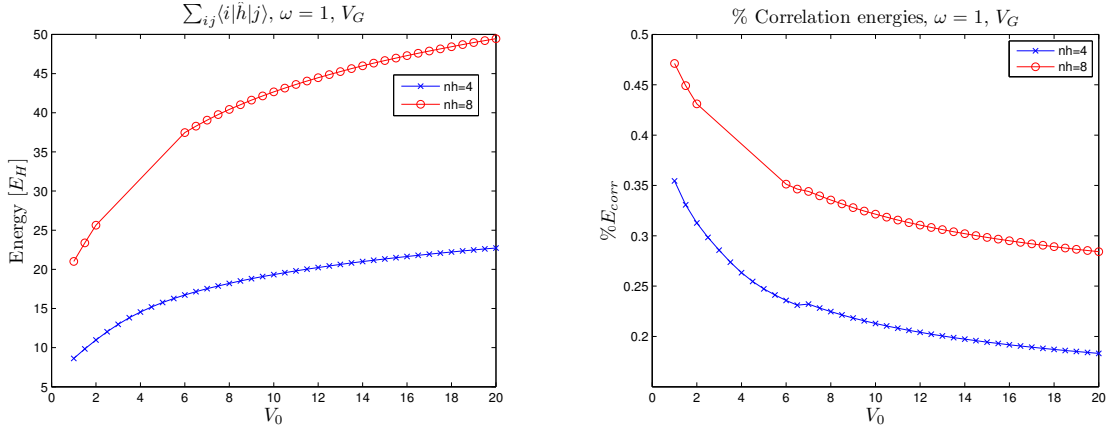


Figure 7.25: The plot on the leftside shows single-particle energies for 4- and 8-particles as a function of V_0 . While on the right we have plotted the correlation energy defined in Eq. (7.14)

makes it difficult to define a possible Slater determinant, therefore we have tried to run the CCSD code with 2,4 and 6-electrons. And as we can see they do not converge at all, except for the 2-electron system that convergences poorly. The conclusion must be that the referebce Slater we start off with is not the correct ones. The coupled-cluster calculation seem to be very dependent on how close the energy levels are together as we have seen in the case of 8-electrons in Fig. 7.23, when V_0 are between 2.5 and 5. It would have been interesting to see if we could tune those parameters so that the 6 states becomes even more degenerate. However, when the energies for 6 electrons in the triple dot potential does not converge,

this does not mean such a state with 6-electrons in the lowest lying single-particle orbitals. We have used a very inferior method for solving the coupled cluster equations. Therefore, we cannot conclude anything at this moment. From a physical perspective it would be reasonable to have 6-electrons in the lowest lying single-particle orbitals for the triple quantum dots.

Chapter 8

Conclusions

"My interest in science is to simply find out about the world, and the more I find out the better it is, like, to find out." (From "The pleasure of finding things out")

R. P. Feynman

We have developed a method for studying several interacting electrons confined in two-dimensional potential wells. In these type of quantum wells the electrons can tunnel to other excited states and in the literature such systems are dubbed two-dimensional double quantum dots systems. This have to our knowledge never been done with an advanced many-body quantum theory like the CCSD. The model that we have considered was a circular quantum dot with a *bump* in one of the dimensions, in the other dimension we still have the one-dimensional harmonic oscillator. The *bump* could be a Gaussian curve, or an absolute value.

One of the first goals was to find the single-particle eigenfunctions of those potentials and expand them in a harmonic oscillator basis. The reason we do this is because of the known two-particle interaction elements Simen Kvaal [42] developed in his PhD thesis for the harmonic oscillator eigenfunctions. The next goal was to transformation his two-particle interaction elements from a polar basis to a Cartesian basis representation. His code gives us effective interaction elements as well. We have implemented this but not used it to produce our results. We have focused on the standard coulomb interaction. But the effective interaction elements would most likely give us a better estimate for the energy. The aim of this thesis was not to give a precise description of our model but to prove that our method of transformation and coupled-cluster theory together with these new interaction elements actually produce meaningful results. We have also developed a Restricted Hartree-Fock (RHF) program to check that the coupled-cluster results are not totally wrong, since RHF gives a variational energy. In addition to this the CCSD from [47] have been optimized with great success and can now be run in parallel with OpenMP.

We have tried to limit ourselves to closed-shell systems. We have considered ground-state Slater determinants based on the lowest single-particle (in energy) states, but sometimes it is difficult to define properly what is a good closed shell systems, like in the triple dots. But for a systems where the ground-state has a single well-defined Slater determinant the coupled-cluster calculations perform well in sense of convergence properties. Other methods for solving the double well have been cumbersome and the dimensionality quickly raises when we try to diagonalize the system [64]. A VMC calculation for this system is possible, but then again, finding the Jastrow-factor is an open issue. We could instead use our CCSD calculations as an starting point in a more precise DMC calculation.

As we have mentioned, one of the sources for errors are the size of the model space. Since our harmonic oscillator basis was not bigger than 20, the model space of our interaction elements could not be big, after $R = 20$, i.e. 40 single-particle basis states, the interaction elements becomes more inaccurate. That is why we have small model spaces.

The CCSD code and the transformations that we have developed are very versatile, we have shown that we can calculate the ground state energies for any potential, and any closed shell number of particles that can be expanded with reasonable number of harmonic oscillator basis functions. The other criteria must be that the groundstate have to be a well-defined single Slater determinant.

8.1 Continuation of this thesis

The first improvement we could do is to do a HF-calculation and use this as input to our coupled-cluster code. This gives us better single-particle states and two-particle interaction elements and will most likely give a better convergence for our coupled-cluster implementation. Another improvement is to include the option of choosing the analytical coulomb interaction elements [62], when using standard interaction. This would speed up the part for generating the interaction elements. Furthermore, the next step is to use an effective Coulomb interaction as this will most likely result in a better estimate of the energies. Another important step is to improve our iteration method, a better choice would be to use Broyden's method [4]

The system that we have studied is a perturbation in one of the dimensions, but the code can easily be expanded to take perturbation in both dimensions and diagonalize a two dimensional problem.

The CCSD code was parallelized with OpenMP, the downside of this is that we can only run our CCSD code on single nodes with shared memory. The next step is to implement a MPI routine. The parallel algorithms that we have developed can easily be translated into MPI code. An even better optimization is to use OpenCL, but this is more difficult because of the limited memory space in the GPUs.

We have used a simple difference method for finding the single-particle eigenvectors and eigenvalues, but we could use the better Richardson's deferred extrapolation method [32] to get more precise eigenvalues and eigenfunctions.

We have shown the versatility of our CCSD code, it is implemented with C++ classes and we would like to have a class implementation for the different potentials we want to use.

The final aim would be to extend our stationary coupled cluster approach to include time-dependent external probes. This would bring in close contact with experiments on quantum dot systems.

"There's beauty not just at the dimension of one centimeter; there's also a beauty at smaller dimensions."

R. P. Feynman

Appendix A

Derivation of the Baker-Campbell-Hausdorff formula

We will now derive the following relation:

$$\begin{aligned} e^{-\lambda\hat{A}}\hat{B}e^{-\lambda\hat{A}} &= \hat{B} + \lambda [\hat{B}, \hat{A}] + \frac{\lambda^2}{2!} [[\hat{B}, \hat{A}], \hat{A}] + \frac{\lambda^3}{3!} [[[\hat{B}, \hat{A}], \hat{A}], \hat{A}] + \dots \\ &= \sum_{n=0}^{\infty} \frac{1}{n!} (\text{ad}(\hat{B}))^n \hat{A}, \quad (\text{ad}(\hat{B}))^n \hat{A} = [[[\hat{B} \dots, \hat{A}], \hat{A}], \hat{A}] \text{ (n times)} \end{aligned} \quad (\text{A.1})$$

We define

$$\hat{G}(\lambda) = e^{-\lambda\hat{A}}\hat{B}e^{\lambda\hat{A}} \quad (\text{A.2})$$

We want to do a Taylor series expansion with this function around $\lambda = 0$,

$$\hat{G}(\lambda) = \hat{G}(0) + \left. \frac{d\hat{G}}{d\lambda} \right|_{\lambda=0} (\lambda - 0) + \frac{1}{2!} \left. \frac{d^2\hat{G}}{d^2\lambda} \right|_{\lambda=0} (\lambda - 0)^2 + \frac{1}{3!} \left. \frac{d^3\hat{G}}{d^3\lambda} \right|_{\lambda=0} (\lambda - 0)^3 + \dots \quad (\text{A.3})$$

0th order:

$$\hat{G}(0) = \hat{B}. \quad (\text{A.4})$$

1th order:

$$\left. \frac{d\hat{G}}{d\lambda} \right|_{\lambda=0} = \left[-\hat{A}e^{-\lambda\hat{A}}\hat{B}e^{\lambda\hat{A}} + e^{-\lambda\hat{A}}\hat{B}e^{\lambda\hat{A}}\hat{A} \right]_{\lambda=0} = [\hat{G}(0), \hat{A}] = [\hat{B}, \hat{A}]. \quad (\text{A.5})$$

2nd order:

$$\frac{d^2\hat{G}}{d^2\lambda} = \frac{d\hat{G}}{d\lambda} [\hat{G}, \hat{A}] = \left[\frac{d\hat{G}}{d\lambda}, \hat{A} \right] = [[\hat{G}, \hat{A}], \hat{A}]. \quad (\text{A.6})$$

$$\Rightarrow \left. \frac{d^2\hat{G}}{d^2\lambda} \right|_{\lambda=0} = [[\hat{B}, \hat{A}], \hat{A}]. \quad (\text{A.7})$$

3rd order:

$$\frac{d^3\hat{G}}{d^3\lambda} = \frac{d\hat{G}}{d\lambda} [[\hat{G}, \hat{A}], \hat{A}] = \left[\left[\frac{d\hat{G}}{d\lambda}, \hat{A} \right], \hat{A} \right] = [[[\hat{G}, \hat{A}], \hat{A}], \hat{A}]. \quad (\text{A.8})$$

$$\Rightarrow \left. \frac{d^3\hat{G}}{d^3\lambda} \right|_{\lambda=0} = [[[\hat{B}, \hat{A}], \hat{A}], \hat{A}]. \quad (\text{A.9})$$

n-th order:

$$\frac{d^n\hat{G}}{d^n\lambda} = \frac{d\hat{G}}{d\lambda} \underbrace{[[[\hat{G} \dots, \hat{A}], \hat{A}], \hat{A}]}_{(n-1) \text{ nested commutators}} = \underbrace{[[[\hat{G} \dots, \hat{A}], \hat{A}], \hat{A}]}_{n \text{ nested commutators}}.$$

Bibliography

- [1] A. Aboussaïd, M. R. Godefroid, P. Jönsson, and C. Froese Fischer. Multiconfigurational hartree-fock calculations of hyperfine-induced transitions in heliumlike ions. *Phys. Rev. A*, 51:2031, 1995.
- [2] G. Arfken. *Mathematical Methods for Physicists*. Academic Press, Orlando, FL, fifth edition, 2000.
- [3] R.C. Ashoori. Electrons in artificial atoms. *Nature*, 379:413, 1996.
- [4] Andrzej Baran, Aurel Bulgac, Michael McNeil Forbes, Gaute Hagen, Witold Nazarewicz, Nicolas Schunck, and Mario V. Stoitsov. Broyden's method in nuclear structure calculations. *Phys. Rev. C*, 78:014318, 2008.
- [5] R. J. Bartlett and G. D. Purvis. Many-body perturbation theory, coupled-pair many-electron theory, and the importance of quadruple excitations for the correlation. *Int. J. Quantum Chem. Symp.*, 14(561), 1978.
- [6] D. Bimberg, M. Grundmann, F. Heinrichsdorff, N. N. Ledentsov, V. M. Ustinov, A. E. Zhukov, A. R. Kovsh, M. V. Maximov, Y. M. Shernyakov, B. V. Volovik, A. F. Tsatsul'nikov, P. S. Kop'ev, and Zh. I. Alferov. Quantum dot lasers: breakthrough in optoelectronics. *Thin Solid Films*, 367:235, 2000.
- [7] Mary L. Boas. *Mathematical Methods in the Physical Sciences*. Wiley, Hoboken, third edition, 2006.
- [8] Parsa Bonderson and Roman M. Lutchyn. Topological quantum buses: Coherent quantum information transfer between topological and conventional qubits. *Phys. Rev. Lett.*, 106:130505, 2011.
- [9] G. E. Bowman. *Essential Quantum Mechanics*. Oxford University Press, first edition, 2008.
- [10] R. R. Burnside and P. B. Guest. A simple proof of the transposed qr algorithm. *SIAM Review*, 38:306, 1996.
- [11] S. J. Chang. *Introduction to Quantum Field Theory (World Scientific Lecture Notes in Physics, V. 29)*. World Scientific Pub Co Inc, n, 1988.
- [12] F. Coester and H. Kümmel. Short-range correlations in nuclear wave functions. *Nucl. Phys.*, 1:015008, 2008.
- [13] T. D. Crawford and H. F. Schaefer. An introduction to coupled cluster theory for computational chemist. *Rev. Comp. Chem.*, 14:33, 2007.
- [14] C. G. Darwin. *Proc. Cambridge Philos. Soc.*, 27:86, 1930.
- [15] D. J. Dean, G. Hagen, M. Hjorth-Jensen, and T. Papenbrock. Computational aspects of nuclear coupled-cluster theory. *Comp. Sci. and Disc.*, 1:015008, 2008.
- [16] W. H. Dickhoff and D. V. Neck. *Many-Body Theory Exposed!* World Scientific, first edition, 2005.
- [17] P. A. M. Dirac. *The principles of quantum mechanics*. Oxford University Press., fourth edition, 1982.
- [18] J. Dongarra and F. Sullivan. Guest editors introduction to the top 10 algorithms. *Comp. in Sci. Eng.*, 2:22, 2000.
- [19] L. N. Drøsdal. *Finite Element Studies of Quantum Dots*. Master thesis, University of Oslo, 2009.
- [20] B. Faires. *Numerical Analysis*. Brooks/Cole, eighth edition, 2004.

- [21] V. Fock. *Z. Physik*, 47:446, 1928.
- [22] J. G. F. Francis. The qr transformation a unitary analogue to the lr transformation part 1. *The Computer Journal*, 4:265, 1961.
- [23] Gene H. Golub and Charles F. Van Loan. *Matrix computations (3rd ed.)*. Johns Hopkins University Press, Baltimore, MD, USA, 1996.
- [24] David J. Griffiths. *Introduction to Quantum Mechanics*. Benjamin Cummings, London, second edition, 2004.
- [25] G. Hagen, T. Papenbrock, D. J. Dean, and M. Hjorth-Jensen. Ab initio coupled-cluster approach to nuclear structure with modern nucleon-nucleon interactions. *Phys. Rev. C*, 82:034330, 2010.
- [26] Detlef Heitmann and Jorg P. Kotthaus. The spectroscopy of quantum dot arrays. *Physics Today*, 46:56, 1993.
- [27] T. Helgaker, P. Jørgensen, and J. Olsen. *Molecular Electronic Structure Theory. Energy and Wave Functions*. Wiley, Chichester, 2000.
- [28] P. C. Hemmer. *Kvantemekanikk*. Tapir akademiske forlag, 5. utgave edition, 2005.
- [29] Thomas M. Henderson, Keith Runge, and Rodney J. Bartlett. Excited states in artificial atoms via equation-of-motion coupled cluster theory. *Phys. Rev. B*, 67:045320, 2003.
- [30] H. B. Schlegel, J. A Pople and J. S. Binkley. Electron correlation theories and their application to the study of simple reaction potential surfaces. *Int. J. Quantum Chem. Symp.*, 14(545), 1978.
- [31] J. D. Jackson. *Classical Electrodynamics*. Wiley, third edition edition, 1998.
- [32] M. H. Jensen. *Computational Physics*. Jensen, University of Oslo, 2010.
- [33] M. H. Jensen. *Slides from FYS-KJEM4480*. University of Oslo, 2010.
- [34] M. H. Joergensen. *Coupled-Cluster Studies of Quantum Dots*. Master’s thesis, University of Oslo, 2011.
- [35] D. Kincaid and W. Cheney. *Numerical Analysis: Mathematics of Scientific Computing*. American Mathematical Society, third edition, 2009.
- [36] Walter Kohn. Cyclotron resonance and de haas-van alphen oscillations of an interacting electron gas. *Phys. Rev.*, 123:1242, 1961.
- [37] A. I. Krylov. Equation-of-motion coupled-cluster methods for open-shell and electronically excited species: The hitchhiker’s guide to fock space. *Ann. Rev. of Phys. Chem.*, 59:433, 2008.
- [38] V. N. Kublanovskaya. On some algorithms for the solution of the complete eigenvalue problem. *USSR Comput. Math.*, 3:637, 1961.
- [39] S. A. Kucharski and R. J. Bartlett. Fifth-Order Many-Body Perturbation Theory and Its Relationship to Various Coupled-Cluster Approaches. *Adv. in Quant. Chem.*, 18:281, 1986.
- [40] Arvind Kumar, Steven E. Laux, and Frank Stern. Electron states in a gaas quantum dot in a magnetic field. *Phys. Rev. B*, 42:5166, 1990.
- [41] S. Kvaal. *Analysis of many-body methods for quantum dots*. University of Oslo, 2008.
- [42] S. Kvaal. Open source FCI code for quantum dots and effective interactions. *ArXiv e-prints*, 2008.
- [43] Simen Kvaal. Harmonic oscillator eigenfunction expansions, quantum dots, and effective interactions. *Phys. Rev. B*, 80(4):045321, 2009.
- [44] D. C. Lay. *Linear Algebra and Its Applications*. Pearson Education, Orlando, FL, third edition, 2006.
- [45] L. E. Lervaag. *Variational monte-carlo calculations of two-dimensional quantum dots*. Master’s thesis, University of Oslo, 2010.

-
- [46] Xiangzhu Li and Josef Paldus. A multireference coupled-cluster study of electronic excitations in furan and pyrrole. *The Jour. of Phys. Chem. A*, 114:8591, 2010.
 - [47] M. P. Lohne. *Coupled-Cluster Studies of Quantum Dots*. Master's thesis, University of Oslo, 2010.
 - [48] G. B. Lubkin. Centenary of Lev Landau, accessed 25.05.2011. <http://www.aps.org/units/fhp/newsletters/fall2009/lubkin.cfm>.
 - [49] T. Lyche. *Lecture notes for INF-MAT 4350, 2010*. 2010.
 - [50] G. Hagen M. P. Lohne, M. Hjorth-Jensen, S. Kvaal, and F. Pederiva. Ab initio computation of circular quantum dots. *Not yet published*, 2010.
 - [51] M. Macucci, Karl Hess, and G. J. Iafrate. Numerical simulation of shell-filling effects in circular quantum dots. *Phys. Rev. B*, 55:R4879, 1997.
 - [52] P. Merlot. *Manybody-Body Approaches to Quantum Dot*. Master's thesis, University of Oslo, 2009.
 - [53] Peter J. Mohr, Barry N. Taylor, and David B. Newell. Codata recommended values of the fundamental physical constants: 2006. *Rev. Mod. Phys.*, 80:633, 2008.
 - [54] H. J. Monkhorst. *Int. J. Quantum Chem. Symp.*, 11, 1977.
 - [55] Nga T. T. Nguyen and S. Das Sarma. Impurity effects on semiconductor quantum bits in coupled quantum dots. *Phys. Rev. B*, 83:235322, 2011.
 - [56] Michael E. Peskin and Dan V. Schroeder. *An Introduction To Quantum Field Theory (Frontiers in Physics)*. Westview Press, 1995.
 - [57] K. D. Petersson, J. R. Petta, H. Lu, and A. C. Gossard. Quantum coherence in a one-electron semiconductor charge qubit. *Phys. Rev. Lett.*, 105:246804, 2010.
 - [58] J. R. Petta, A. C. Johnson, A. Yacoby, C. M. Marcus, M. P. Hanson, and A. C. Gossard. Pulsed-gate measurements of the singlet-triplet relaxation time in a two-electron double quantum dot. *Phys. Rev. B*, 72:161301, 2005.
 - [59] J. R. Petta, A. C. Johnson, A. Yacoby, C. M. Marcus, M. P. Hanson, and A. C. Gossard. Triplet singlet spin relaxation via nuclei in a double quantum dot. *Nature*, 435:7044, 2005.
 - [60] J. J. Quinn and K. Yi. *Solid State Physics-Principles and Modern Applications*. Springer Berlin Heidelberg, first edition, 2009.
 - [61] Stephanie M. Reimann and Matti Manninen. Electronic structure of quantum dots. *Rev. Mod. Phys.*, 74:1283, 2002.
 - [62] M. Rontani. *Ph.D thesis, Electronic States in Semiconductor Quantum Dots*. Universit degli Studi di Modena e Reggio Emilia, Modena, Italy, 2000.
 - [63] C. C. J. Roothaan. New developments in molecular orbital theory. *Rev. Mod. Phys.*, 23:69, 1951.
 - [64] J. Särkkä and A. Harju. Spin dynamics in a double quantum dot: Exact diagonalization study. *Phys. Rev. B*, 77:245315, 2008.
 - [65] I. Shavitt and R. Bartlett. *Quantum Theory of Many-Particle Systems*. Chambridge University Press, first edition, 2009.
 - [66] M. Shur and E. Borovitskaya. *Quantum Dots(Selected Topics in Electronics and Systems S.)*. World Scientific Publishing, first edition, 2002.
 - [67] J. C. Slater. The theory of complex spectra. *Phys. Rev.*, 34:1293, 1929.
 - [68] Lawrence D. True and Xiaohu Gao. Quantum dots for molecular pathology: Their time has arrived. *The Journ. of Mol. Diag.*, 9:7, 2007.
 - [69] M. A. Strosio V. Mitin, V. A. Kochealap. *Quantum Heterostructures - Microelectronics and Optoelectronics*. Chambridge University Press, first edition, 1999.

- [70] J. Čížek. On the correlation problem in atomic and molecular systems. calculation of wavefunction components in ursell-type expansion using quantum-field theoretical methods. *The Journ. of Chem. Phys.*, 45:4256–4266, 1966.
- [71] J. Čížek. On the use of the cluster expansion and the technique of diagrams in calculations of correlation effects in atoms and molecules. *Adv. Chem. Phys.*, 14, 1969.
- [72] G. C. Wick. The evaluation of the collision matrix. *Phys. Rev.*, 80:268, 1950.